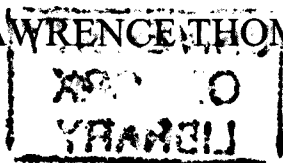


INVESTIGATION INTO BIOCATALYTIC ROUTES
TOWARDS MONOTERPENE ALCOHOLS

MARK LAWRENCE THOMPSON



UNIVERSITY OF YORK

PhD

CHEMISTRY

2009

Abstract

The overall aim of this investigation was to identify novel bacterial and fungal biocatalytic routes towards monoterpene alcohols such as enantiopure linalool and menthol, and geraniol, each of which find many applications within the flavour and fragrance industries.

The first part of the investigation targeted hydrolytic transformations of racemic monoterpene esters. Enantioselective linalyl acetate esterase activity was detected in *Rhodococcus ruber* DSM 43338, offering a potential route towards enantiopure (*R*)- and (*S*)- linalool. Fractions displaying complementary enantioselectivity for the reaction were isolated from anion-exchange chromatography of cell extracts, giving enantiomeric excess values for linalool ranging from 60% (*R*)- to 79% (*S*)-. Attempts to isolate the genes encoding relevant esterases *via* polymerase chain reactions resulted in a gene fragment representing 75% of a putative tertiary alcohol esterase (TAE). An alternative gene putatively encoding a TAE from a closely related Actinomycete *Nocardia farcinica* (NfTAE) was cloned and expressed in *E. coli*, and the enzyme purified and characterised. NfTAE was inactive towards linalyl acetate, but catalysed the hydrolysis of racemic menthyl acetate to give the commercially-preferred 1(*R*)-enantiomer of menthol.

In the second part of the project, a strain of *Rhodococcus erythropolis* MLT1 was isolated by selective enrichment from soil surrounding hop plants using the hop terpene β -myrcene as sole carbon source. Resting-cell preparations transformed β -myrcene to the high-value monoterpene alcohol geraniol. While the relevant enzyme remains to be identified, initial studies suggested an inducible operon for β -myrcene degradation in MLT1.

List of contents

Abstract

List of contents

List of figures

List of tables

Abbreviations

Acknowledgements

Author's declaration

<u>Section</u>	<u>Title</u>	<u>Page</u>
Chapter 1	Introduction	
1.1.	Natural products.....	1
1.2.	Terpenes.....	3
1.3.	Monoterpene alcohols.....	8
1.3.1.	Linalool.....	11
1.3.1.1.	Current methods of linalool production.....	12
1.3.2.	Geraniol and nerol.....	14
1.3.3.	Menthol.....	17
1.4.	The use of <i>Rhodococcus</i> species and Fungi in industrial biocatalysis.....	21
1.4.1.	Fungi.....	21
1.4.2.	<i>Rhodococcus</i> sp.....	24
1.5.	Project outline.....	26

3.2.3.	Extraction and concentration of solutions for GC analysis.....	46
3.2.4.	GC-MS analysis of fungal biotransformations.....	47
3.2.5.	Freeze-drying <i>A. niger</i> by lyophilisation.....	48
3.3.	Results and discussion.....	49
3.3.1.	Fungal biotransformations of geraniol, nerol, and myrcene.....	49
3.3.2.	Studies into the media pH effects on the perceived fungal biotransformation of geraniol to linalool by <i>Aspergillus niger</i>	52
3.3.3.	Biotransformation of geraniol and nerol to citral using <i>A. niger</i> and <i>G. lipsiense</i>	59
3.3.3.1.	Effect of pH on the yield of citral from biotransformation 3.....	62
3.3.3.2.	Use of acetone as a co-substrate to improve the yield of citral in biotransformation 3.....	63
3.4.	Conclusions.....	64

Chapter 4 Screening of *Rhodococcus* sp. for the resolution of linalyl acetate to linalool

4.1.	Introduction.....	67
4.2.	Experimental.....	73
4.2.1.	<i>Rhodococcus</i> strains and growth.....	73
4.2.2.	Growth of <i>Rhodococcus ruber</i> DSM 43338 on linalyl acetate as sole carbon source.....	73
4.2.3.	Screening <i>Rhodococcus</i> sp. for the hydrolysis of linalyl acetate to linalool.....	74
4.2.4.	Use of <i>tert</i> -butyl acetate as an inducer of carboxyl esterase hydrolases in <i>R. ruber</i> DSM 43338.....	75
4.2.5.	Gas chromatography analysis of linalyl acetate hydrolysis.....	75
4.2.6.	Protein purification of potential tertiary alcohol esterases.....	76
4.2.6.1.	Preparation of <i>Rhodococcus</i> cell extracts.....	76
4.2.6.2.	Anion exchange chromatography.....	77
4.2.6.3.	Ammonium sulphate precipitation.....	77
4.2.6.4.	Hydrophobic interaction chromatography.....	78

4.2.6.5.	Gel filtration chromatography.....	78
4.3.	Results and discussion.....	79
4.3.1.	Screening <i>Rhodococcus</i> strains for linalyl acetate hydrolytic activity.....	79
4.3.2.	Investigation of linalyl acetate and <i>tert</i> -butyl acetate as inducers of tertiary carboxyl ester hydrolase activity.....	83
4.3.3.	Purification of enantioselective esterases from <i>Rhodococcus</i> cell extracts.....	86
4.4.	Conclusions.....	95

Chapter 5 A gene-based approach towards an enantioselective esterase for linalyl acetate hydrolysis

5.1.	Introduction.....	97
5.2.	Experimental.....	101
5.2.1.	PCR for potential tertiary alcohol esterases from <i>R. ruber</i> DSM 43338.....	101
5.2.2.	Inverse PCR approach to a full length gene.....	102
5.2.2.1.	Digestion and re-ligation of template DNA.....	102
5.2.2.2.	Inverse PCR.....	103
5.2.3.	PCR for potential tertiary alcohol esterases from <i>Nocardia farcinica</i> (N1-3) and <i>Sulfolobus tokodaii</i> (S1).....	104
5.2.4.	Whole cell activity test for the hydrolysis of linalyl acetate, using over-expressed N2 and N3 esterases.....	105
5.2.5.	Purification of soluble N3 esterase.....	105
5.2.5.1.	Preparation of soluble protein.....	105
5.2.5.2.	Nickel column purification of N3 (1 st step).....	106
5.2.5.3.	Gel filtration of N3 (2 nd step).....	106
5.2.6.	Study of purified N3 esterase kinetics with <i>p</i> -nitrophenyl acetate.....	107
5.2.7.	Activity test with purified N3 esterase.....	107
5.2.8.	GC analysis of monoterpene acetate hydrolysis.....	108

5.3.	Results and discussion	109
5.3.1.	Cloning of potential tertiary alcohol esterases from <i>R. ruber</i> DSM 43338.....	109
5.3.2.	Cloning of potential tertiary alcohol esterases from <i>N. farcinica</i> and <i>S. tokodaii</i>	123
5.3.3.	Characterisation of the activity of N3 esterase from <i>N. farcinica</i>	131
5.4.	Conclusions	137

Chapter 6 Enrichment selection of a microorganism competent for growth on myrcene as the sole carbon source and characterisation of the microbial activity

6.1.	Introduction	140
6.2.	Experimental	146
6.2.1.	Chemicals.....	146
6.2.2.	Enrichment cultures and isolation of <i>Rhodococcus erythropolis</i> MLT1.....	146
6.2.3.	Growth of <i>Rhodococcus erythropolis</i> MLT1.....	147
6.2.4.	Preparation of cell extracts.....	148
6.2.5.	Biotransformation of β -myrcene by <i>R. erythropolis</i> MLT1.....	148
6.2.6.	Anaerobic resting cell assay.....	149
6.2.7.	Metabolite identification.....	150
6.2.8.	Peptide mass spectrometry.....	151
6.3.	Results and discussion	153
6.3.1.	Enrichment selection and characterisation of <i>R. erythropolis</i> MLT1.....	153
6.3.2.	Biotransformation of β -myrcene.....	155
6.3.3.	Metabolite identification.....	157
6.3.4.	Cytochrome P450 inhibition studies.....	159
6.3.5.	Inducibility of β -myrcene biotransformation.....	161
6.4.	Conclusions	166

Chapter 7	Sub-cellular studies of the myrcene degrading strain	
	<i>Rhodococcus erythropolis</i> MLT1	
7.1.	Introduction.....	171
7.2.	Experimental.....	175
7.2.1.	Fermentation of <i>R. erythropolis</i> MLT1.....	175
7.2.2.	Purification of a 15 kDa myrcene induced protein.....	176
7.2.2.1.	Preparation of soluble protein.....	176
7.2.2.2.	Anion exchange chromatography (1 st step).....	176
7.2.2.3.	Gel filtration chromatography (2 nd step).....	177
7.2.3.	Assaying sub-cellular fractions for activity towards myrcene and linalool.....	177
7.2.4.	PCR for genes encoding myrcene induced proteins.....	178
7.3.	Results and discussion.....	179
7.3.1.	Investigation into fermentation as a method of generating increased biomass for sub-cellular studies.....	179
7.3.2.	Purification of a 15 kDa myrcene induced protein.....	185
7.3.3.	Attempted identification of a 15 kDa myrcene induced protein.....	189
7.3.4.	Attempts towards cloning of a myrcene degradation cluster.....	191
7.4.	Conclusions.....	194
Chapter 8	Conclusions and future work.....	197
	References.....	213
	List of structures.....	222
	Appendix.....	230
	Publication of research.....	231

List of figures

<u>Page</u>	<u>Figure</u>	<u>Abbreviated title</u>
2	1	The alkaloids quinine and caffeine
2	2	The polyketide antibiotic erythromycin
3	3	Structure of the 5-carbon isoprene unit
3	4	Monoterpenes: limonene, menthol, and camphor
4	5	The sesquiterpene caryophyllene, and diterpene retinol
5	6	Monoterpene olefins α -pinene and 3-carene with the diterpene abietic acid
6	7	The mevalonic acid pathway
7	8	The non-mevalonate (MEP/DOXP) pathway
9	9	Examples of natural products including monoterpene alcohols of industrial importance
10	10	Industrially important monoterpene alcohols to be targeted in this research
12	11	Synthesis of linalool from α -pinene
12	12	Organic synthesis of (<i>S</i>)-linalool from 2-methyl-2-hepten-6-one <i>via</i> base catalysed ethynylation
13	13	Biosynthesis of (<i>S</i>)-linalool from geranyl diphosphate
14	14	Industrial synthesis of geraniol from β -pinene
15	15	Chemical synthesis of geraniol and nerol from β -myrcene
16	16	Inter-conversion between the isomers of citral
18	17	Pathway of menthol biosynthesis in <i>Mentha</i> sp
19	18	Asymmetric synthesis of menthol
20	19	Preparation of 1 <i>R</i> -(-)-menthol <i>via</i> enantioselective hydrolysis of menthyl acetate
21	20	Regio- and enantioselective 6 β -hydroxylation of the steroid 17 α -hydroxyprogesterone by <i>Botrytis cinerea</i>

<u>Page</u>	<u>Figure</u>	<u>Abbreviated title</u>
22	21	Yeast mediated selective reduction of a pro-chiral double bond, and <i>Candida antartica</i> lipase A catalysed kinetic resolution of (\pm)-2-phenylbut-3-yn-2-ol
23	22	Monoterpene biotransformations catalysed by yeast
24	23	Desulphurisation of naphtho[2-1- <i>b</i>]thiophene found in diesel oil by <i>Rhodococcus</i> sp. WU-K2R
25	24	Biotransformation of limonene to carveol and carvone by <i>Rhodococcus opacus</i> PW4
27	25	Biocatalytic routes towards the monoterpene alcohols of industrial interest for this project
31	26	Overview of the ligation independent cloning (LIC) process
42	27	Regio- and enantioselective hydroxylation of isosteriol by <i>Aspergillus niger</i> and <i>Penicillium chrysogenum</i>
42	28	Biotransformation products of β -myrcene with <i>A. niger</i>
43	29	Biotransformation products of β -myrcene with <i>G. lipsiense</i>
44	30	Diversity of biotransformation products of geraniol and nerol using <i>Botrytis cinerea</i>
50	31	GC-MS analysis for the pH 7 buffered biotransformation of nerol by <i>B. cinerea</i> .
53	32	GC-MS analysis and time-course for the growing-cell biotransformation 1 of nerol by <i>A. niger</i>
54	33	GC-MS analysis and time-course for the growing cell biotransformation 2 of geraniol by <i>A. niger</i>
56	34	Incubation of geraniol in a 50 mM potassium phosphate buffer solution at pH 4.85
57	35	Sample extracted from biotransformation 2 after a 24 h incubation
58	36	Results from published literature for the bioconversion of geraniol by <i>A. niger</i> sporulated surface cultures
59	37	GC-MS analysis and time-course for the resting cell biotransformation 3 of geraniol using <i>A. niger</i>
60	38	GC-MS analysis and time-course for the resting cell biotransformation 4 of nerol by <i>G. lipsiense</i>

<u>Page</u>	<u>Figure</u>	<u>Abbreviated title</u>
61	39	Commercial importance of citral in a synthetic route towards ionones
62	40	Samples extracted for the resting cell biotransformation of geraniol using <i>A. niger</i> at pH 6 and pH 10
63	41	Proposed use of acetone as a co-substrate for the recycling of NAD ⁺ via biocatalytic hydrogen transfer
65	42	Scheme showing the acid catalysed conversion of geraniol and nerol into linalool, nerol, and α -terpineol
68	43	Biocatalytic routes towards tertiary alcohols
70	44	Representation of the catalytic triad residues (Ser, Glu, and His) in <i>p</i> -nitrobenzyl esterase from <i>Bacillus subtilis</i> , and a general serine hydrolase mechanism
71	45	Examples of the industrially important tertiary alcohols linalool and α -terpineol.
71	46	Biocatalytic resolution of racemic linalyl acetate
80	47	GC analysis for the four strains of <i>Rhodococcus</i> that showed activity towards the hydrolysis of linalyl acetate
81	48	Activity of <i>R. ruber</i> DSM 43338 and <i>R. aetherivorans</i> AM1 strains towards linalyl acetate
82	49	Activity of <i>R. sp.</i> HS2 and <i>R. rhodochrous</i> 11Y strains towards linalyl acetate
84	50	Effect of <i>tert</i> -butyl acetate induction on the activity of linalyl acetate hydrolysis by <i>R. ruber</i> DSM 43338
84	51	Acetates used in the induction experiments: tributyrin, α -naphthyl acetate, and <i>tert</i> -butyl acetate
85	52	Cell extracts from <i>R. ruber</i> DSM 43338 grown on: linalyl acetate and glucose as sole carbon sources
85	53	Results of peptide sequencing for the linalyl acetate induced protein
88	54	Chiral GC analysis for the hydrolysis of linalyl acetate using anion exchange fractions
89	55	First step of purifying esterases from <i>R. ruber</i> 43338 cell extract using anion exchange chromatography

<u>Page</u>	<u>Figure</u>	<u>Abbreviated title</u>
90	56	Chiral GC analysis of <i>R. ruber</i> anion exchange fractions
91	57	SDS-PAGE analysis of fractions collected from a second step of purification (HIC)
92	58	Chromatogram showing the first step of a two step purification strategy using a phenyl sepharose column
94	59	Anion exchange chromatography for the second step of a two step purification strategy and GC analysis of the active fraction
94	60	SDS-PAGE analysis of a fraction collected from the second step of purification shows enhanced enantioselectivity towards the hydrolysis of linalyl acetate
97	61	The chiral tertiary alcohol ester, linalyl acetate
98	62	Representation of the tetrahedral intermediate formed within the active site of <i>Bacillus subtilis</i> esterase BS2
100	63	Peptide sequence of the GGG(A)X motif <i>Bacillus subtilis</i> <i>p</i> -nitrobenzyl esterase (BS2)
100	64	Binding of the TAEs 2-phenyl-3-butin-2-yl acetate in the active site of WT <i>Bacillus subtilis</i> <i>p</i> -nitrobenzyl esterase
111	65	Sequence alignment of BS2 esterase with homologues from <i>Rhodococcus</i> sp. RHA1
112	66	Design of PCR primers towards highly conserved regions in the sequence of a potential tertiary alcohol esterase
113	67	Results of PCR and ligation independent cloning showing a ~300bp product
114	68	Results of sequencing and alignment of the cloned esterase 288bp gene fragment
115	69	PCR using the CAT forward primer with reverse primer 2
116	70	Sequence of a probable carboxylesterase from <i>R. sp</i> RHA1
117	71	Agarose gel after running a restriction digest showing the cloned ~1100bp insert
117	72	The results of sequencing for the cloned 1107bp and BLAST for those genes sharing a high degree of homology

<u>Page</u>	<u>Figure</u>	<u>Abbreviated title</u>
118-119	73	Six peptide sequences showing the greatest homology with respect to the cloned 1107bp fragment.
120	74	PCR results showing a product of ~1200bp when using primers CAT for / R1a
121	75	Restriction digest showing a cloned ~1200bp gene fragment
122	76	Summary of the cloning strategy towards a ~1550bp potential tertiary alcohol esterase from <i>R. ruber</i>
124	77	Clustal sequence alignment of the <i>Bacillus subtilis</i> <i>p</i> -nitrobenzyl esterase with the <i>Nocardia farcinica</i> genome
125	78	Clustal sequence alignment of the <i>Bacillus subtilis</i> <i>p</i> -nitrobenzyl esterase with the <i>Sulfolobus tokodaii</i> genome
125	79	PCR products for the carboxylesterases: N1, N2, N3 and S1
126	80	Restriction digest showing the cloned N3 insert
127	81	Expression of N3 protein in <i>E. coli</i> BL21 (DE3) cells
128	82	Expression of N2 protein in <i>E. coli</i> B834 cells
129	83	Activity testing of BL21 whole cells over-expressing N3 esterase, towards the hydrolysis of linalyl acetate
130	84	Second step of N3 esterase purification <i>via</i> gel filtration chromatography (GF)
131	85	Kinetics analysis for the hydrolysis of <i>p</i> -nitrophenylacetate (<i>p</i> NPA) by N3 esterase
132	86	Michaelis-Menten curve and Lineweaver-Burk plot used in the determination of kinetic parameters for the hydrolysis of <i>p</i> NPA by the purified N3 esterase
134	87	Chiral GC analysis of 1(±)-menthyl acetate hydrolysis using the purified N3 esterase
135	88	GC analysis of citronellyl acetate hydrolysis using the purified N3 esterase
136	89	Chiral GC analysis of 1(±)-lavandulyl acetate hydrolysis using the purified N3 esterase
141	90	Chemical structures of some of the main components of oils extracted from the lupulin glands of hop plants

<u>Page</u>	<u>Figure</u>	<u>Abbreviated title</u>
142	91	Products of β -myrcene metabolism in rabbit
144	92	Summary of some existing β -myrcene biotransformations in the literature
154	93	Growth of <i>R. erythropolis</i> MLT1 on M9 minimal media with myrcene as the sole carbon source (SCS)
154	94	Growth of <i>R. erythropolis</i> MLT1 utilising either succinate, glucose, and β -myrcene as the SCS
156	95	GC analysis for the biotransformation of β -myrcene by <i>R. erythropolis</i> MLT1
157	96	Mass spectrum for the geraniol metabolite
160	97	Effect of cytochrome P450 inhibition on the biotransformation of β -myrcene to geraniol
162	98	Activity testing for <i>R. erythropolis</i> MLT1 grown on alternate carbon sources
163	99	SDS-PAGE analysis of the crude soluble cell extracts of <i>R. erythropolis</i> MLT1 grown on either glucose or β -myrcene
167	100	Monooxygenase catalysed oxidation at a terminal alkene position in styrene by <i>Pseudomonas</i> sp. VLB120
168	101	Enantioselective hydration of the conjugated C=C bond in 3-methyl and 3-ethylbutanolide
168	102	Hydration of a non-conjugated double bond in limonene
172	103	The acyclic terpene utilisation (ATU) pathway showing the degradation of geraniol in <i>Pseudomonas citronellolis</i>
173	104	An initial monooxygenase catalysed step in the pathway of isoprene degradation in <i>Rhodococcus</i> strain AD45
180	105	Growth curves for the fermentation of <i>R. erythropolis</i> MLT1 in M9 minimal media with glucose, and glucose supplemented with myrcene
182	106	Growth curves for the fermentation of <i>R. erythropolis</i> MLT1 in M9 minimal media with myrcene as the SCS
184	107	Resting cell assay with myrcene using cells harvested from a 5 L fermentation with myrcene as the SCS

<u>Page</u>	<u>Figure</u>	<u>Abbreviated title</u>
185	108	SDS-PAGE analysis of soluble cell extracts from <i>R. erythropolis</i> MLT1 grown on glucose and myrcene as SCS.
187	109	Purification of an unknown ~15 kDa myrcene induced protein from <i>R. erythropolis</i> MLT1 cell extracts
188	110	Calibration of the Superdex gel filtration column (S75 10/30) used in the second step of purification
190	111	Mass spectrometry (MS) analysis for the purified ~15 kDa myrcene induced protein
190	112	Agarose gel for PCR using primers designed towards the ~15 kDa myrcene induced protein
192	113	Fragments from peptide MS used in the identification of a myrcene induced protein
193	114	Sequence alignment of the putative acyl-CoA dehydrogenase from <i>Frankia alni</i> with a homologous acyl-CoA dehydrogenase from <i>Rhodococcus</i> sp. RHA1
197	115	Summary of the biocatalytic routes observed during this project
207	116	A proposed catabolic pathway of β -myrcene in <i>Pseudomonas</i> strain M1
208	117	The dehydration of linalool to β -myrcene, and isomerisation of geraniol to linalool catalysed by a <i>linalool dehydratase</i> in <i>Castellaniella defragrans</i>
209	118	A proposed mechanism for the conversion of α -myrcene to nerol by different strains of basidiomycetes
210	119	The anaerobic biotransformation of β -myrcene to geranic acid by <i>Alcaligenes defragrans</i>

List of tables

<u>Page</u>	<u>Table</u>	<u>Abbreviated title</u>
8	1	Annual demand for some of the more common monoterpene alcohols
11	2	Enantiomeric distribution (%) of (<i>R</i>) and (<i>S</i>) linalool in different species of plant
51	3	Four fungal biotransformations for further investigation
55	4	pH measurements of the fungal growth medium from the time of substrate addition
66	5	Summary of reactions from this chapter
86	6	Enantiomeric excess of linalool produced in resting whole cell assays for the active strains of <i>Rhodococcus</i>
87	7	Increasing enantioselectivity for the hydrolysis of (<i>S</i>)-linalyl acetate from a single step FFQ purification
158	8	Published GC-MS data for geraniol
165	9	Identification of protein bands II and IV using MS analysis of peptide fragments

Abbreviations

ABT	1-aminobenzotriazole
APS	Ammonium persulphate
ATU	acyclic terpene utilisation
BINAP	2,2'-bis(diphenylphosphino)-1,1'-binaphthyl
BLAST	Basic Local Alignment Search Tool
BSA	Bovine serum albumin
CBS	Centraalbureau voor Schimmelcultures
dATP	Deoxyadenosine triphosphate
DMAPP	Dimethylallyl diphosphate
DMSO	Dimethyl sulfoxide
DNA	Deoxyribonucleic acid
dNTPs	Deoxynucleotide triphosphates
DOXP	1-deoxy-D-xylulose 5-phosphate
DSM	Deutsche Sammlung von Mikroorganismen
DTE	Dithioerythritol
DTT	Dithiothreitol
dTTP	Deoxythymidine triphosphate
E	Enantiomeric ratio
EDTA	Ethylenediaminetetraacetic acid
ee	Enantiomeric excess
EEC	European Economic Community
EI	Electrical ionisation
FFQ	Fast flow Q-sepharose resin

GC	Gas chromatography
GC-MS	Gas chromatography – Mass spectrometry
GF	Gel filtration
GPPS	Geranyl diphosphate synthase
HIC	Hydrophobic interaction chromatography
HMG	3-hydroxy-3-methylglutarate
iPD	Isopiperitenol dehydrogenase
iPI	Isopugelone isomerase
IPP	Isopentenyl diphosphate
iPR	Isopiperitenone reductase
IPTG	Isopropyl β -D-1-thiogalactopyranoside
L3OH	Limonene-3-hydroxylase
LB	Luria Bertani
LIC	Ligation independent cloning
LS	Limonene synthase
M9	Minimal growth medium
MALDI	Matrix-assisted laser desorption/ionization
MEP	Methylerythritol phosphate
MR	Menthone reductase
MS	Mass spectrometry
MVA	Mevalonic acid
MW	Molecular weight
NAD ⁺	Nicotinamide adenine dinucleotide
NADH	Reduced nicotinamide adenine dinucleotide

NCBI	National Centre for Biotechnology Information
NCIMB	National Collection of Industrial and Marine Bacteria
NDMA	<i>N</i> -nitrosodimethylamine
NEB	New England Biolabs
NfTAE	<i>Nocardia farcinica</i> tertiary alcohol esterase
OD	Optical density
pA	Peak area
PCR	Polymerase chain reaction
PES	Polyethersulfone membrane from Millipore
<i>p</i> NBE	<i>p</i> -nitrobenzyl esterase
<i>p</i> NPA	<i>p</i> -nitrophenyl acetate
PR	Pulegone reductase
rRNA	Ribosomal ribonucleic acid
SCS	Sole carbon source
SDS-PAGE	Sodium dodecyl sulfate polyacrylamide gel electrophoresis
TAE	Tertiary alcohol esterase
TAEs	Tertiary alcohol ester(s)
TEMED	Tetramethylethylenediamine
TEMPO	Tetramethylpiperidine oxide
TF	Technology facility (University of York)
TRP	Transient receptor potential (ion channel)
WT	Wild-type

Acknowledgements

I would like to thank my supervisor Dr. Gideon Grogan for giving me the opportunity to work on this project which I have found interesting and enjoyable, and for whom the time and effort devoted, I am extremely grateful for.

I appreciate the financial assistance that has been provided by the Biotechnology and Biological Sciences Research Council, and Botanix Ltd; and acknowledge help from technical staff within the York Structural Biology Laboratory (YSBL), the Technology Facility, and from Prof. Ray Marriott in the Green Chemistry department at the University of York.

I would especially like to thank my parents for all their support, and write this in memory of my brother Stuart. I would finally like to thank Dr. James Edwards, Dr. Radka Snajdrova, and Claudia Szolkowy for their kind support during my three years in the YSBL.

Author's declaration

The research described in this thesis, except where due reference is made, is original and has been carried out by the author.

M. L. Thompson

1. Chapter 1: Introduction

1.1. Natural products

The great diversity of structures produced in nature which possess biological and pharmacological activity has created a wealth of opportunity for their use in drug design and commerce. Natural products can be generally categorised into either primary or secondary metabolites. Proteins, carbohydrates, fats and nucleic acids comprise the primary metabolites that are vital molecules for living organisms, and are generated by common metabolic pathways in microorganisms, animals, and plants. Secondary metabolites are organic compounds which are not directly required for growth and metabolism by the organism. In contrast the secondary metabolites which can be produced from the intermediates of primary metabolism are often prevalent in specific organisms and species depending upon the particular role that they fulfil, and can be generally classified according to their structural properties. One particular category is those natural products which contain basic nitrogen atoms, termed alkaloids, which are frequently found to confer pharmacological and stimulant activity (fig. 1). Polyketides are secondary metabolites synthesised from the polymerisation of acetyl and propionyl groups *via* Claisen condensation reaction, from which further derivatisation yields a diverse group of compounds found to contain many antibiotics such as erythromycin and the tetracyclines (fig. 2). Other classes of secondary metabolite natural products include phenolics and phenazines; however it is the terpenoids which provide the focus of study for this PhD work.

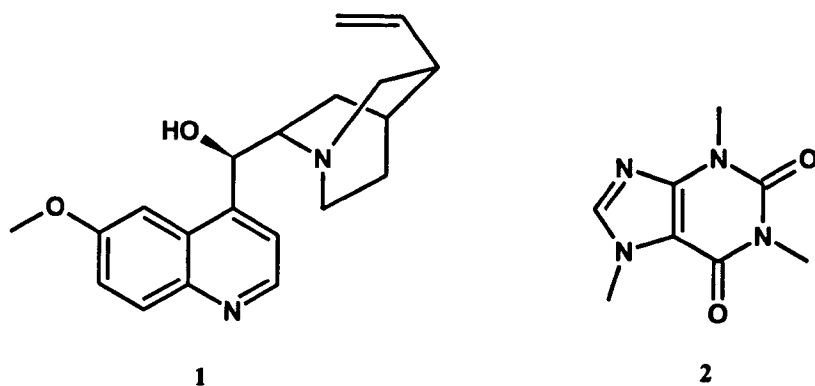


Figure 1: The alkaloids quinine 1 and caffeine 2 which possess well-known pharmacological and stimulatory properties.

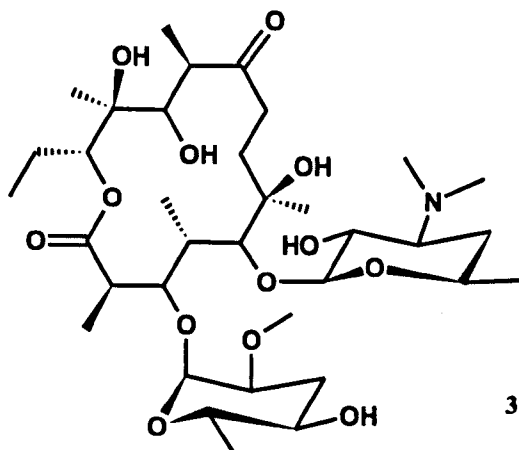


Figure 2: The polyketide antibiotic erythromycin 3 produced by the actinomycete *Saccharopolyspora erythraea*.

1.2. Terpenes

Produced as secondary metabolites in plants, terpenes and their derivatives (terpenoids) account for the largest class of natural products numbering over 23,000 [Cheng et al. 2007]. Terpenes are comprised of a basic C_5H_8 isoprene unit **4** (fig. 3) which forms the backbone for a large range of both acyclic and cyclic derivatives with a variety of functionality.

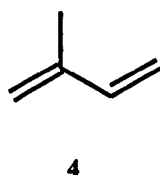


Figure 3: Structure of the 5-carbon isoprene unit.

These isoprene units are linked ‘head-to-tail’ forming chains or rings which can be classified according to the number of these 5 carbon units: monoterpenes (C_{10}), sesquiterpenes (C_{15}), diterpenes (C_{20}), triterpenes (C_{30}). Examples of these are shown in figures 4 and 5.

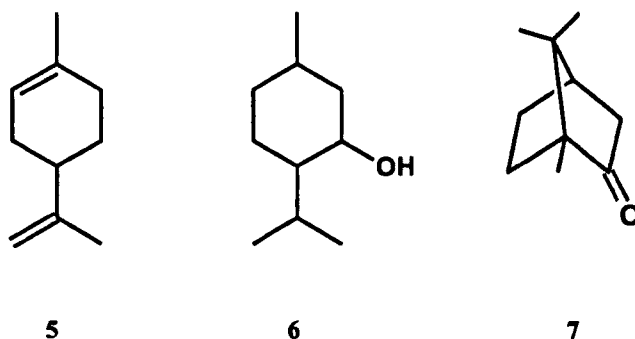


Figure 4: Monoterpenes: limonene **5**, menthol **6**, and camphor **7**.

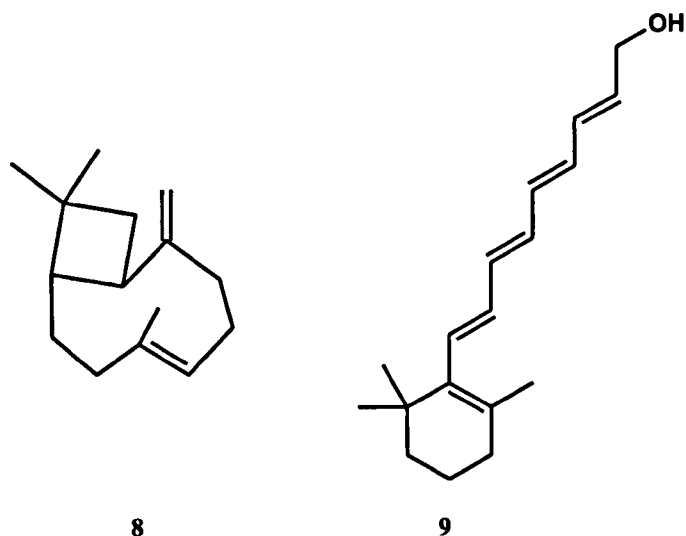


Figure 5: The sesquiterpene: caryophyllene **8**, and an example of a diterpene: retinol **9**.

Terpenes serve diverse metabolic, physiological, and structural roles in plants [McGarvey et al. 1995]. Many examples of the particularly volatile mono- and sesquiterpenes are used in plant communication and defence (fig. 6). Other roles as plant hormones (gibberellins, abscisic acid), photosynthetic pigments (phytol, carotenoids), electron carriers (ubiquinone, plastoquinone) are also fulfilled by these secondary metabolites.

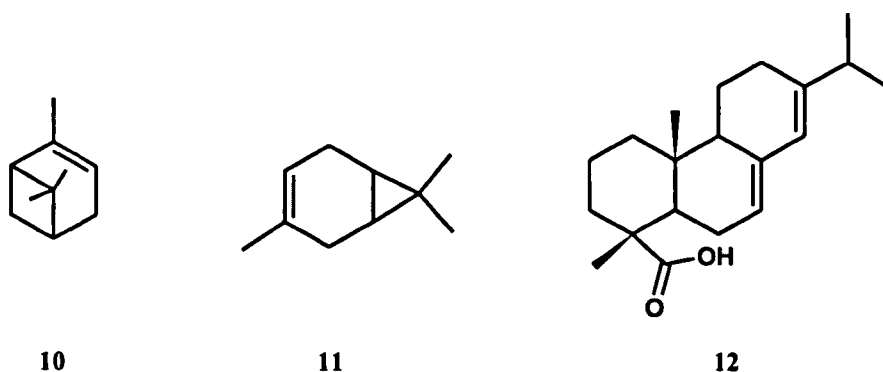


Figure 6: Monoterpene olefins α -pinene **10** and 3-carene **11** along with the diterpene abietic acid **12** are produced in coniferous resin in response to herbivore or pathogen attack. The more volatile monoterpenes enable a quicker flow of abietic acid which is toxic to herbivores, and polymerises during exposure to oxygen, sealing the wound [Gershenzon et al. 2007].

Terpenoids are produced in plants from the 5-carbon precursors isopentenyl diphosphate (IPP) **16** and dimethylallyl diphosphate (DMAPP) **17**, which are derived *via* two different pathways and can freely interconvert through isomerisation. The initial steps of the mevalonic acid (MVA) pathway which occurs in the cell cytosol convert acetyl CoA **13** to an activated form of the isoprene unit IPP, through the action of HMG-CoA reductase (**14-16**). IPP is isomerised to its more reactive form DMAPP by IPP isomerase, before addition to prenyl diphosphate co-substrates to extend the chain in terpenoid biosynthesis (fig. 7, **18-20**). An MVA-independent pathway also exists (termed MEP/DOXP pathway after the identification of a methylerythritol phosphate intermediate) leading to the formation of IPP from pyruvate and glyceraldehyde-3-phosphate, and is found to occur in plastids (fig. 8) [Lichtenthaler et al. 1999, Rohmer et al. 1999]. IPP and DMAPP derived from the cytosolic MVA pathway serve as

precursors of farnesyl diphosphate (FPP) in the synthesis of sesquiterpenes and triterpenes. Whilst the biosynthesis of mono-, di-, and tetra-terpenes is derived from plastidic IPP and DMAPP produced in the MEP/DOXP pathway.

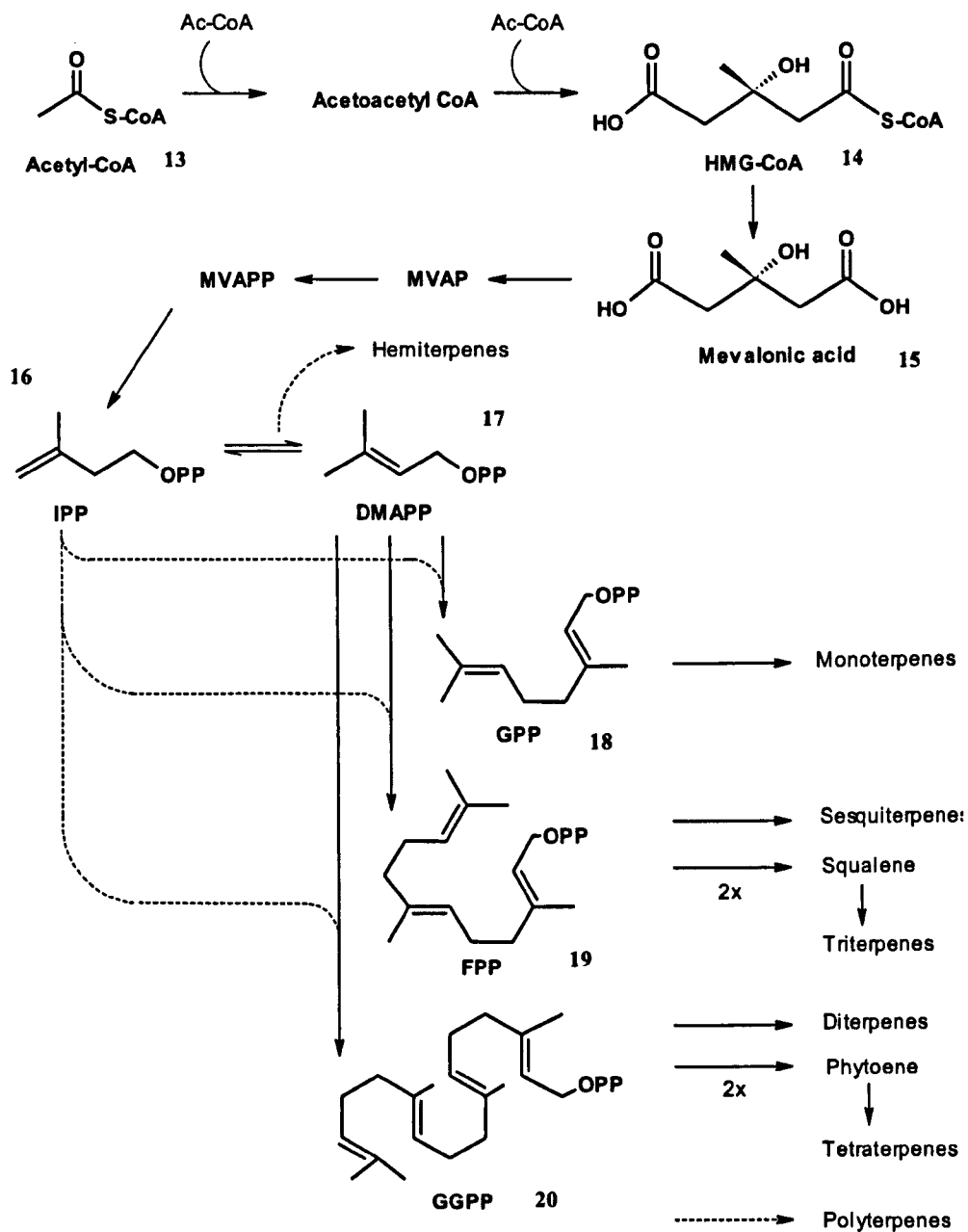


Figure 7: The mevalonic acid pathway giving rise to IPP and DMAPP precursors for subsequent use in terpenoid skeleton biosynthesis in plants. [McGarvey et al. 1995].

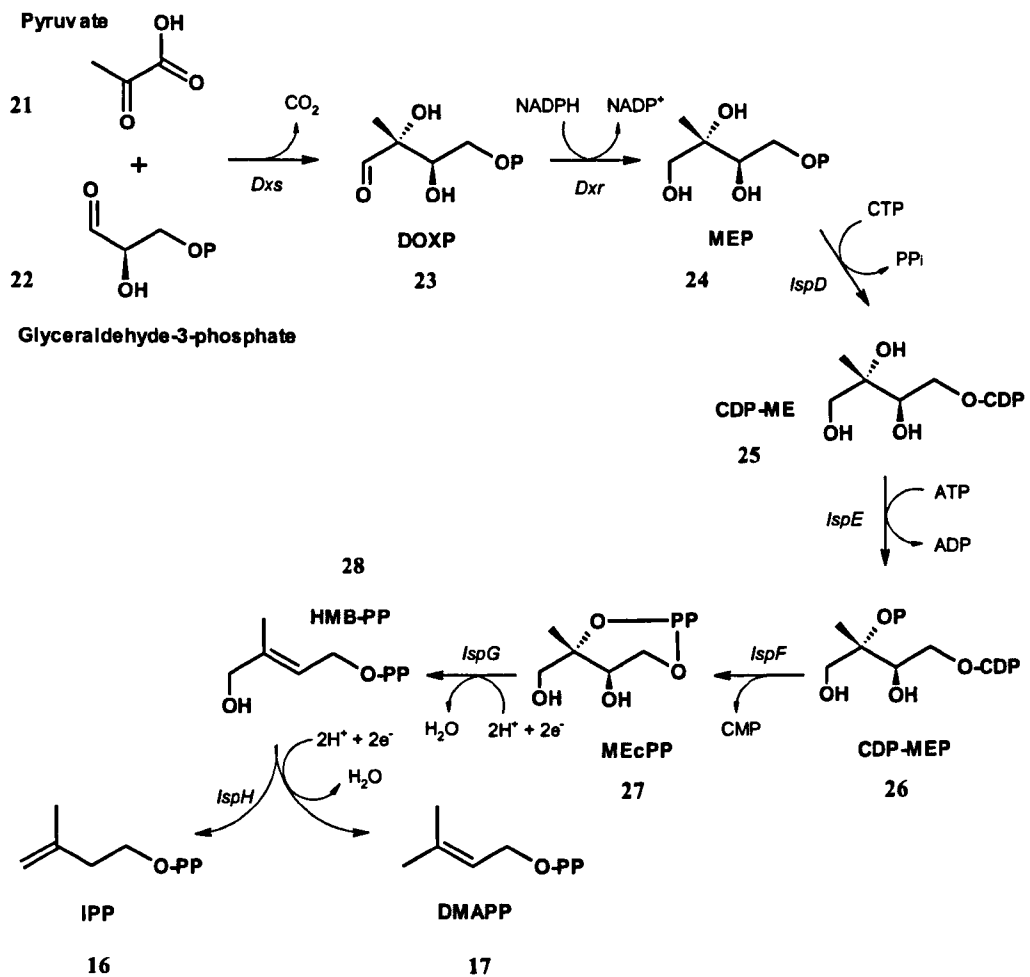


Figure 8: The non-mevalonate (MEP/DOXP) pathway leading to production of universal precursors IPP 16 and DMAPP 17 for isoprenoid biosynthesis *via* the generation of a methylerythritol phosphate intermediate [Lichtenthaler et al. 1999, Rohmer et al. 1999].

1.3. Monoterpene alcohols

Derived from two isoprene units with added hydroxyl functionality the characteristic and diverse organoleptic properties associated with the monoterpene alcohols, ensure that this particular group of natural products have an important role in the flavour and fragrance industries (fig. 9). Primary, secondary, and tertiary alcohols belonging to this class have been extracted from plant essential oils, however synthetic approaches have now been developed to cope with the increase in demand that these industries have created (table 1).

Table 1: Annual demand for some of the more common monoterpene alcohols [Sell 2003].

Monoterpene alcohol	Odour	Approx. annual usage (tons) - 2003
Menthol	Mint	5000
α -terpineol	Pine	3000
Dihydromyrcenol	Citrus, floral	2500
Geraniol / nerol	Rose	6000
Citronellol	Rose	6000
Linalool	Floral	4000

Whilst the use of synthetic chemistry negates some environmental factors, such as variable climatic conditions, that can pose problems for the large scale cultivation and physical extraction of oils from plant specimens; it has in turn brought disadvantages which are of increasing significance. One of the main limitations in following a synthetic rather than biocatalytic route towards these compounds is an inability to generate high levels of enantioselectivity. Many natural products, with the monoterpene alcohol menthol as an example, yield their distinguishing function or fragrance depending upon the absolute configuration [Brenna et al. 2003].

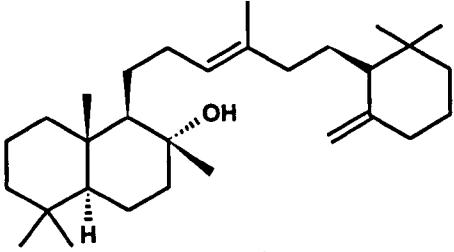
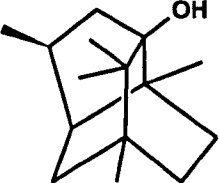
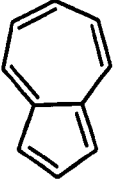
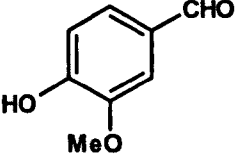
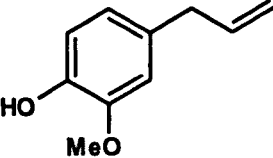
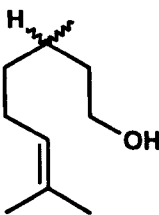
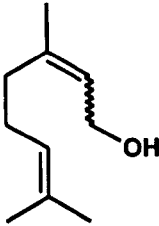
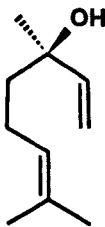
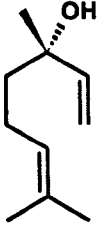
Fragrance	Natural product	Source / properties	
Ocean	 (+)-Ambrein 29	Previously isolated from sperm whales as a main constituent of ambergris; the highly fragrant ambrein is now largely produced synthetically	
Oriental	 Patchouli alcohol 30	 Azulene 31	Azulene extracted from the essential oil of chamomile flowers and patchouli alcohol from <i>P. cablin</i> are used to provide a lasting oriental fragrance
Spicy / floral	 Vanillin 32	 Eugenol 33	The more naturally abundant eugenol has been used in the synthesis of vanillin. Both compounds sort after for sweet and spiced fragrances
Rose / floral	 Citronellol 34	 (Z)-Geraniol 35 / (E)-Nerol 36	Collectively known as the rose alcohols; as extracts from plants of this species constitute a rich source of these monoterpene alcohols which possess a distinctive floral odour
White / floral	 (R)-Linalool 37	 (S)-Linalool 38	Produced in many plant species, the different enantiomers of the monoterpene alcohol linalool are known to possess noticeably contrasting fresh fragrances

Figure 9: Examples of natural products including monoterpene alcohols, which are of importance to the fragrance and cosmetic industries.

The difficulties in obtaining ‘natural’ compounds in significant quantities and their demand within the flavour and fragrance industries are reflected in their commercial value [Serra et al. 2005, Feron et al. 1996, Cheetham 1993]. Vanillin is an important compound in both flavour and fragrance, and whilst the price of synthetically prepared vanillin from guaiacol is around US \$15/kg; natural vanillin extracted from the pods of *Vanilla* orchids can range in value between US \$1200-4000/kg. European legislation restricts the methods of preparation by which ‘natural’ flavours can be prepared to either physical extraction from the natural material, or *via* enzymatic and microbiological approaches using naturally isolated precursors.

‘If the sales description of the flavouring contains a reference to a foodstuff or a flavouring source, the word ‘natural’, or any other word having substantially the same meaning, may not be used unless the flavouring component has been isolated by appropriate physical processes, enzymatic or microbiological processes or traditional food preparation processes solely or almost solely from the foodstuff or the flavouring source concerned.’ [EEC directive 1988].

The use of biocatalysis to target the industrially important monoterpene alcohols in this research not only allows exploitation of enzymatic selectivity but would ensure that any product achieved can be classified as ‘natural’. This could in turn offer potentially desirable alternatives towards the production of these monoterpene alcohols (fig. 10).

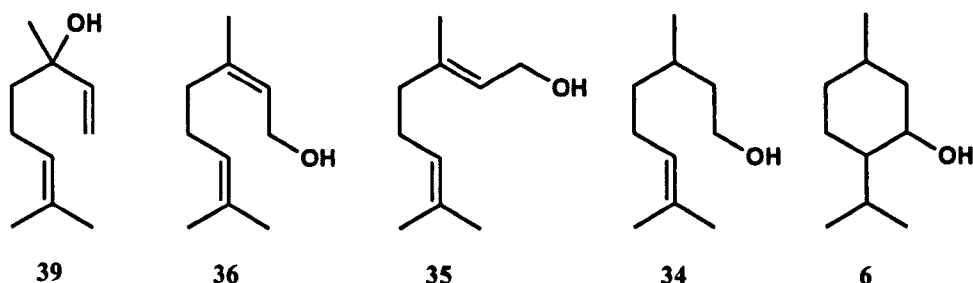


Figure 10: Industrially important monoterpene alcohols to be targeted in this research: linalool 39, nerol 36, geraniol 35, citronellol 34, and menthol 6.

1.3.1. Linalool

Linalool is a particularly important chiral tertiary alcohol, and is widely used in fragrance products such as perfumes, soaps and detergents, whilst also important as an odour-active component in the hopping of beer [Kishimoto et al. 2005, 2006]. Linalool is a naturally occurring monoterpene in many species of plants, in which the proportion of enantiomers can vary significantly (Table 2). The enantiomers of linalool differ in odour with (*S*)-(+)-linalool (coriandrol) **38** yielding a sweet floral fragrance, whilst (*R*)-(-)-linalool (licareol) **37** has a more characteristic woody / lavender odour; therefore production of homochiral linalool is commercially desirable.

Table 2: Enantiomeric distribution (%) of (*R*) and (*S*) linalool in different species of plant [Casabianca et al. 1998].

	<u>Enantiomeric distribution</u>	
	(<i>R</i>)	(<i>S</i>)
Basil	100	0
Eucalyptus	100	0
Thyme	98	2
Lavender	96	4
Rose	60	40
Geranium	50	50
Grapefruit	37	63
Lemon	32	68
Rosemary	23	77
Lilac	11	89
Coriander	10	90
Jasmine	4	96

1.3.1.1. Current methods of linalool production

The importance of linalool for fragrance production and in the industrial preparation of vitamins A and E has led to various literature examples concerning its organic synthesis. One such method uses α -pinene extracted from coniferous wood as a cheaper starting material (fig. 11).

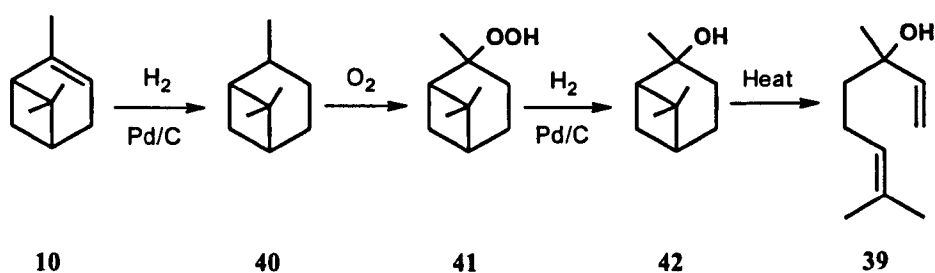


Figure 11: Synthesis of linalool **39** from α -pinene **40** [Semikolenov et al. 2001].

Methods of synthesising single enantiomers of linalool also exist in both organic chemistry (fig. 12), and in Nature (fig. 13) where it is utilised as a key component of the volatile pheromones designed to attract pollinators.

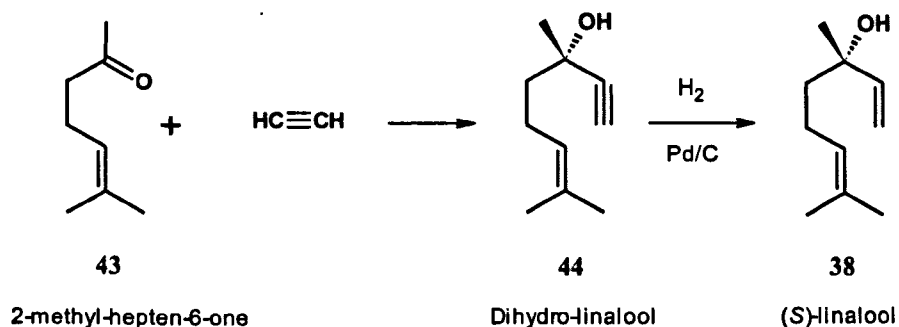


Figure 12: Organic synthesis of (*S*)-linalool from 2-methyl-2-hepten-6-one via base catalysed ethynylation in the presence of a palladium catalyst [Raguso et al. 1999].

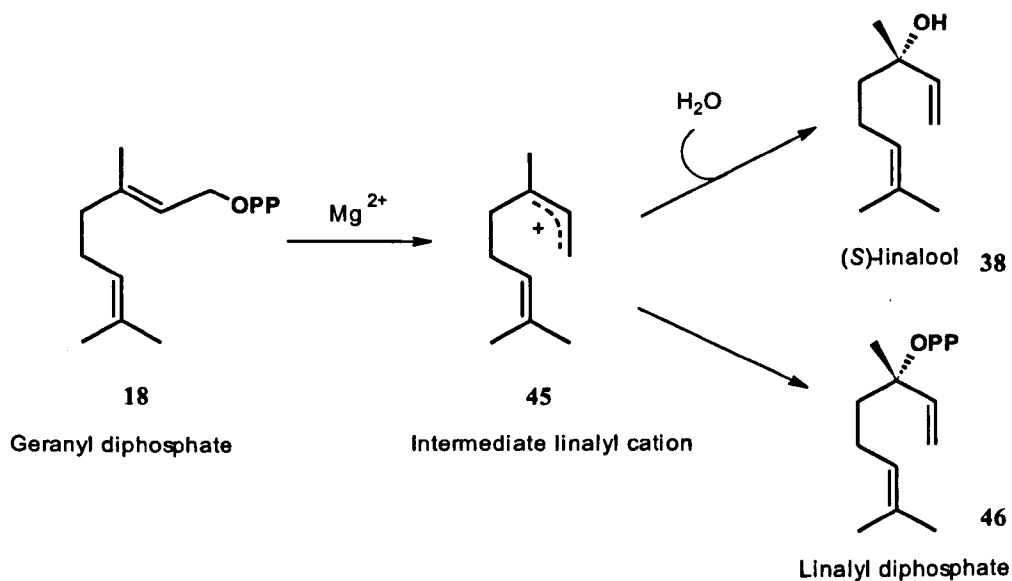


Figure 13: Biosynthesis of (*S*)-linalool from geranyl diphosphate by (*S*)-linalool synthase; an enzyme involved with floral scent production in *Clarkia breweri* [Pichersky et al. 1995].

Until the 1950-60s, the majority of linalool used in the fragrance industry was isolated from essential oils, predominantly rosewood oil. The oil extracted from rosewoods in the Amazon rainforest is particularly rich in linalool (up to 86% w/w) [Maia et al. 2004]. The growing demand for the naturally extracted linalool created harvest pressure on the tree, with this species of rosewood now becoming endangered as a consequence.

1.3.2. Geraniol and nerol

Geraniol is a monoterpene alcohol with a wide range of uses in perfumery, food and also as an insect repellent. The global production of geraniol together with its derived esters was estimated recently to be 12,000 tonnes per year [Schwab et al. 2008]. Whilst some of this material is extracted directly from natural products, the majority is based on an industrial chemical synthesis from β -pinene. In this synthesis, β -pinene is first heated to yield β -myrcene as an intermediate. Chlorination using hydrochloric acid and copper (II) chloride, followed by substitution of chloride with acetate and finally saponification yields a mixture of geraniol, linalool and nerol (fig. 14). Selective abiotic routes from β -myrcene towards geraniol have also been described, through regioselective hydroxylation of Pd(II) [Takahashi et al. 1979] and cobalt [Howell et al. 1990] complexes (fig. 15).

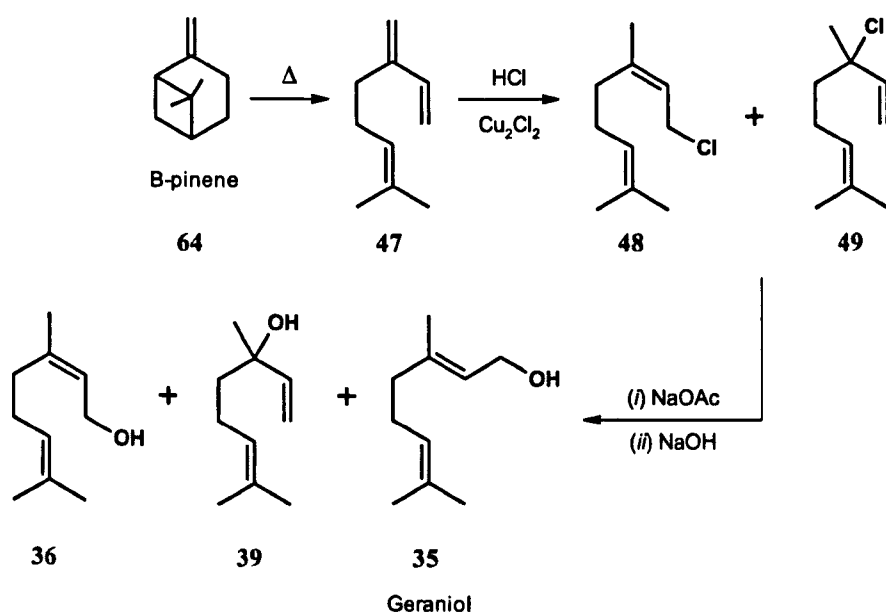


Figure 14: Industrial synthesis of geraniol 35 from β -pinene 64.

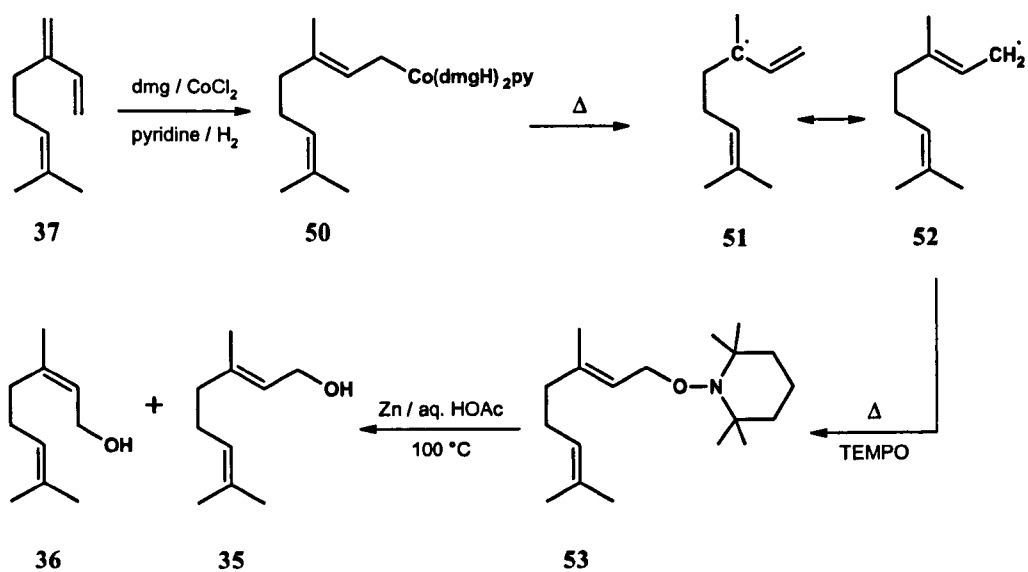


Figure 15: Chemical synthesis of geraniol **35** and nerol **36** from β -myrcene **47** through regioselective hydroxylation of a cobalt complex, *via* trapping at the radical centre with tetramethylpiperidine oxide (TEMPO), and subsequent reduction with zinc [Howell 1990].

Nerol, along with geraniol and citronellol, are often known together as the rose alcohols due to their ubiquitous presence in the essential oils of plants from this species. Nerol is less commonly found than geraniol, and *Palmarosa* sp. constitutes an important natural source of this monoterpene alcohol. The aldehyde derivatives geranial and neral are usually termed citral together, and are interconverted through the enol form (fig. 16). In this form the double bond which previously existed in the aldehyde structures becomes a rotatable single bond and thus after protonation / hydration can yield either isomer of citral. This sequence is unable to proceed from the alcohols geraniol and nerol, and thus their ratio in the extracts of essential oils will exist in similar proportion to the plant from which extracted.

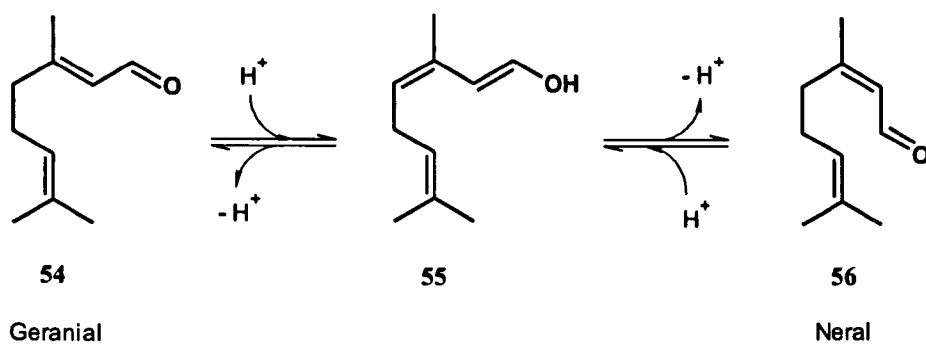


Figure 16: Inter-conversion between the isomers of citral *via* the enol structure.

1.3.3. Menthol

The naturally derived cyclic monoterpene alcohol 1*R*-(-)-menthol has an important role in the flavour and fragrance industries. The biosynthesis and storage of this compound occurs in the glandular trichomes of plants from the *Mentha* species in which it constitutes the main essential oil component. Cultivation of the industrial field crop mint *Mentha arvensis* occurs in many semi-temperate regions. As a product of distilling the essential oils from plants of this species, natural menthol is commonly found as a key ingredient in confectionary and oral hygiene products. Additional uses in cosmetics, pharmaceuticals, cigarettes and pesticides have created a worldwide market value of approximately \$300 million resulting from an annual consumption exceeding 7,000 tons [Patel et al. 2007]. With the production of natural menthol strongly dependent on climatic factors, synthetic routes towards menthol have attracted significant attention. Of the 8 different isomers, it is only L-(1*R*, 2*S*, 5*R*)-menthol which possesses the characteristic minty taste and aroma usually associated with this compound. 1*R*-(-)-menthol has been found to bind to a receptor belonging to the TRP family of excitatory ion channels, enabling it to elicit the cooling sensation that is associated with this compound, and is replicated with exposure to low temperatures [Mckemy et al. 2002, Peier et al. 2002]. 1*R*-(-)-Menthol **63** is derived from a biosynthetic pathway initiated by the cyclisation of the general monoterpene precursor geranyl diphosphate **18** to 4*R*-(+)-limonene **57**. Following a hydroxylation step; a series of four redox reactions creates three chiral centres leading to the formation of (-)-(1*R*, 2*S*, 5*R*)-menthol (fig. 17).

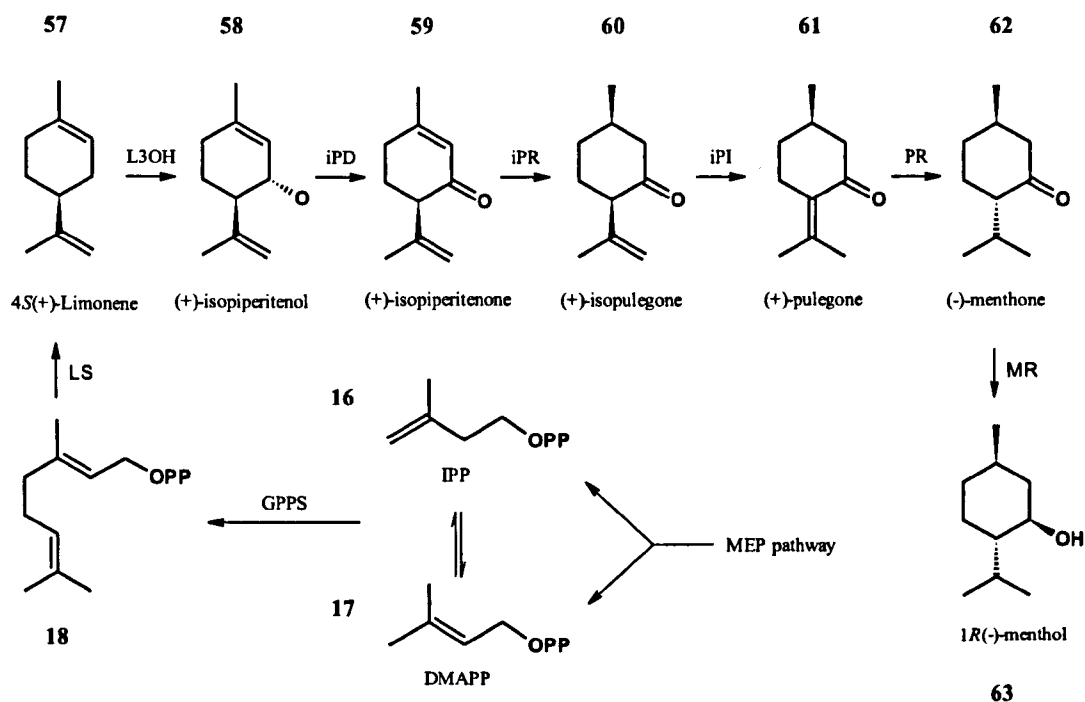


Figure 17: Pathway of menthol biosynthesis in *Mentha* sp. Catalysis occurs through the use of the following enzymes: Geranyl diphosphate synthase (GPPS), limonene synthase (LS), limonene-3-hydroxylase (L3OH), isopiperitenol dehydrogenase (iPD), isopiperitenone reductase (iPR), isopulegone isomerase (iPI), pulegone reductase (PR), menthone reductase (MR) [Croteau et al. 2005].

Industrial production of 1*R*(-)-menthol is performed through asymmetric synthesis from β -pinene **64** or β -myrcene **47** (fig. 18), by the Takasago International Company on a scale of approximately 3000 tonnes per year [Akutagawa et al. 1997, Noyori et al. 2003]. After formation of an allylic amine from β -myrcene, a BINAP rhodium catalyst is used for asymmetric isomerisation yielding enantiomerically pure (*R*)-citronellol after subsequent hydrolysis. Cyclisation *via* a carbonyl-ene reaction catalysed by zinc bromide leads to the formation of isopulegol, which can then be hydrogenated to yield 1*R*, 2*S*, 5*R*-menthol.

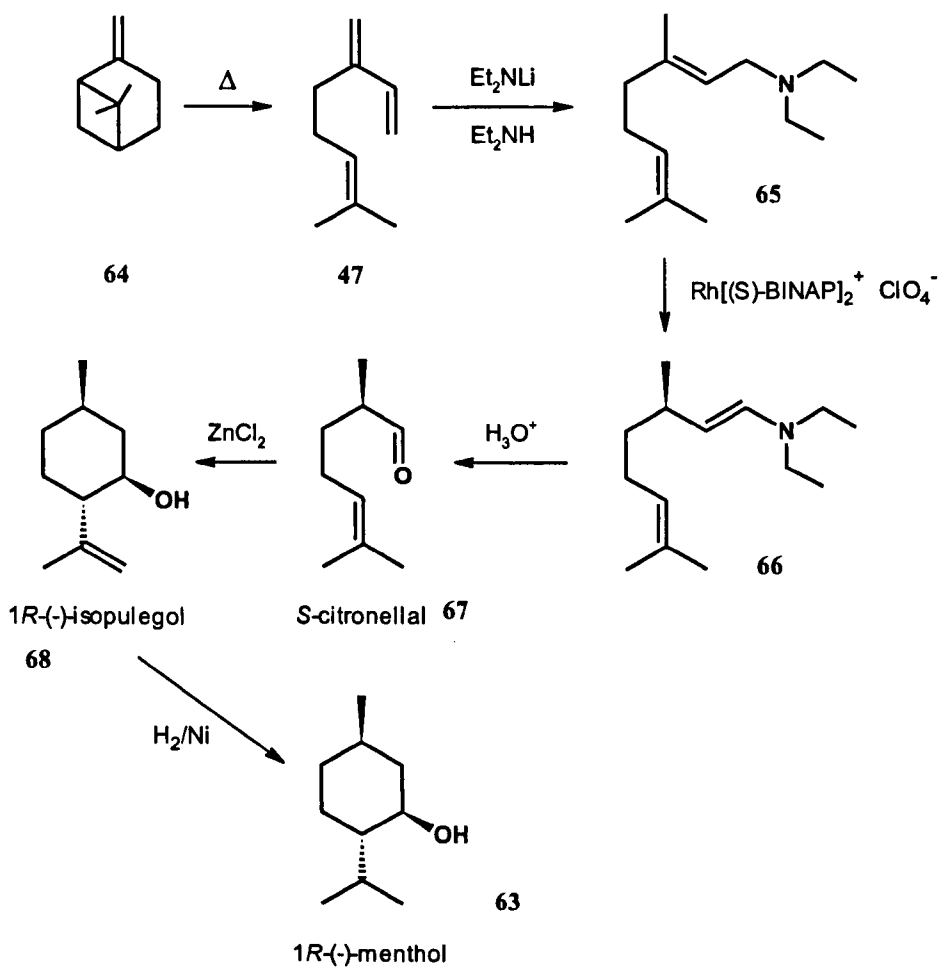


Figure 18: Asymmetric synthesis of menthol [Noyori et al. 2003, Sell 2003].

Whilst this and other asymmetric synthetic routes towards 1*R*-(-)-menthol have been established, the use of biocatalysis confers advantages for high stereo- and regioselectivity without a dependence on expensive catalysts in multi-step inorganic syntheses; namely through the use of hydrolysis or esterification reactions. The use of a stereoselective lipase from *Candida cylindracea* has enabled the resolution of racemic menthol through esterification with acid anhydrides [Wu et al. 1996]. The enantioselective hydrolysis of menthyl acetate

provides an alternative approach towards 1*R*-(-)-menthol. Whole cell lipase activity has been identified in *Burkholderia cepacia* ATCC 25416 [Yu et al. 2007], which after optimisation yielded a high selectivity ($E = 170$) towards this hydrolysis. Subsequent purification of the active enzyme from this species gave a 37 kDa esterase which displayed high enantioselectivity towards the hydrolysis of menthyl acetate (ee_p 97%, $E = 280$, at a conversion of 50% – fig. 19) and a range of other racemic menthyl esters [Yu et al. 2009]. An esterase from *Bacillus stearothermophilus* which was cloned into *E. coli* displayed high enantioselectivity towards the kinetic resolution of menthyl acetate ($E > 100$), but despite sharing a sequence homology >95% with this enzyme, an esterase characterised from *Bacillus subtilis* was found to be inactive with this substrate [Henke et al. 2002].

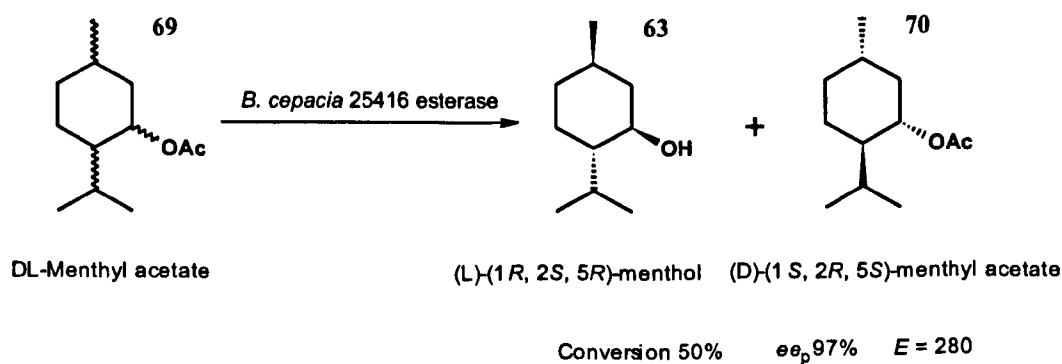


Figure 19: Preparation of 1*R*-(-)-menthol **63** via enantioselective hydrolysis of menthyl acetate **69** [Yu et al. 2007].

1.4. The use of *Rhodococcus* species and Fungi in industrial biocatalysis

1.4.1. Fungi

Fungi are heterotrophic microorganisms which cover great taxonomical diversity, and can be found growing in; soil, dead organic matter, or in symbiosis with other species. A wide variety of environmental degradation processes occur as a result of fungal catalysis, and they are now found increasingly used in industrial reactions which utilise the favourable properties offered by the secreted biodegradative enzymes such as lipases, cellulases, and proteases which facilitate their growth in nature [Wackett et al. 2001]. The ability of many species to carry out novel regio- and enantioselective hydroxylation of a range of polycyclic hydrocarbons has also facilitated their use in the derivatisation of diterpenoids, particularly steroids (fig. 20), and in the synthesis of pharmacological precursors.

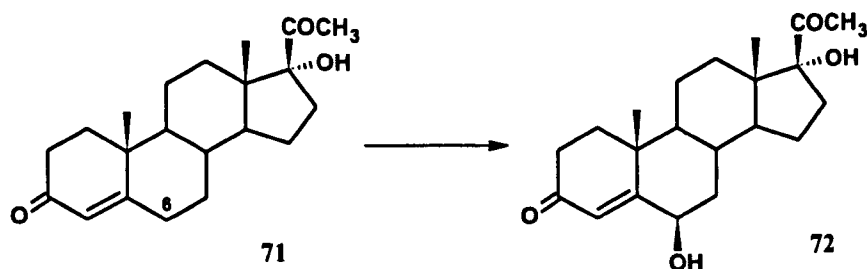


Figure 20: Regio- and enantioselective 6 β -hydroxylation of the steroid 17 α -hydroxyprogesterone by *Botrytis cinerea* [Aleu et al. 2001].

Broadly used in the alcoholic beverages industry, the use of numerous yeast species from the ascomycete phylum has extended towards the biocatalytic

preparation of flavours and fragrances. In particular, *Saccharomyces cerevisiae* is frequently utilised in organic synthesis because it is widely available and a relatively inexpensive option, whilst still offering the potential for high selectivity (fig. 21A). Lipases A and B from *Candida antartica* have also been extensively studied for their biocatalytic capabilities, and are known to exhibit enantioselective properties (fig. 21B) during hydrolysis and esterification reactions [King et al. 2000, Serra et al. 2005, Fukuda et al. 2009].

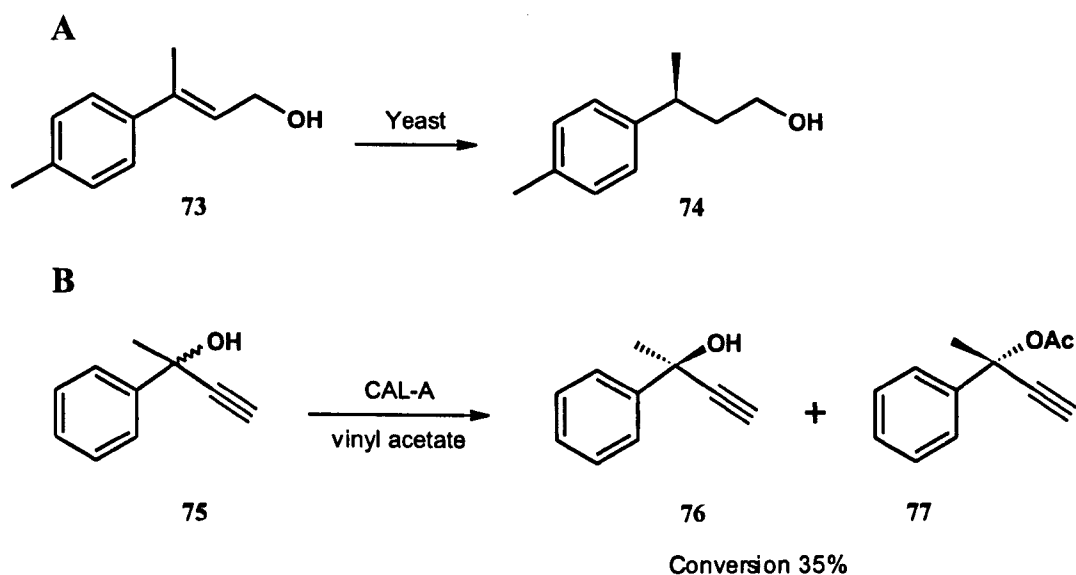


Figure 21: (A) Yeast mediated selective reduction of a pro-chiral double bond, used as an initial step in the synthetic preparation of naturally occurring sesquiterpenes [Serra et al. 2005]. (B) *Candida antartica* lipase A catalysed kinetic resolution of (±)-2-phenylbut-3-yn-2-ol **75** [Kourist et al. 2008].

Certain strains of yeast including: *Ambrosiozyma monospora*, *Torulaspora delbrueckii* and *Kluyveromyces lactis* have proved viable for *de novo* synthesis of terpenoids including geraniol, linalool and citronellol, albeit at low concentrations

[Drawert et al. 1978, Fagan et al. 1981, Klingenburg et al. 1985]. Interesting conversions have been discovered from biotransformations which supplemented these monoterpene alcohols to the yeast growth medium (fig. 22). Catalytic reductions (geraniol **35** to citronellol **34**), translocations (geraniol **35** / nerol **36** to linalool **39**), isomerisations (nerol to geraniol), and cyclisations (nerol / linalool to α -terpineol **78**) resulted in a range of products from a single substrate [King et al. 2000].

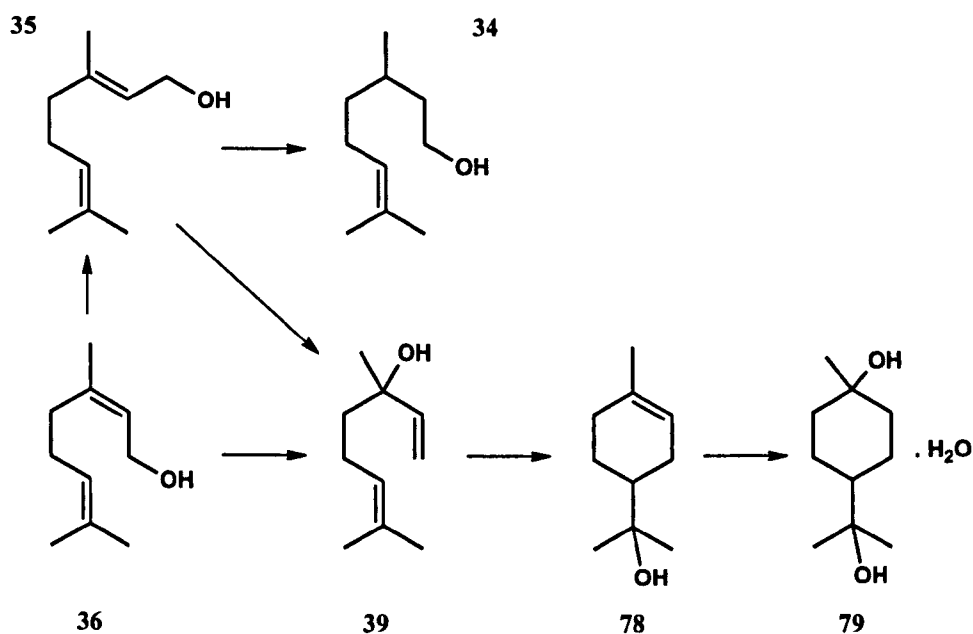


Figure 22: Monoterpene biotransformations catalysed by the yeast: *S. cerevisiae*, *T. delbrueckii* and *K. lactis* [King et al. 2000].

1.4.2. *Rhodococcus* sp.

From the order actinomycetales, *Rhodococci* are non-motile gram-positive bacteria found in a wide variety of environments, including soil and water. The great metabolic capability of *Rhodococci* means that they are of significant biotechnological importance [McLeod et al. 2006, Bell et al. 1998, Van der Geize et al. 2004, Larkin et al. 2005]. The genome of *Rhodococcus* sp. RHA1 was recently published [McLeod et al. 2006], and found to encode a disproportionately large number of oxidoreductases (1085), of which there are 203 oxygenases encoded. They are a heterotrophic species able to degrade a very diverse range of organic compounds including: aliphatic and aromatic hydrocarbons, steroids, and polychlorinated biphenyls. *Rhodococcus erythropolis* has also been shown to assimilate the gaseous hydrocarbon propane [Kulikova et al. 2000, 2001]. It is this diversity of potential substrates which has led to their widespread study and use for bioremediation and biotransformations. One such example is the annual production of over 30,000 tons of acrylamide using an over produced nitrile hydratase from *Rhodococcus rhodochrous*. Another biotechnological application involving this strain is the microbial desulphurisation of fossil fuels, whereby carbon-sulphur bonds are selectively cleaved, as opposed to carbon-carbon bonds which remain intact (fig. 23).

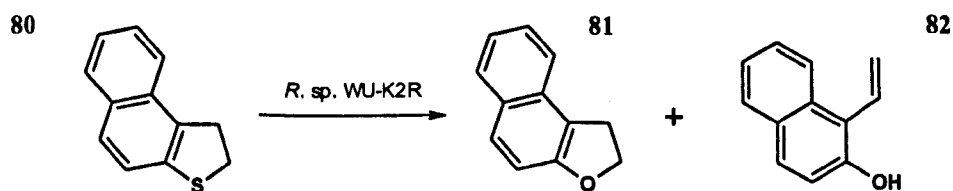


Figure 23: Desulphurisation of naphtho[2-1-*b*]thiophene **80** found in diesel oil to naphtho[2-1-*b*]furan **81** and 2-hydroxynaphthylethene **82** by *Rhodococcus* sp. WU-K2R [Kirimura et al 2002].

1.5. Project outline

The overall aim of the project is to uncover novel biocatalytic routes directed towards the monoterpene alcohols which are of significant interest to the flavour and fragrance industry. Particular emphasis will be placed upon achieving an enantioselective biotransformation in the case of chiral linalool and menthol. A starting material which forms the basis for much of the work, myrcene; is investigated along with geraniol and nerol in chapter 3 as substrates in fungal biotransformations which in literature have yielded a wide diversity of products. The use of these fungal biocatalysts may offer a potential route for the selective oxidation of myrcene to linalool. An alternative approach towards linalool is considered in chapter 4 through attempts at screening and purification of an enantioselective esterase from *Rhodococcus* sp. which shows activity towards linalyl acetate. Following on from these efforts, chapter 5 presents a gene based approach towards an enantioselective esterase, and further investigates the substrate specificity and selectivity with regards to biotransformations generating monoterpene alcohols. The attempts to yield a novel and potentially desirable conversion of myrcene are further studied in chapter 6 which describes the enrichment and characterisation of a bacterial strain competent for growth on this abundant hydrocarbon, and subsequent biotransformation. Chapter 7 comprises a sub-cellular study of the enriched strain with a view to understanding mechanistic details about the biotransformation of myrcene. A summary of the approaches taken in this project are shown in figure 25.

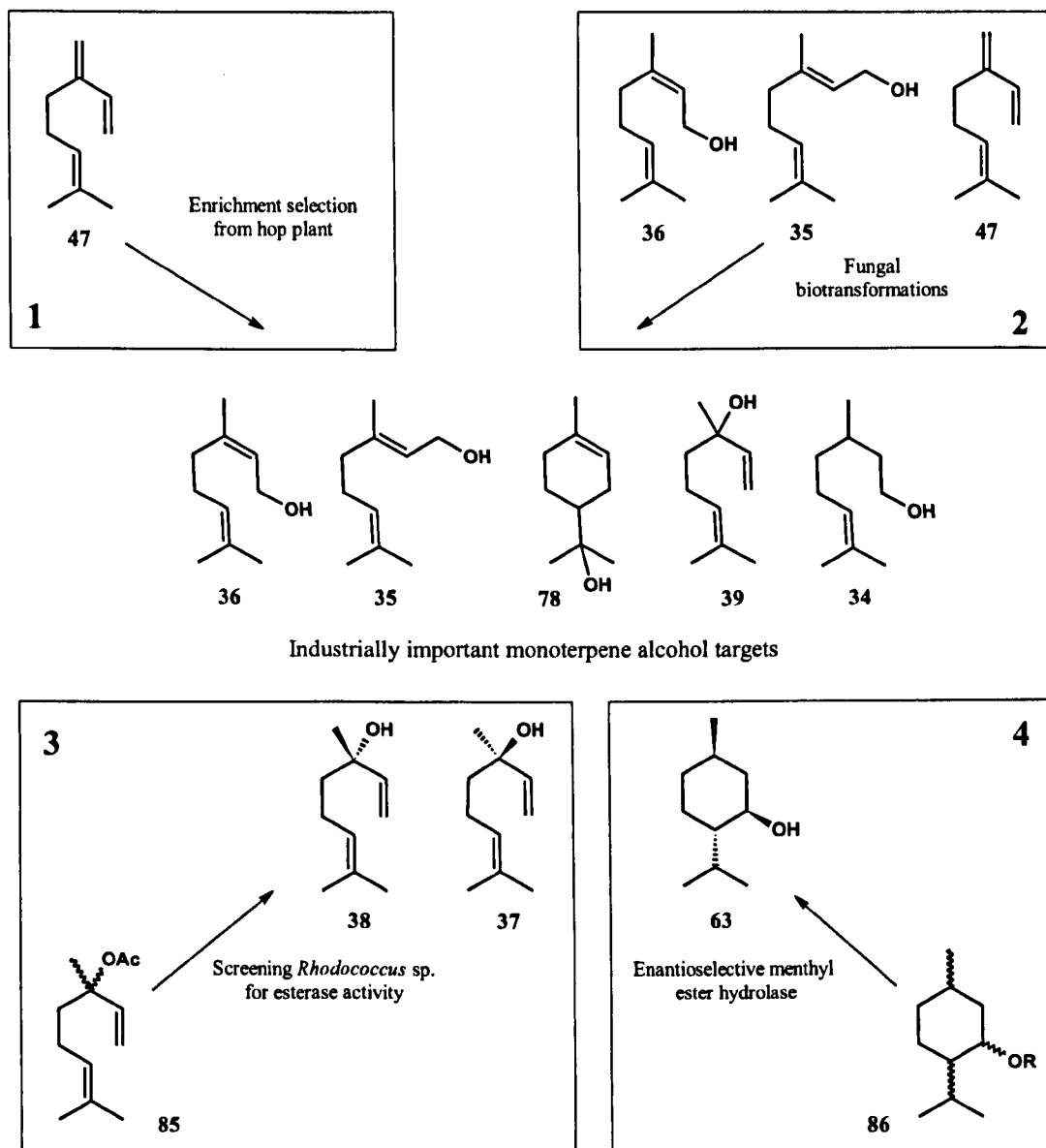


Figure 25: Biocatalytic routes towards the monoterpene alcohols of industrial interest for this project. (1) A selective enrichment strategy to identify a microorganism competent for the growth on and metabolism of β -myrcene. (2) Analysis of fungal biocatalysts towards conversions of nerol, geraniol, and myrcene. (3) A screening and protein purification approach towards a potential enantioselective linalyl acetate **85** esterase. (4) Further study of esterase activity with regard to enantioselective hydrolysis of racemic menthyl esters **86**, directed towards production of 1*R*-(-)-menthol.

2. Chapter 2: General materials and methods

2.1. General materials, chemicals, bacterial and fungal strains

Chemicals purchased for use in this project were of the highest purity available. Authentic single enantiomer GC standards for menthol ($\geq 99\%$), lavandulol (98.5%), linalool (97%), and their corresponding acetates were obtained from Fluka. α -Terpineol ($\geq 97\%$), citronellol (95%), and the corresponding acetates were purchased from Sigma Aldrich. Geraniol ($\geq 96\%$) and nerol ($\geq 90\%$) were purchased from Fluka. An authentic standard of citral was supplied by Botanix Ltd. Naphthyl acetate ($\geq 99\%$) was acquired from Fluka, whilst tributyrin (97%) and *tert*-butyl acetate ($\geq 99\%$) were supplied by Sigma Aldrich. The solvents ethyl acetate and petroleum ether were of analytical reagent grade and were purchased from Fisher Scientific. The cytochrome P450 inhibitors aminobenzotriazole and metyrapone were purchased from Sigma Aldrich.

For molecular biology experiments *Escherichia coli* NovaBlue singles cells, and BL21 (DE3) cells were obtained from Novagen. PCR primers were ordered from MWG-Eurofins (Germany). KOD hot start DNA polymerase was obtained from Novagen. The pET-YSBLIC3C vector was obtained from the Structural Biology Laboratory (University of York). Restriction enzymes *BseRI*, *DpnI*, *NcoI*, and *NdeI*

Chapter 2: General materials and methods

were purchased from New England Bio Labs. PCR clean-up and mini-prep kits were purchased from Qiagen, and a gel extraction kit from Sigma Aldrich. Isopropyl β -D-1-thiogalactopyranoside (IPTG) was purchased from Melford Labs.

The following fungal cultures were purchased: *Mucor piriformis* CBS 256.85 (CBS – Netherlands), *Ganoderma lipsiense* CBS 250.61 (CBS), *Aspergillus niger* DSM 821 (DSM – Germany), and *Botrytis cinerea* DSM 877 (DSM).

A total of 24 strains of *Rhodococcus* was acquired from collections within the University laboratory (Prof. Neil Bruce) and were as follows: *Rhodococcus rhodochromis* 11Y, *Rhodococcus* sp. 11211, *Rhodococcus* sp. DN22, *Rhodococcus* sp. CW25, *Rhodococcus aetherivorans* AM1, and *Rhodococcus* HS 1–19 inclusive. Another strain *Rhodococcus ruber* DSM 43338 was acquired from the DSM collection.

2.2. SDS-PAGE analysis of proteins

Cell extract samples were diluted 1:1 in a loading buffer (50 mM Tris / HCl, pH 6.8), containing: glycerol 10%, SDS 2%, bromophenol blue 0.005%, and β -mercaptoethanol 5%. Resolving gels (12% acrylamide) were set by adding tetramethylethylenediamine (TEMED) to a resolving gel buffer (1.5 M Tris, 0.4% SDS, pH 8.8) containing acrylamide and ammonium persulphate (APS). Stacking gels were poured from a 0.5 M Tris buffer (0.4% SDS, pH 6.8) containing acrylamide, APS, and TEMED. A BioRad low molecular mass marker mixture was used that contained phosphorylase B 97.4 kDa, serum albumin 66.2 kDa, ovalbumin 45 kDa, carbonic anhydrase 31 kDa, Soybean trypsin inhibitor 21.5 kDa, lysozyme 14.4 kDa. Gels were stained with Coomassie Blue dye, and de-stained using a 6:3:1 mixture of water : propan-2-ol : glacial acetic acid.

2.3. Molecular biology techniques

2.3.1 Ligation independent cloning (LIC)

A general overview of the ligation independent cloning process is shown in figure 26 below, with a plasmid map for the pET-YSBLIC vector shown in the appendix. A description of the methods involved at each stage of the process follows.

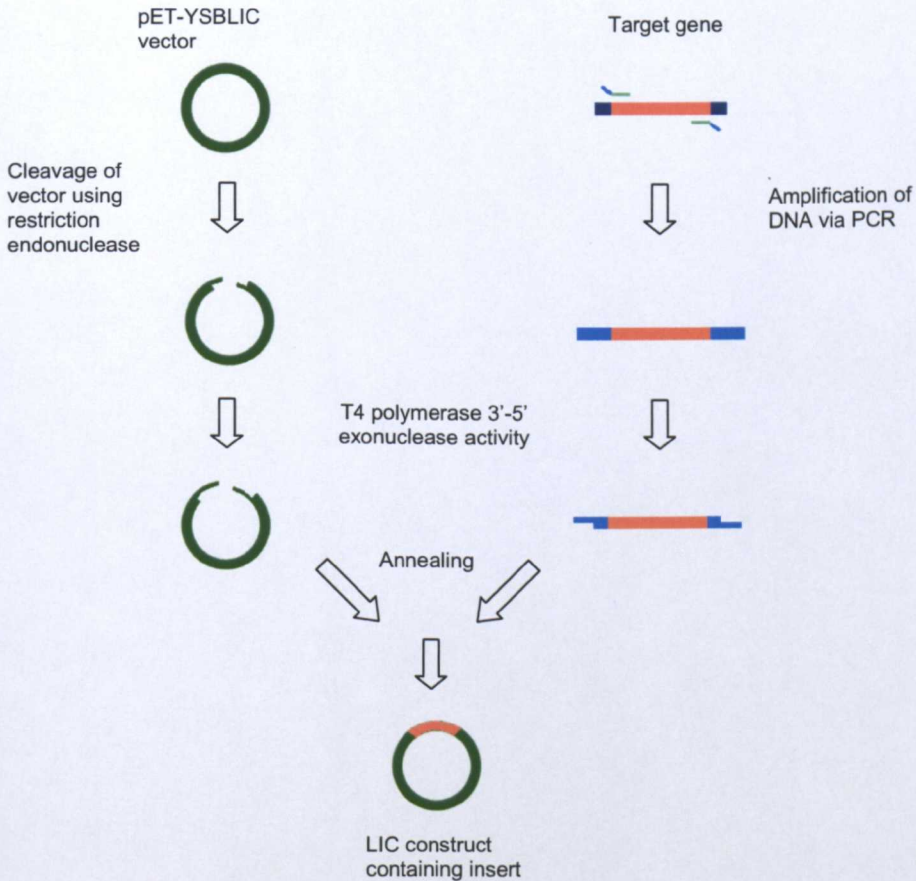


Figure 26: An overview of the ligation independent cloning (LIC) process. Figure adapted from Bonsor et al. 2006.

2.3.1.1. Preparation of LIC vector using PCR method

PCR primers:

5'-TTGCTGGTCCCTGGAACAGAACTTCC-3'

5'-CGCGCCTTCTCCTCACATATGGCTAGC-3'

1 µg of the cleavable His-tagged pET-YSBLIC vector was transformed into competent DH5α cells and plated onto Luria Bertani (LB) agar + kanamycin (30 µg/mL) and incubated at 37°C o/n. A single colony was picked to inoculate a 20 mL culture of LB + kanamycin (30 µg/mL) and incubated at 37°C o/n. The cells were harvested before a mini-prep was carried out to extract the vector DNA (20 µg) which was used as the template for PCR. Each 50 µL PCR volume contained: 0.4 µM of forward and reverse primers (ordered from MWG), 0.2 mM dNTPs, 1 µL KOD hot start DNA polymerase (1 unit/µL), 1 mM MgSO₄, 5 µL 10x buffer, 50 ng template DNA, 5% v/v DMSO, and water to 50 µL. Thermocycling conditions were as follows: initial denature 3 min at 94°C, followed by 35 cycles of: denature 30 s at 94°C, annealing 30 s at 60°C, and extension 2 min at 72°C, with a final extension step 3 min at 72°C. *DpnI* was added to the DNA and incubated at 37°C for 2 h to digest the methylated DNA. The reaction mixture was run on a preparative agarose gel and the bands corresponding to linear vector DNA were cut from the gel and extracted (7.5 µg).

2.3.1.2. Preparation of LIC vector using *BseRI* method

1 μL LIC vector transformed into competent NovaBlue cells, plated out onto LA + kanamycin (30 $\mu\text{g}/\text{mL}$) agar, and incubated at 37°C o/n. A single colony was picked to inoculate 2x 50 mL LB + kanamycin (30 $\mu\text{g}/\text{mL}$) and incubated at 37°C o/n. All 100 mL culture was harvested before a mini-prep was carried out to extract the vector DNA. A restriction digest: 66 μL vector DNA (7.9 μg), 8 μL *BseRI*, 16 μL 10x buffer (NEB2), and 70 μL water was incubated at 37°C for 1 h 50 min. The sample was run on a preparative agarose gel. The bands were cut out and purified to give linear LIC vector DNA which was concentrated to 20 ng/ μL .

2.3.1.3. Vector LIC T4pol reaction

A mixture comprising of the following: 3.75 μg linearised vector DNA, 15 μL T4pol buffer (10x), 15 μL dTTP (25 mM stock), 7.5 μL DTT (100 mM stock), 3 μL T4 polymerase (2.5 U/ μL LIC qualified – Novagen), and H₂O to 150 μL , was incubated at 22°C for 30 min, and then at 75°C for 20 min.

2.3.1.4. Insert LIC T4pol reaction

A mixture comprising of the following: 0.2 pmol PCR product (insert), 2 μL T4pol buffer (10x), 2 μL dATP (25 mM stock), 1 μL DTT (100 mM stock), 0.4 μL T4

polymerase (2.5 U/ μ L LIC qualified – Novagen), and H₂O to 20 μ L, was incubated at 22°C for 30 min, and then at 75°C for 20 min.

2.3.1.5. LIC annealing reaction

1.5 μ L of T4 treated vector (50 ng/ μ L) was added to 2.5 μ L of the insert T4 reaction, and incubated at r/t for 10 min, before the addition of 1.5 μ L EDTA (25 mM stock) and incubation for a further 10 min at r/t. A negative control using water instead of the insert was also set up.

2.3.1.6. Transformation of competent *E. coli* cells

5.5 μ L of the LIC annealing reaction was added to 25 μ L of competent *E. coli* NovaBlue singles cells, and then incubated on ice for 5 min. The cells were heat-shocked at 42°C for 30 s, and then incubated on ice for a further 5 min. 0.5 mL of LB medium was added and the cells incubated at 37°C for 2.5 h. The cells were harvested (12,000 \times g, 3 min, 4°C) and 400 μ L of the supernatant removed, before re-suspension of the remaining 100 μ L which was plated out onto LB agar + kanamycin (30 μ g/mL) and incubated o/n at 37°C.

2.3.1.7. *NdeI* / *NcoI* restriction digest

Colonies from the transformation of NovaBlue cells were picked to inoculate 5 mL cultures of LB + kanamycin (30 µg/mL) and incubated o/n at 37°C before carrying out a mini-prep. Extracted DNA was then digested: 1 µg DNA, 1 µL NE buffer 2 (10x), 1 µL *NcoI*, 1 µL *NdeI*, water to 10 µL, and incubated at 37°C for 3 h. The mixture was then run on an agarose gel.

2.3.2. DNA Sequencing

Sanger sequencing of cloned genes and PCR products was carried out by the Technology Facility (University of York).

2.3.3. Purification of plasmid DNA using mini-prep kit (Qiagen)

A single colony was picked from an antibiotic selective plate and used to inoculate a 5 mL o/n culture. The 5 mL culture was harvested using a microcentrifuge and the cell pellet resuspended in 250 µL of P1 (resuspension buffer). 250 µL of P2 (lysis buffer) was added to the suspension and mixed thoroughly before the addition of 350 µL N3 (neutralisation buffer). The solution was centrifuged for 10 min at 12,000 × g,

and the supernatant applied to a QIAprep spin column. Following centrifugation for 1 min at 12,000 x g, the spin column was washed with 0.5 mL PB (binding buffer) and 0.75 mL PE (wash buffer), before eluting the DNA with 100 µL water.

2.3.4. Preparation of genomic DNA using DNeasy kit (Qiagen)

Rhodococcus ruber DSM 43338, *R. aetherivorans* AM1, *R. sp* 11Y, and *R. HS2* cells were harvested in microcentrifuge tubes for 10 min at 10,000 x g. The cell pellets were resuspended in 180 µL of enzymatic lysis buffer and incubated at 37°C for 30 min. 25 µL of proteinase K and 200 µL of buffer AL (-EtOH) were added and then incubated at 56°C for a further 30 min. 200 µL of EtOH was then added and the sample mixed by vortexing, before adding to a DNeasy mini spin-column and centrifuged for 1 min (10,000 x g). The supernatant was discarded and 500 µL of buffer AW1 added before centrifugation (10,000 x g, 1 min, 4°C). The supernatant was discarded and 500 µL buffer AW2 added to the column then centrifuged again (14,000 x g, 3 min, 4°C). The DNeasy spin column was placed in a clean microcentrifuge tube and 200 µL buffer AE added onto the DNeasy membrane then incubated at r/t for 1 min before centrifuging for 1 min (10,000 x g) to elute. DNA concentration was calculated from measuring the absorbance at 260 nm.

2.3.5. Agarose gel analysis of DNA

0.48 g of agarose was heated in a 60 mL solution of Tris-acetate buffer pH 8.0 containing EDTA using a microwave until dissolved. Upon cooling 2 μ L of the DNA stain Sybr safe® was added, and the gel set. 8 μ L samples were mixed with 2 μ L of loading buffer (New England Biolabs) prior to loading onto the gel in addition to a DNA ladder (New England Biolabs), before running at 100 V and 400 mA for 1 h.

2.3.6. Extraction of DNA from agarose gels

DNA bands were cut from agarose gels with a scalpel and using a gel extraction kit (Sigma), dissolved in a gel solubilisation solution (300 μ L solution / 100 mg gel) at 55°C for 10 min before precipitating the DNA with isopropanol (100 μ L / 100 mg gel). The DNA binding column was prepared by adding 0.5 mL of preparation solution and centrifuging (10,000 \times g, 1 min, 4°C) before binding the DNA and further centrifugation for 1 min. The column was washed, and the DNA eluted in 100 μ L of distilled water before determining the concentration using a spectrophotometer.

2.3.7. Preparation of competent cells

Autoclaved LB medium (5 mL) was inoculated with *E. coli* cells grown on LB agar + antibiotic, and incubated at 37°C o/n. LB medium (20 mL) was inoculated with 200 µL of this starter culture, and the cells grown at 37°C to $A_{600} = 0.3-0.5$. The cells were harvested (5,000 × g, 15 min, 4°C), the supernatant removed, and the cells resuspended in 20 mL of chilled CaCl₂ (0.1 M). The mixture was incubated on ice for 10 min, and the cells harvested again. The supernatant was removed and the cells resuspended in 2 mL of chilled CaCl₂ (0.1 M) containing 10% (w/v) glycerol. The suspension was divided into 100 µL aliquots and frozen in liquid nitrogen immediately. Competent cells were stored at -80°C until use.

2.3.8. Expression of cloned genes in *E. coli*

1 µL of the LIC construct containing the insert was added to 50 µL of competent *E. coli* cells (BL21, B834, BL21-Ros, or Ros-PlysS), and then incubated on ice for 5 min. The cells were heat-shocked at 42°C for 30 s, and then incubated on ice for a further 5 min. 0.5 mL GS96 or LB medium was added and the cells incubated at 37°C for 1.5 h. The cells were harvested (12,000 × g, 3 min, 4°C) and 400 µL of the supernatant removed, before re-suspension of the remaining 100 µL which was plated out onto LB agar + kanamycin (30 µg/mL) (also + chloramphenicol 30 µg/mL when

using BL21-Ros, or Ros-PlysS cells), and incubated o/n at 37°C. Expression tests were carried out by picking colonies from these plates to inoculate 5 mL o/n cultures of LB + kanamycin (+ chloramphenicol). Cultures were incubated initially at 37°C until reaching an optical density $A_{600} = 0.5$ at which point they were induced with isopropyl β -D-1-thiogalactopyranoside (IPTG) (0.1 mM). Cultures were then incubated o/n at a range of temperatures between 18-37°C.

2.3.9. Auto-induction of protein expression

Stock solutions were prepared for the following: 20x NPS solution (90 mL water, 6.6 g $(\text{NH}_4)_2\text{SO}_4$, 13.6 g KH_2PO_4 , 14.2 g Na_2HPO_4 , pH 6.75 at 20-fold dilution in water); 1x ZY solution (10 g/L tryptone, 5 g/L yeast extract); 1000x metals solution (36 mL water, 50 mL 0.1 M $\text{FeCl}_2 \cdot 6\text{H}_2\text{O}$ in 0.1 M HCl, 2 mL 1 M CaCl_2 , 1 mL 1 M $\text{ZnSO}_4 \cdot 7\text{H}_2\text{O}$, 1 mL 0.2 M $\text{CoCl}_2 \cdot 6\text{H}_2\text{O}$, 2 mL 0.2 M $\text{CuCl}_2 \cdot 2\text{H}_2\text{O}$, 1 mL $\text{NiCl}_2 \cdot 6\text{H}_2\text{O}$, 2 mL 0.1 M $\text{Na}_2\text{MoO}_4 \cdot 5\text{H}_2\text{O}$, 2 mL 0.1 M $\text{Na}_2\text{SeO}_3 \cdot 5\text{H}_2\text{O}$, 2 mL H_3BO_3).

A single colony was picked and incubated in 10 mL LB + antibiotic (30 $\mu\text{g}/\text{mL}$) for 6-8 h at 37°C, before inoculating 500 mL of auto-induction media + antibiotic (30 $\mu\text{g}/\text{mL}$), and incubating at 30°C o/n.

2.3.10. Buffer screen for solubilisation of over-expressed protein

A screen of 30 re-suspension buffers listed below were tested to improve the solubility of proteins over-expressed in *E. Coli* [Lindwall et al. 2000].

1. 100 mM Tris, 10% glycerol, pH 7.6
2. 100 mM Tris, 50 mM LiCl, pH 7.6
3. 100 mM HEPES, 50 mM $(\text{NH}_4)_2\text{SO}_4$, 10% glycerol, pH 7.0
4. 100 mM HEPES, 100 mM KCl, pH 7.0
5. 100 mM Tris, 50 mM NaCl, 10% isopropanol, pH 8.2
6. 100 mM $\text{K}_2\text{HPO}_4/\text{KH}_2\text{PO}_4$, 50 mM $(\text{NH}_4)_2\text{SO}_4$, 1% Triton X-100, pH 6.0
7. 100 mM triethanolamine, 100 mM KCl, 10 mM DTT, pH 8.5
8. 100 mM Tris, 100 mM sodium glutamate, 10 mM DTT, pH 8.2
9. 250 mM $\text{KH}_2\text{PO}_4/\text{K}_2\text{HPO}_4$, 0.1% CHAPS, pH 6.0
10. 100 mM triethanolamine, 50 mM LiCl, 5 mM EDTA, pH 8.5
11. 100 mM sodium acetate, 100 mM glutamine, 10 mM DTT, pH 5.5
12. 100 mM sodium acetate, 100 mM KCl, 0.1% *n*-octyl- β -D-glucoside, pH 5.5
13. 100 mM HEPES, 1 M MgSO_4 , pH 7.0
14. 100 mM HEPES, 50 mM LiCl, 0.1% CHAPS, pH 7.0
15. 100 mM $\text{KH}_2\text{PO}_4/\text{K}_2\text{HPO}_4$, 2.5 mM ZnCl_2 , pH 4.3
16. 100 mM Tris, 50 mM NaCl, 5 mM calcium acetate, pH 7.6
17. 100 mM triethanolamine, 50 mM $(\text{NH}_4)_2\text{SO}_4$, 10 mM MgSO_4 , pH 8.5
18. 100 mM Tris, 100 mM KCl, 2 mM EDTA, 1% Triton X-100, pH 8.2
19. 100 mM sodium acetate, 1M MgSO_4 , pH 5.5
20. 100 mM Tris, 2 M NaCl, 0.1% *n*-octyl- β -D-glucoside, pH 7.6
21. 100 mM Tris, 1 M $(\text{NH}_4)_2\text{SO}_4$, 10 mM DTT, pH 8.2
22. 100 mM sodium acetate, 50 mM LiCl, 5 mM calcium acetate, pH 5.5
23. 100 mM HEPES, 100 mM sodium glutamate, 5 mM DTT, pH 7.0
24. 100 mM triethanolamine, 100 mM sodium glutamate, 0.02% *n*-octyl- β -D-glucoside, 10% glycerol, pH 8.5
25. 100 mM Tris, 50 mM NaCl, 100 mM urea, pH 8.2
26. 100 mM triethanolamine, 100 mM KCl, 0.05% dextran sulfate, pH 8.5
27. 100 mM $\text{KH}_2\text{PO}_4/\text{K}_2\text{HPO}_4$, 50 mM $(\text{NH}_4)_2\text{SO}_4$, 0.05% dextran sulfate, pH 6.0
28. 100 mM HEPES, 50 mM LiCl, 0.1% deoxycholate, pH 7.0
29. 100 mM Tris, 100 mM KCl, 0.1% deoxycholate, 25% glycerol, pH 7.6
30. 100 mM potassium acetate, 50 mM NaCl, 0.05% dextran sulfate, 0.1% CHAPS, pH 5.5

3. Chapter 3: Investigation into the fungal biotransformations of myrcene, geraniol, and nerol

3.1. Introduction

Fungal biocatalytic systems have been widely studied for many biotransformations of terpenoids, and find purpose for the introduction of functionality to molecules that through synthetic methods would prove far more complicated. One such example is the fungal hydroxylation of the diterpenoid isosteriol using *Aspergillus niger* (fig. 27), which has been targeted as a way of influencing the binding of this bioactive compound to its corresponding receptor [de Oliveira et al. 1999]. The potential for regio- and stereo- selectivity that can be achieved through the use of fungal biocatalysts means that the systems to be investigated in this chapter of work represent a prospective enantioselective route towards the monoterpene alcohols.

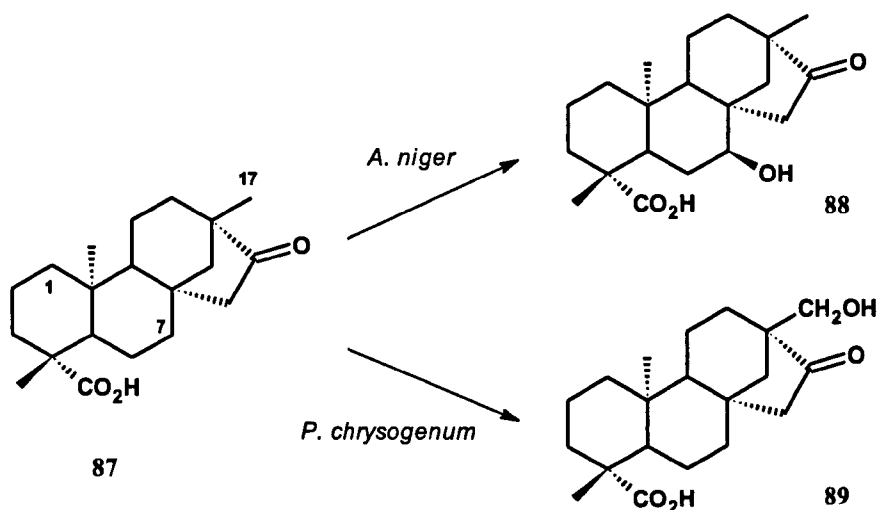


Figure 27: Regio- and enantioselective hydroxylation of the diterpenoid isosteriol 87 by *A. niger* and *Penicillium chrysogenum* [de Oliveira et al. 1999].

Literature examples show myrcene to have been used as a substrate in a number of fungal biotransformations. With the use of *A. niger*, different diols have been produced from myrcene at positions across each of the three double bonds (fig. 28).

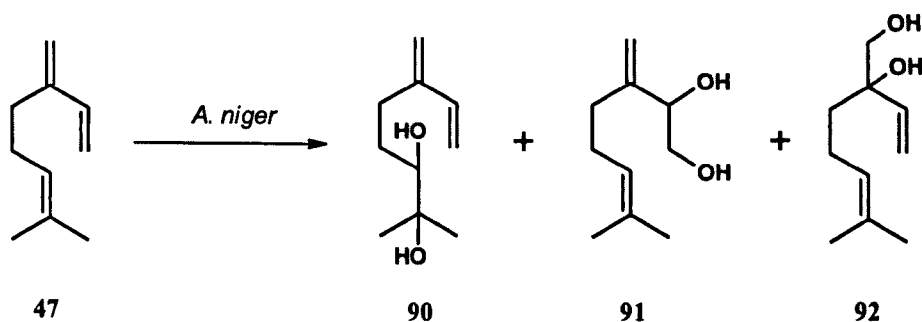


Figure 28: Biotransformation products of β -myrcene 47 with *A. niger* [Yamazaki et al. 1988]. Products: myrcene-6,7-glycol 90, myrcene-1,2-glycol 91, and myrcene-3(10)-glycol 92.

Other strains of fungi have been screened for the biotransformation of myrcene [Busmann et al. 1994]. Shown in figure 29 are three examples from the numerous acyclic and monocyclic products found in these screens. Many of these individual monoterpenes have characteristic desirable organoleptic properties.

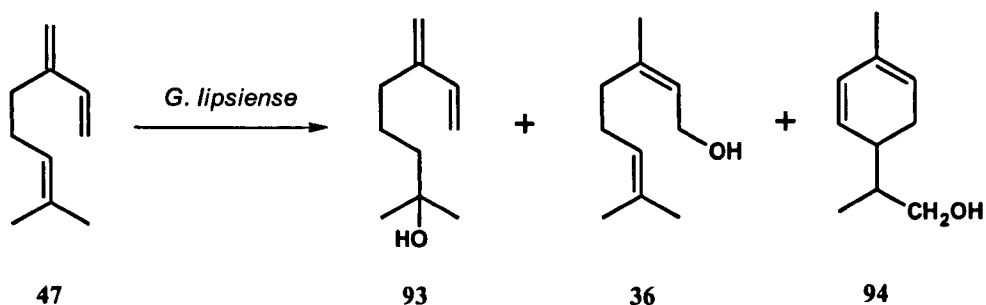


Figure 29: Biotransformation products of myrcene 47 with *G. lipsiense* [Busmann et al. 1994]. Products: myrcenol 93, nerol 36, and *p*-mentha-1,5-diene-8-ol 94.

Aspergillus niger, *Botrytis cinerea*, *Ganoderma lipsiense*, and *Mucor piriformis* have all been cited in literature sources [Farooq et al. 2004, Bock et al. 1988, Busmann et al. 1994, Yamazaki et al. 1988, de Carvalho et al. 2006, Demyttenaere et al. 2001] for a range of biotransformations involving the monoterpene alcohols geraniol and nerol as substrates whereby a great diversity of biotransformation products can be obtained (fig. 30). These substrates, in addition to myrcene, will form the basis of study for this chapter of work.

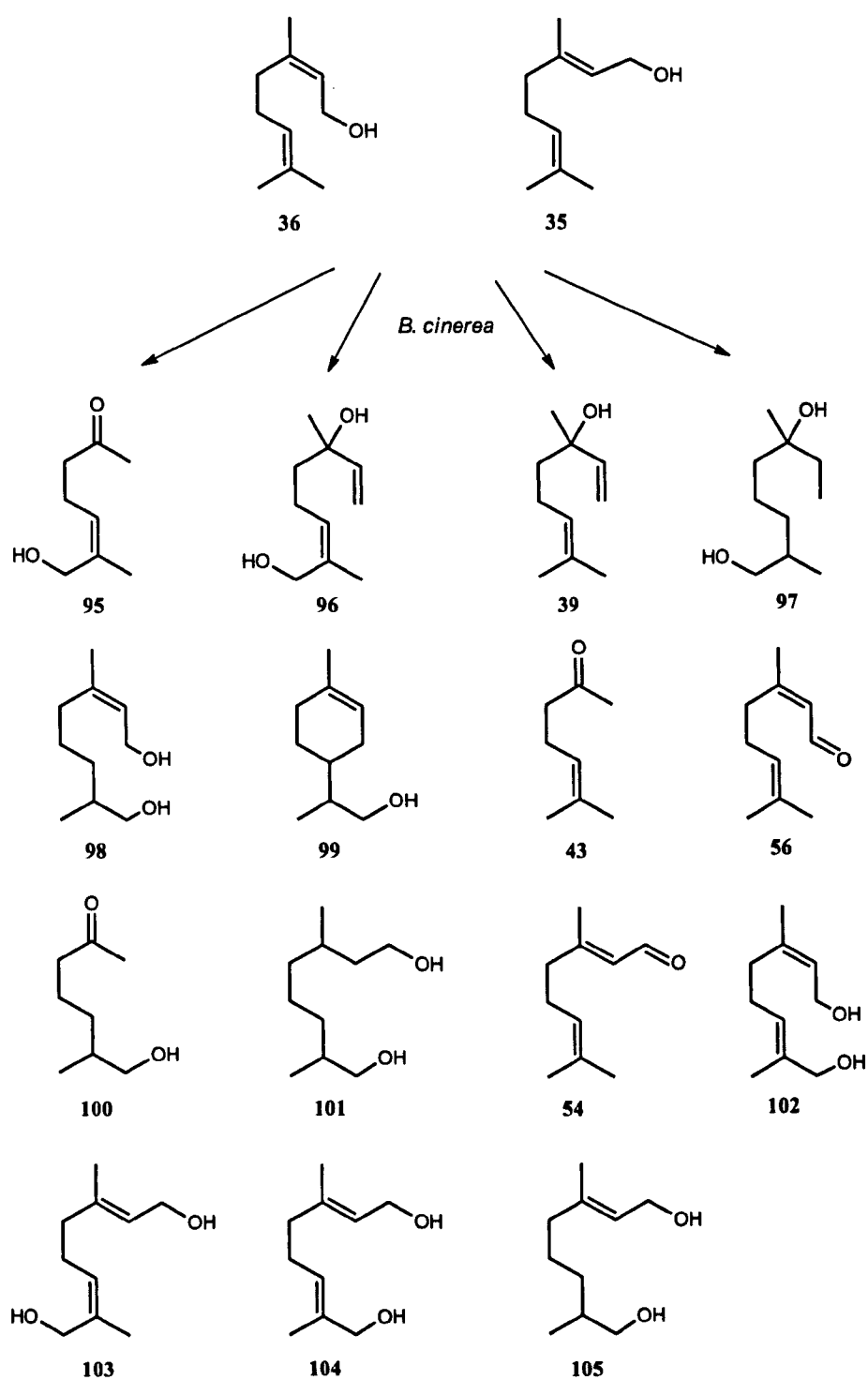


Figure 30: Diversity of biotransformation products of geraniol 35 and nerol 36 using *Botrytis cinerea* [Farooq et al. 2004, Bock et al. 1988].

3.2. Experimental

3.2.1. Fungal biotransformations

Fungal cultures for biotransformations were maintained on potato dextrose agar plates (potato starch 4 g/L, dextrose 20 g/L, and agar 15 g/L). For long term storage at -80°C and provision of future inocula, 30% glycerol stocks were made from liquid cultures inoculated with the initial freeze-dried isolates obtained from culture collections. Sections of agar (approx. 10 mm²) containing fungal growth were cut and homogenised under sterile conditions with 2 mL of deionised water using an autoclaved pestle and mortar. The homogenised cells were added to a medium of corn steep solids (7.5 g/L) and glucose (20 g/L) at pH 4.85, and incubated at 25°C for 48 h. For resting cell assays, cells were harvested before washing and re-suspending in 50 mM phosphate buffer pH 7.0. Growing cell assays were performed with direct addition of the substrate after a growth period of 48 h. Substrates were added at a concentration of 0.5 g/L with the detergent Tween 20 v/v (3:1) in both types of assay. During the incubation period, 0.5 mL aliquots were withdrawn after: 0, 2, 5, 24, 48, 72 h, for extraction and analysis by GC. Due to restrictions on the use of an electronic pH probe with biohazard material, graded pH paper covering set ranges (lower limit pH 1.8) was used for monitoring the pH of inoculated fungal solutions.

3.2.2. Use of acetone as a co-substrate in resting cell biotransformations

A. niger was grown in 2 x 50 mL liquid cultures as before. These were combined, washed, filtered and weighed. Four equal masses of fungi (2.1 g wet weight) were split, and re-suspended into the four 25 mL solutions shown in the table below.

% v/v acetone	Phosphate buffer (mL)	Acetone (mL)
0	25	0
5	23.75	1.25
10	22.5	2.5
20	20	5

Geraniol was added as the primary substrate. The assay was stopped after 21 h and the solution extracted and concentrated prior to GC analysis.

3.2.3. Extraction and concentration of solutions for GC analysis

The assays were stopped by filtering off the fungal biomass. The filtrate was retained and NaCl added to the solution, which was then extracted with 3 x 30-40 mL of CH₂Cl₂. The organic layers were recombined, and dry MgSO₄ added to remove excess water. The MgSO₄ was filtered off, and the solution concentrated by rotary evaporation to leave an oily residue. The oil was re-dissolved in 1 mL of CH₂Cl₂ and transferred to a GC vial. A silica plug was also used in the preparation of samples for chiral GC to ensure that all the water was removed.

3.2.4. GC-MS analysis of fungal biotransformations

Gas chromatographic analysis of samples was performed routinely using an Agilent 6890N gas chromatograph equipped with a J&W HP5 column (length 30 m, internal diameter 0.32 mm, film 0.25 μm). 2 μL samples were injected at 250°C in the split mode. An initial oven temperature of 60°C was increased through a 10°C/min gradient to 200°C, and held at this temperature for 5 min. Total run time was 19 min. Using this gradient, retention times (min) were as follows: linalool (5.4), α -terpineol (6.7), nerol (7.25), neral (7.4), geraniol (7.6), geranial (7.8). GC-MS analysis was performed at Botanix Limited with a Clarus 500 gas chromatograph (Perkin-Elmer) equipped with a J&W DB-1 column (30 m x 0.32 mm x 1 μm), coupled with a Clarus 500 mass spectrometer. 1 μL samples were injected at 250°C in the split mode. An initial oven temperature of 60°C was held for 1.5 min before increasing at 4°C/min to 280°C with a further hold at this temperature for 15 min. The carrier gas helium was provided at a flow rate of 1.5 mL/min. The instrument was run in electrical ionisation (EI) mode at an energy of 70 eV. Mass spectra were scanned in the range of 25 to 250 m/z .

For chiral GC analysis samples were prepared by passing through a silica plug to remove water. 1 μL of sample was injected onto an Agilent cyclosil-B column (length 30 m, internal diameter 0.25 mm, film 0.25 μm) at 250°C in the split mode. An isothermal oven temperature of 115°C was maintained for 22 min. Under these conditions, the retention times (min) were as follows: (*R*)-linalool (15.4), (*S*)-linalool (15.9).

3.2.5. Freeze-drying *A. niger* by lyophilisation

A 50 mL culture of *A. niger* was grown for 48 h, and the resulting biomass was washed with 50 mM phosphate buffer and vacuum filtered before transferring to a small petri dish and storing at -80°C overnight. Water was removed from the fungal sample by lyophilizing at -46°C for 24 h, leaving a crisp mat of fungi. 0.25 g dry weight of the lyophilized fungi was re-suspended in 50 mL of 50 mM phosphate buffer pH 7.0, and left to re-hydrate for 1 h. Biotransformation (3) (geraniol → citral) was carried out as before, and analysed by GC.

3.3. Results and discussion

3.3.1. Fungal biotransformations of geraniol, nerol, and myrcene

Initial experiments aimed to identify potentially interesting biotransformations by assaying each of the four fungal strains (*A. niger*, *G. lipsiense*, *M. piriformis*, and *B. cinerea*) with geraniol, nerol, and myrcene as substrates. Myrcene proved relatively insoluble in the aqueous solutions despite the addition of Tween20 detergent. Low levels of substrate detection *via* GC may also indicate this non-polar hydrocarbon is partitioning to the fungal cell surface rather than being taken up for biotransformation. Consequently no products could be detected for the biotransformation of myrcene with any of the fungal strains. The diversity of fungal biotransformation products that could be achieved using nerol **36** as a substrate was demonstrated in an initial resting cell assay using *Botrytis cinerea* (fig. 31). GC-MS analysis revealed the production of an unknown epoxide **106** and cyclic monoterpene derivative **107**, which were formed in addition to geraniol **35**, geranial **54** and neral **56**.

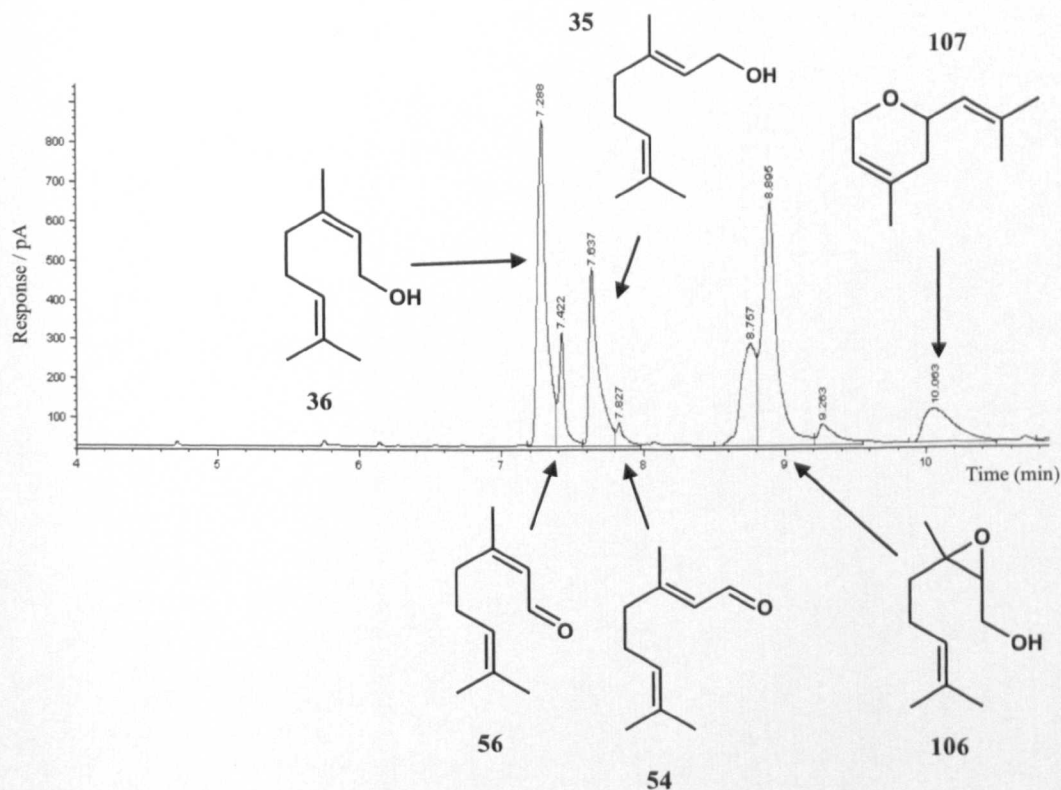


Figure 31: GC-MS analysis for the pH 7 buffered biotransformation of nerol by *B. cinerea*. Sample identification was validated with the MS analysis of authentic standards available for compounds: 35, 36, 54, and 56.

The results of GC-MS highlighted a further four biotransformations of interest whereby the utilisation of geraniol and nerol as substrates led to the formation of potentially desirable monoterpenes, namely linalool and citral (geranial and nerol together) (table 3 and figures 32, 33, 37, 38).

Table 3: Four fungal biotransformations for further investigation.

Fungal sp.	Assay cell type	Substrate	Main products
1. <i>Aspergillus niger</i>	Growing	nerol	α -terpineol, linalool
2. <i>Aspergillus niger</i>	Growing	geraniol	linalool
3. <i>Aspergillus niger</i>	Resting	geraniol	geranial, neral
4. <i>Ganoderma lipsiense</i>	Resting	nerol	geranial, neral

In each instance fungal cultures were prepared fresh prior to either direct substrate addition to the growth media (growing cell assay), or to a pH 7 buffered suspension of the fungal biocatalyst (resting cell). Single samples were extracted at each time-point for analysis *via* GC-MS, with comparisons to calibrations with authentic standards made where possible. The effect of freeze-drying the fungal cultures prior to biotransformations was also studied; as the ability to re-hydrate the fungal biocatalyst would enable a convenient scale-up and allow more accurate quantitative comparisons using dry-weights, as vacuum-filtered fungi still retain some water after harvesting from the growth medium. Comparisons were made between equal culture volumes of freeze-dried *A. niger* and cells harvested fresh from a growing culture, for their ability to carry out the conversion of geraniol to citral in biotransformation 3 (section 3.3.3. fig. 37). However up to 50% decreases in the product yield were observed when using freeze-dried fungal biocatalysts. Subsequent assays therefore utilised freshly prepared fungal cultures.

3.3.2. Studies into the media pH effects on the perceived fungal biotransformation of geraniol to linalool by *Aspergillus niger*

The growing cell assays **1** and **2** into which nerol and geraniol were added direct to the *A. niger* culture medium both showed increasing concentrations of linalool, produced at conversions between 12-30% (up to 0.65 mM) over a 24 h incubation period (figures 32 and 34). α -terpineol was also produced as a major biotransformation product in **1**, with rates of conversion up to 35%. The absence of linalool production using the same biocatalyst and substrate geraniol in the pH 7 buffered biotransformation **3** (fig. 37) was noted and further work aimed to investigate the effect of pH on this reaction. Chiral-GC was also used to analyse a 24 h sample from biotransformation **2** to determine whether the linalool is racemic, or if there is any significant enantiomeric excess resulting from some degree of selectivity in the conversion.

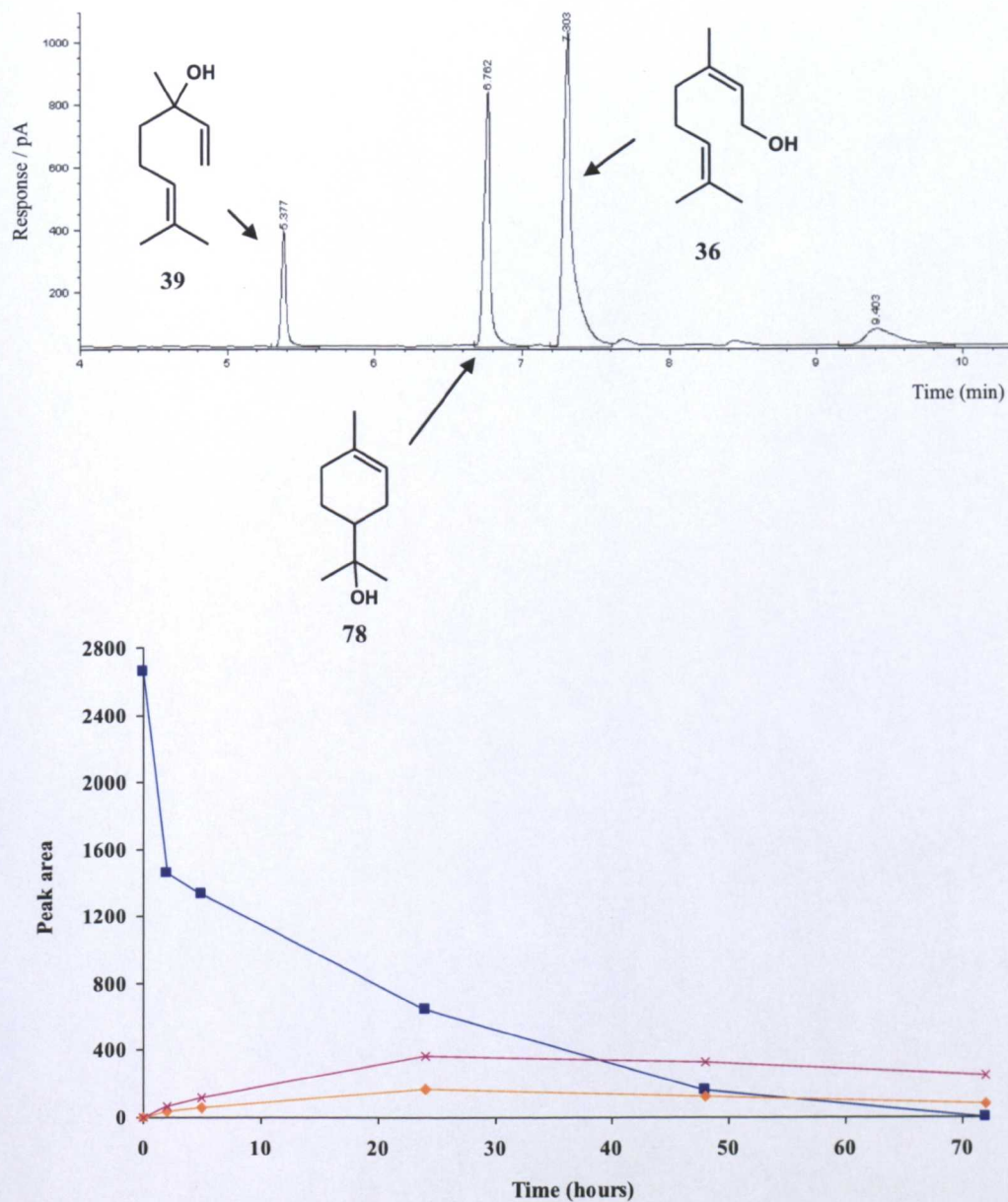


Figure 32: GC-MS analysis and time-course for the growing-cell biotransformation 1 of nerol **36** (■) by *A. niger*, showing the production of linalool **39** (♦) and α -terpineol **78** (×). Authentic standards for each compound were also analysed *via* GC-MS.

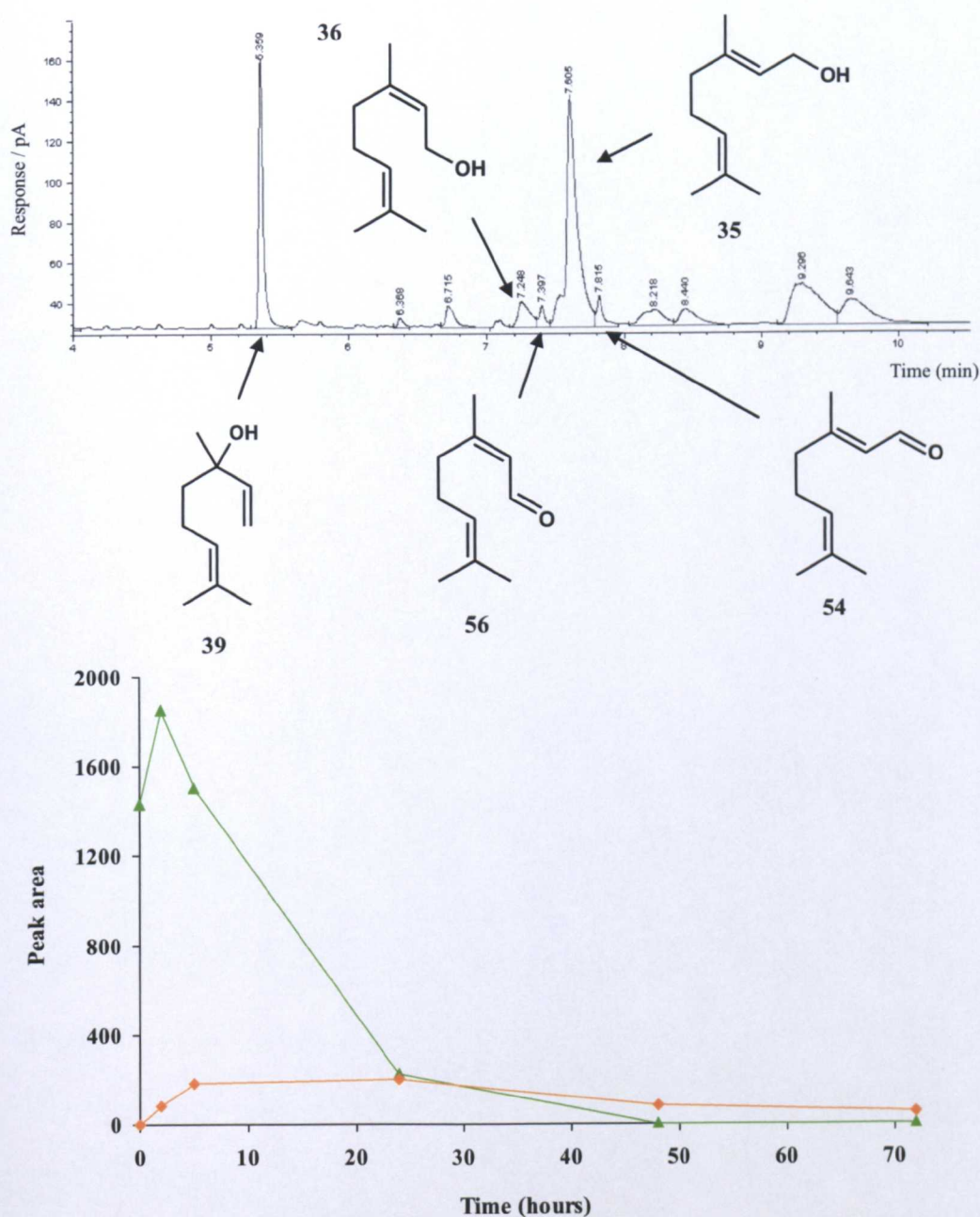


Figure 33: GC-MS analysis and time-course for the growing cell biotransformation of geraniol **35** (\blacktriangle) by *A. niger*, which shows the production of linalool **39** (\blacklozenge) in addition to low concentrations of neral **56** and geranial **54**. Authentic standards for each compound were also analysed *via* GC-MS.

Two of the highlighted *A. niger* biotransformations 2 and 3 use geraniol as a substrate (one giving linalool as a product, and the other citral). Comparisons between the gas chromatograms highlight one particular difference, with the apparent formation of linalool in the growing cell incubation only, and not in the pH 7 buffered assay. The pH of these assays was monitored over a 24 h period (table 4).

Table 4: pH measurements of the fungal growth medium from the time of substrate addition. Initial pH of the media prior to inoculation with fungi was pH 4.85. Dead cell control pH was measured after autoclaving.

Dead cell + nerol	Time (h)	0	1	2	4	6	24
	pH	4.7	4.6	4.5	4.2	4.3	4.2
Growing cell + nerol	Time (h)	0	1	2	4	6	24
	pH	≤ 1.8	≤ 1.8	≤ 1.8	≤ 1.8	≤ 1.8	≤ 1.8
Growing cell + geraniol	Time (h)	0	1	2	4	6	24
	pH	≤ 1.8	≤ 1.8	≤ 1.8	≤ 1.8	≤ 1.8	≤ 1.8

The resting cell biotransformation 3 remained at a buffered pH of 7.0 throughout this period. The corn steep / glucose media used to grow the fungus was at an initial pH of 4.85. However after the 48 h period of growth the pH of the solution was measured at ≤ 1.8 (limit of the graded pH paper available). With these fungal biotransformation assays a dead cell control was run simultaneously with substrate incubations. The effect of autoclaving a fungal culture after 48 h growth is a return to a pH (4.7) similar to that of the initial medium. The fact that linalool is not produced in the dead cell controls with either nerol or geraniol as the substrate, suggested that the effects of this low pH must be taken into consideration before assigning a particular product as a result of biotransformation by *A. niger*.

A separate experiment incubating geraniol in 50 mM phosphate buffer pH 7.0 (without *A. niger*), gave no potential products as a result of incubation at this pH. However *A. niger* in the growing cell flasks (for biotransformations **1** and **2**) (initial media pH = 4.85) were found previously to decrease the pH of the solution to ≤ 1.8 . To check the effect of this acidity on the substrate, geraniol was incubated for 24 h in the growing cell medium (corn steep / glucose) without *A. niger*, at a pH ≤ 1.8 . GC analysis showed linalool to be produced as a result of this (fig. 34), indicating that the acidity is resulting in the formation of linalool from geraniol in solution rather than the fungal biocatalyst.

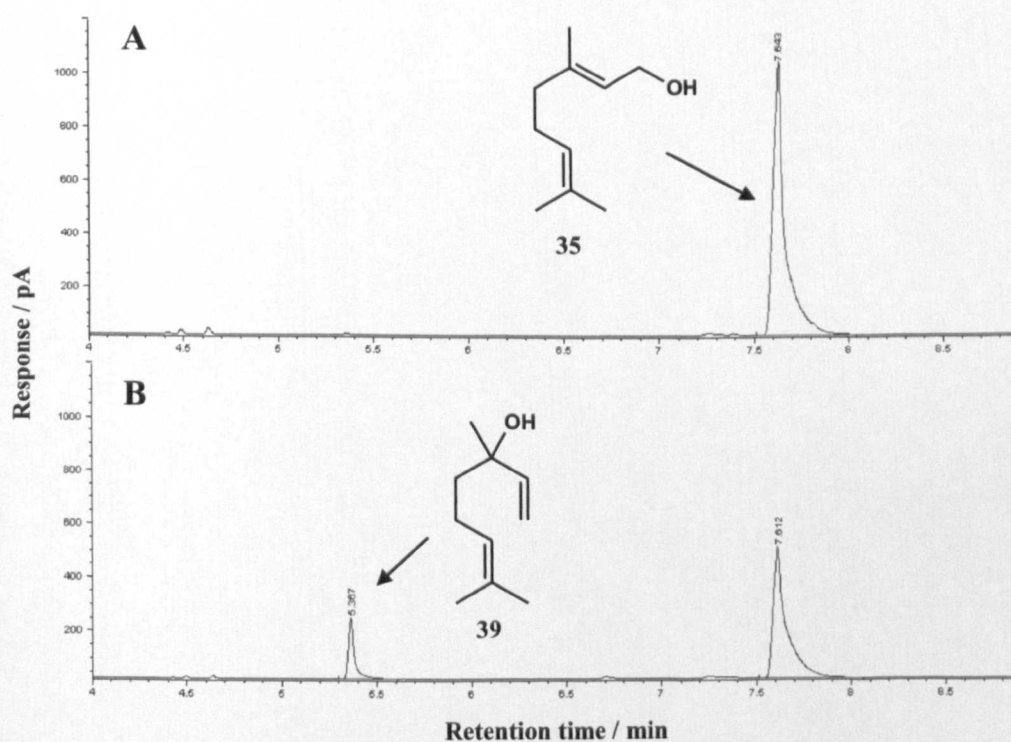


Figure 34: Geraniol incubated in a 50 mM potassium phosphate buffer solution at pH 4.85 (A), and pH ≤ 1.8 (B). Samples extracted after a 24 h incubation at 30°C.

Homochiral linalool is a desirable target for this project, and investigation of the enantiomeric composition of linalool produced in this assay would determine whether further progress would be made into this biotransformation. The results of chiral GC showed the linalool produced from biotransformation **2** to be racemic (fig. 35) and hence no selectivity from this acid catalysed conversion is observed.

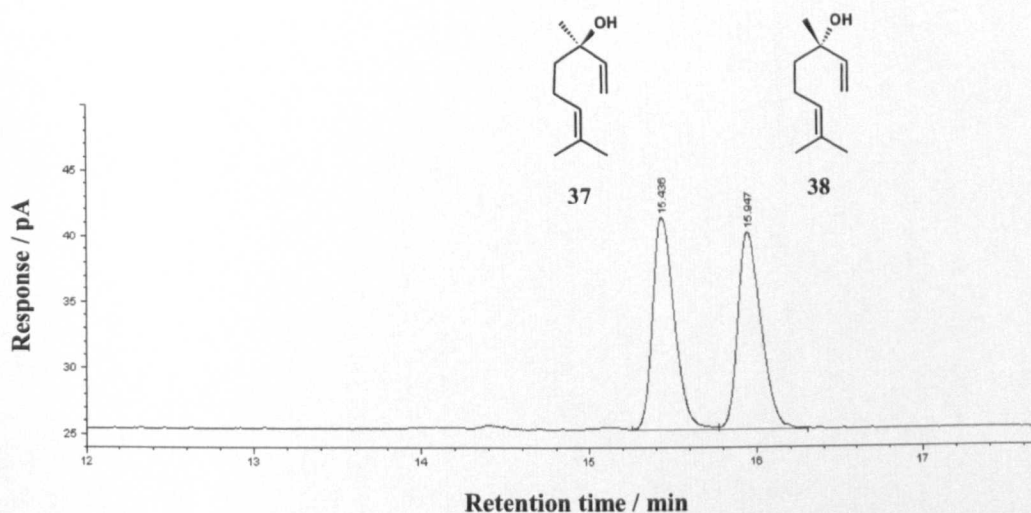


Figure 35: Sample extracted from biotransformation **2** after a 24 h incubation. The corresponding peak areas are: (*R*)-linalool 15.4 min (144.9), and (*S*)-linalool 15.9 min (143.7), a ratio of 50.2 / 49.8%, therefore racemic.

Previously published work on a biotransformation of geraniol using a sporulated surface culture of *A. niger* however yielded linalool as the main product (fig. 36).

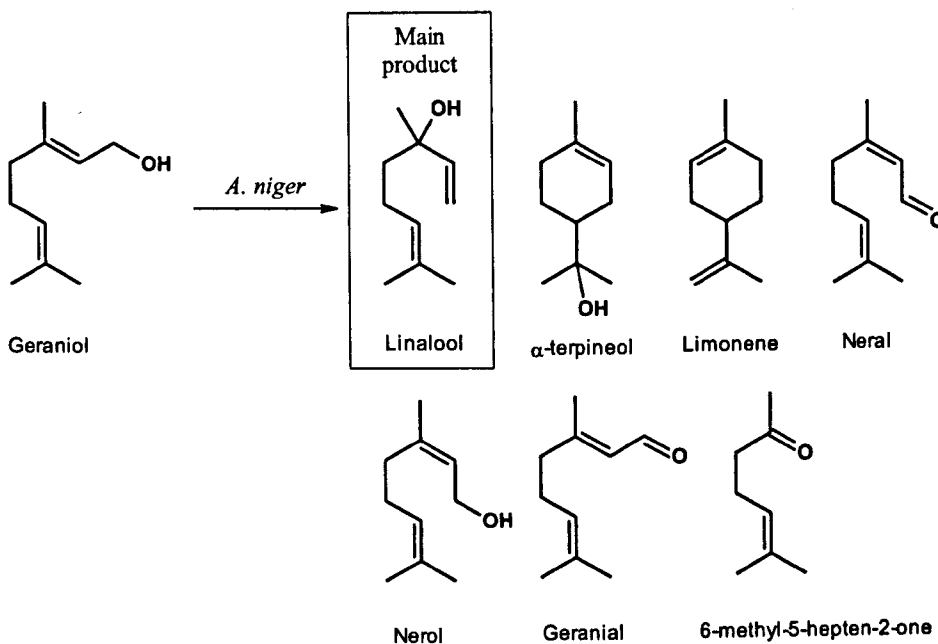


Figure 36: Results from published literature for the bioconversion of geraniol by *A. niger* sporulated surface cultures [Demyttenaere et al. 2000].

As with the observations made here, the authors of this work describe that neither geraniol nor nerol were converted to linalool in controls without the fungal biocatalyst at pH 5 and 7. However at pH 3.5, the authors noted that there was 0.5% conversion to linalool and 1% to α -terpineol in a blank medium over a 7 day period. A media pH 3.5 – 4 was measured for the growing *A. niger* cultures in the literature, despite an approximate pH 1 measured in the investigations described here. It is this low pH which has given rise to the observed conversion of geraniol to linalool after 24 h in these assays.

3.3.3. Biotransformation of geraniol and nerol to citral using *A. niger* and *G. lipsiense*

The results of GC-MS for biotransformations 3 and 4 identified products of oxidation and isomerisation of the substrates geraniol and nerol. A mixture of geraniol and nerol (termed citral) were formed in these two assays (figures 37 and 38).

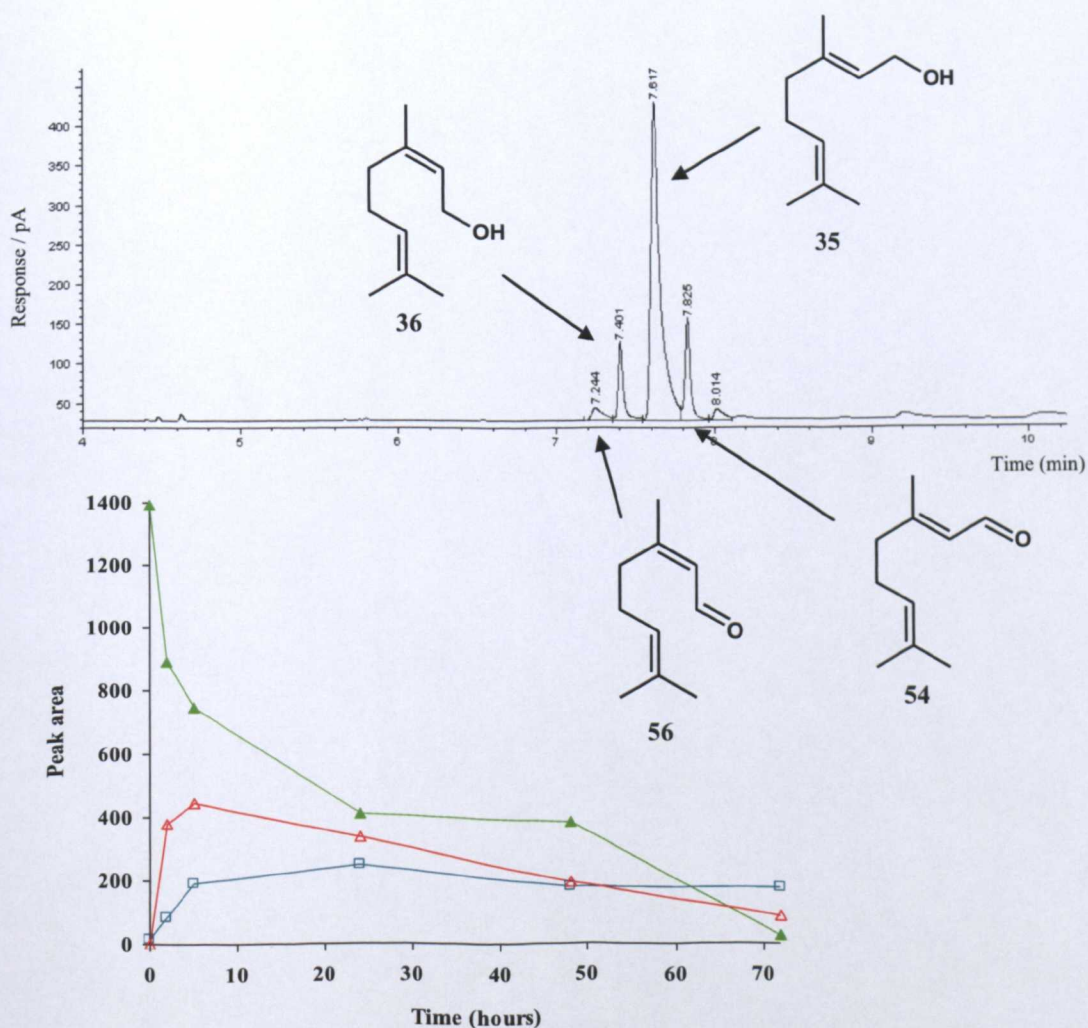


Figure 37: GC-MS analysis and time-course for the resting cell biotransformation 3 of geraniol 35 (\blacktriangle) using *A. niger*, showing the oxidation and isomerisation products, neral 56 (\square) and geraniol 54 (\triangle). Authentic standards for each compound were also analysed *via* GC-MS.

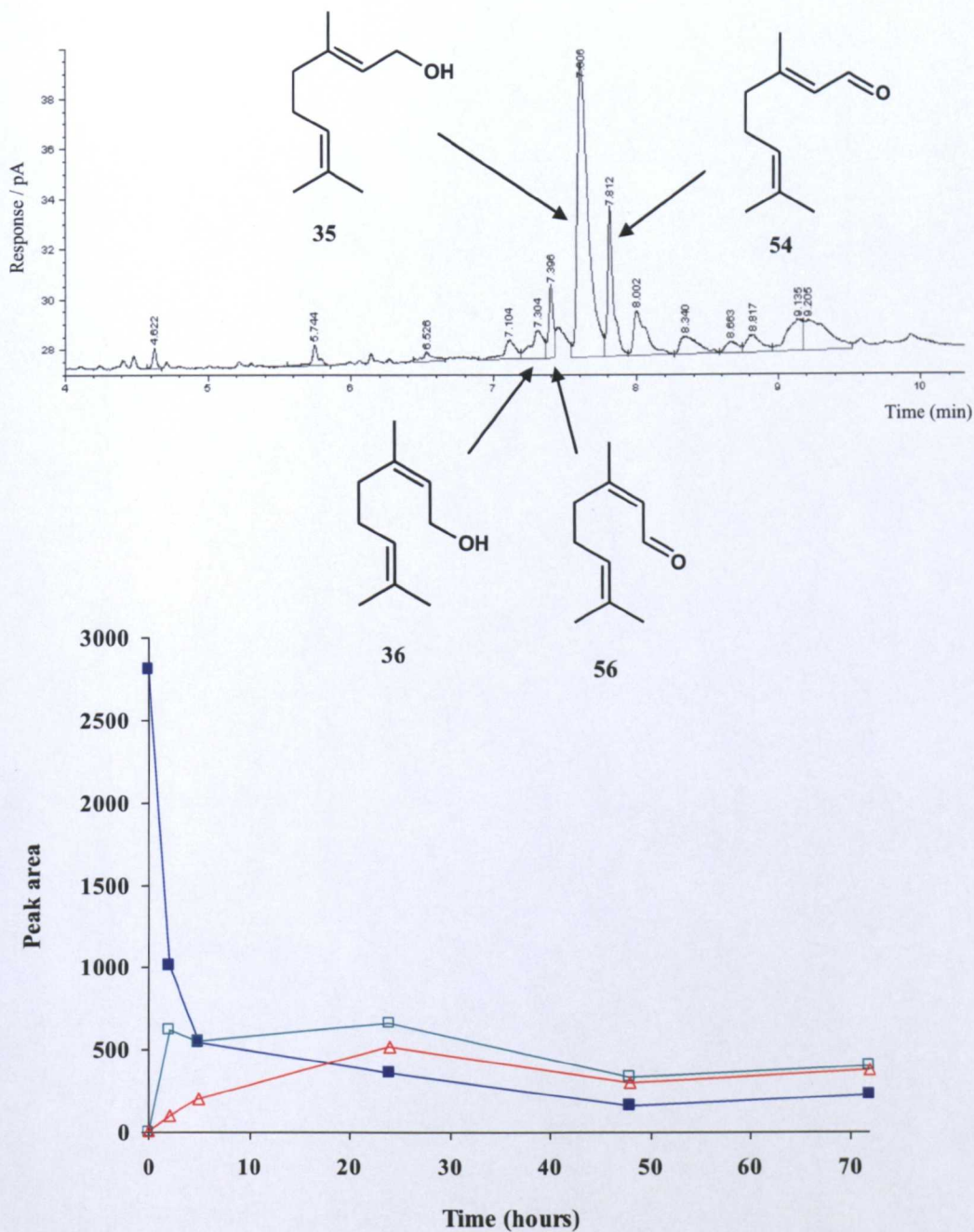


Figure 38: GC-MS analysis and time-course for the resting cell biotransformation 4 of nerol (■) by *G. lipsiense*, showing the oxidation and isomerisation products, nerol (□) and geranial (△). Authentic standards for each compound were also analysed via GC-MS.

Citral is widely used in the fragrance industry as a citrus aroma compound occurring as the main component in lemon and lemongrass oils; and is primarily extracted from the oils of: hops, rose, ginger, orange and basil [Sell 2003]. It is also used as an intermediate in the synthetic routes towards vitamins A, E and K, and the fragrant ionones (fig. 39).

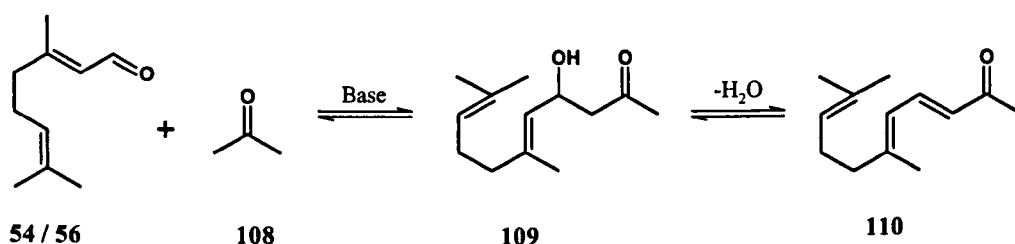


Figure 39: Commercial importance of citral **54/56** used in a synthetic route towards ionones. The condensation of citral with acetone under basic conditions yields ψ -ionone **109**, which undergoes rearrangement to form α -ionone **110** [Hibbert et al. 1924, Jablonski et al. 2006].

The characteristic violet and woody odorous properties associated with the ionones, makes them a highly desirable class of monoterpene. The prohibitive costs involved with the extraction of these compounds from the roots and flowers of violet plants, has placed significant emphasis on their chemical synthesis, to which citral has formed a useful starting material, and thus creating an additional demand for the aldehyde. With this potential commercial interest; different approaches were taken to optimise the geraniol and neral produced in biotransformation **3** (fig. 37).

3.3.3.1. Effect of pH on the yield of citral from biotransformation 3

A pH range from 5.5 – 10.5 was investigated for the washing and re-suspension of *A. niger* in these resting cell assays. These changes in pH however were found to have negligible and no consistent effect on the levels of citral production. Figure 40 below shows a comparison between biotransformations at pH 6 and 10. Conversions of geraniol to neral across the pH range were observed between 0.6 – 4.9%, and to geranial 5.8 – 9.5%.

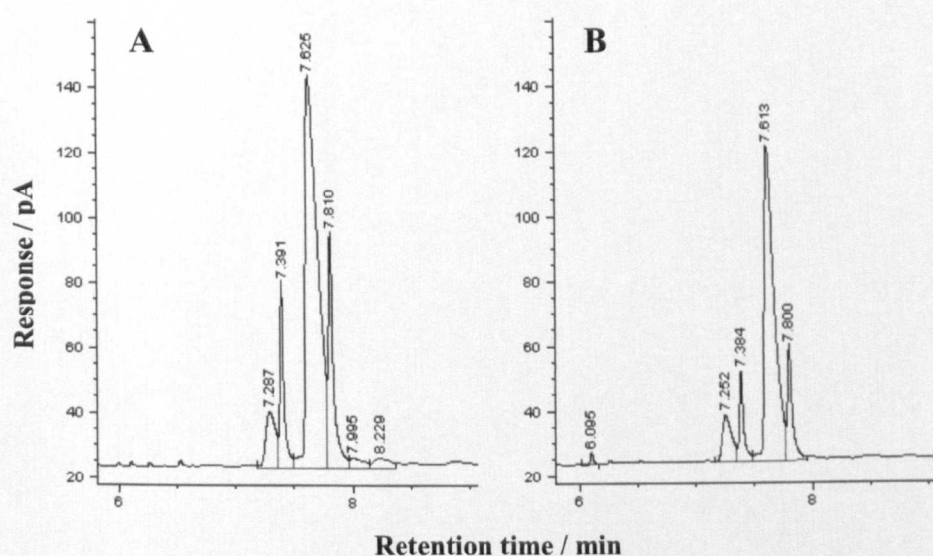


Figure 40: Samples extracted after 24 h for resting cell biotransformation of geraniol using *A. niger* at pH 6 (A), and pH 10 (B).

3.3.3.2. Use of acetone as a co-substrate to improve the yield of citral in biotransformation 3

The use of co-solvents and co-substrates has been found in literature examples to facilitate oxidation of alcohols *via* an NAD^+/NADH hydrogen transfer, recycling system [Kroutil et al. 2004, Edegger et al. 2006]. The majority of dehydrogenases which oxidise primary and secondary alcohols require NAD^+ as a cofactor, and in principle this system offers a method of improving the yield from biotransformations of this nature. In the literature, concentrations of acetone up to 20% v/v have been used for cofactor regeneration when using whole-cells of *Rhodococcus ruber* DSM 44541 [Stampfer et al. 2003, Kosjek et al. 2003]. Experiments have been carried out to study the effect of using acetone as a co-substrate for biotransformation 3; to facilitate the observed oxidation of the secondary alcohol geraniol to citral using *A. niger* (proposed scheme fig. 41). Concentrations of acetone from 0-20% were added to the resuspended culture of *A. niger*. Results from quantitative GC analysis over the 21 h assay period however are inconclusive as to any possible increases in the yield of citral.

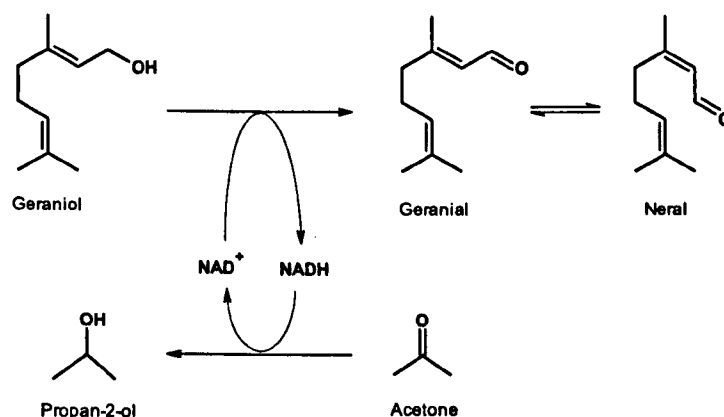


Figure 41: Proposed use of acetone as a co-substrate for the recycling of NAD^+ *via* biocatalytic hydrogen transfer [Kroutil et al. 2004, Edegger et al. 2006].

3.4. Conclusions

The three strains of fungi: *Aspergillus niger*, *Ganoderma lipsiense*, and *Botrytis cinerea*, were assayed with myrcene, geraniol, and nerol as substrates for potential bioconversions to monoterpene alcohols of industrial interest. Problems with the poor solubility of myrcene in aqueous solution meant that no biotransformation products were observed when used as the substrate. However GC-MS analysis revealed five biotransformations of interest when using geraniol and nerol as substrates, with linalool and citral (mixture of neral and geranial) identified as particular products of potential commercial interest. Linalool production was found only in growing cell assays using *A. niger*, and could not be reproduced at a buffered pH 7. Studies into the pH of the growing cell assays however revealed this linalool to be produced as a result of an acidic medium pH ≤ 1.8 which had been generated over a 48 h period of growth rather than by fungal biotransformation. Chiral GC showed an absence of selectivity in the conversion of geraniol to linalool, with a racemic mixture of product enantiomers confirming this view of an acid-catalysed reaction. Studies have been carried out in the literature into the effects of acidic conditions on the rearrangement of linalool, geraniol, nerol, and their derivatives. Acid catalysed rearrangements of nerol were found to yield predominantly cyclic products, mainly α -terpineol and limonene [Cori et al. 1986]. In contrast, reactions of geraniol led to the formation of linalool and other acyclic alkenes (fig. 42). These findings show a relationship to the results presented in this chapter whereby the products yielded from the pH ≤ 1.8 growing cell assay of nerol with *A. niger* (reaction 1 – fig. 32) were α -terpineol

and linalool (conversions 35% and 30% respectively). However only trace amounts of α -terpineol could be detected *via* GC analysis in reaction 2 (fig. 33) with geraniol as the substrate. In this instance linalool was clearly observed as the main product of acid-catalysed rearrangement. In acidic medium the authors found the rate of inter-conversion between linalool and its isomers to be low, thus accumulating in acid catalysed rearrangements of geraniol and nerol; and hence explaining the formation observed in the *A. niger* growth media here (fig. 42).

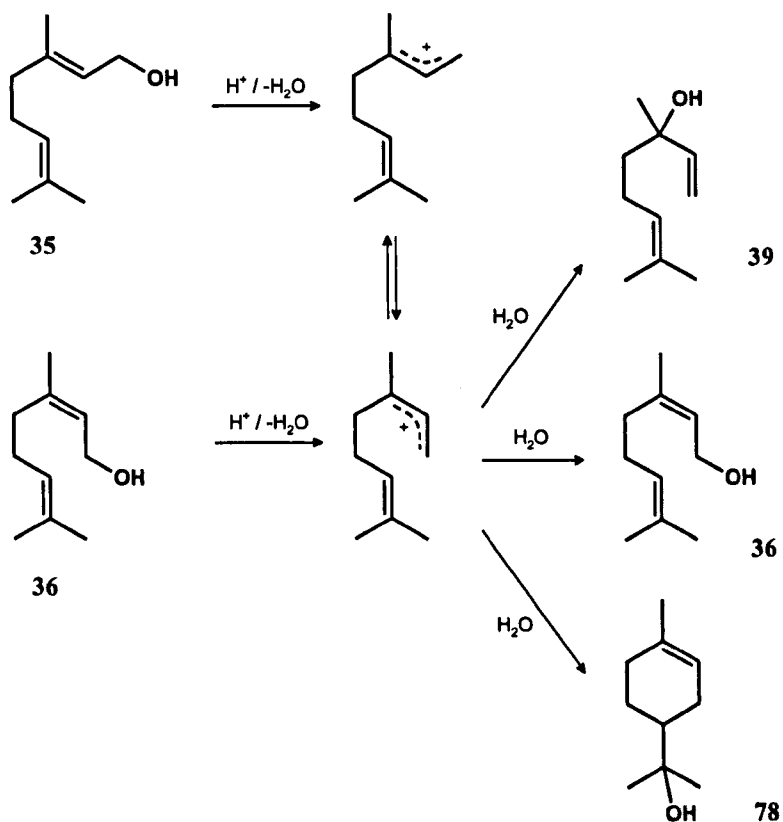


Figure 42: Scheme showing the acid catalysed conversion of geraniol 35 and nerol 36 into linalool 39, nerol, and α -terpineol 78. Figure adapted from Cori et al. 1986.

Linalool has been described as a product in a number of published fungal biotransformations. Literature values for the media pH of a growing *A. niger* culture which yield this product have been quoted in the range pH 3.5-4, which led to levels of background conversion no greater than 0.5% [Demyttenaere et al. 2000]. In contrast the significantly lower pH of growing cell assays described in this chapter and its known effect on the acid catalysed rearrangement of geraniol to linalool does not find precedent in published fungal biotransformations of a similar nature. Citral was confirmed as a fungal biotransformation product in pH 7 buffered assays using *A. niger* and *G. lipsiense*, with geraniol and nerol utilised as substrates respectively (figs. 37 and 38). Optimisation of citral production was attempted *via* changes in pH (6-10), and the use of acetone as a co-substrate (up to 20% v/v). Neither factor was found to have a positive effect on this biotransformation, with rates of conversion not exceeding 10%. A summary of the reactions observed during this chapter is shown in table 5 below. Despite the known potential offered by fungal biocatalysts for the generation of monoterpene alcohols amongst a great diversity of other products; the biotransformations investigated in this chapter could not yield sufficient conversion or selectivity towards the targets of this project to warrant their further study.

Table 5: Summary of reactions from this chapter.

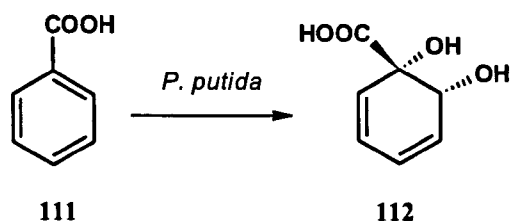
Substrate	Catalyst / pH	Main products (% conversion)
nerol	<i>B. cinerea</i> / 7.0	geraniol (21), neral (5.0), geranial (3.2)
nerol	Acid / ≤ 1.8	α -terpineol (35), linalool (30)
geraniol	Acid / ≤ 1.8	linalool (23)
geraniol	<i>A. niger</i> / 7.0	geranial (9.5), neral (4.9)
nerol	<i>G. lipsiense</i> / 7.0	geranial (3.7), neral (3.1)

4. Chapter 4: Screening of *Rhodococcus* sp. for the resolution of linalyl acetate to linalool

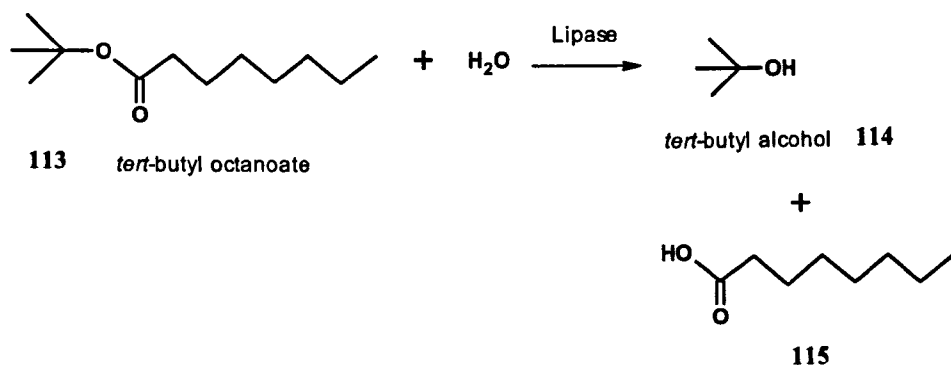
4.1. Introduction

The advantage of high enantio- and regio-selectivity offered by biocatalysis over chemical synthesis has stimulated the use of enzyme-catalysed reactions for generation of chiral tertiary alcohols as intermediates in pharmaceutical and natural product synthesis. An example in this case is the use of the tertiary alcohols 2-phenylbut-3-yn-2-ol and 1,1,1-trifluoro-2-phenylbut-3-yn-2-ol as precursors in the synthesis of triazolopyrazine derivatives as A_{2A} adenosine receptor antagonists [Yao et al. 2005, Kourist et al. 2007]. Requirements for compounds containing a chiral tertiary alcohol moiety have led to the study of a number of biocatalytic routes for their generation (fig. 43); including developments on industrial scale processes such as the synthesis of a tertiary alcohol containing diol from an aromatic carboxylic acid *via* a dihydroxylation reaction (fig. 43A). In addition to hydroxylations, alternative biocatalytic routes exist for the synthesis of tertiary alcohols, predominantly *via* the use of hydrolytic enzymes such as esterases and lipases (fig. 43B). Epoxide hydrolases from *Rhodococcus ruber* and *Bacillus subtilis* have also been shown to carry out the stereoselective ring opening of epoxides (fig. 43C). Kinetic resolution of tertiary alcohols has been achieved in this case with high enantioselectivities (ranging from $E = 70$ to ~ 200) [Hellstrom et al. 2001, Kourist et al. 2008].

A



B



C

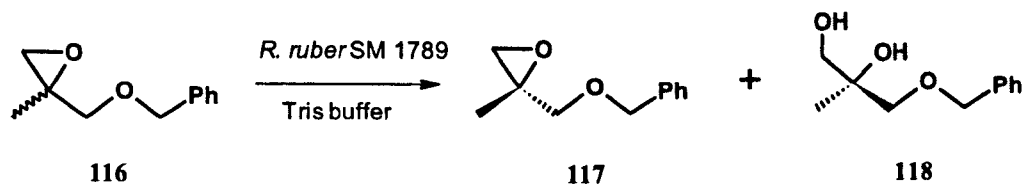


Figure 43: Biocatalytic routes towards tertiary alcohols. (A) Preparative whole cell catalysed di-hydroxylation using the mutant *Pseudomonas putida* U103 to yield a tertiary alcohol-containing diol **112** [Jenkins et al. 1995]. (B) *Tert*-butyl octanoate-hydrolysing lipase from *Burkholderia* sp. YY62 [Yeo et al. 1998]. (C) Stereoselective epoxide hydrolase from *Rhodococcus ruber* SM 1789 [Hellstrom et al. 2001].

Hydrolytic enzymes, particularly lipases and carboxy esterases, are commonly used in biocatalysis to accept a wide range of substrates. The three-dimensional structures of lipases (triacylglycerol hydrolases) and esterases (carboxyl ester hydrolases) both contain the characteristic α/β – hydrolase fold, consisting of 8 β -sheets interconnected with α -helices (fig. 44A) [Ollis et al. 1992, Pleiss et al. 2000]. The catalytic triad of these enzymes comprises Ser-Asp (or Glu)-His amino acids with a conserved consensus sequence (Gly-x-Ser-x-Gly) around the active site serine, and are present on the highly conserved loop regions on one side of this structure. The arrangement of the catalytic triad residues in close proximity causes a decrease in the pK_a -value of the serine hydroxyl group, facilitating its nucleophilic attack on the substrate carbonyl group. This results in the formation of a covalent acyl-enzyme intermediate with subsequent release of the R^2 -OH leaving group in ester hydrolysis (mechanism shown in fig. 44B).

A



B

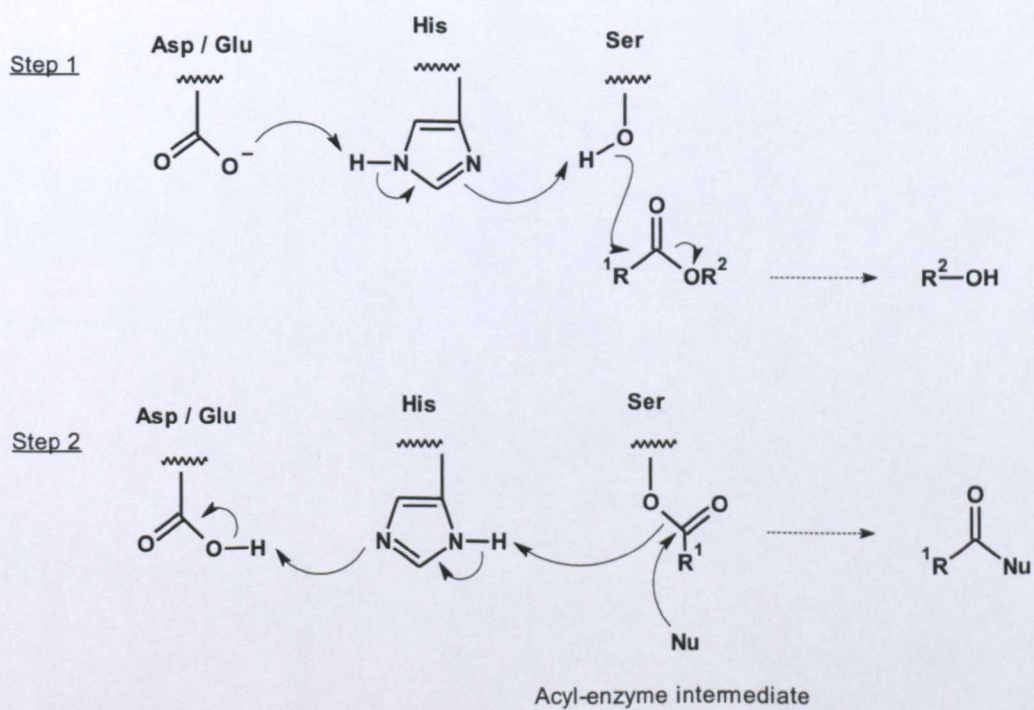


Figure 44: (A) Representation of the catalytic triad residues (Ser, Glu, and His) in *p*-nitrobenzyl esterase (an α/β – hydrolase) from *Bacillus subtilis*. (B) General serine hydrolase mechanism [Faber 2004].

Whilst esters of tertiary alcohols are not so commonly used as substrates in biotransformations, their hydrolysis can be targeted for synthesis of natural products (fig. 45) which are important in the flavour and fragrance industries.

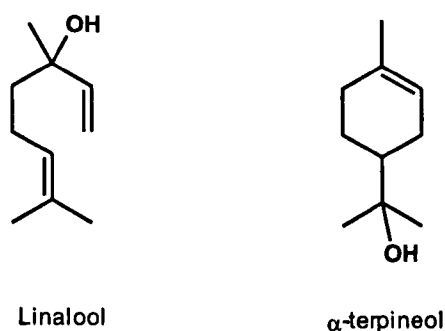


Figure 45: Examples of the industrially important tertiary alcohols linalool and α -terpineol.

Previous literature examples have utilised both whole-cell and cell-extract approaches to the resolution of linalool from hydrolysis of linalyl acetate (fig. 46) [Osprian et al. 1996]. In this instance *Rhodococcus ruber* DSM 43338 was used to obtain a conversion of 25%, with (*S*)-linalool at an enantiomeric excess (*ee*) 56%, and selectivity (*E*) of 4.2.

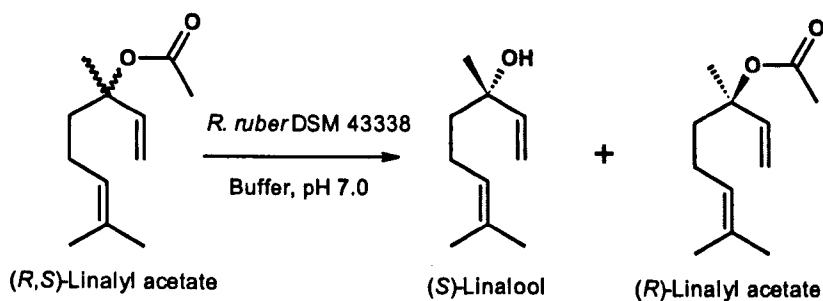


Figure 46: Biocatalytic resolution of racemic linalyl acetate [Osprian et al. 1996].

The ability of several *Rhodococcus* spp. to cleave the sterically hindered tertiary alcohol ester (TAEs) linalyl acetate was noted by the authors, as many hydrolases and whole bacterial cells had previously proved inactive. Later work took an approach based upon cell extracts from *R. ruber* DSM 43338 [Pogorevc et al. 2000]. In this case protein purification was used to isolate two active fractions with opposite enantioselectivity for the acetate, thus revealing that low selectivities using whole cells is due to the presence of competing carboxyl esterases. Selectivities up to $E = 100$ were obtained for the individual fractions. This chapter describes work aiming to build upon these preliminary studies by screening a number of *Rhodococcus* spp. for activity towards the hydrolysis of linalyl acetate. With the intention of purifying enantioselective esterases from the crude cell extracts to homogeneity, this approach offers potential for achieving the objective of a biocatalytic route towards individual enantiomers of linalool.

4.2. Experimental

4.2.1. *Rhodococcus* strains and growth

The 25 species of *Rhodococcus* screened during this investigation were: *Rhodococcus rhodochrous* 11Y, *Rhodococcus* sp. 11211, *Rhodococcus* sp. DN22, *Rhodococcus* sp. CW25, *Rhodococcus aetherivorans* AM1, *Rhodococcus ruber* DSM 43338, and *Rhodococcus* HS 1–19 inclusive (general materials and methods). Luria Bertani media (LB – NaCl 10 g/L, tryptone 10 g/L, and yeast extract 5 g/L) agar plates of each strain were maintained by sub-culturing every 4–5 weeks. 30% glycerol stocks made from liquid cultures were frozen at -80°C for long term storage. Growth in liquid cultures was performed by inoculating 25 mL of LB medium was from agar plates and incubating at 30°C for 24 h. The optical density (OD) was measured using the absorbance at 600nm (A_{600nm}) and 5 mL of culture used to inoculate 3 separate 50 mL volumes of LB medium in 250 mL flasks. For determination of growth curves (43338, HS2, AM1, 11Y) optical density measurements were taken in triplicate from each flask over a period of time, until stationary phase of the growth curve was reached.

4.2.2. Growth of *R. ruber* DSM 43338 on linalyl acetate as sole carbon source

25 mL starter cultures containing M9 minimal medium (KH_2PO_4 3.1 g/L, K_2HPO_4 8.2 g/L, $(NH_4)_2SO_4$ 2.4 g/L, yeast extract 0.1 g/L, tryptone 0.1 g/L, $MgSO_4 \cdot 7H_2O$

0.5 g/L, MnSO₄·H₂O 0.05 g/L, CaCl₂·2H₂O 0.01 g/L, molybdic acid 0.01 g/L, FeSO₄·7H₂O 2.5 g/L) plus either glucose (1 g/L) or linalyl acetate (1 µL/mL) as the sole carbon source were inoculated from agar plates, and incubated at 30°C shaking at 170 rpm for 3 days.

4.2.3. Screening *Rhodococcus* sp. for the hydrolysis of linalyl acetate to linalool

Rhodococcus cells grown on LB agar were used to inoculate 50 mL of LB medium, and grown for 48 h at 30°C. The cells were harvested using a Sorvall RC5B centrifuge equipped with an SS34 rotor (25,000 x g, 15 min, 4°C) and re-suspended in 5 mL of 50 mM potassium phosphate buffer (pH 7.0). 5 µL of the substrate linalyl acetate (1.0 g/L, ~20 mM) was added at T = 0. During the assay 0.5 mL aliquots were withdrawn at time-points: 0, 0.5, 1, 3, and 20 h, and extracted with an equal volume of EtOAc for analysis by GC. For measurement of activity across different stages of the growth curves, *Rhodococcus* strains: *R. ruber* DSM 43338, *R. rhodochrous* 11Y, *R. aetherivorans* AM1, and *R. HS2* grown in 50 mL pre-cultures of LB medium for 24 h at 30°C, were used to inoculate 900 mL volumes of LB medium. The A_{600nm} was monitored, and 100 mL of cells harvested (27,000 x g, 20 min, 4°C) at each time-point. The cell pellet was weighed then re-suspended in 15 mL 50 mM potassium phosphate buffer (pH 7.0) before dividing into 3 x 5 mL aliquots (assay in triplicate). Linalyl acetate (1 µL/ml) was added to each tube and incubated at 30°C, with samples extracted as previously for GC analysis at t = 0 and 4 h.

4.2.4. Use of *tert*-butyl acetate as an inducer of carboxyl ester hydrolases in *Rhodococcus ruber* DSM 43338

R. ruber DSM 43338 grown in 25 mL pre-cultures for 24 h was used to inoculate (3.3% vol) 150 mL cultures of: LB, M9, and M9 + glucose media for growth at 30°C for 24 h. *Tert*-butyl acetate (1 mM) was then added to one of the M9 + glucose cultures, and the flasks incubated for a further 48 h. The cells were harvested (6000 x g, 20 min, 4°C) and washed with 50 mM potassium phosphate buffer (pH 7.0). The cells were harvested, before weighing and re-suspension in 24 mL phosphate buffer. The cell solution was split into 3 x 8 mL aliquots for assay in triplicate, before adding linalyl acetate (1 µL/mL) and extracting samples of 0.5 mL extracted with an equal volume of EtOAc at $t = 0$ and 4 h for GC analysis.

4.2.5. Gas chromatography analysis of linalyl acetate hydrolysis

Gas chromatographic analysis of samples was performed using an Agilent 6890N gas chromatograph equipped with a J&W HP5 column (length 30 m, internal diameter 0.32 mm, film 0.25 µm). 2 µL samples were injected at 250°C in the split mode. An initial oven temperature of 60°C was increased through a 10°C/min gradient to 200°C, with a flow rate of the carrier gas helium at 10 mL/min. Under these conditions, the retention times (min) were as follows: linalool (5.4), linalyl acetate (7.6).

For chiral GC analysis, samples were prepared by passing through a silica plug to remove water. 1 μL of sample was injected onto an Agilent cyclosil-B column (length 30 m, internal diameter 0.25 mm, film 0.25 μm) at 250°C in the split mode. An isothermal oven temperature of 115°C was maintained for 22 min. Under these conditions, the retention times (min) were as follows: (*R*)-linalool (15.4), (*S*)-linalool (15.9), (\pm)-linalyl acetate (20.0).

4.2.6. Protein purification of potential tertiary alcohol esterases

4.2.6.1. Preparation of *Rhodococcus* cell extracts

Rhodococcus strains grown on LB agar plates were subsequently used to inoculate 25 mL starter cultures of LB, and incubated for 24 h at 30°C. The starter cultures were then added to 2 L flasks containing 850 mL of LB medium, and grown for 3 days at 30°C. The cells were harvested (GS3 rotor, 6,000 x *g*, 30 min, 4°C) and re-suspended in 40 mL of 50 mM phosphate buffer (pH 7.0). The cells were lysed by passing twice through a continuous flow French press at 270 MPa, and centrifuged (27,000 x *g*, 15 min, 4°C), before retaining the supernatant as the soluble protein fraction, which was then filtered using a 0.22 μm filter (Millipore – PES membrane).

4.2.6.2. Anion exchange chromatography

For initial purification steps an anion exchange FFQ column (volume 50 mL) was pre-equilibrated with 50 mM potassium phosphate buffer (pH 7.0). The column was loaded with the filtered cell extract and unbound protein eluted with 100 mL phosphate buffer. The run started with a further 100 mL phosphate buffer before applying a gradient from 0 – 0.7 M NaCl over a volume of 500 mL, which was then held at this concentration for a further 100 mL. For increased resolution during purification a pre-packed Mono Q anion exchange column of volume 1 mL was equilibrated with phosphate buffer. Pooled 1 mL fractions from an initial phenyl sepharose column were dialysed with phosphate buffer overnight, before concentration with a centricon 5k molecular-weight cut-off filter (centrifuged at 4,500 x g, 30 min, 4°C). The sample was filtered using a 0.45 µm filter (Millipore – PES membrane) before injecting a 2 mL volume onto the Mono Q column. A gradient was run from 0 – 0.7 M NaCl (in 50 mM phosphate buffer) over a volume of 70 mL.

4.2.6.3. Ammonium sulphate precipitation

Solutions of protein collected from anion exchange chromatography were precipitated by adding $(\text{NH}_4)_2\text{SO}_4$ (52 g / 100 mL) and stirred at 4°C o/n. Solutions were centrifuged (27,000 x g, 20 min, 4°C), retaining the protein pellet before re-suspending in 2 M $(\text{NH}_4)_2\text{SO}_4$ in 50 mM potassium phosphate buffer (pH 7.0) for hydrophobic interaction chromatography.

4.2.6.4. Hydrophobic interaction chromatography

A pre-packed phenyl superose column (volume 1 mL) was equilibrated with 50 mM potassium phosphate buffer (pH 7.0) containing 2 M $(\text{NH}_4)_2\text{SO}_4$. The column was loaded with 0.5 mL of protein in phosphate buffer containing 1 M $(\text{NH}_4)_2\text{SO}_4$. Elution started with 10 mL of phosphate buffer containing 2 M $(\text{NH}_4)_2\text{SO}_4$, before decreasing the concentration to zero over a volume of 10 mL, before holding at this concentration for a further 10 mL. For the preparation of a phenyl sepharose column, powdered phenyl sepharose was mixed into a slurry with 50 mM potassium phosphate buffer (pH 7.0) and packed into a 10 mL column volume. The column was pre-equilibrated with phosphate buffer containing 2 M $(\text{NH}_4)_2\text{SO}_4$. The filtered cell extract was loaded onto the column, and 50 mL of unbound protein collected in the flow-through with the equilibration buffer. A gradient was run from 2 M $(\text{NH}_4)_2\text{SO}_4$ to 0 M, over a volume of 100 mL, collecting 2 mL fractions.

4.2.6.5. Gel filtration chromatography

A HiLoad S200 16/60 gel filtration column (volume of 120 mL) was equilibrated and run with 50 mM potassium phosphate buffer (pH 7.0) containing 0.2 M NaCl. 2 mL of pooled concentrated FFQ fractions from the first step of purification were loaded onto the column.

4.3. Results and discussion

4.3.1. Screening of *Rhodococcus* strains for linalyl acetate hydrolytic activity

A screen of 25 species of *Rhodococcus* including: *Rhodococcus rhodochrous* 11Y, *Rhodococcus* sp. 11211, *Rhodococcus* sp. DN22, *Rhodococcus* sp. CW25, *Rhodococcus aetherivorans* AM1, *Rhodococcus ruber* DSM 43338, and *Rhodococcus* HS 1–19 inclusive, was used to determine the best strains for carrying out the hydrolysis of linalyl acetate to linalool. Using GC analysis, significant hydrolytic activity was observed in four strains: *R. aetherivorans* AM1 (39 % conversion after 3 h at 30°C), *R. ruber* DSM 43338 (50%), *R. rhodochrous* 11Y (30%), and *R. HS 2* (15%) (fig. 47). The background level of hydrolysis of linalyl acetate in the pH 7 phosphate buffer over a 3 h period was observed at 2%. The remaining 21 strains showed negligible activity towards this bulky acetate substrate with activities in the region of 2-5% over the same time period. Growth of the *Rhodococcus* strains was checked by measuring the optical density at 600nm, with cells harvested at different stages and the activity / (g) cell weight / hour measured for cultures in triplicate during a 4 h resting cell assay at 30°C. These results confirmed that optimal activity for the hydrolysis of linalyl acetate is observed at the end of the log phase of growth (figures 48 and 49).

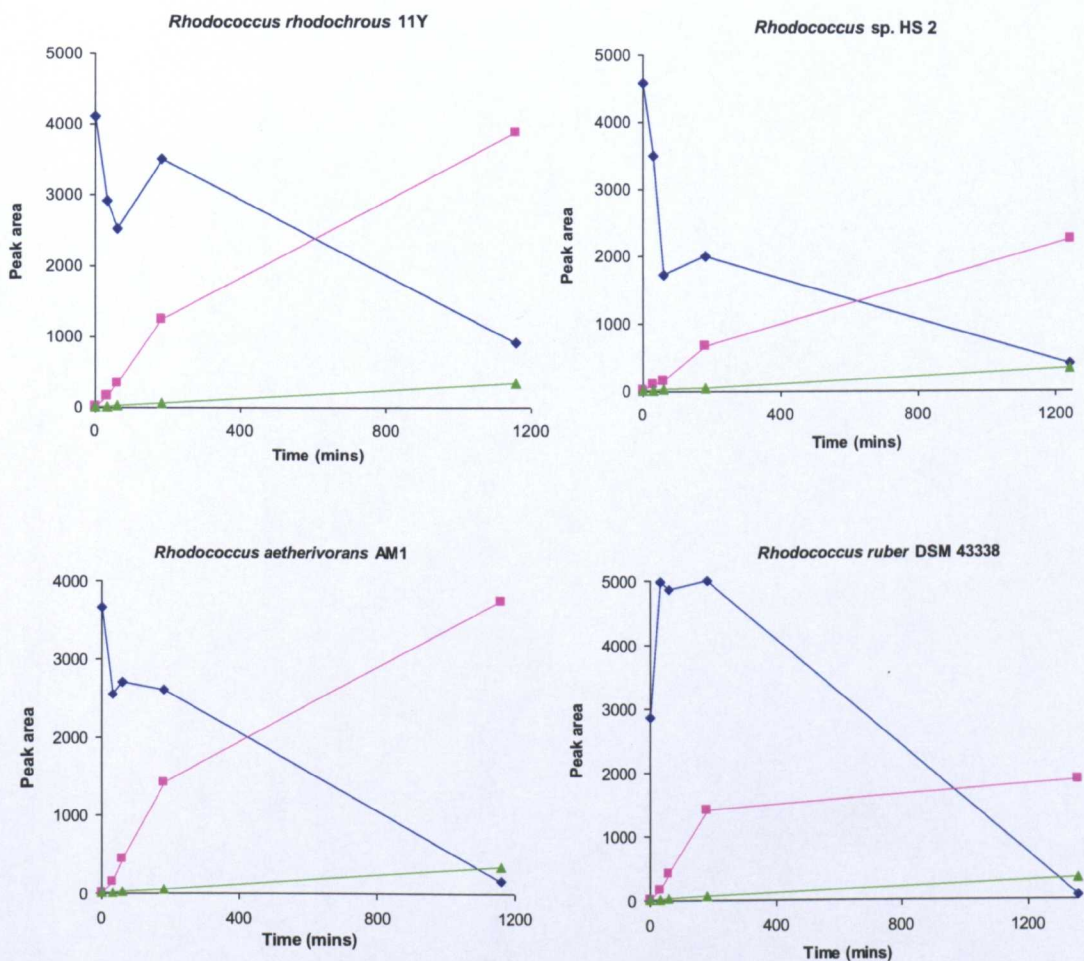


Figure 47: Results of GC analysis for the four strains of *Rhodococcus* that showed activity towards the hydrolysis of linalyl acetate (♦) to linalool (■). The background (control) level of hydrolysis in buffer (without cells) is also shown (▲). Samples were extracted from isolated assays. Measurements of the loss of linalyl acetate and appearance of linalool show some fluctuation due to mixing of samples and incomplete solubility in aqueous solution.

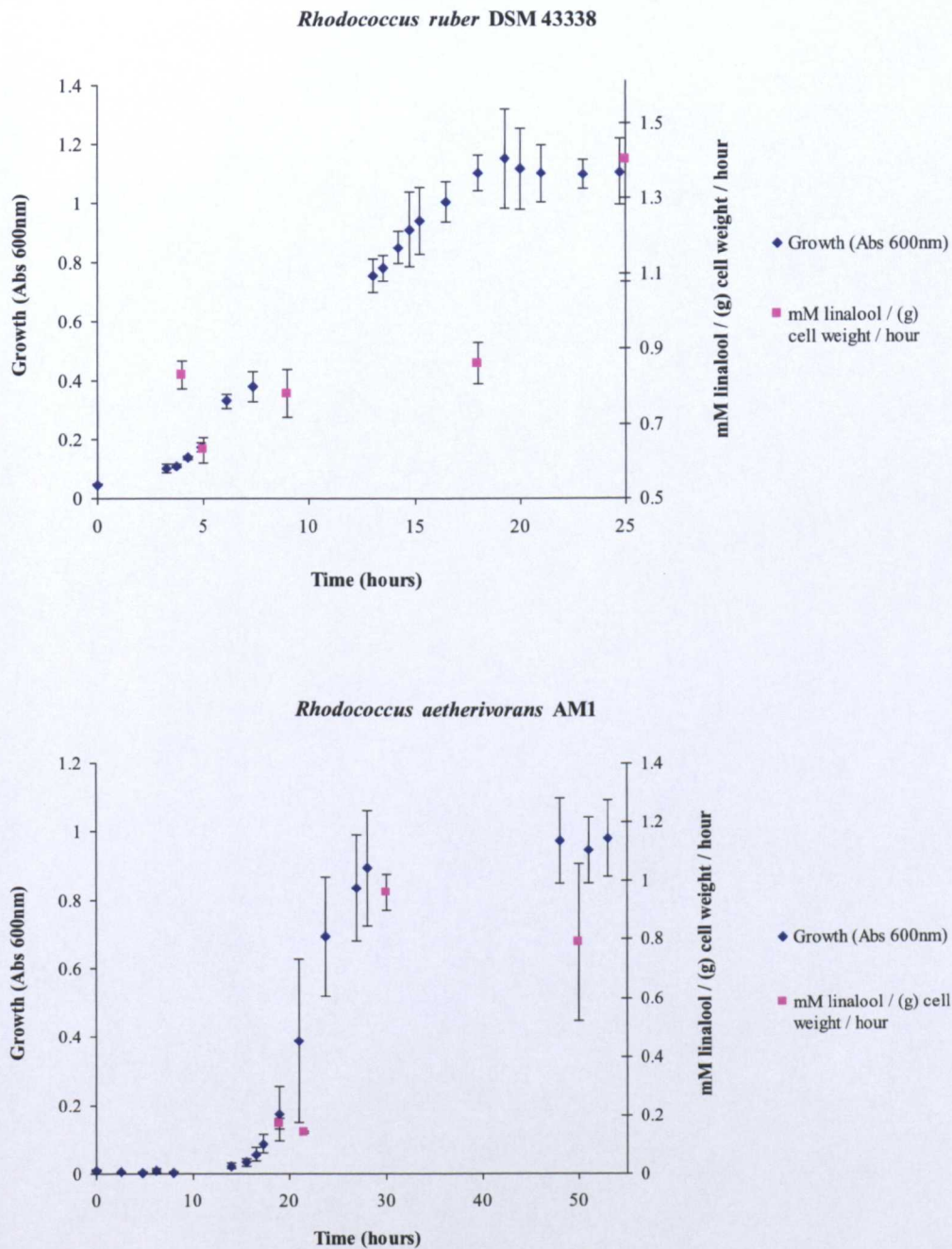


Figure 48: Activity of *R. ruber* DSM 43338 and *R. aetherivorans* AM1 strains towards linalyl acetate (production of linalool) at different stages of the growth curve. Incubations were carried out at 30°C for 4 h in triplicate for determination of error.

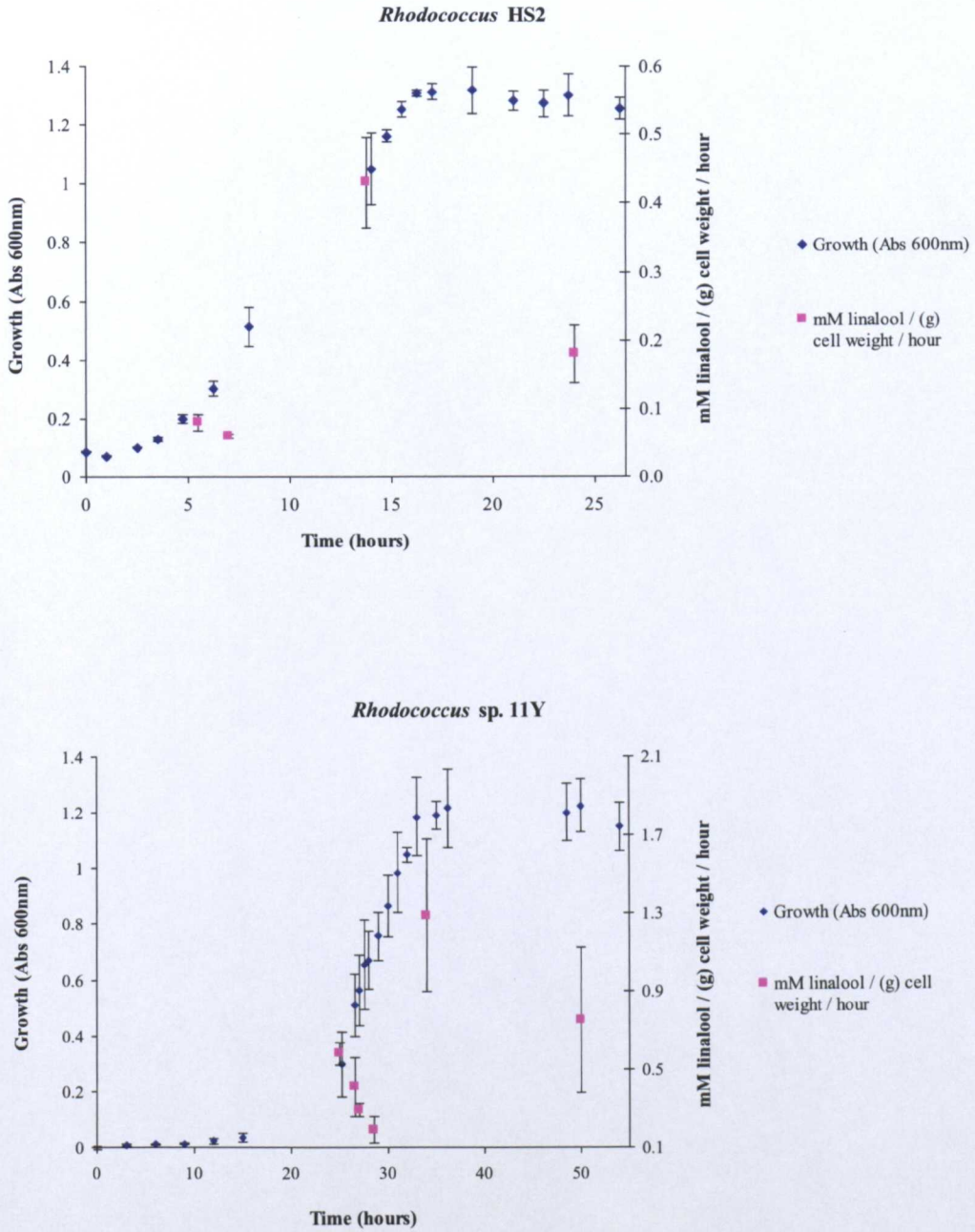


Figure 49: Activity of *R. sp.* HS2 and *R. rhodochrous* 11Y strains towards linalyl acetate (production of linalool) at different stages of the growth curve. Incubations were carried out at 30°C for 4 h in triplicate for determination of error.

4.3.2. Investigation of linalyl acetate and *tert*-butyl acetate as inducers of tertiary carboxyl ester hydrolase activity

Whereby the enzymatic resolution of linalyl acetate has been previously studied in literature examples [Osprian et al. 1996, Pogorevc et al. 2000], the effect of enzyme induction has also been investigated for enhancement of this biotransformation. The addition of either racemic or (*R*)-linalyl acetate was found in the literature to have no positive effect on the induction of carboxyl ester hydrolases. However those enzymes which accept linalyl acetate as a substrate were found to be inducible with *tert*-butyl acetate. These experiments aimed to replicate the observed effects of TAE induction with *tert*-butyl acetate (1 mM) in *R. ruber* DSM 43338 cells grown on either glucose or succinate as a sole carbon source (SCS). A 6-fold increase in activity of linalyl acetate hydrolysis was observed when cells grown on either 1 g/L glucose and succinate were induced in the early log-phase of growth by the addition of 1 mM *tert*-butyl acetate (fig. 50). Cells were harvested at the end of log-phase when previously shown to be at their most active. Analysis of the cell extracts from these incubations *via* SDS-PAGE however failed to show increased expression of proteins in response to this induction. The induction of TAE activity in *R. ruber* DSM 43338 was tried with a further two bulky acetates (α -naphthyl acetate and tributyrin – figure 51) which were also added at a 1 mM concentration after 24 h of growth (early log phase). However no positive inductive effects were observed as was the case with *tert*-butyl acetate.

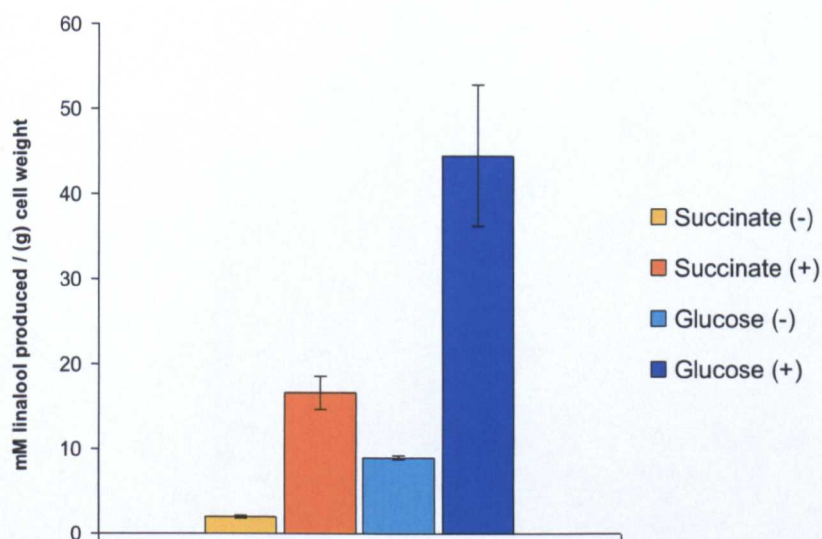


Figure 50: The effect of *tert*-butyl acetate induction on the activity of linalyl acetate hydrolysis by *R. ruber* cells grown on either succinate or glucose as SCS (\pm inducer).

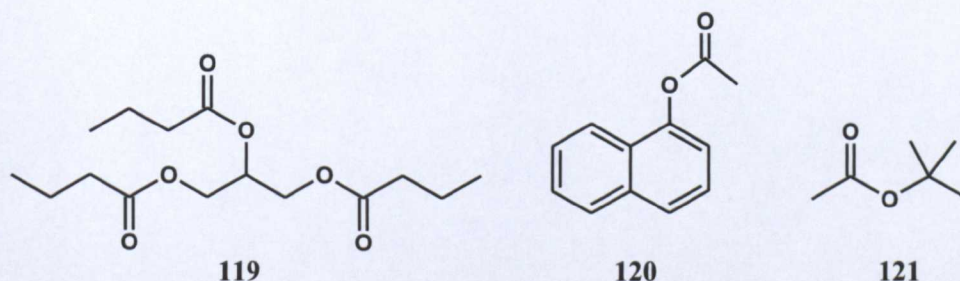


Figure 51: Acetates used in the induction experiments: tributyrin **119**, α -naphthyl acetate **120**, and *tert*-butyl acetate **121**.

Experiments whereby *R. ruber* was grown on linalyl acetate also targeted the induction of enzymes specifically for the metabolism of this substrate in order for the *Rhodococcus* cells to survive and grow on it as a SCS. Comparative SDS-PAGE analysis of cell extracts grown on glucose and linalyl acetate as SCS revealed the apparent induction of one protein at approximately 50 kDa (fig. 52),

which following a tryptic digest and peptide sequencing was identified as a type of aldehyde dehydrogenase from a strain of *R. ruber* (fig. 53).

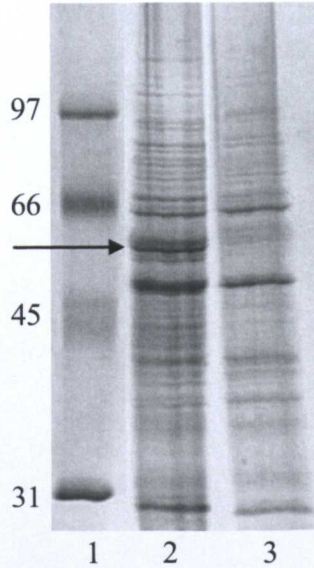


Figure 52: Cell extracts from *R. ruber* DSM 43338 grown on: linalyl acetate (lane 2) and glucose (lane 3) as sole carbon sources. Highlighted band cut out for protein identification (TF). BioRad molecular weight marker (kDa) lane 1.

Match to: [gi|29893039](#) Score: 230
aldehyde dehydrogenase [Rhodococcus ruber]

Nominal mass (M_r): 44777; Calculated pI value: 4.97
 NCBI BLAST search of [gi|29893039](#) against nr
 Unformatted [sequence string](#) for pasting into other applications

Taxonomy: [Rhodococcus ruber](#)

Fixed modifications: Carbamidomethyl (C)
 Variable modifications: Oxidation (M)
 Cleavage by Trypsin: cuts C-term side of KR unless next residue is P
 Sequence Coverage: 19%

Matched peptides shown in **Bold Red**

1	AAERERMIWR	VGDLTQRAE	EFGQLEALDN	GK SAVIAAAV	DTAWSADIFR
51	YYAGWATKIE	GSTVNVTMPF	VPGGEFHAYT	LREPVGVCGL	IVPWNFLLM
101	AAFKLAPALA	AGNTVILKPA	EQTPLTALLL	AEIFEEAGFP	PGVVNIVPGF
151	GDAGAALAAH	DDVDKIAFTG	STEVGKKVVD	AAKGNLKKVS	LELGGKSPNI
201	VFADADFDAA	VQGSLDAWLF	NHGQCCVAGT	RLFVERPIFE	RFTEAVAEAA
251	SKVK IGPGLD	PATQLGPLVS	QEQLDRVTGY	LREGLIDGAR	ALTGGKRWGD
301	KGFFVEPTVL	VDVQPDFSVV	REEIFGPVVN	AMPFDADDGI	SAAANDSIYG
351	LAAGIWTRDL	SKAHRTARRL	KAGSVWINQY	NGFDTAMPFG	GFKQSGWGRE
401	LGAGALDLYT	QTKAVNIAL			

Figure 53: Results of peptide sequencing carried out by the Technology Facility (TF), identifying the induced protein (highlighted in fig. 52) as an aldehyde dehydrogenase.

4.3.3. Purification of enantioselective esterases from *Rhodococcus* cell extracts

Table 6 shows the results of chiral GC analysis for the four (whole-cell) assays with selected *Rhodococcus* strains. (*R*) and (*S*)-linalool could be clearly resolved using a cyclosil-B column under the GC conditions developed however resolution of linalyl acetate can not be achieved using this column. Time-points were taken at both 5 and 24 h to check whether there is a decrease in selectivity over a prolonged incubation. These initial results show a relatively low whole cell enantioselectivity (*ee* between 14-19%) leading predominantly to production of (*S*)-linalool. A literature example studying the hydrolysis of racemic linalyl acetate also found whole cell biocatalysts from *Nocardia* and *Rhodococcus* sp. proceeded with an (*S*)-selectivity for this hydrolysis [Osprian et al. 1996]. The authors found that with levels of conversion between 12-30%, enantiomeric excesses (*ee*) of (*S*)-linalool were generated in the range 11-56%.

Table 6: The enantiomeric excess of linalool produced in resting whole cell assays for the active strains of *Rhodococcus*. Samples were analysed *via* chiral GC after 5 and 24 h.

Strain	Linalool <i>ee</i> (%)	
	5 h	24 h
<i>R. HS2</i>	19 (<i>S</i>)	16 (<i>S</i>)
<i>R. aetherivorans</i> AM1	14 (<i>R</i>)	14 (<i>S</i>)
<i>R. ruber</i> DSM 43338	16 (<i>S</i>)	17 (<i>S</i>)
<i>R. rhodochrous</i> 11Y	17 (<i>S</i>)	15 (<i>S</i>)

In a previous literature example [Pogorevc et al. 2000] fractionation of *R. ruber* DSM 43338 cell extract was studied to give improved selectivity towards linalyl acetate hydrolysis. Through the use of ion exchange and hydrophobic interaction chromatography, partially purified fractions with opposite enantioselectivity were obtained. The work for this project continued with this study of *Rhodococcus* cell extracts for the four selected strains from the previous screening. An initial purification step of anion exchange chromatography (FFQ) was tried in each case. A range of the resultant fractions were assayed with linalyl acetate and the selectivity determined using chiral GC. With each of: *R. aetherivorans* AM1, *R. rhodochrous* 11Y, and *R. HS 2*, the predominant selectivity led to (*S*)-linalool as the main product of this hydrolysis. There were fractions in each example with limited or no selectivity. As a first step of purification however, there were partially purified fractions with an enhanced selectivity towards (*S*)-linalyl acetate over the cell extract from which the fractions were derived. Table 7 and figure 54 summarise the results for these three strains.

Table 7: Increasing enantioselectivity for the hydrolysis of (*S*)-linalyl acetate from a single step FFQ purification.

Strain	Fraction	Selectivity ee (%)
11Y	Whole cell	15 (S)
	Cell extract	24 (S)
	FFQ - 23	49 (S)
HS2	Whole cell	16 (S)
	Cell extract	15 (S)
	FFQ - 42	33 (S)
AM1	Whole cell	14 (S)
	Cell extract	6 (S)
	FFQ - 31	50 (S)

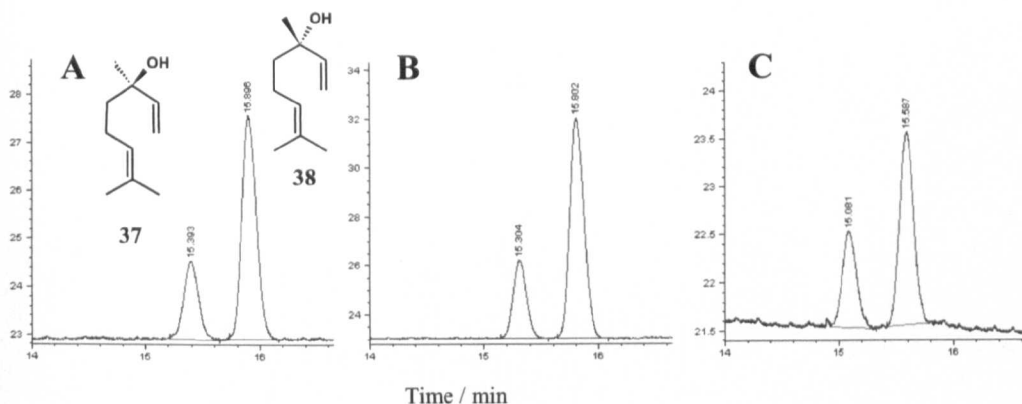
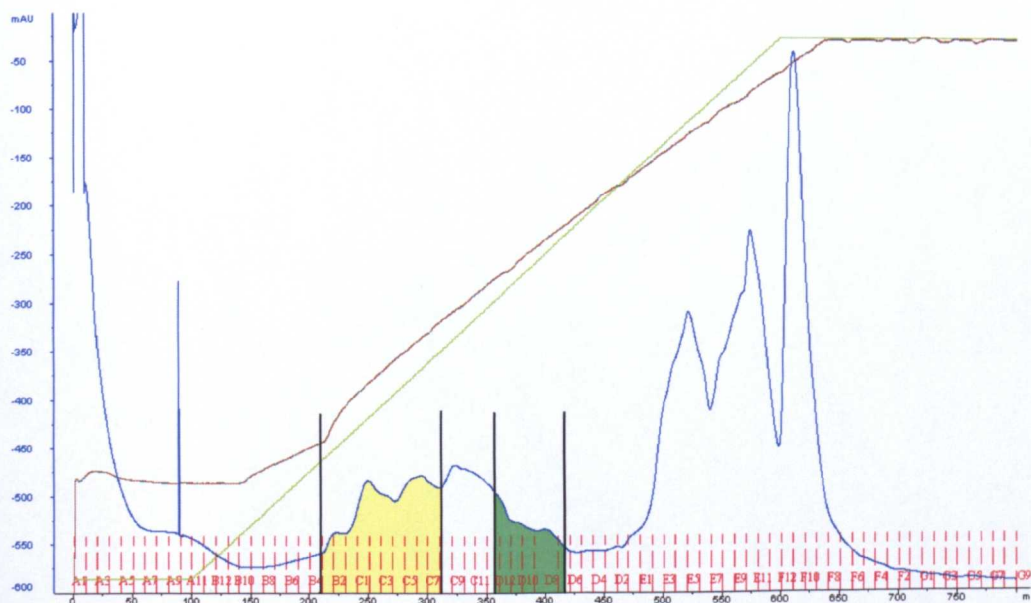


Figure 54: Chiral GC analysis for the hydrolysis of linalyl acetate after a 6 h assay using anion exchange fractions: (A) 11Y fraction 23; (B) AM1 fraction 31; (C) HS2 fraction 42. Retention times (min): (*R*)-linalool (15.4), (*S*)-linalool (15.9).

Anion exchange fractions assayed for activity from the first step of purification from *R. ruber* DSM 43338 cell extracts show interesting results regarding esterase selectivity, which relate to those previously published [Pogorevc et al. 2000, Osprian et al. 1996]. Activity for linalyl acetate hydrolysis was observed within two distinct regions on the FFQ chromatogram with chiral GC analysis revealing opposite enantioselectivity in each case (fig. 55). Through running an elution gradient of increasing salt concentration (0-0.7 M NaCl over 10 column volumes), fractions collected at salt concentrations of between 0.14-0.28 M all displayed a predominant *R*-selectivity with enantiomeric excess (*ee*) values of up to 60%-*R* at levels of conversion between 7-21% over a period of 6 h (conversions with the crude cell extract prior to loading on the column were measured at 37% over the same time period). Chiral GC analysis of fractions eluting at slightly higher salt concentrations 0.39-0.46 M showed the hydrolysis of linalyl acetate proceeding at conversions in the range of 12-27% with opposite enantiopreference (*ee* up to 76%-*S*) (figures 55 and 56).



FFQ fraction	Enantioselectivity ee (%)
Cell extract	17 (S)
3	0
11	0
21	60 (R)
25	52 (R)
27	31 (R)
30	27 (R)
31	20 (R)
34	14 (R)
36	0
37	9 (R)
39	76 (S)
42	45 (S)
49	0
54	0
61	0
65	0
Control (no protein)	0

Figure 55: First step of purifying esterases from *R. ruber* 43338 cell extract using anion exchange chromatography. The highlighted regions on the chromatogram show active fractions displaying opposite enantioselectivity towards linalyl acetate hydrolysis.

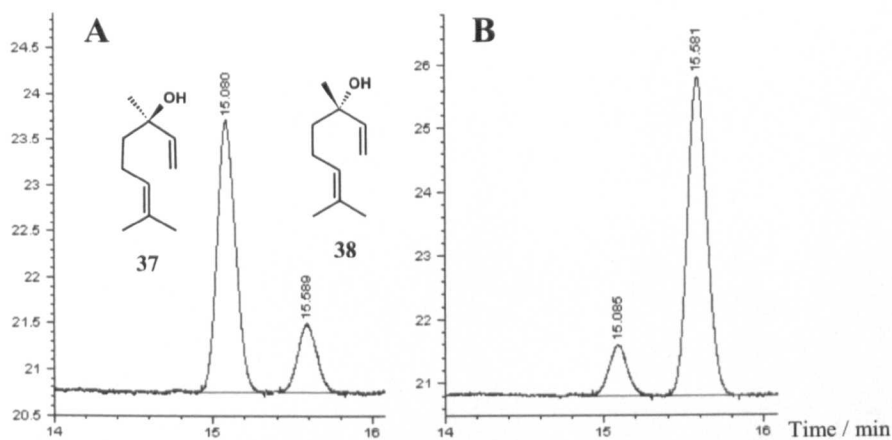


Figure 56: Chiral GC analysis of *R. ruber* DSM 43338 anion exchange fractions 21 (A) and 39 (B) after 6 h. Retention times (min): (*R*)-linalool (15.4), (*S*)-linalool (15.9).

Fractions 20-31 (*ee* of *R*-linalool produced), and fractions 38-43 (*ee* of *S*-linalool) from the FFQ column were pooled separately for further purification with hydrophobic interaction chromatography (HIC). Separation of the proteins was improved with this second step of purification when using an extended gradient decreasing the concentration of 2 M $(\text{NH}_4)_2\text{SO}_4$ over 30 column volumes. Proteins bound to the hydrophobic column were found to elute below a concentration of 1 M $(\text{NH}_4)_2\text{SO}_4$. Despite collecting 1 mL fractions, SDS-PAGE analysis revealed these eluted fractions to still contain many proteins (fig. 57). Whilst the initial step of purification (FFQ) reduced the activity observed quite significantly when compared to the soluble cell extract (between 10-30%); assays using the collected HIC fractions revealed a complete absence of active protein, with no difference between a control (no protein) and the fractions collected from the column. It is not clear whether the loss of activity can be attributed to the extended duration of time required for this two step purification, or is due to significant dilution of the active proteins.

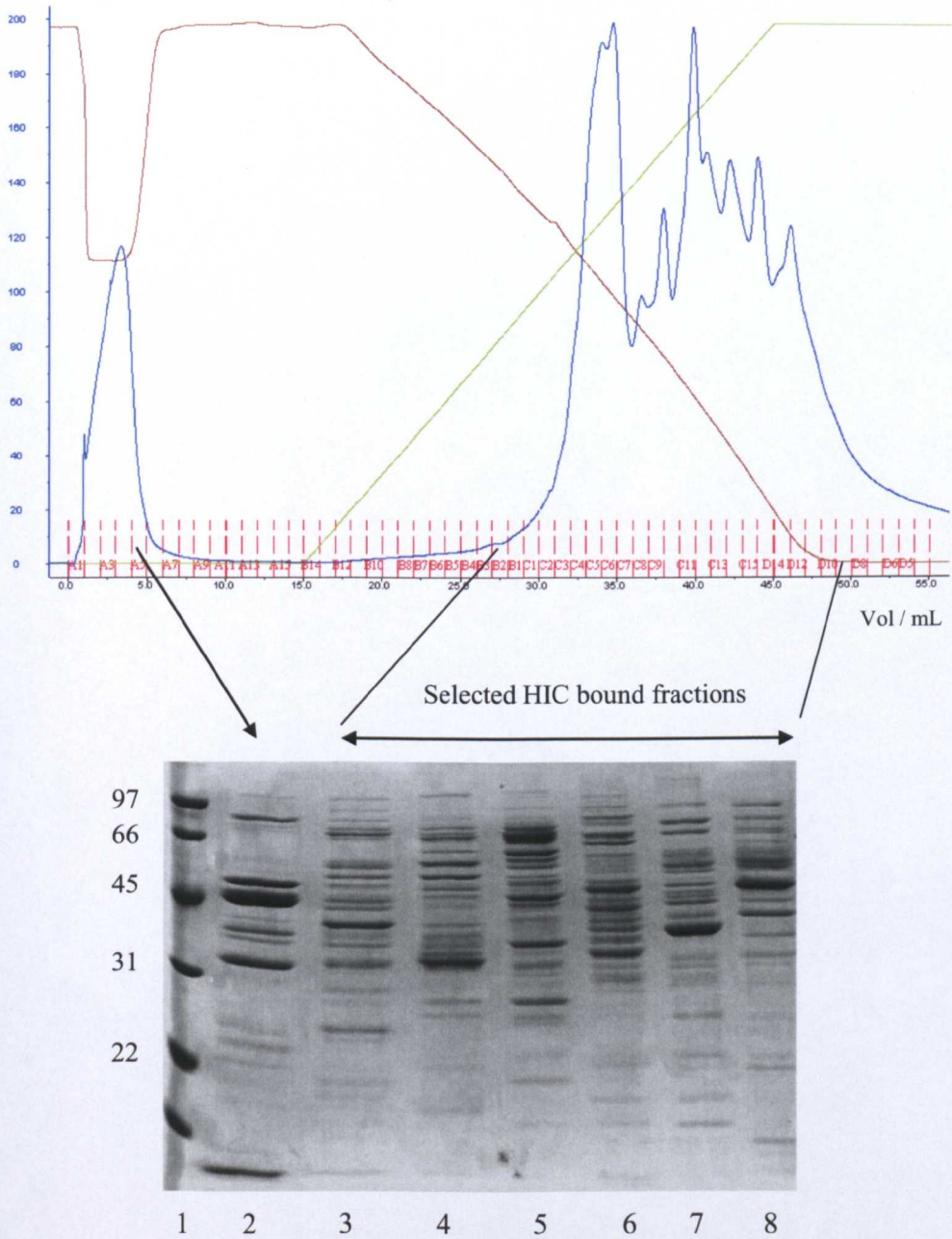


Figure 57: SDS-PAGE analysis of fractions collected from a second step of purification (HIC) lanes 2-8, which was run using the pooled *R*-selective fractions from the first step of anion exchange (FFQ) chromatography. BioRad molecular weight marker (kDa) lane 1.

An alternative method of protein purification was considered, which utilised an initial step of phenyl sepharose chromatography (column volume 10 mL). A gradient was run from 2 M $(\text{NH}_4)_2\text{SO}_4$ to 0 M, over a volume of 100 mL, with collection of 2 mL fractions. The protein containing fractions were found to elute over a salt concentration between 1.8-1.4 M $(\text{NH}_4)_2\text{SO}_4$ (fig. 57). Fractions eluting between 1.6-1.5 M showed activity towards the hydrolysis of linalyl acetate with a rate of conversion up to 7.5% (0.4 mM linalool generated) over a 2 h assay period with *ee* 28% (*S*)-linalool.

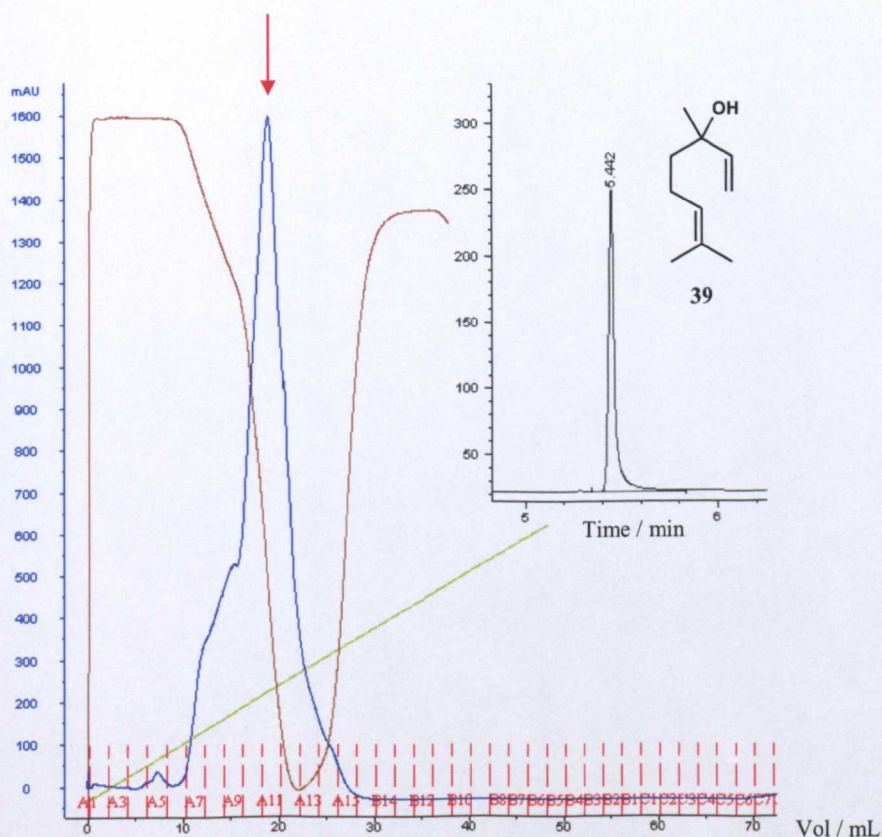


Figure 58: Chromatogram showing the first step of a two step purification strategy using a phenyl sepharose column (inset displaying the results of quantitative GC analysis with 0.4 mM linalool generated from activity testing of the highlighted fraction).

The fractions containing proteins active for the hydrolysis of linalyl acetate were pooled for attempts at further purification to homogeneity. With the previous elution from the phenyl sepharose column occurring at high salt concentrations, methods of removing this salt were investigated prior to running anion exchange chromatography to facilitate protein binding to a Mono Q resin. It was found that a greater concentration of protein was retained from an overnight dialysis in comparison to the use of a PD-10 desalting column; however it was also necessary to reduce the time of prolonged storage of protein solutions in the sub-cellular fractions which tended to reduce the observed activity of these esterases. Following the removal of ammonium sulphate *via* dialysis, the protein was bound to an anion exchange column (fig. 59), and an active 1 mL fraction eluted at 1.1 M NaCl. The rate of conversion for linalyl acetate hydrolysis after the same 2 h period was 4.1%, which is a 1.8-fold decrease in activity when compared to protein eluted from the first step of this purification. A prolonged 18 h incubation of this Mono Q fraction with linalyl acetate resulted in an 11% conversion to linalool. SDS-PAGE analysis in figure 60 shows that despite an enhanced level of enantioselectivity after this second step of purification *ee* 79% (*S*)-linalool (up from 28%) there is still a vast number of proteins present in this active fraction particularly in the 30-45 kDa molecular weight region (as revealed by SDS-PAGE analysis) typically associated with the microbial carboxyl esterases [Bornscheuer 2002]. A number of chromatographic methods were investigated for further purification of this active fraction however in each case activity of the esterase towards linalyl acetate could not be detected.

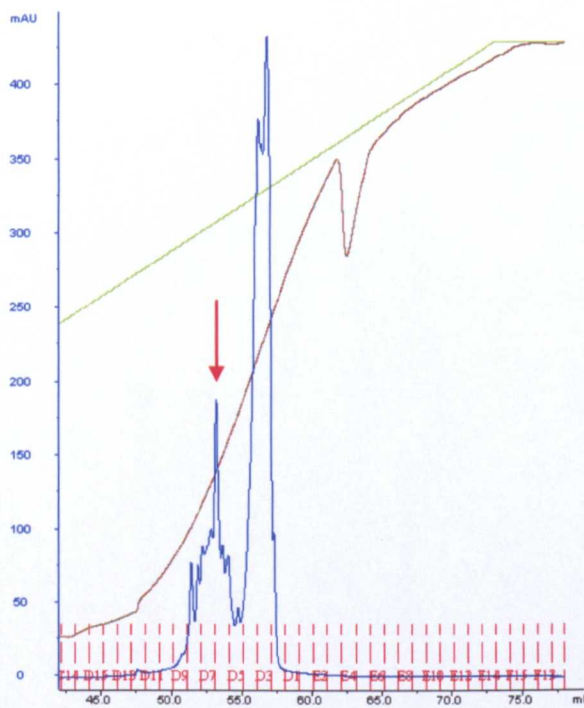


Figure 59: Anion exchange chromatography for the second step of a two step purification strategy using a 1 mL Mono Q column. GC analysis of the fraction showing activity is highlighted below.

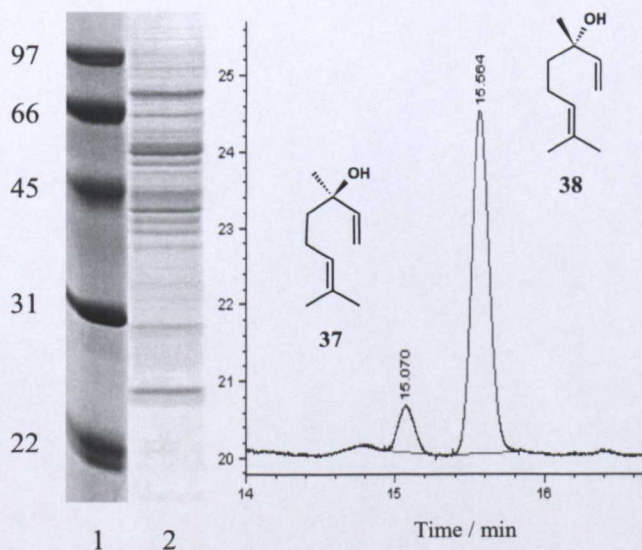


Figure 60: SDS-PAGE analysis (left) of a fraction collected from the second step of purification shows enhanced enantioselectivity towards the hydrolysis of linalyl acetate (*lane 2*). BioRad molecular weight marker (kDa) *lane 1*. Chiral GC analysis (right) showing an *ee* 79% (*S*)-linalool.

4.4. Conclusions

Through screening of 25 *Rhodococcus* strains for the biotransformation of linalyl acetate to the commercially desirable linalool there were four identified: *R. ruber* DSM 43338, *R. rhodochrous* 11Y, *R. aetherivorans* AM1, and *R. sp.* HS2 which demonstrated significant activity (15-50% conversion) when compared to the minimal activity observed in the remaining 21 strains and control assay (conversions up to 5%) towards this sterically demanding ester. In each case there was a predominant *S*- enantioselectivity (*ee* 15-20%) displayed in whole-cell assays. Cultures were found to be at their most active towards this hydrolysis when harvested in the late log-phase of the growth curve. Experiments whereby 1 mM *tert*-butyl acetate was added to *R. ruber* DSM 43338 cells in the early log-phase of growth revealed an induction of activity by 6-fold, yet sub-cellular extracts from induced and non-induced cells failed to clearly highlight the overexpression of any particular proteins in response to this induction which could have provided the information required for the start of a molecular biological approach towards these enzymes. Further attempts to induce activity with other bulky acetates (α -naphthyl acetate and tributyrin) and the substrate linalyl acetate did not lead to increases in the activity of resting cell biotransformations.

Traditional protein purification methods were employed to isolate enantioselective linalyl acetate esterases in each of these four active strains. After a single step of anion exchange chromatography the most interesting results were achieved with

extracts from *R. ruber* DSM 43338 whereby two distinct sets of fractions of opposing enantioselectivity were collected, with enantiomeric excess values ranging from 60% (*R*) to 76% (*S*). A two step purification strategy was developed utilising a phenyl sepharose column followed by anion exchange chromatography to yield a fraction which upon assaying for linalyl acetate hydrolysis showed an *ee* of 79% (*S*)-linalool. However despite running two columns, purification to homogeneity of an enantioselective esterase could not be achieved. Without a system of over-expressing the desired enzyme in this instance, it was found that the protein concentration became significantly reduced following successive rounds of purification despite using preparations of 10 L culture volume, with the consequential loss in esterase activity that was required for successful enzyme isolation from fractions of unknown proteins. The following chapter of work will describe an alternative gene-based approach towards achieving the target of an enantioselective linalyl acetate esterase.

5. Chapter 5: A gene-based approach towards an enantioselective esterase for linalyl acetate hydrolysis

5.1. Introduction

Whilst the stability of hydrolases in organic solvents and their stereoselectivity are advantageous, there are, however, only a few that will accept tertiary alcohol esters (TAEs) as substrates [Henke et al. 2002, 2003]. Linalyl acetate (fig. 61) has been used as a model substrate in literature examples for investigating carboxylesterase enantioselectivity towards chiral TAEs.

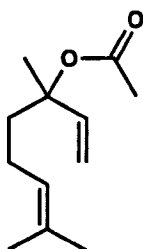


Figure 61: The chiral tertiary alcohol ester, linalyl acetate.

One reason suggested for the low enantioselectivity towards the acetate is due to the steric similarity of the methyl and ethenyl groups, which it is proposed, impedes the chiral recognition process [Pogorevc et al. 2000]. Studies using linalyl acetate as a model substrate have found that hydrolases containing a highly conserved GGG(A)X motif (located in the active site), are able to accept TAEs as substrates by stabilising

the tetrahedral intermediate formed during ester hydrolysis within an oxyanion hole (fig. 62) [Heinze et al. 2007]. The anionic carbonyl oxygen atom of the tetrahedral intermediate is stabilised by the formation of two hydrogen bonds provided by two amide groups of the protein backbone. Most esterases however contain a GX motif within the active site instead, whereby the bulky residue (X) forming the hydrogen bond prevents TAEs from binding. Comparison of a number of GGG(A)X and GX structures in literature sources [Kourist et al. 2008, Henke et al. 2002, 2003] showed that the alcohol binding pockets in GGG(A)X hydrolases are 1.5-2Å wider than in GX structures, due to the carbonyl oxygen atoms of the flexible triple glycine motif lying parallel to the wall of the binding pocket thus creating more space for TAEs substrates.

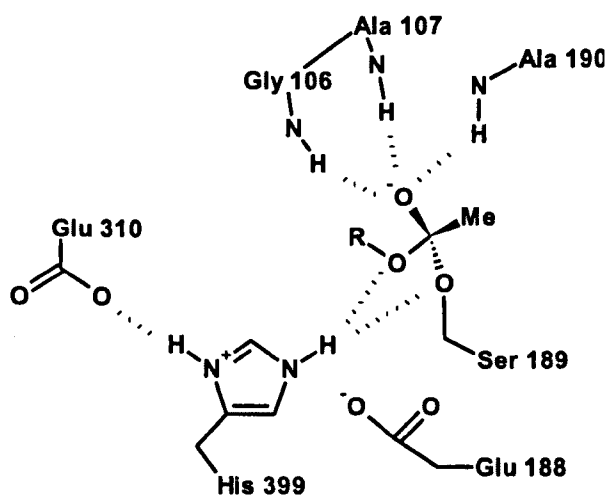


Figure 62: Representation of the tetrahedral intermediate formed within the active site of *Bacillus subtilis* esterase BS2 from Heinze et al. 2007.

This conserved GGG(A)X motif has been used as a target for identifying TAE with high enantioselectivity from environmental DNA libraries [Kourist et al. 2007].

Esterases found to contain this motif were screened for activity with a number of TAEs including linalyl acetate. An enantiomeric excess of 54% for the product (*S*)-linalool was yielded from the hydrolysis of linalyl acetate, with a selectivity *E* of up to 5 in some cases.

A number of methods have been used to improve the enantioselective resolution of tertiary alcohols [Bornscheuer et al. 2002, Bartsch et al. 2008]. An esterase from *Bacillus subtilis* identified as containing this GGG(A)X motif showed activity towards a number of tertiary alcohol esters, and was used as a model for studies aiming to improve and alter the enantioselectivity of these biotransformations. Changes in substrate structure and physical parameters of the reaction system, as well as directed evolution techniques, are among those methods that have been tried for these purposes. The published sequence (Swiss-Prot entry no: PNBA_BACSU) corresponding to this enzyme is shown in figure 63 with the arrangement of active site residues in this esterase shown in figure 64. This sequence forms the basis for a gene based approach towards an enantioselective esterase from the *R. ruber* DSM 43338 strain that was shown in the previous chapter to possess enantioselective activity towards linalyl acetate. The results of protein purification in chapter 4 suggested that esterases of complementary enantioselectivity for this hydrolysis are to be found in this strain of *Rhodococcus*. The aim of the work in this chapter was to clone potential tertiary alcohol esterases that confer this activity already demonstrated in the wild-type strain of *R. ruber* DSM 43338. The cloning of GGG(A)X motif

esterases (N1-3) from the closely related Actinomycete *Nocardia farcinica* for which the genome sequence is known, and (S1) from *Sulfolobus tokodaii*, for which genomic DNA is also available will be targeted as well. A method of over-expressing a recombinant esterase with enantioselective activity towards linalyl acetate would therefore offer a potentially desirable route towards ‘natural’ homochiral linalool.

```
MTHQIVTTQYGKVKGTTENGVHKWKGIPYAKPPVGQWRFKAPEPPEVWEDVLDATAYGSI
CPQPSDLLSLSYTELPRQSEDCLYVNVFAPDTPSKNLPVMVWIHGGA FYLGAGSEPLYDGG
SKLAAQGEVIVVTLNRYLGPFGFLHLSSFNEAYS DNLGLLDQAAA LKVVRENI SA FGGDP
DNVTVFGE SA GGMS IA ALLAMPAAKGLFQKAIMESGASRTMTKEQAASTSA AFLQVLGIN
EGQLDKLHTVSAEDLLKAADQLRIA EKENIFQLFFQPALDPKTLPEEPEKAI AEGAASGI
PLLIGTTRDE GYLFFTPDS DVHSQETLDAALEYLLGKPLAEKVADLYPRSLESQIHMMTD
LLFWRPAVAYASAQSHYAPVWMYRFDWHPKPKPPYNKAFH ALELPFVFGNLDGLERMAKAE
ITDEVKQLSHTIQSAWITFAKTGNPSTEAVNWPAYHEETRETLILDSEITIENDPESEKR
QKLFPSKGE
```

Figure 63: Peptide sequence of the GGG(A)X motif *Bacillus subtilis* *p*-nitrobenzyl esterase (BS2). The conserved oxyanion hole residues are shown in blue, and catalytic triad in red, with the GGG(A)X motif underlined.

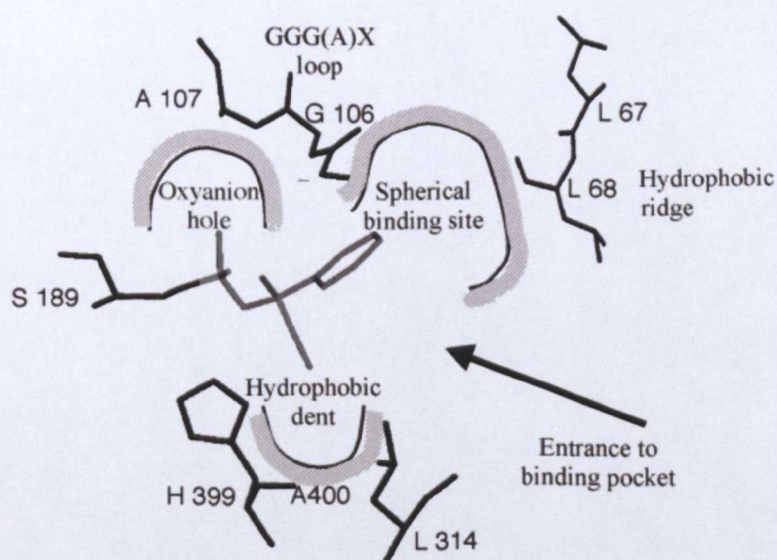


Figure 64: Binding of the TAEs 2-phenyl-3-butin-2-yl acetate in the active site of WT *Bacillus subtilis* *p*-nitrobenzyl esterase from [Henke et al. 2003].

5.2. Experimental

5.2.1. PCR for potential tertiary alcohol esterases from *R. ruber* DSM 43338

A standard PCR mixture contained 0.4 μM of forward and reverse primers (ordered from MWG), 0.2 mM dNTPs, 1 μL KOD hot start DNA polymerase (1 unit/ μL), 1 mM MgSO_4 , 5 μL 10x buffer, 50 ng template DNA, 5% v/v DMSO, and water to 50 μL . Thermocycling conditions were as follows: initial denature 4 min at 94°C, followed by 35 cycles of: denature 1 min at 94°C, annealing 1.5 min at 48°C, and extension 1.5 min at 72°C, with a final extension step 3 min at 72°C. For optimisation in individual reactions changes were made to the concentration of MgSO_4 (0.5-2.5 mM), DMSO (0-15% v/v), and annealing temperature (45-70°C). For the use in touchdown PCR programs a decreasing annealing temperature (-1°C per cycle) was used.

Primers for 300bp fragment:

CAT for: 5'-CCAGGGACCAGCAATGGTCTKSATCCACGGCGGCGCCTAC-3'

CAT rev: 5'-GAGGAGAAGGCGCGTTAGCCGGCCGACTCGCCGAAGACGGTGAC-3'

Primers for 1100bp fragment:

CAT for: 5'-CCAGGGACCAGCAATGGTCTKSATCCACGGCGGCGCCTAC-3'

R2: 5'-GAGGAGAAGGCGCGTTACGGGGTGCCSTGACKGGCGAAGTGCAGCCA-3'

Primers for touchdown PCR:

F9/9: 5'-CCAGGGACCAGCAATGGGCATCCCGTACGCCGCCGCCCG-3'
R9/9: 5'-GAGGAGAAGGCGCGTTACGGGGTGCCGTGCGAGGCGAA-3'

Primers for nested PCR – round 1:

Q5 For: 5'-CCAGGGACCAGCAATGGCAGGGGTGGTCCGCCGCCGGCGC-3'
Q6 For: 5'-CCAGGGACCAGCAATGGCCGGCGCCGTCCGAGGACGCCGG-3'
R2: 5'-GAGGAGAAGGCGCGTTACGGGGTGCCSTGACKGGCGAAGTGCAGCCA-3'
R1a: 5'-GAGGAGAAGGCGCGTTAGCGGCGCTCGCSGHSCGGGTC-3'
R9/9: 5'-GAGGAGAAGGCGCGTTACGGGGTGCCGTGCGAGGCGAA-3'

Primers for nested PCR – round 2:

F1: 5'-CCAGGGACCAGCAATGTGGAAGGGCATCCCGTWCGCCGCCSCGCCGGT-3'
F2: 5'-CCAGGGACCAGCAATGTGGCGCGGCATCCCGTACGCCGCCCGCCGGT-3'
F3: 5'-CCAGGGACCAGCAATGTTCTGGGCATCCCGTACGCCGCCGCCCGGC-3'
F9/9: 5'-CCAGGGACCAGCAATGGGCATCCCGTACGCCGCCGCCCG-3'
CATrev: 5'-GAGGAGAAGGCGCGTTAGCCGGCCGACTCGCCGAAGACGGTGAC-3'

(where K = G or T; S = G or C; W = A or T; H = A or T or C)

5.2.2. Inverse PCR approach to a full length gene

5.2.2.1. Digestion and re-ligation of template DNA

In a 140 μ L incubation: 4 μ g of *R. ruber* DSM 43338 DNA, 14 μ L 10x NE buffer 1, 1.4 μ L 100x BSA, and 10 μ L *Sac I* restriction enzyme (20 unit/ μ L activity) were added before incubating at 37°C o/n. The restriction enzyme was heat inactivated at

65°C for 20 min, before PCR clean-up was used to purify the DNA to 50 ng/μL. 24 μL of the *Sac I* digested DNA was incubated at 16°C o/n with 3 μL 10x ligase buffer, and 2 μL T4 DNA ligase (400 unit/μL activity).

5.2.2.2. Inverse PCR

Primers:

Inverse For: 5'-ATGGTCTGGATCCACGGCGGCGCCTAC-3'

Inverse rev: 5'-CACGGCATTGCCCGCGGCGACTCGCC-3'

Each 50 μL PCR volume contained: 0.4 μM of forward and reverse primers (ordered from MWG-Eurofins), 0.2 mM dNTPs, 1 μL KOD hot start DNA polymerase (1 unit/μL), 1.5 mM MgSO₄, 5 μL 10x buffer, 50 ng template DNA, 10% v/v DMSO, and water to 50 μL. Thermocycling conditions were as follows: initial denature 4min at 94°C, followed by 15 cycles of: denature 1 min at 94°C, annealing 1 min at 70°C (-1°C per cycle), and extension 2.5 min at 72°C; followed by 20 cycles of: denature 1 min at 94°C, annealing 1 min at 55°C, and extension 2.5 min at 72°C with a final extension step 10 min at 72°C. Re-amplification of round 1 PCR was carried out using a 1/10,000 dilution of this initial reaction as a template for a second PCR whereby the extension time was increased to 5 min per cycle.

5.2.3. PCR for potential tertiary alcohol esterases from *Nocardia farcinica* (N1-3) and *Sulfolobus tokodaii* (S1)

Primers:

Sulfolobus (for): 5'-CCAGGGACCAGCAATGATAGACCCTAAAATTAAAAATTA-3'

Sulfolobus (rev): 5'-GAGGAGAAGGCGTTATTCTTTTCATAAAATGCCTTTTATT-3'

Nocardia (F1): 5'-CCAGGGACCAGCAATGGTGGCAACGATCGACATCACGACC-3'

Nocardia (R1): 5'-GAGGAGAAGGCGTTAGCAGTCCCACGGCTGGGACTGGACT-3'

Nocardia (F2): 5'-CCAGGGACCAGCAATGACCATCCGATACGACACCACCGTC-3'

Nocardia (R2): 5'-GAGGAGAAGGCGTTAGCTGGTCCGCCAGCCGAAGTCGACT-3'

Nocardia (F3): 5'-CCAGGGACCAGCAATGGACAACGTGGTCTGAAGCGCCCTCG-3'

Nocardia (R3): 5'-GAGGAGAAGGCGTTATGCACGGCAAGCTGTCGAGGGGACT-3'

Each 50 μ L PCR volume contained: 0.4 μ M of forward and reverse primers (ordered from MWG), 0.2 mM dNTPs, 1 μ L KOD hot start DNA polymerase (1 unit/ μ L), 1 mM MgSO₄, 5 μ L 10x buffer, 50 ng template DNA, 10% v/v DMSO, and water to 50 μ L. Thermocycling conditions were as follows: initial denature 4 min at 94°C, followed by 35 cycles of: denature 1 min at 94°C, annealing 1 min at 55°C, and extension 1.5 min at 72°C, with a final extension step 3 min at 72°C.

5.2.4. Whole cell activity test for the hydrolysis of linalyl acetate, using over-expressed N2 and N3 esterases

Single colonies of B834 (transformed with N2) and BL21 (transformed with N3) *E. coli* cells were used to inoculate 25 mL cultures of LB containing kanamycin (30 µg/mL) and incubated at 37°C until an optical density (OD) A_{600nm} 0.5 when expression was induced with the addition of IPTG (0.1 mM). Negative controls included incubations without cells, and BL21 cells transformed with just the vector (no insert). The cells were incubated for a further hour at 30°C before the substrate linalyl acetate was added (1 µL/mL). Samples were extracted for GC analysis over a period of 16 h with EtOAc.

5.2.5. Purification of soluble N3 esterase

5.2.5.1. Preparation of soluble protein

500 mL cultures of BL21-N3 grown in LB (kanamycin 30 µg/mL) at 37°C until an OD 0.5, before inducing with IPTG (0.1 mM) and growing overnight at 18°C. A 2 L culture volume was harvested using a Sorvall RC5B – GS3 (6,000 x g, 45 min, 4°C) and the cell pellet re-suspended in 80 mL of 50 mM Tris / HCl, 300 mM NaCl, pH 7.1 buffer. The cells were lysed by sonication for 3 x 40 s. The cell debris was removed by centrifugation using a Sorvall RC5B – SS34 (34,500 x g, 20 min, 4°C)

before retaining the soluble cell extract which was filtered using a 0.45 μm filter (Millipore – PES membrane).

5.2.5.2. Nickel column purification of N3 (1st step)

A 5 mL HiTrap chelating Ni column was pre-equilibrated with 25 mL of 0.1 M Ni_2SO_4 followed by 25 mL of the re-suspension buffer (50 mM Tris / HCl, 300 mM NaCl, pH 7.1). The filtered cell extract was loaded, and the unbound protein eluted in a 30 mL wash with 30 mM imidazole (50 mM Tris / HCl, 300 mM NaCl, pH 7.1). A gradient from 30-500 mM imidazole was run over a volume of 100 mL. The bound protein N3 eluted over the range of 250-300 mM imidazole.

5.2.5.3. Gel filtration of N3 (2nd step)

A Superdex HiLoad S200 16/60 gel filtration column was pre-equilibrated with 50 mM Tris/HCl buffer (pH 7.1) containing 300 mM NaCl. 2 mL of concentrated pooled Ni column fractions was loaded and run with the same buffer. 5 mL fractions were collected with the N3 protein eluting at ~80 mL.

5.2.6. Study of purified N3 esterase kinetics with *p*-nitrophenyl acetate

Into a quartz cuvette containing 960 μL of the 50 mM Tris/HCl, 300 mM NaCl, resuspension buffer (pH 7.1), 20 μL of *p*-nitrophenyl acetate (pNPA) (final concentrations from 0-8 mM) dissolved in EtOH was added then shaken before taking a baseline absorbance reading at 412 nm over a period of 1 min. 20 μL of a 0.4 mg/mL solution of purified N3 esterase (final concentration 8 $\mu\text{g}/\text{mL}$) was then added and the cuvette shaken before measuring the increase in absorbance due to *p*-nitrophenol ($\epsilon = 14,200 \text{ M}^{-1}\text{cm}^{-1}$) release over a period of 3.5 min.

5.2.7. Activity tests with purified N3 esterase

The purified esterase in 50 mM Tris/HCl buffer (pH 7.1) containing 300 mM NaCl was utilised at concentrations between 0.4 – 1.0 mg/mL for 1.5 mL incubations shaken at 30°C and 37°C in sealed screw-cap glass vials. The substrates (citronellyl-, lavandulyl-, terpinyl-, menthyl- and linalyl acetates) were added (1 $\mu\text{L}/\text{mL}$) and 250 μL samples extracted for GC analysis with an equal volume of EtOAc over a time-course. Assays for the enzyme activity towards (\pm)-menthyl acetate at 22°C were conducted in a 25 mL round-bottom flask connected to a stoppered reflux condenser. A stirred 5 mL volume of 0.4 mg/mL enzyme in buffer was used, and 1 $\mu\text{L}/\text{mL}$ substrate added before extraction of samples as before over a period of 48 h. Control reactions were prepared in each assay, without the presence of enzyme.

5.2.8. GC analysis of monoterpene acetate hydrolysis

Chiral gas chromatographic analysis of samples using an Agilent Technologies cyclosil-B column (length 30 m, internal diameter 0.25 mm, film 0.25 μm) was performed using an Agilent GC 6890N. 2 μL samples were injected at 250°C in the split mode. An isothermal oven temperature of 115°C was maintained for 35 min, with a flow rate of helium 10 mL/min. Under these conditions, the retention times (min) were as follows: 1*R*-(-)-menthyl acetate (24.94), 1*S*-(+)-menthyl acetate (28.61), 1*R*-(-)-menthol (29.82), 1*S*-(+)-menthol (29.28), *R*-(-)-lavandulyl acetate (23.25), *S*-(+)-lavandulyl acetate (23.56), *R*-(-)-lavandulol (23.99), and *S*-(+)-lavandulol (22.38). The enantiomeric ratio (*E*-value) was calculated as described by Chen et al. 1982.

Analysis of samples using an Agilent Technologies J&W HP5 column (length 30 m, internal diameter 0.32 mm, film 0.25 μm) was again performed using an Agilent GC 6890N. 2 μL samples were injected at 250°C in the split mode. An initial oven temperature of 60°C was increased through a 10°C/min gradient to 200°C, with a flow rate of the carrier gas helium at 10 mL/min. Under these conditions, the retention times (min) were as follows: menthyl acetate (8.6), menthol (6.8), lavandulyl acetate (8.5), lavandulol (6.7), citronellyl acetate (9.4), citronellol (7.6), linalyl acetate (8.0), linalool (5.7), terpinyl acetate (9.4), α -terpineol (7.1).

5.3. Results and discussion

5.3.1. Cloning of potential tertiary alcohol esterases from *R. ruber* DSM 43338

The results from chapter 4 of this thesis showed the WT strain of *R. ruber* DSM 43338 to possess activity towards the hydrolysis of linalyl acetate. Whilst purification attempts did not result in the isolation of a single protein, they did uncover fractions of heterogeneous protein displaying opposite enantioselectivity towards this hydrolysis. An alternative gene-based approach towards obtaining enantioselective linalyl acetate hydrolases from the *R. ruber* DSM 43338 strain was attempted in this section of work. The results of a BLAST search of the closely related *Rhodococcus* RHA1 genome [McLeod et al. 2006] sequence using the *Bacillus subtilis* *p*-nitrobenzyl esterase are shown in figure 65, with subsequent alignment of carboxylesterase sequences that were found. The conserved oxyanion hole residues are shown in blue, and catalytic triad in red. This sequence information was used for two different approaches towards cloning of tertiary alcohol esterases from *R. ruber* DSM 43338. The first method used PCR primers designed against fairly well conserved regions of the peptide sequence which were located towards the N- and C-terminals. The sequence used for the design of these primers is highlighted in yellow (N-) and green (C-) on figure 65. The PCR primers were designed using an RHA1 codon usage table as the 43338 genome had not been sequenced.

Amplified gene sequences were to be inserted into the cleavable N-terminal His-tagged pET-YSBLIC3C vector using a ligation independent cloning (LIC) protocol [Aslanidis et al. 1990]. Ligation independent cloning has developed into an important and convenient method for the generation of novel recombinant biocatalysts [Bonsor et al. 2006]. In this instance, initial amplification of the DNA by PCR is carried out using primers with an overhanging LIC specific sequence attached. Separate incubations of the PCR product and linear pET-YSBLIC3C vector with a T4 polymerase plus adenine and thymine nucleotides respectively, creates complementary single stranded overhangs from the LIC specific sequence, *via* the natural 3'-5' exonuclease activity of this enzyme. This process facilitates subsequent annealing of the T4 polymerase treated insert and vector, prior to transformation into *E. coli*. An overview of this LIC process is shown in figure 26 of the general materials and methods section (chapter 2).

For design of the PCR primers a start codon (ATG) was added in the forward direction along with the LIC specific sequence. Reverse primers were designed against the complementary C-terminus strand with a LIC specific sequence added containing a stop codon (TTA – reverse direction). A number of PCR experiments were performed using different pairs of degenerate primers under various conditions (changes in annealing temperature / time, MgSO₄ concentration and DMSO %); however there appeared to be a lot of non-specific binding using these primers with smearing on agarose gels, and no clear bands to suggest a single PCR product.

Chapter 5: A gene-based approach towards an enantioselective esterase for linalyl acetate hydrolysis

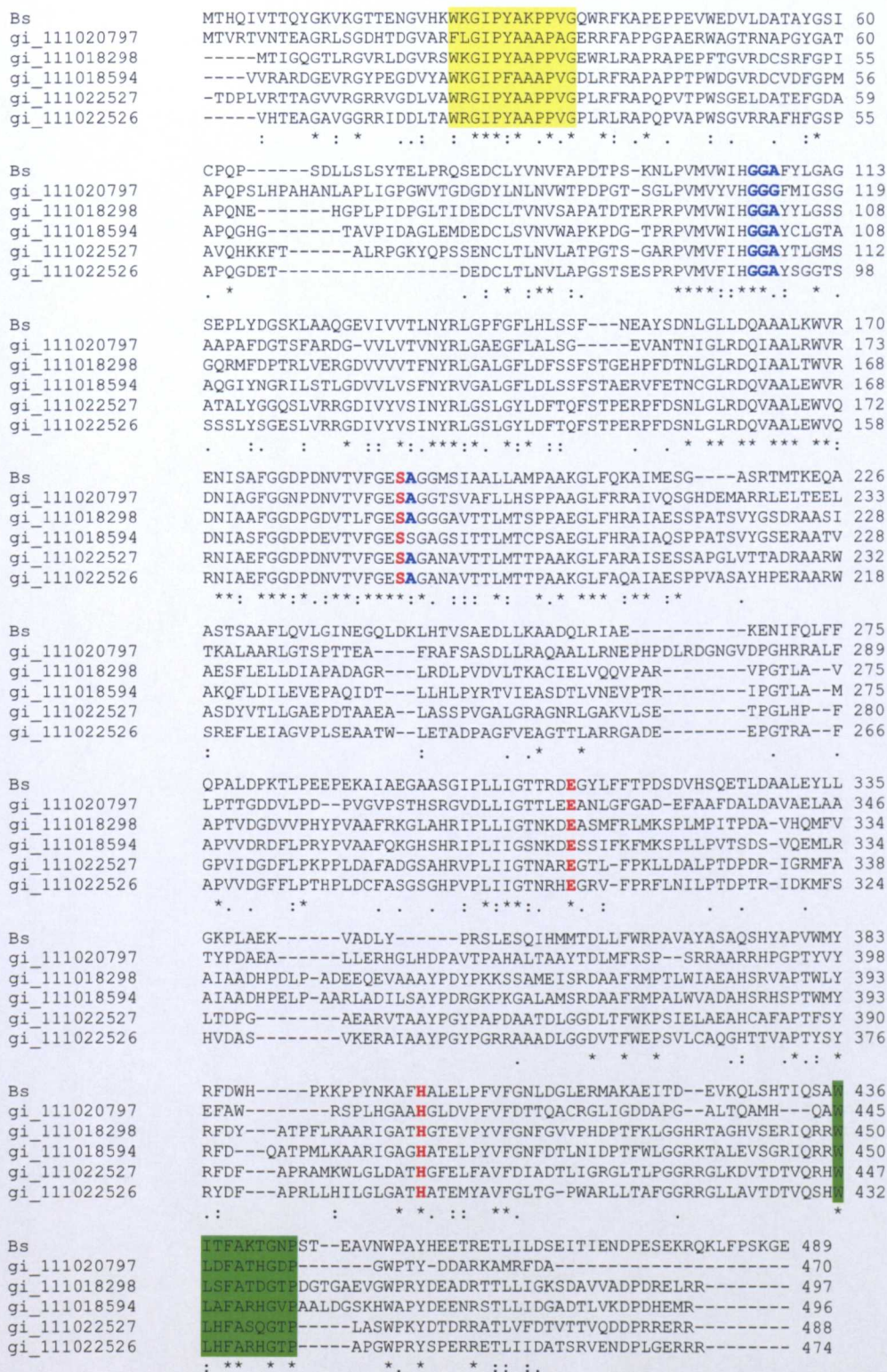


Figure 65: Sequence alignment of BS2 esterase with homologues from RHA1 showing the conserved catalytic triad (red) and oxyanion hole residues (blue). Regions for design of initial degenerate PCR primers (yellow and green).

The second approach towards the cloning of tertiary alcohol esterases from *R. ruber* was initially targeted at a smaller fragment in the sequence which contains regions highly conserved in carboxyl esterases. PCR primers were again designed using an RHA1 codon usage table. The forward primer (CATfor) was designed from a methionine (ATG start codon). The sequence for this forward primer encodes within it three amino acids which are involved in formation of the oxyanion hole in these enzymes (fig. 66). The reverse primer (CATrev) was designed against the complementary C-terminus strand, encoding the catalytic serine, and a conserved alanine residue involved in the formation of the oxyanion hole (fig. 66). Optimisation of PCR conditions (5% DMSO added, 48.2°C annealing temperature) led to a product of ~300bp being observed (fig. 67A).

Forward primer against:

MV (W/F) IH GGAY	Bs	PVMVWIH GGA FYLGAG 113
	gi_111020797	PVMVYVH GGG FMIGSS 119
	gi_111018298	PVMVWIH GGAY YLGS 108
	gi_111018594	PVMVWIH GGAY CLGTA 108
	gi_111022527	PVMVFIH GGAY TLGMS 112
	gi_111022526	PVMVFIH GGAY SGGTS 98
		****:****: * .

Reverse primer against:

VTVFGE SAG	Bs	ENISAFGGDPDNTVFGE SAG GMSIAALLA 196
	gi_111020797	DNIAGFGGNPDNTVFGE SAG GTSVAFLLH 203
	gi_111018298	DNIAAFGGDPDVTLFGE SAG GGAVTTLMT 198
	gi_111018594	DNIASFGGDPDVTVFGE SAG SAGSITLMT 198
	gi_111022527	RNIAEFGGDPDNTVFGE SAG ANAVTTLMT 202
	gi_111022526	RNIAEFGGDPDNTVFGE SAG ANAVTTLMT 188
		** : ** : * . : ** : ** : * . : : : * :

Figure 66: The design of PCR primers towards highly conserved regions in the sequence of a potential tertiary alcohol esterase. The oxyanion hole residues are shown in blue, and catalytic triad in red.

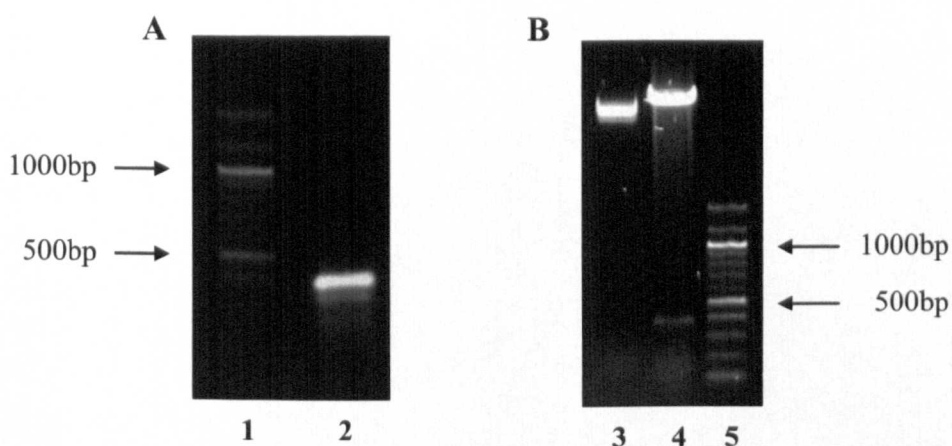


Figure 67: (A) Results of PCR showing a ~300bp product (*lane 2*). (B) A restriction digest following ligation independent cloning. *Lane 3* shows an uncut plasmid (–restriction enzyme control), and *lane 4* the digested plasmid containing the ~300bp insert.

The band at ~300bp from the above PCR experiment was cut out, extracted from the gel, and concentrated prior to carrying out ligation independent cloning and transformation into competent *E. coli* Novablue cells (as described in chapter 2). Transformed cells were plated onto LB agar + kanamycin and incubated overnight. A single colony which had grown on the plate was picked to inoculate a 5 mL overnight culture, prior to extracting the plasmid using a miniprep kit. A restriction digest (fig. 67B) with *NcoI* and *NdeI* showed the colony contained the LIC vector with this ~300bp insert. The information gained from sequencing was used in an alignment which showed a number of carboxylesterases sharing a high percentage sequence homology in this cloned region of the gene (fig. 68).

(A)

MVWIHGGAYVLGYSGQRIYDGRLLAERGDVVVVTVNYRLGALGFLDFS
SFSTAGTTFESNVGLRDQIAALEWVRDCISAFGGDPDRVTVFGESAG

(B)



Figure 68: (A) Results of sequencing the cloned esterase gene fragment. Underlined regions correspond to forward and reverse primer binding regions. The oxyanion hole residues are shown in blue, and conserved serine from the catalytic triad shown in red. Total length of the sequence is 288bp. (B) Results of BLAST with the sequenced 288bp fragment shown above.

The majority of carboxyl esterases particularly those identified in previous sequence alignments with *Rhodococcus* RHA1 are of the order 1500-1600bp (~50-60 kDa). Whilst the initial attempt to clone a full length sequence with pairs of degenerate N- and C- terminal primers did not yield any specific products, it could be possible to achieve this aim by using this cloned 288bp fragment as a starting point. The following experiments aimed to build upon these results of cloning so far.

Sequencing of the cloned 288bp fragment using the primers designed towards the highly conserved catalytic motifs confirmed that both the forward and reverse primers were binding their complementary sequence within the 43338 DNA template. A range of PCR experiments (at different annealing temperatures and times) was carried out using one of these conserved region primers with corresponding N/C terminal primers so as to extend the length of gene sequence that can be amplified from PCR:

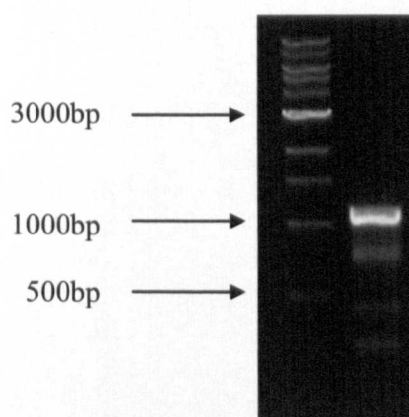


Figure 69: PCR results using the CAT forward primer with reverse primer 2 (C-terminal), at an annealing temperature of 53°C.

Four PCR products at approximately 250, 400, 800, 1100bp were observed when using the CAT forward primer (conserved motif) in combination with reverse primer 2 (C-terminal) (fig. 69). Optimal PCR conditions for generation of these products were with an annealing temperature of 53°C, and the addition of 10% DMSO. Looking at the length of gene sequence for a RHA1 carboxylesterase contained within these primers (fig. 70) reveals a potentially larger fragment of 369 amino acids (hence 1107bp), making the PCR product at ~1100bp (above) of considerable interest.

```
MTIGQGTLRGVRLDGVRSWKGI PYAAPPVGEWRLRAPRAPEPFTGVRDCSRFGPIAPQNE
-----HGPLPIDPGLTIDEDCLTVNV SAPATDTERPRPV MVWIHG GAY YLGSSGQRMFD
PTRLVERGDVVVTFNYRLGALGFLDFSSFSTGEHPFDTNLGLRDQIAALTWVRDNIAAF
GGDPGDVTLFGESAGGGAVTTLMTSPPAEGLFHRAIAESSPATSVYGS DRAASIAESFLE
LLDIAPADAGRLRDL PVDVLT KACIELVQQV PARVPGTLAVAPTVDGDVVPHY PVAAFRK
GLAHRIPLLI GTNKDEASMFRLMKS PLMPITPDA-VHQM FVAIAADHPDL PADEEQEVAA
AYPDYPKKSSAMEISRDAAFRMPTLWIAEAHSRVAPTWLYRFDY---ATPFLRAARIGAT
HGTEVPYVFGNFGVPHDPTFKLGGHRTAGHVSERIQRR WLSFATDGT DGTGAEVGPWR
YDEADRTLLIGKSDAVVADPDRELRR
```

Figure 70: Sequence for the probable carboxylesterase (ref: gi 111018298) from RHA1 with the sequences for binding with the forward CAT primer (pink), and reverse primer 2 (green) highlighted. The binding of primers to such positions should yield an 1107bp PCR product.

The PCR product at 1100bp was cut out, extracted from the agarose gel, and concentrated prior to ligation independent cloning into the pET-YSBLIC vector and transformation into competent Novablue cells. Transformed cells were plated onto LB agar + kanamycin and incubated overnight. Ten colonies had grown on the agar plate, of which four were picked to inoculate 5 mL overnight cultures, prior to extracting the plasmid using a miniprep kit. A restriction digest (fig. 71) with *NcoI* and *NdeI* showed colonies to contain the LIC vector with this ~1100bp insert. A sample of this DNA was submitted for sequencing (fig. 72). The information gained from this was used for BLAST (fig. 72). The six sequences showing the highest degree of homology to the sequenced 1107bp fragment included carboxylesterases from the closely related *Rhodococcus* sp. RHA1 and other Actinobacteria including *Nocardia farcinica* and *Clavibacter michiganensis*. These sequences were then aligned against each other (fig. 73) to assist in the design of PCR primers towards the most conserved regions.

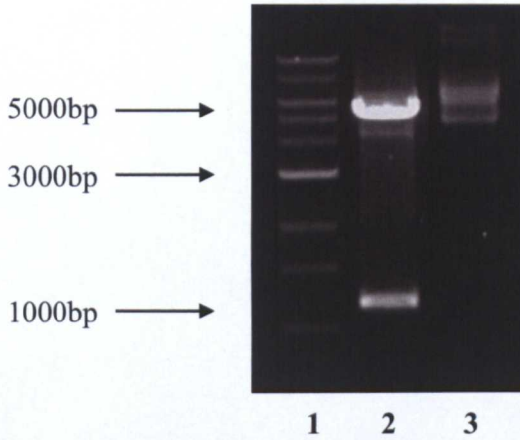


Figure 71: Agarose gel after running a restriction digest. *Lane 1:* DNA ladder. *Lane 2:* Digested plasmid with ~1100bp insert. *Lane 3:* Uncut plasmid (– restriction enzyme control).

MVWIHGGAYTLGTTALPLYGGESLVRRGDLIYVSINYLRLGSLGYLDFTEFSTAERPFDNS
 LGLRDQVAALAWVRRNIAAFGGDPDNITIFGESAGGNAVTTLLATPAAEGLFARAVAQSS
 APNLVVDAEHAAEWARRFVELLGADRDSAVEALGSATPVDFGRAARRLSGRILHETPGLH
 AFGPVVDGDYLPPTTVEAYETGAAHRVPLVIGTNAREGLTFPRVLDALPTNQLRIEQMFG
 LTDPTAQERVVAAYPGYPDARAAVDLGGDLTFWHPSIEIAQAHSRHAPTYSYRFDYAPPL
 LRWTGFHATHAFELLSVFGQADTALGRVVTAAGRRALRTVSDAVQRQWLHFASHGTF

Db AC	Description	Score	E-value
tr Q08545	_RHOSR Carboxylesterase (EC 3.1.1.1) [RHA1_ro05561] [Rh...	363	1e-98
tr Q08546	_RHOSR Carboxylesterase (EC 3.1.1.1) [RHA1_ro05560] [Rh...	301	4e-80
tr A5C5S8	_CLAM3 Carboxylesterase (EC 3.1.1.1) [lipT] [Clavibacte...	263	1e-68
tr Q5YPM0	_NOCFA Putative carboxylesterase [nfa50190] [Nocardia f...	263	2e-68
tr B0RGS7	_CLAMS Putative carboxylesterase [CMS1144] [Clavibacter...	262	2e-68
tr A4TB12	_MYCGI Carboxylesterase, type B [Mflv_3125] [Mycobacter...	258	5e-67
tr Q73223	_MYCPA LipT [lipT] [Mycobacterium paratuberculosis]	253	1e-65
tr AOQFHO	_MYCA1 LppT protein [MAV_2466] [Mycobacterium avium (st...	253	1e-65
tr AOQ201	_MYCS2 Para-nitrobenzyl esterase (EC 3.1.1.-) [MSMEG_38...	251	6e-65
tr A1TAK4	_MYCVP Carboxylesterase, type B [Mvan_3408] [Mycobacter...	244	7e-63

Figure 72: The results of sequencing for the cloned 1107bp fragment and BLAST for those genes sharing a high degree of homology.

Chapter 5: A gene-based approach towards an enantioselective esterase for linalyl acetate hydrolysis

```

tr|Q0S545|Q0S545_RHOSR_Carboxy  -----MASDTLTTDPLVRTTAGVVGRRRVGDLVAWRGIP
tr|Q0S546|Q0S546_RHOSR_Carboxy  -----MSALEVHTEAGAVGRRIDDLTAWRGIP
tr|B0RGS7|B0RGS7_CLAMS_Putativ  MRADRKLDVRTSDADVPTPAYDPSELDVEVTGGTVRGVREERGIEAWRGIP
tr|A4TB12|A4TB12_MYCGI_Carboxy  -----MVRQAGREFDVTGVMHEHTVVRVKIASGTVEGFTRDGVVHRWSIP
tr|Q73Z23|Q73Z23_MYCPA_LipT_OS  -----MRARRRRHVGYRRFMHRTVRRATATGIVEGFTRDGVVHRWSIP
tr|Q5YPM0|Q5YPM0_NOCFA_Putativ  -----MVATIDITTAGVVGRRRGRRVLRWRALP
                                  * * * : *.:*

tr|Q0S545|Q0S545_RHOSR_Carboxy  YAAPPVGPLRFRAPQVPTPWSGELDATEFGDAAVQHKKFTALRPG----K
tr|Q0S546|Q0S546_RHOSR_Carboxy  YAAPPVGPLRLRAPQVAPWSGVRRAFHFGSPAPQ-----
tr|B0RGS7|B0RGS7_CLAMS_Putativ  FAAPPRGDLRFRAPQVLVGWEGARFAQHFGKVAPQVSAGAFMGAP----Q
tr|A4TB12|A4TB12_MYCGI_Carboxy  YARPPVGPLRYRPRPVQPWPGVRYCHGFGACAPQRMYTLLAPG----R
tr|Q73Z23|Q73Z23_MYCPA_LipT_OS  YARPPVGDLRFRAPQPAQPWSGVRHCHGFANCAPQRRYTLLGLSLGGR
tr|Q5YPM0|Q5YPM0_NOCFA_Putativ  YAAPPVGELRFRAPQVQWSGVRDEFASASFQHRGGARIGAR----T
                                  : * * * * * * * * * . * * . * . : *

tr|Q0S545|Q0S545_RHOSR_Carboxy  YQPSSENCLTLNVLATP-----GTSG-ARVMFIHGGAYTLGMSA
tr|Q0S546|Q0S546_RHOSR_Carboxy  -DETEDECLTLNVLAPG-----STSEPRFMVMFIHGGAYSGTSS
tr|B0RGS7|B0RGS7_CLAMS_Putativ  GTPMEDCLTVNIAPSGLSPDAARVNRESQLRPVMVFIHGGAYVGSSR
tr|A4TB12|A4TB12_MYCGI_Carboxy  YQPMSEDCLTLNVVAPAD-----AEARAADGLPMVMFIHGGYLLGSSA
tr|Q73Z23|Q73Z23_MYCPA_LipT_OS  YQPMSEDCLTLNVVTP-----EAPAEGFLPMVMFIHGGYFLGSSA
tr|Q5YPM0|Q5YPM0_NOCFA_Putativ  YQTSEDSLTLNVIVP-----ATPAITPRPMVMFIHGGYVMLTSA
                                  *.:*.:*.:*.. *****.* * *

tr|Q0S545|Q0S545_RHOSR_Carboxy  TALYGGQSLVRRGDIVVSINYRLGSLGYLDFTQFSTPERFDSNLGLRD
tr|Q0S546|Q0S546_RHOSR_Carboxy  SSLYSGESLVRRGDIVVSINYRLGSLGYLDFTQFSTPERFDSNLGLRD
tr|B0RGS7|B0RGS7_CLAMS_Putativ  ENPVQEGLVRGGIVYSFNYRLGALGYLDFSRYSRPDRPIESNLGLRD
tr|A4TB12|A4TB12_MYCGI_Carboxy  TPVYDGASLARKG-CVYISVNYRLGALGCLESLSTPEAPIDDNLFLD
tr|Q73Z23|Q73Z23_MYCPA_LipT_OS  LVMALRWRYDNVAAFGGDPGNVTIFGSAGAHAVSTLVATPEAEGLFAQA
tr|Q5YPM0|Q5YPM0_NOCFA_Putativ  LGLYSGARLALRGDVVVTLNYRLGAFGYVDFSEFATPARPFDNLGLRD
                                  * * . : * * : . : * : : : : * * * : . : * * *

tr|Q0S545|Q0S545_RHOSR_Carboxy  QVAALEWQRNIAEFGGDPDNVTVFGESAGANAVTLMTTPAAKGLFARA
tr|Q0S546|Q0S546_RHOSR_Carboxy  QVAALEWQRNIAEFGGDPDNVTVFGESAGANAVTLMTTPAAKGLFAQA
tr|B0RGS7|B0RGS7_CLAMS_Putativ  QVQVALQWRDNIRAFFGGDPDNVTVFGESAGGANAVTLMAVPAAHGLFARA
tr|A4TB12|A4TB12_MYCGI_Carboxy  LVMALRWRYDNVAAFGGDPGNVTIFGSAGAHAVSTLVATPEAEGLFAQA
tr|Q73Z23|Q73Z23_MYCPA_LipT_OS  LVLALQWRDNIAEFGGDPDNVTIFGESAGACITALLAVPAAKGLFAQA
tr|Q5YPM0|Q5YPM0_NOCFA_Putativ  QVAALEWRRNIAEFGGDPDNVTIFGESAGAHAVLLALLATPAAHGLFHRG
                                  * * * . : * : * * * . : * * * . : * * * : .

tr|Q0S545|Q0S545_RHOSR_Carboxy  ISESSAPLVTTADRAARWASDYVTLLG-----AEPDTAEALSSPVG
tr|Q0S546|Q0S546_RHOSR_Carboxy  IAESPPASAYHPERAARWSREFLEIAG-----VPLSEAATWLETADPA
tr|B0RGS7|B0RGS7_CLAMS_Putativ  IAQSSPTNAVYPAEQTARWAEFVGLLAGRAGRAPDDAEAVRLLTAASAS
tr|A4TB12|A4TB12_MYCGI_Carboxy  IAQSPASGMISDADIAADYAQRFARQLG-----ADGKDGARALLAARPA
tr|Q73Z23|Q73Z23_MYCPA_LipT_OS  ISESPAGLVRSQEVAAEFANRFANLLG-----VRRQDAANALMLQSAA
tr|Q5YPM0|Q5YPM0_NOCFA_Putativ  IAQSPPADWGLSAADAAEFARRLVERLG-----IDPADAARALTDLPAN
                                  *.:*.. *.:* : : . . . *

tr|Q0S545|Q0S545_RHOSR_Carboxy  ALGRAGNRLGAKVLSETPGLHPFGPVIDGDFLPKPPLDAFADGSAHRVPL
tr|Q0S546|Q0S546_RHOSR_Carboxy  GFVEAGTLARRGADEEPGTRAFAPVDGFFLPHTPLDCFASGSGHPVL
tr|B0RGS7|B0RGS7_CLAMS_Putativ  TLAAANELMVRTPDEEPGTITFSPVIDGDLPERPLDAFKHGRAARVPL
tr|A4TB12|A4TB12_MYCGI_Carboxy  DLVDALERLIVEGQRDLVGAFAIGPTYGTEYLPEDFVEAMRSGRAHPVPL
tr|Q73Z23|Q73Z23_MYCPA_LipT_OS  QLVKTQHRLIDEGMQDRLGAFPIGPVGDDILPDFVEAMRRGEAHRVPL
tr|Q5YPM0|Q5YPM0_NOCFA_Putativ  DIRRADRAMAAAGRQRPGFFPICPVADGDYLPQAPVDAIAGTAAVPL
                                  : : : * . : * . * * * . : : * . * *

tr|Q0S545|Q0S545_RHOSR_Carboxy  IIGTNAREGTLFPKLLDALPTDPDRIGRMFALDPGAEARVTAAYPGYPA
tr|Q0S546|Q0S546_RHOSR_Carboxy  IIGTNHREGRVFPRFLNILPTDPTRIDKMFSHVDASVKERAIAAYPGYPG
tr|B0RGS7|B0RGS7_CLAMS_Putativ  IIGTNEREGSLTGRLDILATTPPRIEAVFAKTDESHRAELAAYPGLPKP
tr|A4TB12|A4TB12_MYCGI_Carboxy  IVGTNADEGRLFTRLKLLPTNEQAIEQLLSAVEPEARQRVLAAYPKYPA
tr|Q73Z23|Q73Z23_MYCPA_LipT_OS  IVGTNAEGRLFTRLAMLPTNESMVELLADAEPAVRRITAAYPNYPD
tr|Q5YPM0|Q5YPM0_NOCFA_Putativ  IIGTCRDEGQLFARFADYLTNPDRLHRLSAEGDEVEKRVVAAYPYGPG
                                  *.:* *.:* *.:* *.:* : : : . . * * * *

tr|Q0S545|Q0S545_RHOSR_Carboxy  PDAATDLGGDLTFWKPSIELAEAHCAFAPTFSYRFDAPRAMKWLGLDAT
tr|Q0S546|Q0S546_RHOSR_Carboxy  RRAAADLGGDVTFWEPSVLCAQGHTTVAPTYSYRYDFAPRLLHLILGLGAT
tr|B0RGS7|B0RGS7_CLAMS_Putativ  RRAALDFGGDYAFWFSIKVAERHARYAPVHFYRFDIAPRLVLMLGLDAT
tr|A4TB12|A4TB12_MYCGI_Carboxy  VDACVAFGGDFIFGSAVWQIAHASAFAPTYVYRDYDATAALRLSGMGAT

```

Chapter 5: A gene-based approach towards an enantioselective esterase for linalyl acetate hydrolysis

```

tr|Q73Z23|Q73Z23_MYCPA_LipT_OS
tr|Q5YPM0|Q5YPM0_NOCPA_Putativ
RSACIQLGDFAFGSAAWQIAEAHCAHAPTYLYRYDYAPRTLRLWSGFGAT
ARAARVMGGDYVFWRPSVEVMEGHSRHAPTYAYRYDYAPRALQLAGIGAT
* . :*** * . * *.. **:* * . : : * :.**

tr|Q0S545|Q0S545_RHOSR_Carboxy
tr|Q0S546|Q0S546_RHOSR_Carboxy
tr|B0RGS7|B0RGS7_CLAMS_Putativ
tr|A4TB12|A4TB12_MYCGI_Carboxy
tr|Q73Z23|Q73Z23_MYCPA_LipT_OS
tr|Q5YPM0|Q5YPM0_NOCPA_Putativ
HGFEFVAVFDIADTLIGRGLTLPGGRRGLKDVDTVQRHHLHFASQGTPL
HATEMYAVFGLTG-PWARLLTAFGGRRGLLAVTDTVQSHWLHFAHGTTPA
HGLELFALFDRMDSMLGRGMTLLGGRRAFVAAGERMRIAWLRFADQDGTVD
HATELLAVFDVYRSRFGKLLAAGLDSRSAAKVTDDVQKRWLGFRAERAVPG
HATELLAVFDVYRTRFGALLTAAADRRRAALRVSNQVQRWRRAFRTGVPG
HATDLIPVFGAADTPLGRALTAAGGARGLAAVTRQFDNWLAFARTGTPL
* . : : . : * . . . : * * : . .

tr|Q0S545|Q0S545_RHOSR_Carboxy
tr|Q0S546|Q0S546_RHOSR_Carboxy
tr|B0RGS7|B0RGS7_CLAMS_Putativ
tr|A4TB12|A4TB12_MYCGI_Carboxy
tr|Q73Z23|Q73Z23_MYCPA_LipT_OS
tr|Q5YPM0|Q5YPM0_NOCPA_Putativ
ASWPKYD-----TDRRATLVFDVTTVQDDDPRRERRL
PGWPRYS-----PERRETLIIDATSRVENDPLGERRR
ESWPPYVGGDDDAPGTGAADADAGASGERATLVFDVVDRVEHDPHAERRV
GDWPQYTR-----DERAVLVLDRRRRVEFDPHSERRQ
EDWPRYTA-----AERAVLVDRKSRVEFDPHPHRRM
PSWPEYTE-----ENRRLTIIDDPTRVIGDPRRERRL
* * * . * * : : * * * * * *

tr|Q0S545|Q0S545_RHOSR_Carboxy
tr|Q0S546|Q0S546_RHOSR_Carboxy
tr|B0RGS7|B0RGS7_CLAMS_Putativ
tr|A4TB12|A4TB12_MYCGI_Carboxy
tr|Q73Z23|Q73Z23_MYCPA_LipT_OS
tr|Q5YPM0|Q5YPM0_NOCPA_Putativ
AWQGYRGGYQGGL
AWLGYEHRR----
AWRDFVPHI----
AWEGFFLATR---
ARDGFSLAR----
AWSGVRVPTLT--
* .

```

Figure 73: Six sequences showing the greatest homology with respect to the cloned 1107bp fragment. Highlighted in yellow and green are the previous N- and C-terminal primers; in pink and blue are the forward and reverse primers designed against conserved motifs. The underlined regions indicate where the latest N- and C-terminal PCR primers have been designed to obtain a near full length product.

Using the N- and C- terminal primers underlined in figure 73 above (designated F1a and R1a from here on) a number of PCR experiments were tried to generate an expected product of ~1550bp (full length gene sequence ~1500-1600bp). However variations in annealing temperature, MgSO₄ concentration, DMSO addition, and PCR cycle times failed to yield a specific product. Various combinations of forward and reverse primers (degenerate and non-degenerate) from those available were tested with the aim of cloning as much of a potential tertiary alcohol esterase gene sequence as possible. Listed below are the primer pairs used with the approximate size of PCR product expected:

F1a / R2	~1350bp
CAT for / R1a	~1200bp
F1, F2, or F3 / R1a	~1450bp

A PCR product (fig. 74) was observed at ~1200bp when using CAT for / R1a primers (purple / underlined on figure 73 above).

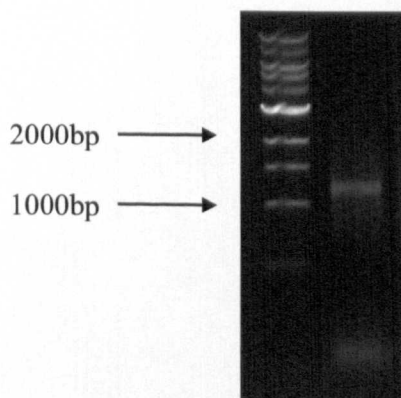


Figure 74: PCR results showing a product of ~1200bp when using primers CAT for / R1a with a 53°C annealing temperature, and 5% DMSO.

The PCR product at ~1200bp was cut out, extracted from the gel, and concentrated prior to transformation into competent Novablue cells. Transformed cells were plated onto LB agar + kanamycin and incubated overnight. Five colonies had grown on the plate, and all were picked to inoculate 5 mL overnight cultures, prior to extracting the plasmid using a miniprep kit. A restriction digest (fig. 75) with *NcoI* and *NdeI* showed a transformed colony to contain the LIC vector with this ~1200bp insert.

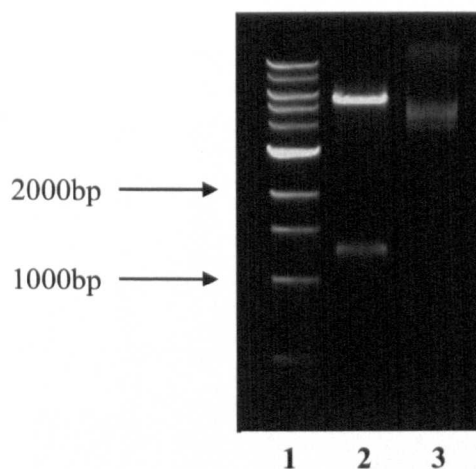


Figure 75: Agarose gel after running a restriction digest. *Lane 1:* DNA ladder. *Lane 2* shows the digested plasmid with insert for colony number 2. *Lane 3* shows an uncut plasmid (– restriction enzyme control).

The other primer combinations above failed to show any positive results from PCR, through changes in: annealing temp, $MgSO_4$ concentration, PCR cycle time, and the use of touchdown PCR and nested PCR. The results of sequencing however showed that the cloned fragment of ~1200bp is a result of non-specific binding in the earlier PCR experiments. The results of a BLAST with the sequenced DNA did not highlight any of the conserved motifs expected, nor was there any homology to known carboxylesterases. It was anticipated that this product was an extension of the 1100bp fragment already achieved which showed good homology to known carboxylesterases, particularly with respect to RHA1. With the sequence information gained from previous experiments, new primers specific to *R. ruber* 43338 DNA were designed for an approach using inverse PCR. This particular method involved digestion of the genomic DNA followed by intra-molecular ligation to generate circularised DNA for use as a template in PCR. The primers were designed for amplification in opposite directions to encompass the N- and C- terminal regions required, however the results

of PCR failed to highlight any specific products. The cloned fragment corresponding to ~75% of the esterase gene showed good levels of expression in *E. coli* BL21 (DE3) cells but was not found in the soluble protein fraction. Whole cells expressing this fragment however were shown to be inactive towards the hydrolysis of linalyl acetate. A summary of the results from these cloning experiments is shown in figure 76. Attempts to clone a full length gene were repeated using DNA extracted from the other three *Rhodococcus* strains which showed enantioselective activity towards the hydrolysis in chapter 4, but were not successful.

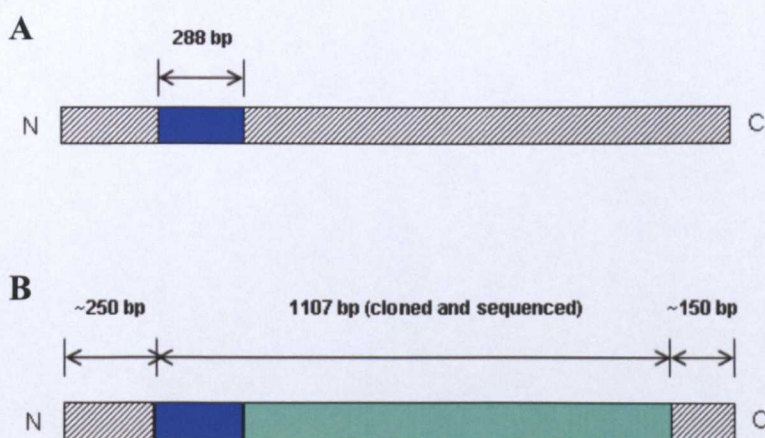


Figure 76: Summary of the cloning strategy towards a ~1550bp potential tertiary alcohol esterase from *R. ruber* DSM 43338. (A): initial cloning of a 288bp fragment based on highly conserved regions. (B): using degenerate primers in combination with those previously used for conserved regions, an 1100bp fragment corresponding to approximately 75% of the total gene sequence was cloned.

5.3.2. Cloning of potential tertiary alcohol esterases from *Nocardia farcinica* and *Sulfolobus tokodaii*

During sequence alignments with the cloned 1107bp gene fragment from *R. ruber* it was noted that an esterase from the closely related *Nocardia farcinica* showed good sequence homology. Classified in the same Nocardiaceae family as *Rhodococcus* sp. *Nocardia farcinica* is an aerobic gram-positive species commonly found in soil environments. The genome for this organism has been sequenced [Ishikawa et al. 2004], and as with *Rhodococcus* RHA1 the DNA contains a high GC content of 71%. The *Bacillus subtilis* *p*-nitrobenzyl esterase (BS2) peptide sequence (fig. 63) was again used for alignments with the *Nocardia farcinica* genome to check whether any full length gene sequences containing the conserved GGG(A)X motif typically associated with the tertiary alcohol esterases could be cloned and if the expressed enzymes were active towards linalyl acetate. The results of BLAST and Clustal sequence alignment (fig. 77) revealed three *Nocardia* carboxylesterases termed N1, N2, and N3 (accession numbers: Q5YPM0, Q5YQP8, Q5YYP18 respectively) with good homology to this known tertiary alcohol esterase. The same method was used to identify a potential tertiary alcohol esterase in *Sulfolobus tokodaii* for which genomic DNA was also readily available (fig. 78). The known gene sequences were used to design PCR primers enabling ligation independent cloning. Products could only be obtained from the amplification of these genes *via* PCR when increasing the DMSO concentration to 10% and using an annealing temperature of 55°C, due to the relatively high GC content of the template (fig. 79).

Chapter 5: A gene-based approach towards an enantioselective esterase for linalyl acetate hydrolysis

```

sp|P37967|PNBA_BACSU          -----MTHQI-----VTQYGVKVKGTENGVHKWKGIPYAKPPVGQWR 38
tr|Q5YPM0|Q5YPM0_NOCF        -----MVATID-----ITTADGVVVRGRRRVLWRALPYAAPVVGELR 39
tr|Q5YQP8|Q5YQP8_NOCF        MTIRYDITVEIDTAGPVAHTTHGRVVRGVMGPIAVWRSIPYAAPVTGPRR 50
tr|Q5YP18|Q5YP18_NOCF        -----MDN---VVEAPSGGWRGVVADGVRTFRGIRYAR----AER 33
:                               : * : * : : * *
:                               : * : * : : * *

sp|P37967|PNBA_BACSU          FKAPEPPEVWEDVLDATAYGSICPQPSD--LLSLSYTELPRQSEDCLYVN 86
tr|Q5YPM0|Q5YPM0_NOCF        FRAPQPVQFWSGVRDATEFASASFQHRG--GARIGARTYQPTSEDSLTLN 87
tr|Q5YQP8|Q5YQP8_NOCF        FRPAEPPEPVDGVRECVRFVDIAPQTMG--TMVPVDSLEL--MGEDCLWLN 97
tr|Q5YP18|Q5YP18_NOCF        FAAPEPEPAHDGVIDASTRGFSAPQLPSRLEAVMGAPAAFEQSEDCLRLT 83
* : * : * : * : * : * : * : * : * : * : * : * : * : * : *

sp|P37967|PNBA_BACSU          VFAPDTP--SKN-LPVMVWIHGGAFYLGAGSEPLYDGSKLAAQGEVIVVT 133
tr|Q5YPM0|Q5YPM0_NOCF        VIVPATP--AITPRPVMVFIHGGGYVMGTSALGLYSGARLALRGDVVVVT 135
tr|Q5YQP8|Q5YQP8_NOCF        VWAPTEPREPEEPVPLVWLHGGAYCLGTAAQKIYDGRKLAETGDVVVVT 147
tr|Q5YP18|Q5YP18_NOCF        VTAPVQP--PPGGSVAVLVLHGGAYLTGGGEWNLYDADRLVRETGIVVVV 131
* . * * . . * : * : * : * : * : * : * : * : * : * : * : *

sp|P37967|PNBA_BACSU          LNYRLGPFGLHLSSFN---EAYS DNGLLDQAAALKWVRENI SAFGGDP 180
tr|Q5YPM0|Q5YPM0_NOCF        LNYRLGAFGYVDFSEFATPARPFDDNNLGLRDQVALEWVRRNIAAFGGDP 185
tr|Q5YQP8|Q5YQP8_NOCF        VNYRIGVLGFLDLSSVV---DGCTPNLGLHDQIRALEWVRENI AAFGGDP 194
tr|Q5YP18|Q5YP18_NOCF        VSYRLGVLGWLRAAGVS-----EGNGLLDDQALALGWVRENIRAFGGDP 175
: . * : * : * : * : * : * : * : * : * : * : * : * : * : * : *

sp|P37967|PNBA_BACSU          DNVTVFGE SAGGMSIAALLAMPAAKGLFQKAIMESG-ASRTMT-KEQAA 228
tr|Q5YPM0|Q5YPM0_NOCF        DNVTIFGESAGAHAVLALLATPAAHGLFHRGIAQSPADWGLS-AADA 234
tr|Q5YQP8|Q5YQP8_NOCF        DNVTLFGES SAGACVTALLTAPAAAGLPHKAIQSPPATTVFG-RQRAEL 243
tr|Q5YP18|Q5YP18_NOCF        ARVTVAGQ SAGGQCVAAVMGMPRARGLFAQAI VQSAPFFGIFGHDA 225
. * : * : * : * : * : * : * : * : * : * : * : * : * : *

sp|P37967|PNBA_BACSU          TSA AFLQVLGIN-EGQLDKLHTVSAEDLLKAADQLRIA EKENIFQLF-FQ 276
tr|Q5YPM0|Q5YPM0_NOCF        FARRLVERLGIDPADAARALTDLPANDIRRAADRAMAAAGRQRPGFFPIC 284
tr|Q5YQP8|Q5YQP8_NOCF        VAHRFLELLDLP-PDRAAEV GELPIERLVQAAGVLFDEVLPREGR LAAA 292
tr|Q5YP18|Q5YP18_NOCF        AA AVFLAELGTD----PR TAPVPELLAAQARTAIRRAGPGGLNAA PPF 270
: : : * . : : : *

sp|P37967|PNBA_BACSU          PALDPKTLPEEPEKAI AEGAASGIPLLIGTTTRDEG YLFFT----PDS-D 320
tr|Q5YPM0|Q5YPM0_NOCF        PVADGDYLPQAPVDAIAAGTAAVPLIIGTCRDEGQLFAR----FAD-Y 328
tr|Q5YQP8|Q5YQP8_NOCF        PVDGELL PDYPI TRFQQGRSHRVP LIIGTNKDEASLFR L----FRSPI 337
tr|Q5YP18|Q5YP18_NOCF        PVEETDVLPG-PAQWAAAVRAAPV PALVGCTAAEMRAFFGGPHVFGR-- 317
* . : . * * * : : * : * : * * *

sp|P37967|PNBA_BACSU          VHSQETLDAALEYLLGK-----PLAEKVADLYP--RSLESQIHMMTDL 361
tr|Q5YPM0|Q5YPM0_NOCF        LPTNPDRHLHRILSAEGD-----EVEKRVVAAYPGYPGARA AAVRMGGDY 371
tr|Q5YQP8|Q5YQP8_NOCF        MPVTPEAVTIMLRDVAESHSDPMSPERVAEIASAYPLDGKARGALAMSTDA 387
tr|Q5YP18|Q5YP18_NOCF        -----VRRIPVAGP--RMVTLAERVVGRK 339
: : : * : :

sp|P37967|PNBA_BACSU          LFWRP AVAYASAQSHYAPVVMYRFWDWHPKPPYP--KAFH ALELFFVFGN 409
tr|Q5YPM0|Q5YPM0_NOCF        VFWRPSVEVMEGHSRHAPTYAYRYDYAPRALQLAGIGATHATDLIPVFGA 421
tr|Q5YQP8|Q5YQP8_NOCF        AFRMPAHWVADGHCTHSMTWVYRFDHATPMLRAARVGAHATEL P YVFGN 437
tr|Q5YP18|Q5YP18_NOCF        AFEDGVFRFADLLTDAG--AVARCYRVGALHPSGLGACHCIELPLLF 387
* . : . * : * : * : * : * : * : * : * : * : * : *

sp|P37967|PNBA_BACSU          LDG-LER-MAKAEITDEVKLSHTIQSAWITFAKTGNPSTE--AVNWPAY 455
tr|Q5YPM0|Q5YPM0_NOCF        ADTPLGRALTAAGGARGLAAVTRQFQDNWLA FARTGTP----LPSWPEY 466
tr|Q5YQP8|Q5YQP8_NOCF        FGTLNHDPTFWLGGKQATEVSGRMRRRWFARHGVPAALD GSKHWPY 487
tr|Q5YP18|Q5YP18_NOCF        PDDWRAAPMVRPTT PAELDELGARTRRSWGEFVRTGAV-----ADWPAH 431
. : : * * : * : * : * : *

sp|P37967|PNBA_BACSU          HEETRETLLDSEITIENDPESEKRQKLFPSKGE--- 489
tr|Q5YPM0|Q5YPM0_NOCF        TEENRLTLIIDDPTRVIGDPRDRERLAWSGVRVPTLT 503
tr|Q5YQP8|Q5YQP8_NOCF        DRDRTRHTLLI DAIDRVVDDPDRDLHTAWGDQAVGFS- 523
tr|Q5YP18|Q5YP18_NOCF        RHGSAVRQLP----- 442
. * . :
    
```

Figure 77: Clustal sequence alignment of the *Bacillus subtilis* p-nitrobenzyl esterase with the *Nocardia farcinica* genome. The conserved oxyanion hole residues are shown in blue, and catalytic triad in red.

Chapter 5: A gene-based approach towards an enantioselective esterase for linalyl acetate hydrolysis

```

sp|P37967|PNBA_BACSU      MTHQIVTTQYGKVKGTENGVHKWKGIPIYAKPPVQGWRFKAPEPEVWED 50
tr|Q976W8|Q976W8_SULTO  ----MIDPKIKKLESTIQ-----LPIGKASVEEIRSLFKQ----- 32
          :: : * : * :           : * . * . * : * :

sp|P37967|PNBA_BACSU      VLDATEYGSICQPQSDLLSLSYTELPRQSEDCLYVNVFADPTPSKNLPVM 100
tr|Q976W8|Q976W8_SULTO  ----FSSLTPR-EEVGKIEDITIPG-SETNIKARVYYPKTQG-PYGVL 73
          : . * : * : . : . :   : * ** : . : * : * . * : * :

sp|P37967|PNBA_BACSU      VWIHGGAFYLGAGSEPLYDGSKLAAQGEVIVVTLNYRLGPPGFHLHSSFN 150
tr|Q976W8|Q976W8_SULTO  VYYHGGGFVLGDIESYDPLCRAITNSQCQCVTISVDYRLAPE----NKFP 118
          * : * * . * * * ..      : : . : : : : * * * . * * .. *

sp|P37967|PNBA_BACSU      EAYSNDNLGLDQAAALKWVRENISAFGGDPDNTVTFGESAGGMSIAALLA 200
tr|Q976W8|Q976W8_SULTO  AAVVDSF-----DALKWVYNNSEKFNKYG-IAVGGDSAGGN-LAAVTA 160
          * * . :           * * * * : * . * . . . : * * : * * * : * * : *

sp|P37967|PNBA_BACSU      MPAAKGLFQKAIMESGASRTMTKEQAASTSAAFQLVGINEGQLDKLHTV 250
tr|Q976W8|Q976W8_SULTO  ILSKK----- 165
          : : *

sp|P37967|PNBA_BACSU      SAEDLLKAADQLRIAENKIFQLFFQPALDPKTLPEEPEKAIIEGAASGI 300
tr|Q976W8|Q976W8_SULTO  -----ENIKLK----YQVLIYPAVS----- 181
          : : : :           : * : : : * * . .

sp|P37967|PNBA_BACSU      PLLIGTTRDEGYLFFTPDSDVHSQETLDAALEYLLGKPLAEKVADLYPRS 350
tr|Q976W8|Q976W8_SULTO  -----FDLITKSLYDNGEGFFLTRHIDWFGQQYLR 213
          * : . :   * . : * : :   : . : * * *

sp|P37967|PNBA_BACSU      LESQIHMMTDLLFWRPAVAYASASHYAPVWVYRFDWHPKPPYNKAFHA 400
tr|Q976W8|Q976W8_SULTO  FADLLDFR-----FSPILADLNDLPP----- 234
          : . : :           : * :           * *

sp|P37967|PNBA_BACSU      LELPFVFGNLDGLERMAKAEITDEVKQLSHTIQSAWITFAKTGNPSTEAV 450
tr|Q976W8|Q976W8_SULTO  ---ALIITAEHDPLRDQGEAYANKLLQSGVQVTSVRFNNVIHG----FV 276
          : : :   .. *           : : : * . : * . . . * *

sp|P37967|PNBA_BACSU      NWPAYHEETRETLILDSEITIENDPESEKRQKLFPSKGE 489
tr|Q976W8|Q976W8_SULTO  SFFPFIEQGRDAIGLIGYVLR-----KVfyGK-- 303
          . : . : * : * : : * . :           : * * . *
    
```

Figure 78: Clustal sequence alignment of the *Bacillus subtilis* p-nitrobenzyl esterase with the *Sulfolobus tokodaii* genome. The conserved oxyanion hole residues are shown in blue, and catalytic triad in red.

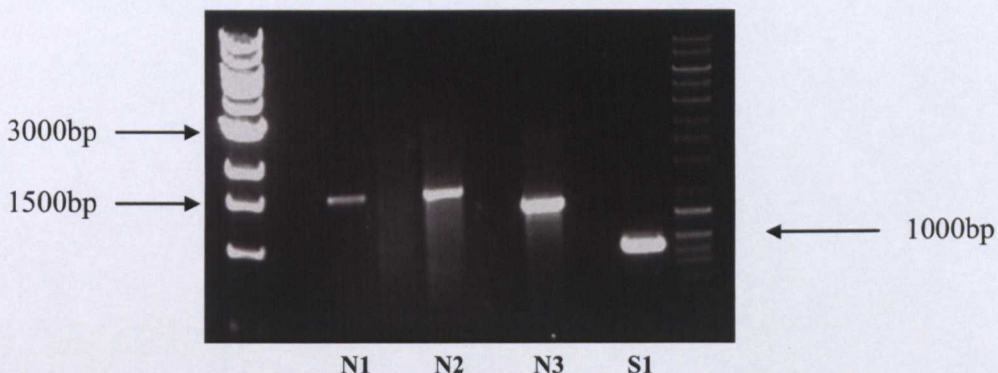


Figure 79: PCR products for the carboxylesterases: N1 (1512bp), N2 (1572bp), N3 (1329bp) and S1 (912bp) (left to right), using DMSO at final concentrations of 10%, and an annealing temperature of 55°C.

Ligation independent cloning of N2 and N3 genes into *E. coli* cells was confirmed with a restriction digest, showing the plasmid to contain the correct sized insert (fig. 80). In this case only the digests for N2 and N3 showed positive results from this ligation independent cloning, with attempts for the N1 and S1 genes proving unsuccessful.

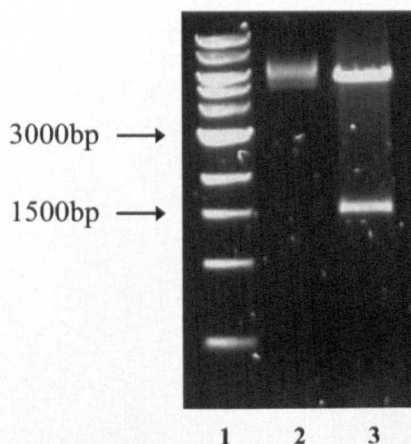


Figure 80: Agarose gel after running a restriction digest with LIC-N3 vector. *Lane 1:* DNA ladder. *Lane 2:* Uncut LIC vector with N3 insert (– restriction enzyme control). *Lane 3:* Digested vector with the N3 insert. Results for N2 not shown.

Samples from the cloning of N2 and N3 were sequenced, confirming that the correct gene sequence had been cloned without the presence of any mutations. The plasmids containing N2 and N3 inserts were initially transformed into *E. coli* BL21 (DE3) cells to test the expression. 5 mL cultures were prepared and cells were induced with IPTG when an A_{600} 0.5 was reached. Samples were taken at 5 h and overnight. Total insoluble protein and soluble protein fractions were prepared. Protein N3 (~50 kDa) was clearly expressed (fig. 81) in BL21 at 18, 30 and 37°C. The N3 protein expressed at 18 and 30°C using these cells was soluble, but insoluble when incubated at 37°C.

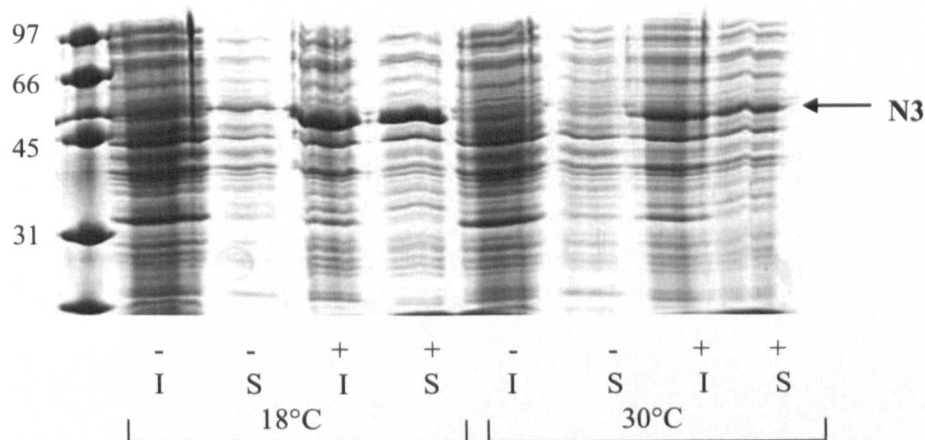


Figure 81: Expression of N3 protein in *E. coli* BL21 (DE3) cells. Overnight samples taken, ± IPTG induction, with insoluble (I) and soluble (S) fractions. Lane 1: Molecular weight marker showing kDa.

Protein N2 (~60 kDa) was not expressed in *E. coli* BL21 cells. A further three different cell types: B834, BL21-Ros, and Ros-PLysS were tested for the expression of N2. Good levels of N2 expression were observed using B834 cells (fig. 82), however whilst all three cell types were able to express this protein, it was only in the insoluble fraction. A range of temperatures with and without the addition of IPTG were tried with expression in B834 cells without a positive effect on the solubility of N2. Alternative methods using an auto-induction medium, and a screen of 30 resuspension buffers [Lindwall et al. 2000] also failed to generate N2 protein in the soluble fraction.

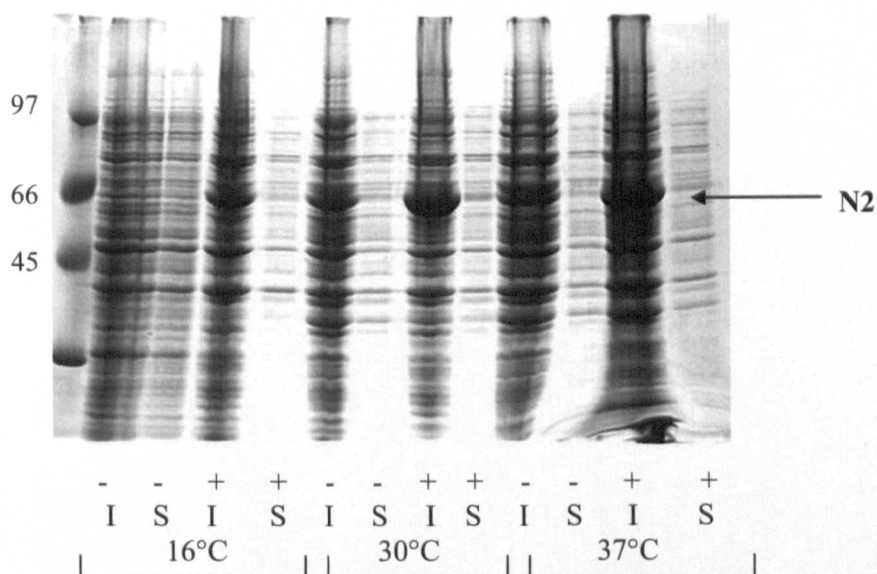


Figure 82: Expression of N2 protein in *E. coli* B834 cells. Overnight samples taken, \pm IPTG induction, with insoluble (I) and soluble (S) fractions. Lane 1: Molecular weight marker showing kDa.

An initial whole cell activity test for the hydrolysis of linalyl acetate was tried with *E. coli* cells BL21 and B834 over-expressing N3 and N2 cloned esterases respectively. Cells were induced with IPTG at an $A_{600\text{nm}}$ 0.5, and incubated at 30°C for a further hour before the substrate linalyl acetate was added. Samples were extracted for GC analysis over a period of 0-16 h however no hydrolytic activity for either N2 or N3 was observed when compared to a negative control of BL21 cells transformed with the LIC vector only (no insert) (fig. 83). For investigations into substrate specificity and selectivity of the esterase, the soluble N3 protein was first purified to homogeneity. The protein was found to elute from the nickel column in the first step of purification at an imidazole concentration of between 250-300 mM. Complete purification could not be achieved through a single step, and to prevent protein

precipitation that was observed with prolonged storage in the imidazole containing elution; the fractions containing the esterase were pooled and concentrated prior to immediate gel filtration chromatography. This second step of purification resulted in a solution of purified esterase (fig. 84) with a molecular weight of 46 kDa, which was stored in aliquots at 0.4 and 1.0 mg/mL concentrations at -80°C prior to use in the enzyme assays.

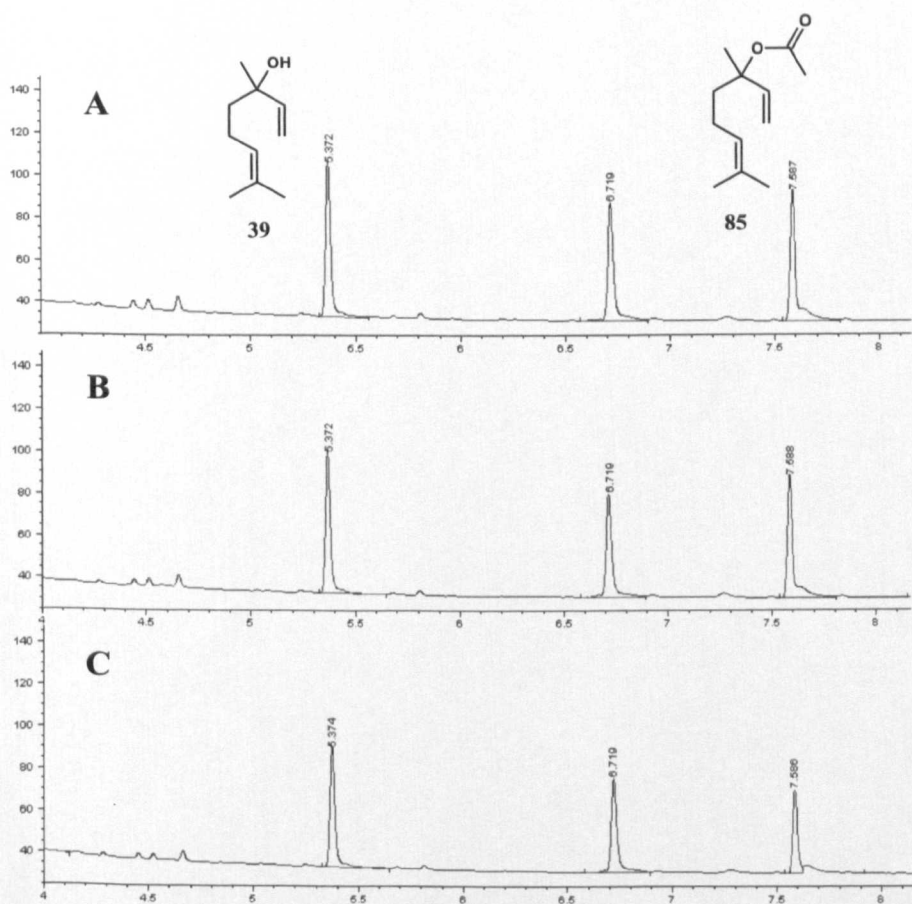


Figure 83: GC analysis from testing the activity of BL21 whole cells over-expressing N3 esterase, towards the hydrolysis of linalyl acetate **85** after 16 h. (A): Control minus cells. (B): Control with BL21 cells expressing an 'empty' LIC vector. (C): BL21 cells expressing N3. Results for N2 not shown.

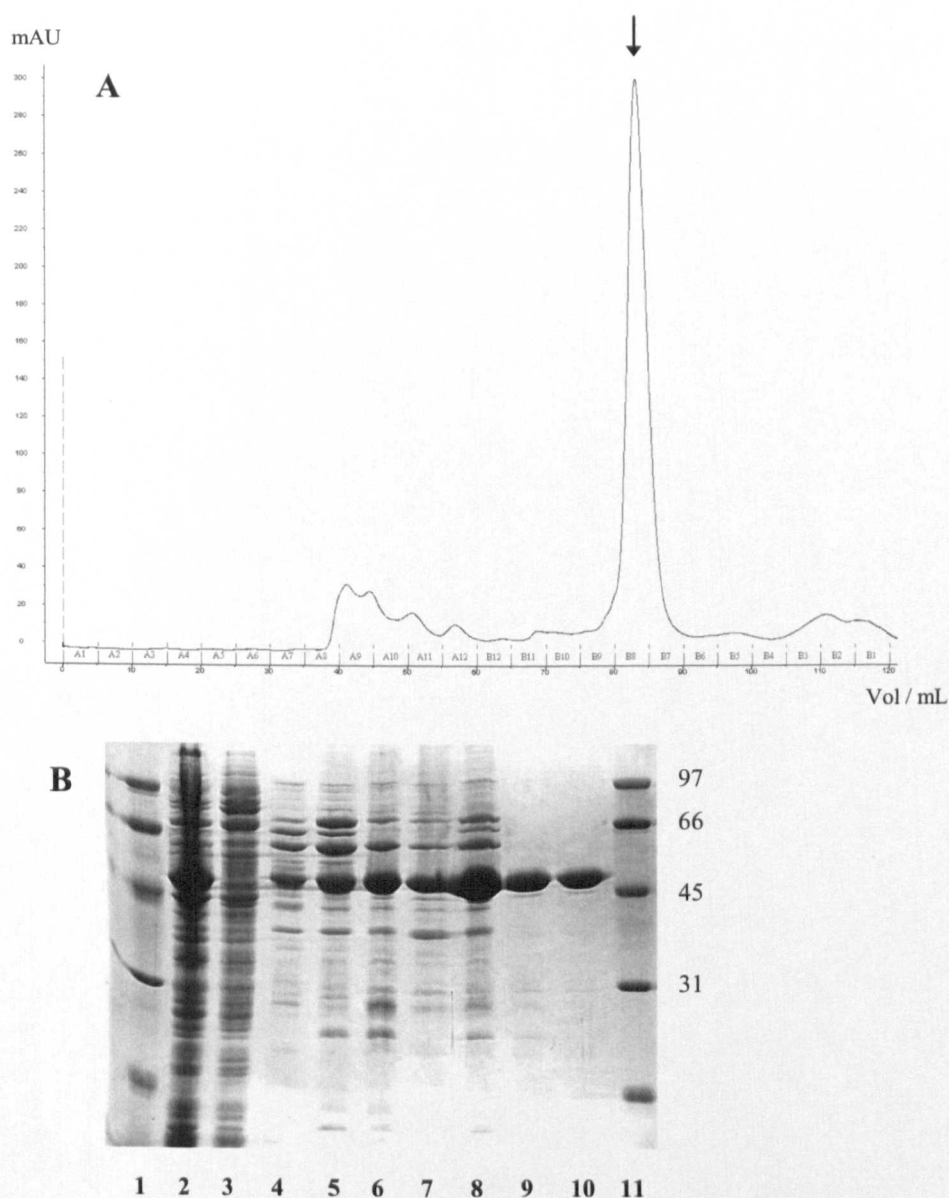


Figure 84: (A): Chromatogram showing the second step of N3 purification *via* gel filtration chromatography (GF). (B): SDS-PAGE summary of purification. *Lanes 1 and 11:* BioRad low MW marker showing mass (kDa). *Lane 2:* Total soluble protein. *Lane 3:* flow-through from nickel column. *Lanes 4-7:* Fractions from Ni-column. *Lane 8:* Concentrated nickel column fractions loaded onto GF column. *Lanes 9 and 10:* Fractions from GF showing purified N3 esterase.

5.3.3. Characterisation of the activity of N3 esterase from *N. farcinica*

The hydrolysis of *p*-nitrophenyl acetate to *p*-nitrophenol by the purified esterase was studied using a spectrophotometer for determination of kinetic parameters (fig. 85). With a concentration of purified enzyme $1.72 \times 10^{-7} \text{ mol dm}^{-3}$ (0.008 mg/mL), the V_{max} equalled $4.7 \times 10^{-7} \text{ mol dm}^{-3} \text{ s}^{-1}$ with a K_m of 1.2 mM (fig. 86A and B). When the concentration of enzyme was halved, a 30% reduction in rate of hydrolysis was observed. Doubling of the concentration of enzyme led to a 3-fold increase in rate. A calculated k_{cat} of 2.73 s^{-1} was determined from these studies. A pH optimisation assay revealed a maximum rate of activity for this hydrolysis occurred at a pH 7.5 (fig. 86C). Similar rates of activity were observed with different types of buffer at the same pH.

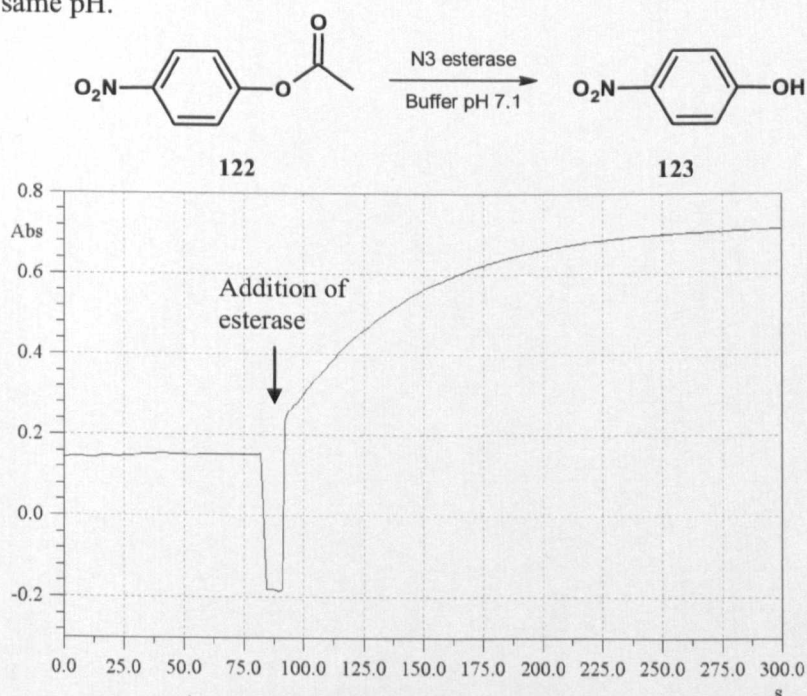


Figure 85: Absorbance measured at 412nm for the release of *p*-nitrophenol upon hydrolysis of *p*-nitrophenylacetate (*p*NPA) by N3 esterase at 25°C. Background level of absorbance was measured for an initial 60s before the addition of enzyme after 90s.

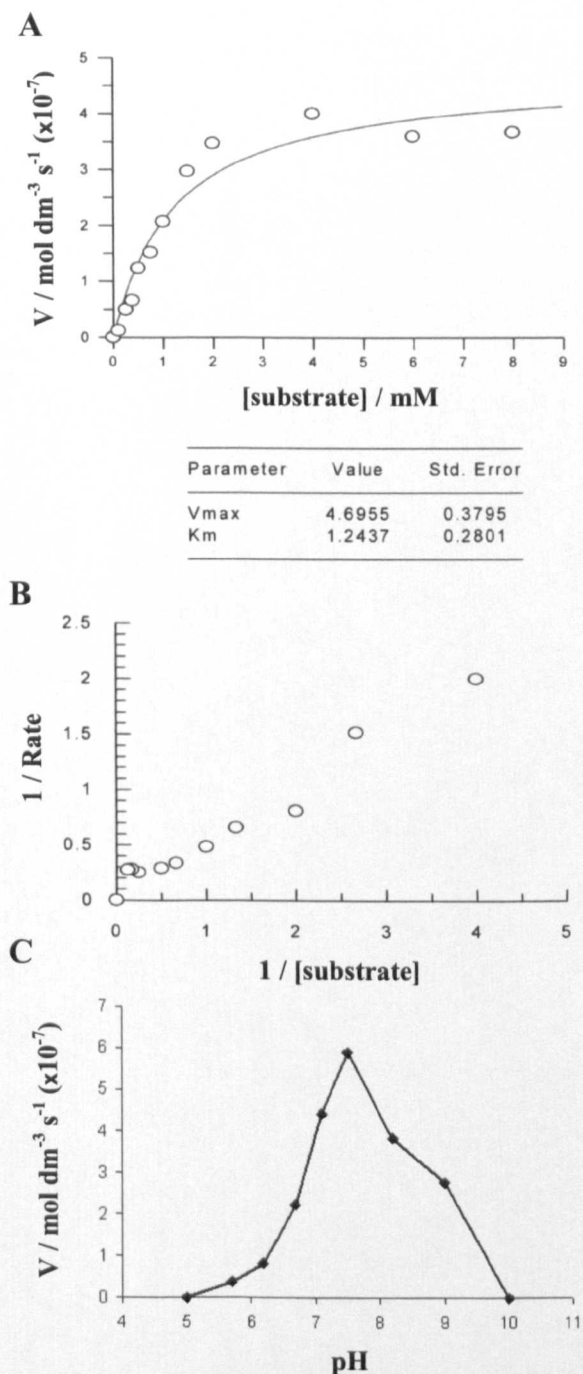


Figure 86: Michaelis-Menten curve (**A**) and Lineweaver-Burk plot (**B**) used in the determination of kinetic parameters by non-linear regression with the program GRAFIT. pH optimisation assay for the hydrolysis of *p*NPA by the purified N3 esterase at 25°C, generated in an overlapping range of 50 mM MES / Tris buffers (**C**).

As previously observed for whole cells expressing N2 and N3 esterases, the purified soluble esterase N3 was shown to be inactive towards the hydrolysis of linalyl acetate when compared to control assays without protein. Another commercially available tertiary monoterpene ester, α -terpinyl acetate was tested as a potential substrate that could yield another commercially desirable monoterpene alcohol α -terpineol upon hydrolysis; however no activity was observed in this case.

Further investigation into the activity of this protein towards other monoterpene esters revealed highly enantioselective activity towards menthyl acetate hydrolysis, observed in incubations at both 30 and 37°C. In each instance an ee_p of $\geq 99\%$ towards the commercially desirable 1*R*(-)-menthol **63** enantiomer product was achieved (fig. 87). However assays at these temperatures revealed problems with the volatility of menthyl acetate which prevented an accurate quantitative determination of selectivity (*E*). With a boiling point of 57°C, significant loss of the substrate to evaporation was noticed from these investigations. Over an assay period of 23 h, 47% of the menthyl acetate was found to evaporate at 30°C during incubations with sealed screw-cap glass vials. This factor seemed to limit the conversion rates which were achieved in these assays, with 8% and 21% 1*R*(-)-menthol formed after 5 and 23 h respectively at 30°C using 0.5 mg/mL enzyme. Lowering of the incubation temperature to 22°C, in conjunction with stirring under reflux condensation led to a reduction in rate of substrate evaporation to 36% over a 23 h period, however detectable levels of conversion could not be achieved.

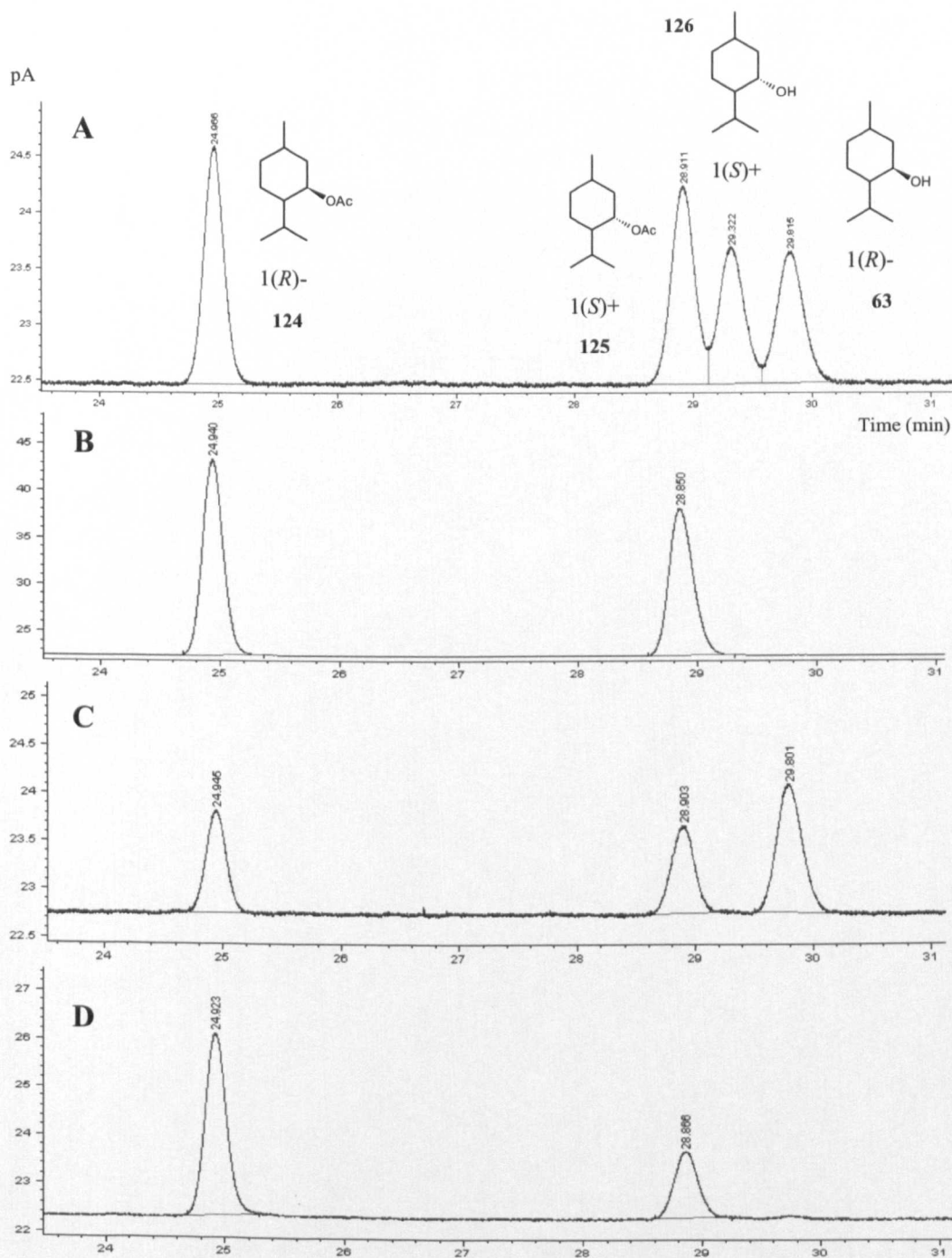


Figure 87: Chiral GC analysis of a mixture of 1(±)-menthyl acetate and 1(±)-menthol standards (A). Incubation of N3 esterase with 1(±)-menthyl acetate at $t = 0$ (B), and $t = 21$ h (C). Control without protein at $t = 21$ h (D).

In addition to 1*R*(-)-menthol, the fragrant monoterpene alcohols lavandulol and citronellol, are also highly valued in the flavour and fragrance industries. Activity for the hydrolysis of citronellyl acetate **127** to citronellol **34** was observed with a 23% conversion after 20 h at 30°C (fig. 88). The hydrolysis of racemic lavandulyl acetate (**128/129**) was also investigated with a conversion of 25% reached after a period of 20 h, with an *ee*_p 26% (*S*)-lavandulol **130** and *E*-value 1.7 (fig. 89).

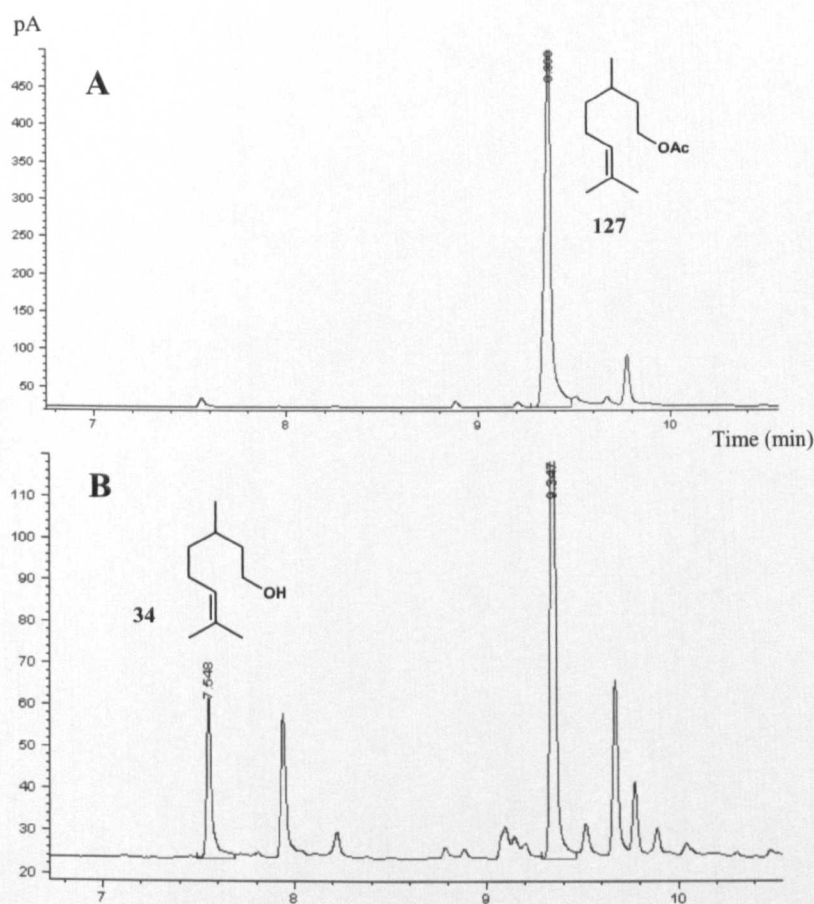


Figure 88: Control incubation of citronellyl acetate **124** without protein at $t = 23$ h (A). Incubation of N3 esterase with citronellyl acetate at $t = 23$ h (B).

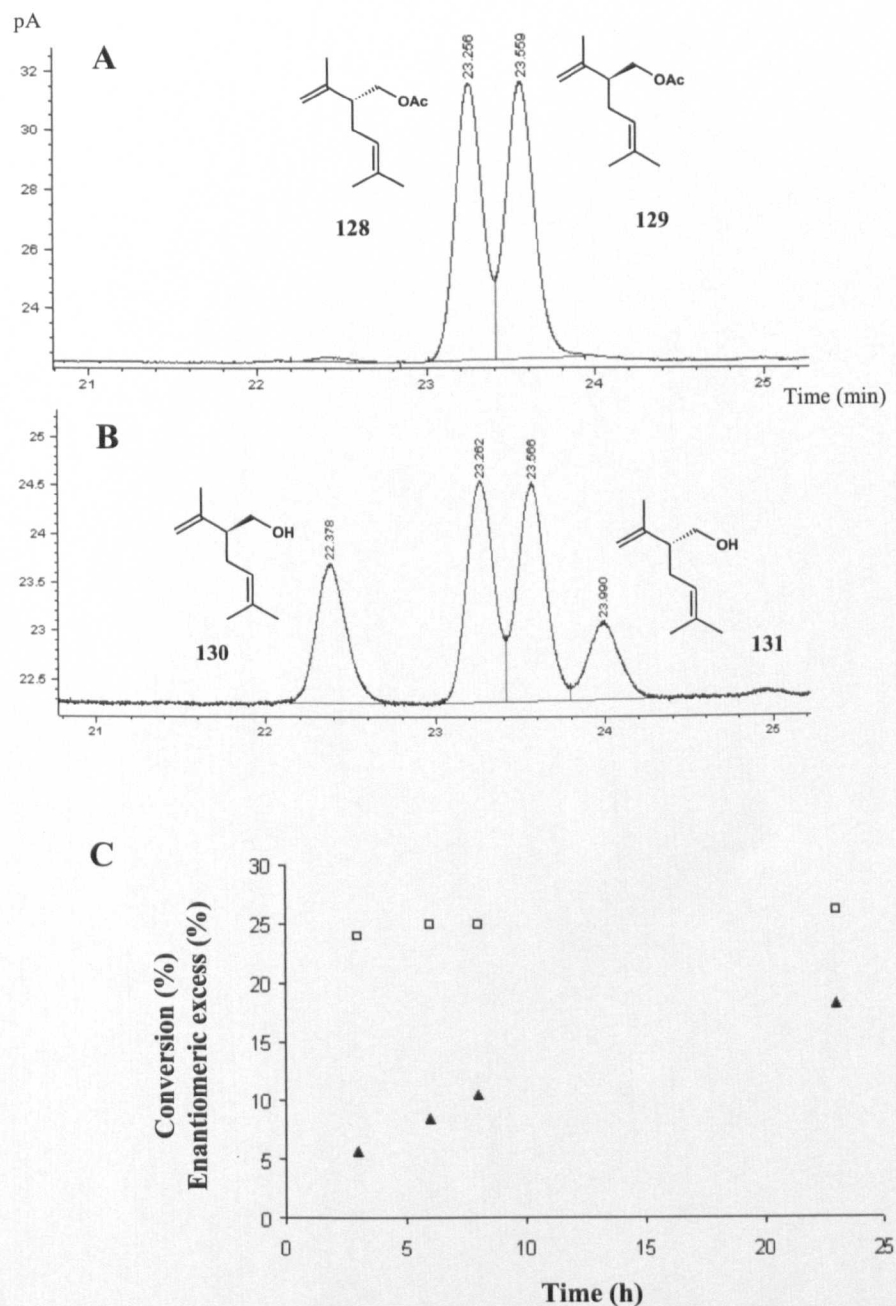


Figure 89: Control incubation of (\pm)-lavandulyl acetate without protein at $t = 23$ h (A). Incubation of N3 esterase with (\pm)-lavandulyl acetate at $t = 23$ h (B). Conversion (\blacktriangle) and ee_p (\square) measured over a time-course for the hydrolysis of lavandulyl acetate at 30°C and pH 7.1 using 0.4 mg/mL purified N3 esterase (C).

5.4. Conclusions

The results in chapter 4 highlighted sub-cellular fractions from *Rhodococcus ruber* DSM 43338 extracts which displayed opposite enantioselectivity towards the hydrolysis of linalyl acetate. A traditional protein purification approach in that instance did not yield an isolated enzyme responsible for this activity, and hence the work described in this chapter targeted an alternative gene-based approach for identifying an enzyme responsible for the interesting activity and enantioselectivity towards linalyl acetate. Problems were encountered with an absence of sequence information for the 43338 strain. Based upon the conserved motifs that confer activity for tertiary alcohol esterases and genome information available for *Rhodococcus* sp. RHA1, sequence alignments revealed 5 GGG(A)X motif esterases in this RHA1 strain. An initial 288bp fragment (~20%) of a gene from the 43338 strain containing these motifs was cloned into the pET-YSBLIC vector using PCR primers that were designed towards these conserved regions. Sequencing and alignment of this cloned fragment against all bacterial genomes in the NCBI database enabled the design of further PCR primers based upon sequence knowledge from the closest homologues. Although a variety of PCR methods failed to amplify a full-length gene, it was possible to clone and sequence a stretch of gene corresponding to approximately 75% of a tertiary alcohol esterase from *R. ruber*.

A different approach targeted the cloning of three possible tertiary alcohol esterases from another actinomycete closely related to *Rhodococcus* sp. A GGG(A)X motif

esterase from *Nocardia farcinica* was noted in earlier sequence alignments to share high levels of homology to those genes from RHA1 and the model *Bacillus subtilis* *p*-nitrobenzyl esterase (BS2). Ligation independent cloning enabled the over-expression and purification of an esterase from *N. farcinica*, which shows promising characteristics for the biocatalytic preparation of commercially desirable monoterpene alcohols. The purified esterase was found to be highly enantioselective towards the hydrolysis of racemic menthyl acetate ($ee_p = \geq 99\%$ 1*R*(-)-menthol). However the volatility of menthyl acetate in these biotransformations even at moderate temperatures prevented accurate determination of conversion and selectivity (*E*), and thus relevant comparisons with literature could not be made. Substrate specificity extended to the other monoterpene esters citronellyl acetate, and lavandulyl acetate whereby a certain degree of enantioselectivity was also demonstrated.

Whilst activity of the purified esterase has been described towards primary and secondary alcohol esters it has yet to show substrate specificity extending towards the TAEs. These acetates are not so commonly used as substrates in biotransformations; however their hydrolysis can be targeted for synthesis of natural products which are also important in the flavour and fragrance industry. Linalool and α -terpineol are particularly important tertiary monoterpene alcohols in this sense, and can be found in products such as perfumes, soaps and detergents. There are however only a few hydrolases which will accept TAEs as substrates, when compared to enzymes accepting esters of primary and secondary alcohols [Henke et al. 2002, Pogorevc et al.

2000, Gudelj et al. 1998]. In comparison to the 50% conversion for the hydrolysis of linalyl acetate that has been achieved in literature with *B. subtilis* pNBE, the presence of such homologous regions in the amino acid sequence does not seem to confer activity in every case [Henke et al. 2002]. Whilst negligible activity was observed towards linalyl- and terpinyl acetates in this investigation, there is potential for hydrolysis of more diverse TAEs using this *N. farcinica* esterase. In the literature a number of esterases containing the GGG(A)X motif have shown a lack of activity towards linalyl- and terpinyl acetate, yet still show high levels of conversion and enantioselectivity for the hydrolysis of other compounds in this class which has facilitated their use in the generation of pharmacological precursors [Kourist et al. 2007]. Further work with this purified esterase will aim to increase the knowledge of substrate specificity and selectivity with other menthyl esters; and to uncover function for hydrolysis of a tertiary alcohol ester by screening a wide range of compounds from this class. The high levels of expression for this recombinant enzyme also offer the potential for further characterisation and structural studies.

6. Chapter 6: Enrichment selection of a microorganism competent for growth on β -myrcene as the sole carbon source and characterisation of the microbial activity

6.1. Introduction

Hops, classified in the *Cannabaceae* family and from the genus *Humulus*, are an abundant crop largely grown in central temperate regions, widely cultivated for their favourable properties which can be exploited in the brewing of beer [King et al. 2003, Murakami et al. 2006]. Lupulin glands from the flowers (cones) of the female *Humulus lupulus* plant contain valuable secondary metabolites comprising bitter β -acids (lupulones), α -acids (humulones), prenylflavonoids, and essential oils (fig. 90), of which the contents differentiate the flavour and aroma characteristics of many commercial varieties [Cheng et al. 2007, Kishimoto et al. 2005, 2006].

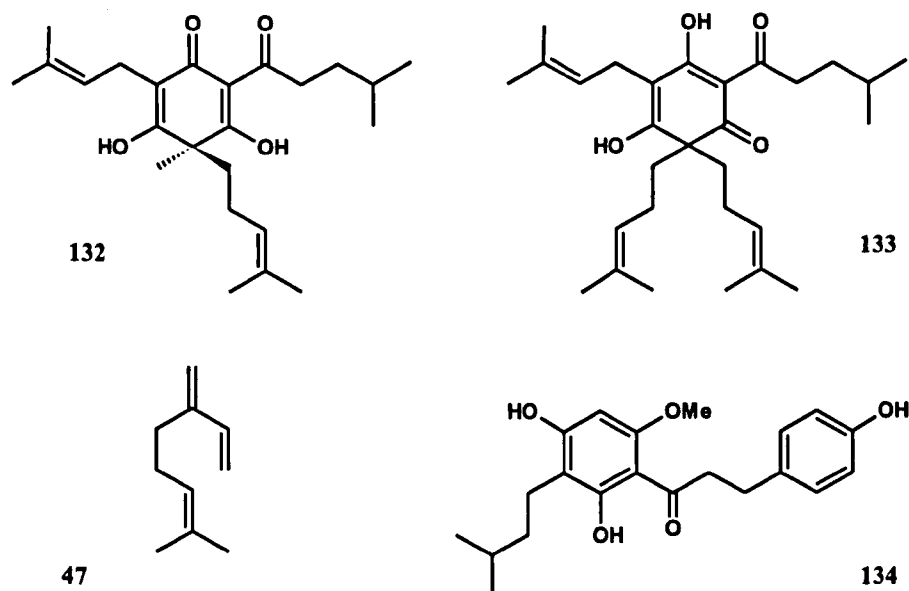


Figure 90: Chemical structures of some of the main components of oils extracted from the lupulin glands of hop plants. From top left (clockwise): Humulone **132** (an α -acid), lupulone **133** (a β -acid), xanthohumol **134** (a prenylflavonoid), and β -myrcene **47** (a monoterpene essential oil).

Hops are known to contain a complex mixture of C-10 terpenes as part of their natural essential oils, including the fragrant monoterpene alcohols, linalool, geraniol, and lavandulol [Bernotiene et al. 2004]. Whilst these monoterpene alcohols are produced in many species of plant, they comprise only a very small fraction of the total essential oil content extracted from the hops; oils of which have been shown to contain these compounds at approximately 0 – 0.2% w/w [Bernotiene et al. 2004].

The acyclic monoterpene β -myrcene (7-methyl-3-methylene-1,6-octadiene) accounts for a relatively large fraction of monoterpenes extracted from the essential oils of hop plants. The chemical composition of essential oils extracted from *H. lupulus* cones at

different geographical locations revealed β -myrcene to constitute 74-99% of the monoterpene fraction [Bernotiene et al. 2004, Mockute et al. 2008], and in commercial varieties can account for 70% of the total essential oil extract [from the Hop Union Directory of Hop Data, available at <http://www.hopunion.com/education.shtml>]. β -myrcene may therefore be considered a relatively inexpensive starting material for biotransformations that target more commercially attractive derivatives.

β -Myrcene has been the subject of a number of biotransformation studies in the past (fig. 91 – Ishida 2005), including descriptions of its metabolism in mammalian [de Oliveira et al. 1997; Madyastha et al. 1987] and insect cells [Miyazawa and Murata 2000].

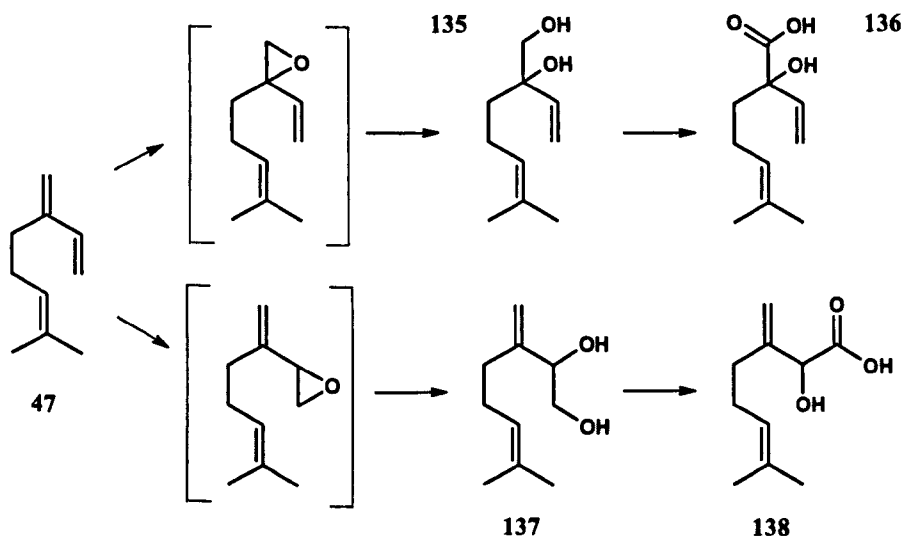


Figure 91: Biotransformation products 135-138 of β -myrcene 47 metabolism in rabbit [Ishida et al. 2005]. The literature example suggests that production of diols as an end product shows that the corresponding epoxides are involved as intermediates.

One example of a natural biotransformation involving myrcene is found in the biosynthetic pathway of aggregation pheromones in the pine engraver beetle *Ips pini*, in which β -myrcene was demonstrated to be hydroxylated stereoselectively to (4*R*)-(–)-ipsdienol (**139**, figure 92) [Sandstrom et al. 2006]. β -myrcene has also been used as a substrate in microbial reactions. Biotransformation of **47** by *Aspergillus niger* yielded different 1, 2-diol compounds **140**, **141** and **142** (figure 92) via the apparent epoxidation, followed by hydrolysis, of β -myrcene at each of the three double bonds [Farooq et al. 2004; Yamazaki et al. 1988]. A wide range of fragrant monoterpene alcohols was also produced by incubation of **47** with submerged cultures of *Ganoderma applanatum*, *Pleurotus flabellatus* and *Pleurotus sajor-caju* [Busmann and Berger 1994]. Further strains of *Pleurotus* have been shown to metabolise **47** to, in one instance, α -acaridiol **143** [Krings et al. 2008] and in another, two endoperoxide derivatives **144** and **145** (fig. 92) [Krugener et al. 2009].

Reports of the biotransformation of β -myrcene by bacterial species are rare, but in one study, it was used as the sole source of carbon for growth by *Pseudomonas* sp. M1 [Iurescia et al. 1999]. Resting cells of a β -myrcene negative mutant of M1, created using transposon mutagenesis and designated N22, accumulated 2-methyl-6-methylen-2,7-octadien-1-ol **93** (myrcen-8-ol) as the major metabolite of biotransformation of **47** (fig. 92). The ability to grow on **47** was conferred on N22 through the transfer of a cosmid which contained four open-reading frames *myrA*, *myrB*, *myrC* and *myrD*, potentially encoding an aldehyde dehydrogenase, an alcohol

dehydrogenase, an acyl-Coenzyme A synthetase and an enoyl-CoA hydratase respectively. The identification of these genes enabled the authors to propose a pathway for degradation of **47** by *Pseudomonas* sp. M1.

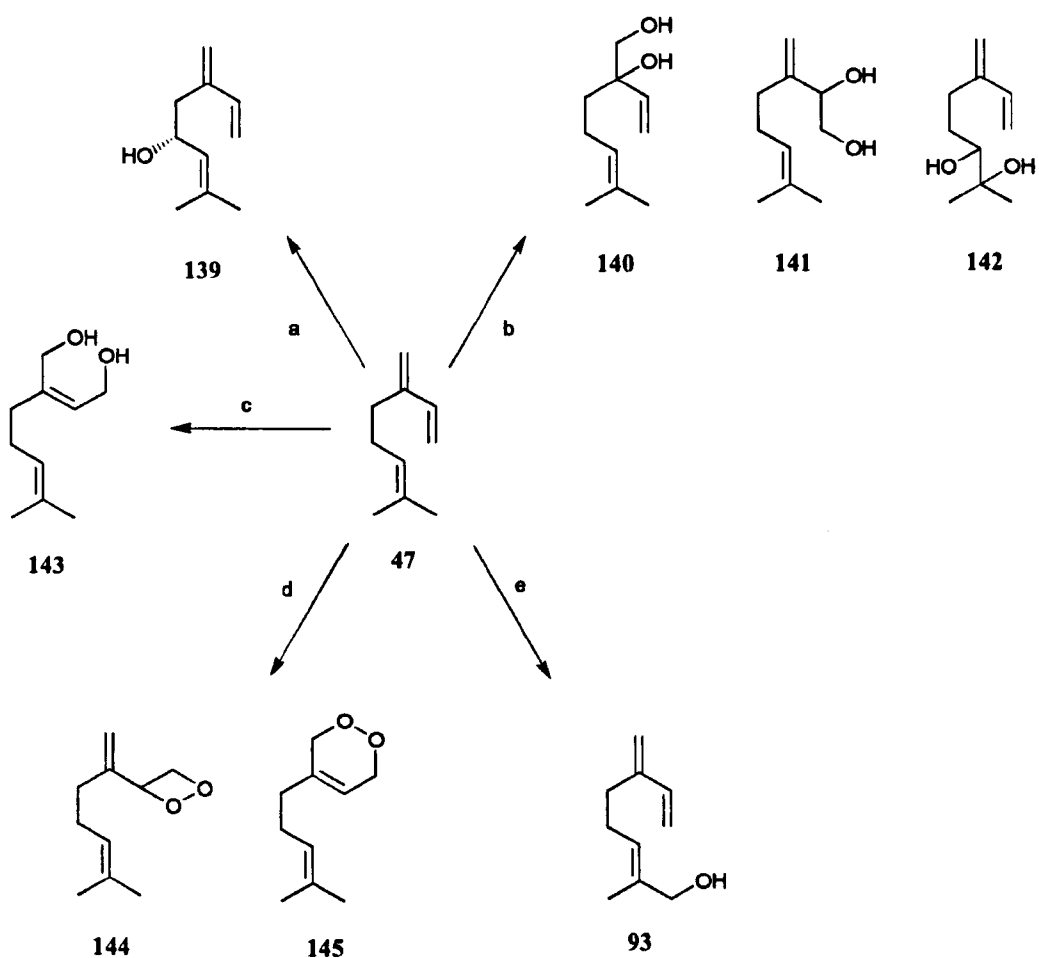


Figure 92: Summary of some existing β -myrcene **47** biotransformations in the literature. Pathway a: to ips-dienol **140** in the bark beetle *Ips pini* [Sandstrom et al. 2006]; b: to three diol **140**, **141** and **142** compounds by *Aspergillus niger* [Farooq et al. 2004; Yamazaki et al. 1988]; c: to α -(Z)-acaridiol **143** by *Pleurotus ostreatus* [Krings et al. 2008]; d: to myrcene 1,2-endoperoxide **144** and myrcene 1,4-endoperoxide **145** by *Pleurotus* spp. [Krugener et al. 2009]; e: to 2-methyl-6-methylen-2,7-octadien-1-ol **93** (myrcen-8-ol) by *Pseudomonas* sp. strain M1 [Iurescia et al. 1999].

With β -myrcene widely available, it is therefore a relatively inexpensive starting material, from which the more substituted desirable monoterpene alcohols can be targeted as products from its potential biotransformation. Routes of biotransformation with β -myrcene as the substrate will investigate bacterial selective enrichment cultures in addition to the fungal approaches already highlighted in chapter 3, based upon a similar approach cited in the literature [Iurescia et al. 1999]. In this instance, the isolation of a *Pseudomonas* strain competent for the biotransformation of myrcene to myrcen-8-ol was achieved from an enrichment culture containing a river-sediment sample with β -myrcene as the SCS. Identification and sequencing of β -myrcene catabolism genes from the *Pseudomonas* isolated was possible in this case. Similar methods will be used in this chapter for enrichment selection of organisms competent for the biotransformation of β -myrcene from hop plants material; with the aim of isolating an organism that can yield a commercially desirable monoterpene alcohol from its metabolism of myrcene.

6.2. Experimental

6.2.1. Chemicals

β -myrcene of 90% purity was purchased from Fluka. For use in enrichment and biotransformation experiments, the commercial compound was distilled by heating at 120°C under a reduced pressure of 15 mbar. Authentic geraniol (purity $\geq 96\%$) and nerol ($\geq 90\%$) standards were purchased from Fluka. A *Humulus lupulus* plant (Goldings variety) and soil surrounding the roots were obtained from Botanix Ltd.

6.2.2. Enrichment cultures and isolation of *Rhodococcus erythropolis* MLT1

Soil, root, leaf, and flower samples from *Humulus lupulus* were homogenised individually in 20 mL of sterile water, 5 mL of which was used to inoculate 250 mL Erlenmeyer flasks containing 50 mL of M9 minimal medium (KH₂PO₄ 3.1 g/L, K₂HPO₄ 8.2 g/L, (NH₄)₂SO₄ 2.4 g/L, yeast extract 0.1 g/L, tryptone 0.1 g/L, MgSO₄·7H₂O 0.5 g/L, MnSO₄·H₂O 0.05 g/L, CaCl₂·2H₂O 0.01 g/L, molybdic acid 0.01 g/L, FeSO₄·7H₂O 2.5 g/L). The cultures were incubated aerobically at 25°C for 7 days with shaking at 150 rpm, before the addition of β -myrcene (1 g/L). After a further 12 days incubation, samples showing growth from the soil incubations were transferred (2% inoculum) to fresh M9 media (50 mL) with concentrations of β -

myrcene at 1 and 5 g/L. After 6 days of growth, M9 agar plates containing β -myrcene (5 g/L) were inoculated with 100 μ L dilutions (10^{-2} – 10^{-4}) of this culture, and incubated at 30°C for 7 days. Plates were sub-cultured onto the same media and incubated for a further 7 days, before picking individual colonies and plating again. Further incubation led to the appearance of a single strain. 16S rRNA sequence analysis of this strain was carried out by the National Collection of Industrial and Marine Bacteria (NCIMB, Aberdeen, Scotland) revealing 99.93% sequence identity to *Rhodococcus erythropolis*. The strain designated MLT1 has been deposited with NCIMB with the accession number NCIMB 14574.

6.2.3. Growth of *Rhodococcus erythropolis* MLT1

To enable growth on β -myrcene in the vapour phase, adaptations of 250 mL Erlenmeyer flasks were made using glassblowing facilities. Glass tubing (50 mm in length, and 6 mm diameter) was attached to the internal base of the flask, the top of which protrudes 25 mm above the level of a 50 mL culture shaken at 150 rpm. 0.5 mL β -myrcene was added into this hollow central well allowing the vapour to fill into the headspace above the culture medium. For the monitoring of growth, 50 mL cultures of M9 media with either glucose 1.0 g/L, succinate 1.0 g/L, or β -myrcene (vapour phase) as sole carbon sources were inoculated from agar plates as described previously and incubated at 30°C for 24 h. The optical density (OD, measured at a wavelength of 600 nm) of these pre-cultures was measured prior to inoculation (10%)

of three separate 50 mL cultures for each of glucose, succinate, and β -myrcene. OD measurements were taken from each flask over a period of time, until stationary phase of the growth curve was reached.

6.2.4. Preparation of cell extracts

Cells were harvested using a Sorvall RC5B centrifuge equipped with an SS34 rotor (27,000 \times g, 20 min, 4°C) then re-suspended in one-tenth growth volume of 50 mM potassium phosphate (KH_2PO_4 6.8 g/L, K_2HPO_4 8.7 g/L) buffer (pH 7.0). Cells were lysed by three passages through a continuous flow French press at 270 MPa. The cell debris was removed by centrifugation (34,500 \times g, 40 min, 4°C) before retaining the soluble cell extract, which was concentrated by ultracentrifugation using a Centricon with a 3,000 molecular-weight cut-off filter (Millipore, Amicon Ultra-15). The total concentration of protein was estimated after lysis using the method of Bradford [Bradford 1976].

6.2.5. Biotransformation of β -myrcene by *Rhodococcus erythropolis* MLT1

R. erythropolis MLT1 was incubated in M9 media as described above, with β -myrcene as the sole carbon source administered in the vapour phase for 3 days.

Harvested cells were washed twice with phosphate buffer, before re-suspension (50 g/L) in 5 mL of buffer and the addition of β -myrcene (1 μ L/mL, 7.4 mM). Controls with dead (autoclaved) cells, and β -myrcene (1 μ L/mL) in buffer (no cells) were prepared under the same conditions. The samples were incubated for 1 h with shaking at 30°C. Cells were separated by centrifugation as before, and the solution saturated with NaCl before extracting three times with 5 mL of a 1:1 (petroleum ether : ethyl acetate) mixture. The organic layers were recombined, and dry $MgSO_4$ added to remove excess water. The $MgSO_4$ was filtered off, and the solution concentrated by leaving to evaporate overnight, before re-dissolving the resultant oil with 300 μ L of a 1:1 petroleum ether : ethyl acetate mixture. For cytochrome P450 inhibition studies, cells were prepared using the methods previously mentioned, then pre-incubated with 1 and 5mM concentrations of the inhibitors metyrapone and 1-aminobenzotriazole (ABT), shaking at 30°C for 0.5, 1, and 2 h before repeating the resting cell assay with β -myrcene.

6.2.6. Anaerobic resting cell assay

Resuspended cells were split into two aliquots. The standard resting cell assay with β -myrcene was repeated with one aliquot by incubating for 1 h at 25°C, whilst the other aliquot was stirred for 15 min in an anaerobic chamber to remove any dissolved oxygen from the solution prior to the addition of pre-equilibrated β -myrcene (1

$\mu\text{L}/\text{mL}$). The stirred solution was incubated for 1 h at 25°C under anaerobic conditions, and extracted with a pre-equilibrated 1:1 (petroleum ether : ethyl acetate) mixture. Samples were kept sealed airtight prior to GC analysis.

6.2.7. Metabolite identification

Gas chromatographic analysis of samples was performed routinely using an Agilent 6890N gas chromatograph equipped with a J&W HP5 column (length 30 m, internal diameter 0.32 mm, film 0.25 μm). 2 μL samples were injected at 250°C in the split mode. For analysis of myrcene-geraniol biotransformations, an initial oven temperature of 60°C was increased through a $10^\circ\text{C}/\text{min}$ gradient to 200°C , with a flow rate of the carrier gas helium at 10 mL/min. GC-MS analysis was performed with a Clarus 500 gas chromatograph (Perkin-Elmer) equipped with a J&W DB-1 column (30 m x 0.32 mm x 1 μm), coupled with a Clarus 500 mass spectrometer. 1 μL samples were injected at 250°C in the split mode. An initial oven temperature of 60°C was held for 1.5 min before increasing at $4^\circ\text{C}/\text{min}$ to 280°C with a further hold at this temperature for 15 min. The carrier gas helium was provided at a flow rate of 1.5 mL/min. The instrument was run in EI mode at an energy of 70 eV. Mass spectra were scanned in the range of 25 to 250 m/z .

6.2.8. Peptide mass spectrometry analysis

Peptide mass spectrometry analysis was carried out by the Technology Facility (University of York). In-gel tryptic digestion was performed after reduction with dithioerythritol (DTE) and *S*-carbamidomethylation with iodoacetamide. Gel pieces were washed twice with 50% (v:v) aqueous acetonitrile containing 25 mM ammonium bicarbonate, and then once with acetonitrile before drying in a vacuum concentrator for 20 min. Sequencing-grade, modified porcine trypsin (Promega) was dissolved in 50 mM acetic acid, then diluted 5-fold by adding 25 mM ammonium bicarbonate to give a final trypsin concentration of 0.01 $\mu\text{g}/\mu\text{L}$. Gel pieces were rehydrated by adding 10 μL of trypsin solution, and after 30 min the gel pieces were submerged in a 25 mM ammonium bicarbonate solution. Digests were incubated overnight at 37°C. A 0.5 μL aliquot of each peptide mixture was applied directly to the ground steel MALDI target plate, followed immediately by an equal volume of a freshly-prepared 5 mg/mL solution of 4-hydroxy- α -cyano-cinnamic acid (Sigma) in 50% aqueous (v:v) acetonitrile containing 0.1%, trifluoroacetic acid (v:v).

Positive-ion MALDI mass spectra were obtained using an Applied Biosystems 4700 Proteomics Analyzer (Applied Biosystems, Foster City, CA, USA) in reflectron mode, equipped with a Nd:YAG laser. MS spectra were acquired over a mass range of m/z 800-4000. Final mass spectra were internally calibrated using the tryptic autoprolysis products at m/z 842.509 and 2211.104. Monoisotopic masses were

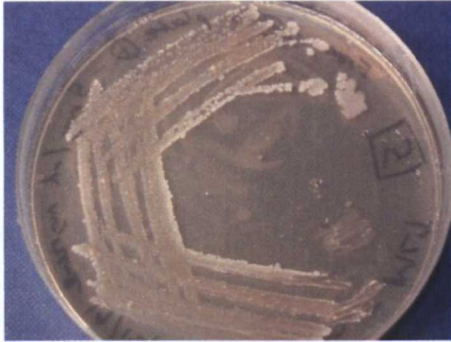
obtained from centroids of raw, unsmoothed data. The twenty strongest peaks with a signal to noise greater than 40 were selected for CID-MS/MS analysis. For CID-MS/MS, a Source 1 collision energy of 1 kV was used, with air as the collision gas. The precursor mass window was set to a relative resolution of 50, and the metastable suppressor was enabled. The default calibration was used for MS/MS spectra, which were baseline-subtracted (peak width 50) and smoothed (Savitsky-Golay with three points across a peak and polynomial order 4); peak detection used a minimum S/N of 5, local noise window of 50 m/z, and minimum peak width of 2.9 bins. Filters of S/N 20 and 30 were used for generating peak lists from MS and MS/MS spectra, respectively. Tandem mass spectral data were submitted to database searching against the NCBI non-redundant database (20070926 version, 5519594 sequences, 1911975371 residues) and the *Rhodococcus jostii* RHA1 genome (<http://www.rhodococcus.ca>; 9161 sequences, 2893055 residues) using a locally-running copy of the Mascot program (Matrix Science Ltd., version 2.1), through the Applied Biosystems GPS Explorer software interface (version 3.6). Where required MS/MS spectral data were also submitted to DeNovo sequencing using GPS Explorer TM software – DeNovo Explorer Version 3.6. The following parameters were used: Enzyme: Trypsin, Mass Tolerance; 0.2 Da, Fixed Modifications; Carbamidomethyl (C), Variable Modification; Oxidation (M). The top ten sequence matches were submitted to an MSBlast search against the nrdb95 database using the facility provided by the European Molecular Biology Laboratory [Shevchenko et al. 2001].

6.3. Results and discussion

6.3.1. Enrichment selection and characterisation of *R. erythropolis* MLT1

Rhodococcus erythropolis MLT1 NCIMB 14574 was isolated from an enrichment culture using β -myrcene as a sole carbon source (SCS) inoculated initially with soil surrounding the roots of a hop plant, as described in the Methods section, and identified through 16S rRNA sequence analysis (NCIMB). Growth of this strain in liquid media with β -myrcene (0.1-0.5 g/L) was very limited, and was likely to be a result of the poor solubility and toxicity observed at higher concentrations of β -myrcene. Improved growth was observed when the β -myrcene was supplied in the vapour phase in Erlenmeyer flasks that had been fitted with a central glass well, into which the β -myrcene was deposited (fig. 93). GC analysis of organic extracts of the growth medium at intervals showed an absence of β -myrcene, and it appears therefore that the substrate in the vapour phase is taken up from the flask headspace by the cells. In cultures using β -myrcene in the vapour phase as SCS a prolonged exponential phase of 15 h preceded a maximum OD (recorded at 600 nm) of 0.45 (fig. 94). Growth rates were increased using glucose or succinate as SCS with exponential phases lasting 7 and 9 h respectively, before reaching optical densities as measured by absorbance at 600 nm of 0.6 and 1.5 respectively (fig. 94).

A



B

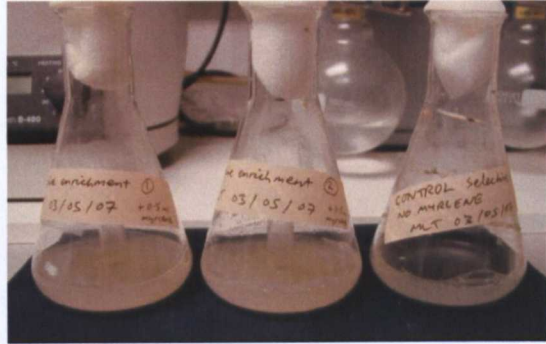


Figure 93: (A) Growth of *R. erythropolis* MLT1 on M9 minimal media agar with myrcene as the SCS (5 g/L). (B) Growth in M9 with myrcene as SCS in the vapour phase (flasks 1 and 2), and M9 medium without myrcene (flask 3).

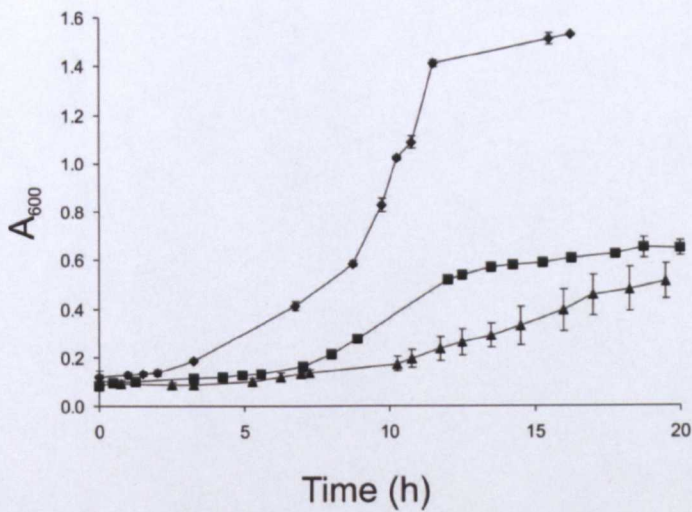


Figure 94: Growth curves plotting absorbance recorded at 600 nm (A_{600}) against time for *R. erythropolis* MLT1 utilising: succinate (\blacklozenge), glucose (\blacksquare), and β -myrcene (\blacktriangle) as the sole sources of carbon for growth. Each point corresponds to the average value calculated on the basis of results recorded for three cultures grown in parallel.

6.3.2. Biotransformation of β -myrcene

Resting cells of *R. erythropolis* MLT1 harvested from the late exponential phase of growth were resuspended (50 g/L) in a pH 7.0 phosphate buffer and incubated with β -myrcene (7.4 mM) for 1 h at 30°C (fig. 95A). A variety of control experiments were performed that included incubating cells without β -myrcene, and incubating phosphate buffer and cells inactivated through autoclaving, with the substrate (figure 95E). No biotransformation products were observed in any of the controls, however a single GC peak with retention time 7.60 min not present in the background was found to be produced only on incubation of β -myrcene-grown cells with β -myrcene. A time-course for this assay showed an increasing concentration of this product over an initial 5 min period (fig 95, B–D), after which the concentration remained constant for approximately 2 h. The dependence of this biotransformation on the presence of molecular oxygen was studied in a control experiment carried out under anaerobic conditions. A single batch of cells was prepared as before with β -myrcene as the SCS in the vapour phase. Division of the cell resuspension into two aliquots enabled reproduction of the standard biotransformation, again showing the formation of the peak at 7.60 min from 1 h incubation at a temperature of 25°C, replicating the ambient temperature measured in the anaerobic hood for the control assay. The second aliquot of active cells was pre-equilibrated in the anaerobic environment, and then challenged with the substrate. GC analysis of the anaerobic biotransformation mixture revealed no production of the peak at 7.60 min under anaerobic conditions.

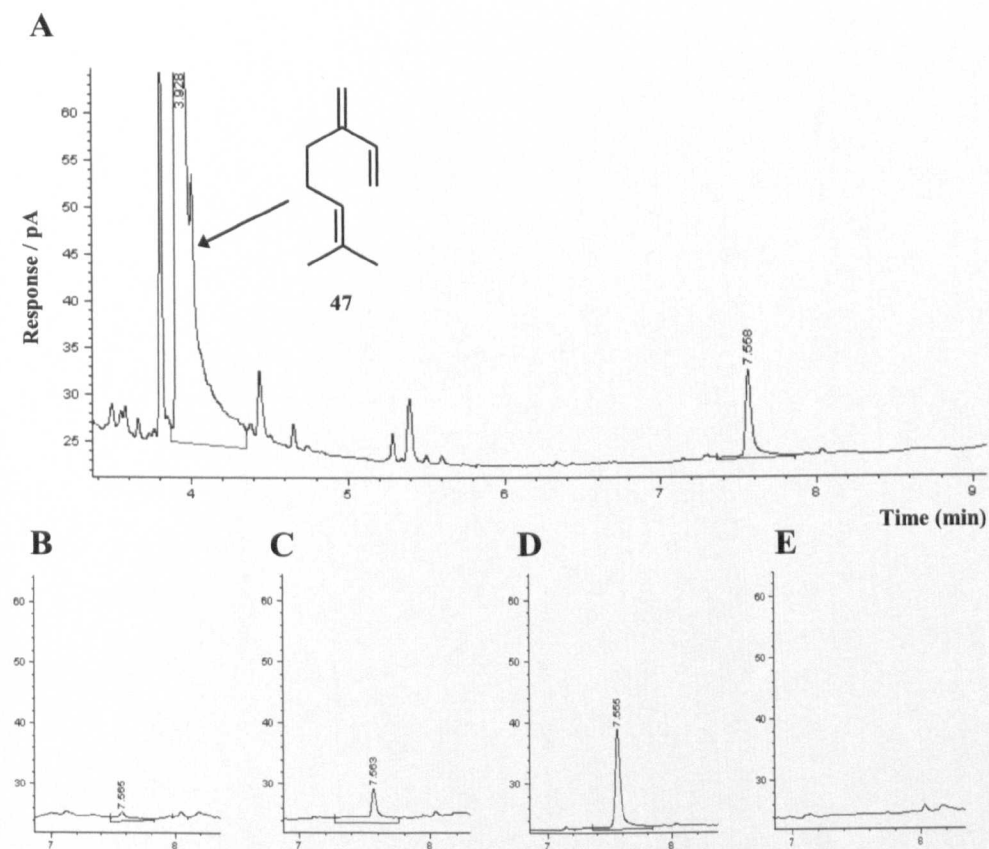


Figure 95: Chromatograms of injections of the β -myrcene biotransformation extracts after: (A) $t = 1$ h; (B) $t = 0.1$ min; (C) $t = 0.5$ min; (D) $t = 5$ min; (E) dead cell control at $t = 1$ h. β -myrcene eluted at 3.93 min.

6.3.3. Metabolite identification

The MS of the biotransformation product (fig. 96) revealed good correlation to existing published data [Adams 1995; Jennings and Shibamoto 1980; Ojala et al. 1999] for the GC-MS analysis of geraniol (3,7-dimethylocta 2,6-dien-1-ol) **7**. The correlation is detailed in Table 8, where the major peaks at m/z : 41, 69, and 67 are consistent with the fragmentation pattern observed in this analysis. The absence of the expected molecular ion at m/z 154 from GC/MS studies presented herein was not without precedent [Ojala et al. 1999].

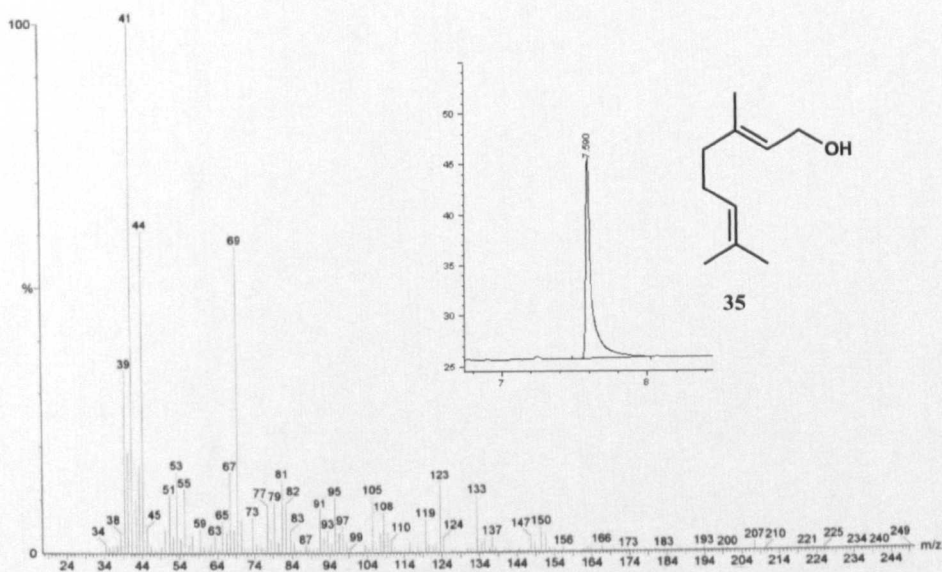


Figure 96: Mass spectrum for the geraniol metabolite (inset shows GC analysis for an authentic geraniol standard 50 μ M).

Table 8: Published GC-MS data for geraniol.

Reference	Ions <i>m/z</i> (relative abundance)							
	1	2	3	4	5	6	7	8
Jennings 1980	69 (100)	41 (93)	68 (52)	93 (44)	44 (37)	67 (34)	55 (32)	84 (30)
Adams 1995	41 (100)	69 (95)	68 (20)	67 (16)	93 (12)	53 (12)	123 (10)	43 (10)
Ojala 1999	69 (100)	93 (24)	68 (19)	67 (18)	53 (14)	91 (13)	55 (10)	79 (10)

Evidence was also obtained to demonstrate that isomers of geraniol are not responsible for the major product peak. An authentic standard of the stereoisomer nerol ((*2Z*)-3,7-dimethylocta-2,6-dien-1-ol) run under the same GC conditions was found to have a HP5 retention time of 7.25-7.30 min compared to that for geraniol of 7.60 min. The structural isomer, isogeraniol ((*3Z*)-3,7-dimethylocta-3,6-dien-1-ol) has published retention indexes lower than those for nerol [Rocha et al. 2007]. A calibration line generated from a geraniol standard shows an approximate 50 μ M product concentration from the biotransformation in a 1 h assay representing a conversion from β -myrcene of ~2%. Further samples were prepared from three separate cultures for the biotransformation of β -myrcene each showing the product with a retention time of 7.60 min. In addition to these samples, three standards of geraniol at: 0.03, 0.05, and 0.5 mM were also prepared for further analytical work to confirm the product identity. A standard linear n-alkane series (C10-C18) was run on both DB5 (non-polar) and DB17 (polar) GC columns giving incremental retention times with increasing chain length. All samples and standards were then run on the

DB17 column where a shift (increase) in retention time was observed for geraniol due to interactions of the hydroxyl group with the polar column, when compared to the standard alkane series (giving a retention time similar to the C14 alkane on the same column). The retention times of the three samples run on DB17 column (11.16-11.21 min) overlapped with those for the geraniol standards (11.13-11.20 min). Peak areas were proportional in samples and standards run on both HP5 and DB17 columns, again confirming the identity of the product peak as geraniol.

6.3.4. Cytochrome P450 inhibition studies

Cells were harvested from cultures grown in parallel and combined before splitting into separate aliquots to study the effects of cytochrome P450 inhibition on the biotransformation. GC analysis of the reactions catalysed by cells in the absence of inhibitors revealed concentrations of geraniol that were consistent with previous observations. Pre-incubation of cells at 30°C for 1 h with metyrapone (1 mM) led to a 23% reduction in the concentration of geraniol produced. The effect of incubation with 5 mM 1-aminobenzotriazole (ABT) for the same period was a 73% decrease in the yield of geraniol (fig. 97). A range of concentrations from 0-5 mM was investigated for both inhibitors however there was no correlation observed between concentration of inhibitor and the negative effect on β -myrcene biotransformation. Extended pre-incubation times of up to 2 h with the inhibitors also did not result in

greater levels of inhibition. Complete inhibition of the biotransformation of β -myrcene to geraniol was not observed for any of the assays conducted using cytochrome-P450 inhibitors.

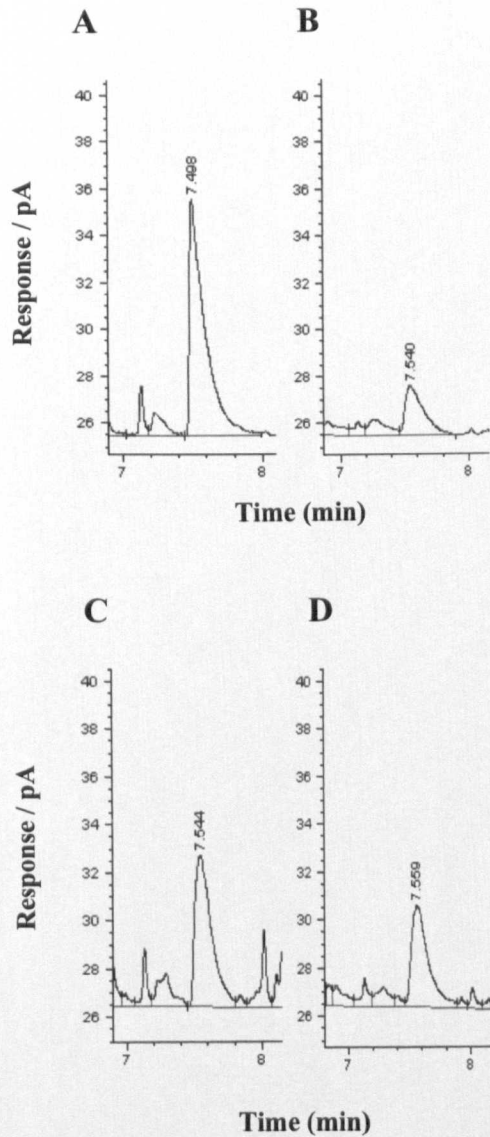


Figure 97: Comparison of resting cell biotransformations of β -myrcene to geraniol without P450 inhibitors (**A** and **C**) to assays with 1 h pre-incubation of the inhibitors 5 mM ABT (**B**) and 1 mM metyrapone (**D**).

6.3.5. Inducibility of β -myrcene biotransformation

The resting cell assay was repeated using cells grown on glucose and succinate as the sole sources of carbon for growth. GC analysis of the extracts from these assays showed no geraniol product peak as previously described for those cells grown on β -myrcene in the vapour phase (fig. 98). *R. erythropolis* cells were also grown on glucose until reaching late log-phase before β -myrcene was added to the flask and incubated for a further 24 h in an attempt to induce the expression of enzymes required for activity. Extracts from these resuspended cells did not show any activity towards the biotransformation of β -myrcene. The ability of *R. erythropolis* MLT1 to convert β -myrcene into geraniol was shown previously to be dependent upon growth of the cells with β -myrcene as the sole carbon source, and that no biotransformation was observed when grown on glucose. These results suggested that the expression of some proteins may be inducible with growth on β -myrcene as the sole carbon source. Insoluble and soluble extracts from cells grown on either glucose or β -myrcene were obtained and analysed by SDS-PAGE (fig 99A). Gel A clearly shows induced expression of a band of protein at a MW of approximately 16 kDa labelled I. Analysis of tryptic digests of this band by mass spectrometry with subsequent comparison of peptide mass fragments against database searches using Mascot failed to identify any clear hits. Gel A also shows additional bands induced in the molecular mass region corresponding to between 43 kDa and 66 kDa.

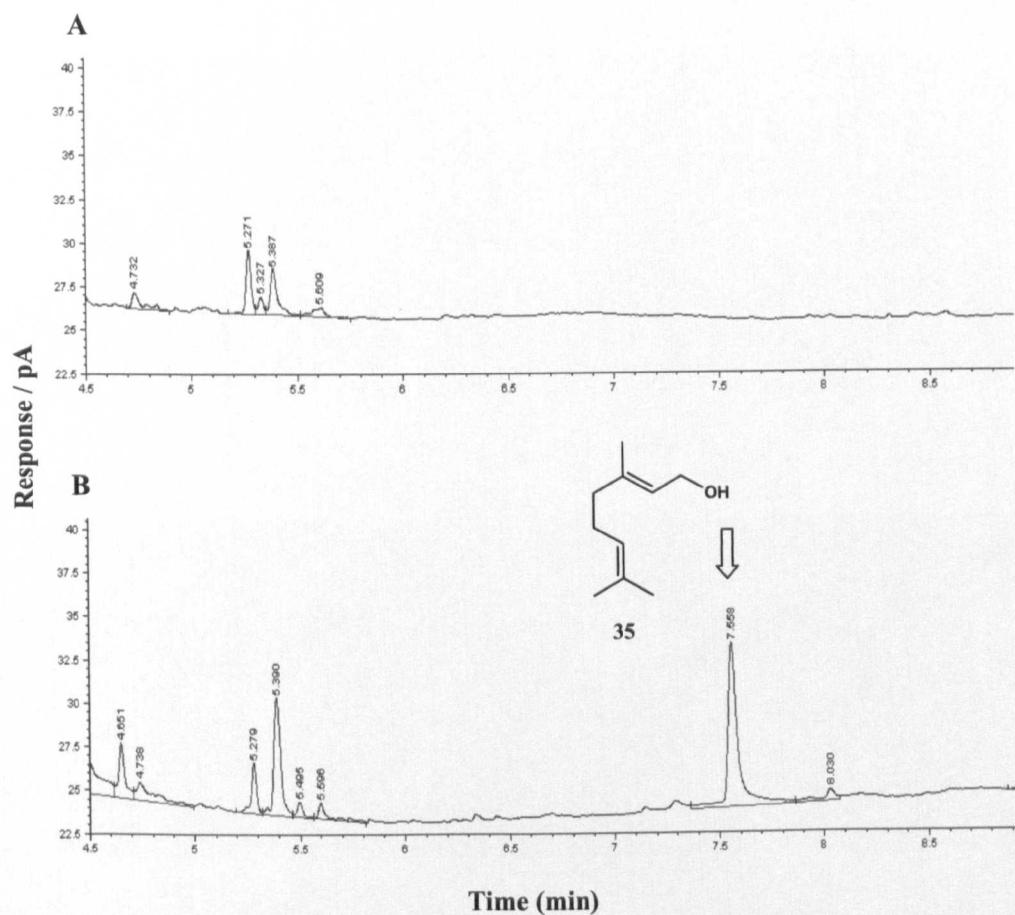


Figure 98: Comparison between cells grown on M9 supplemented with glucose (no β -myrcene) (A), and those grown on M9, with β -myrcene in the vapour phase as SCS (induced) (B). Results for succinate grown cells not shown.

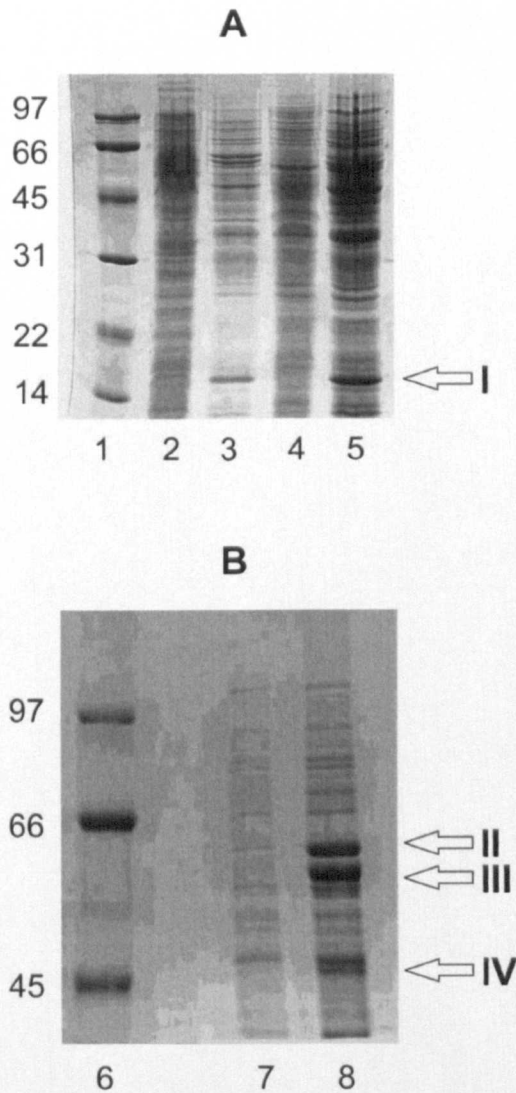


Figure 99: SDS-PAGE analysis of the crude soluble cell extracts of *R. erythropolis* MLT1 grown on either glucose or β -myrcene as SCS. Gel **A** shows denatured proteins in the molecular mass range 14–97 kDa analysed on a 12% acrylamide gel: Lane **1**: BioRad low molecular mass markers with molecular mass shown in kDa; Lane **2**, Soluble extract from cells grown on glucose; Lane **3**, soluble extract from cells grown on β -myrcene; Lane **4**, Insoluble extract from cells grown on glucose; Lane **5**, Insoluble extract from cells grown on β -myrcene. Gel **B** showing denatured proteins in the molecular mass range 45–97 kDa analysed on an 8% acrylamide gel: Lane **6**: BioRad low molecular mass markers with molecular mass shown in kDa; Lane **7**, soluble extract from cells grown on glucose; Lane **8**, soluble extract from cells grown on β -myrcene. Equal concentrations of protein were loaded into lanes on the same gel.

Increased resolution of proteins in this region was achieved between these molecular masses (fig 99B) by decreasing the percentage acrylamide in the gel, and running for a longer period of time. At least three further bands, **II**, **III** and **IV** on the gel were enhanced in samples having been obtained from cells grown on β -myrcene. MS analysis of tryptic fragments obtained from bands **II** and **IV** followed by a BLAST search and comparison with entries in the Mascot database suggested **II** was homologous to the 60 kDa chaperonin GroEL from *Rhodococcus jostii*. RHA1 (Table 9). **IV** was assigned as a putative acyl-CoA dehydrogenase based on the similarity to a peptide fragment from *Frankia alni* (Table 9). Equivalent analysis of band **III** did not yield any clear hits within the Mascot database, however, De Novo sequencing followed by searching against the BLAST database suggested that the protein was homologous to 2-hydroxymuconic acid semialdehyde dehydrogenase from *Pseudomonas*, based on the identification of peptide fragments LSYVEEAVSEGATLVTGG and DEFVAR.

Table 9: Identification of protein bands II and IV (Figure 99) using MS analysis of peptide fragments followed by matching against the Mascot database.

Band	Protein	Database	Peptide Sequences matched	Mowse score	Mowse score identity threshold	Expect score
II	60 kDa chaperonin GroEL	<i>Rhodococcus jostii</i> RHA1	IIAFDEEAR	45	22	0.00032
			WGAPTITNDGVSIAK	37	22	0.0018
			QEAVLEDAYILLVSSK	50	21	7.50E-05
			TDDVAGDGTTTATVLAQALVR	28	21	0.012
			KTDDVAGDGTTTATVLAQALVR	35	21	0.0023
			EGVITVEESNTFGLQLELTEGMR	20	20	0.053
IV	Putative Acyl-CoA dehydrogenase [<i>Frankia alni</i> ACN 14a]	NCBI nr	ILEIFEGANELQQWIIAR	117	49	8.60E-09

6.4. Conclusions

In this chapter of work, a strain of *Rhodococcus erythropolis* was isolated that is observed in resting cell biotransformations to convert β -myrcene to the important flavour compound geraniol [Thompson et al. 2010]. Although much is known about the mechanisms by which some bacteria oxygenate alkene substrates [Ensign 2001], the chemical-enzymatic mechanism of this particular transformation is at this stage unclear, and an explanation must await labelling experiments to reveal the origin of the oxygen atom that has been introduced into β -myrcene.

Mechanisms for biotransformations of this nature routinely involve epoxidation by a multicomponent monooxygenase enzyme, of which different types have been observed in, for example *Xanthobacter* strain Py2 [Small and Ensign 1997] and *Rhodococcus* strain AD45 [Van Hylckama Vlieg et al. 2000]. No component of such a monooxygenase was yet identified in 1-D gels of extracts resulting from cells induced with β -myrcene from mass spectrometric analysis of tryptic fragments, although the biotransformation of β -myrcene by *R. erythropolis* MLT1 clearly required an aerobic environment. Another possible route for the incorporation of a single atom of molecular oxygen into an alkene substrate was described in styrene-oxidising bacteria, in which the successive action of styrene monooxygenase, followed by an isomerase enzyme, results in the terminally monooxygenated

compound phenylacetaldehyde from styrene oxide (fig. 100) [Panke et al. 1998], but as yet, no such system has been described in the metabolism of aliphatic alkenes.

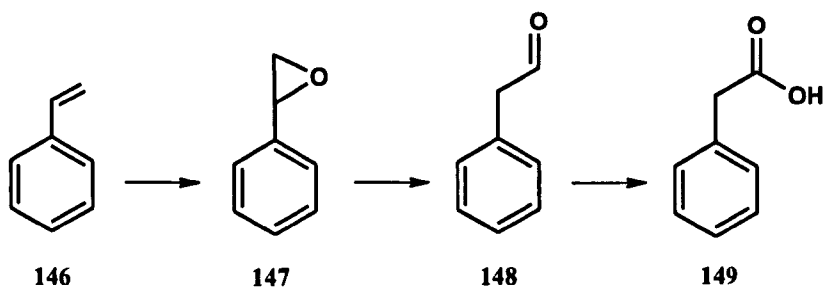


Figure 100: Oxidation at a terminal alkene position in styrene **146** catalysed by a monooxygenase from *Pseudomonas* sp. VLB120 [Panke et al. 1998].

Of other enzymes that catalyse the incorporation of a single atom of oxygen into an alkene substrate, the contribution of cytochrome-P450 in the oxygenation of β -myrcene by *R. erythropolis* MLT1 has not been discounted by the relevant inhibition studies. Alkenes such as myrcene have been shown to act as substrates for cyt-P450 enzymes [Sandstrom et al. 2006], although in previous studies, such as those on the cytochrome-P450 steroid 9- α hydroxylase from *Mycobacterium fortuitum* [Kang and Lee 1997], the level of inhibition by metyrapone increased with increasing inhibitor concentration. This was not the case for the transformation by *R. erythropolis* MLT1 presented in this chapter.

The chemical transformation of β -myrcene to geraniol is formally a hydration reaction. The hydration of myrcene could also lead to linalool, and, whilst there is a precedent for the microbial transformation of linalool to geraniol through a putative 3,1-hydroxyl- Δ^1 - Δ^2 -mutase [Fo β and Harder 1997], there are relatively few lyases

describing the hydration of an alkene not part of α , β -unsaturated systems conjugated to ketone or (thio)ester functionality (figure 101 shows a whole cell *Rhodococcus* catalysed hydration of one such conjugated position). However one example was the limonene hydratase described by Oriol and co-workers, which was used to convert limonene to α -terpineol, carvone and perillyl alcohol (fig. 102) [Savithiry et al. 1997].

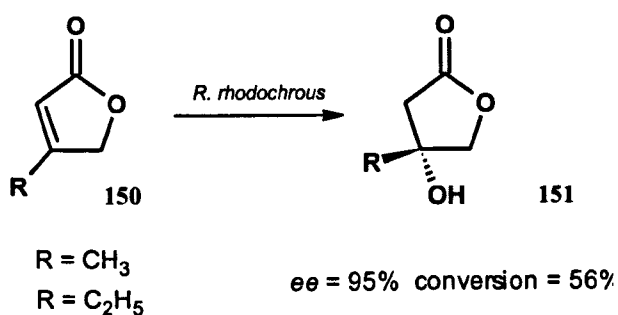


Figure 101: Enantioselective hydration of the conjugated C=C bond in 3-methyl and 3-ethylbutanolide [Holland et al. 1998].

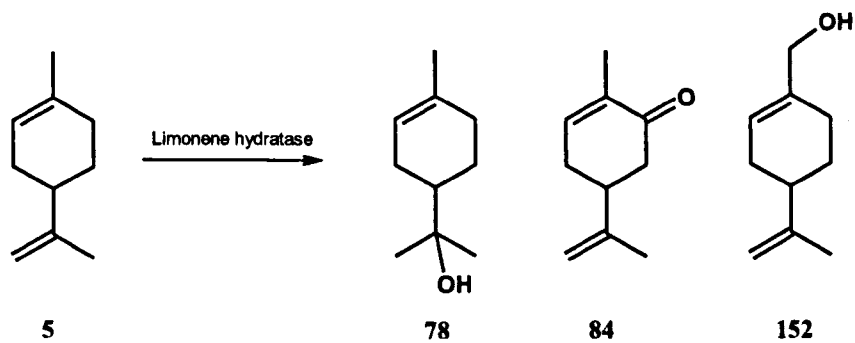


Figure 102: A thermostable limonene hydratase cloned from *B. stearothersophilus* hydrates a non-conjugated double bond in limonene **5** leading to the formation of α -terpineol **78**, in addition to other products carvone **84** and perillyl alcohol **152** [Savithiry et al. 1997].

The other chemical methods of conversion to geraniol described in the chapter 1 Introduction are dependent on, for example, hydrocobaltation of the terminal alkene, followed by radical trapping with TEMPO and subsequent reduction with zinc [Howell and Pattenden 1990]. Whilst these mechanisms of hydroxylation have no formal equivalent in biochemistry, the use of metal assisted catalysis for the transformation of β -myrcene by MLT1 cannot at this stage be ruled out.

Of the enzymes that are apparently induced in MLT1 by growth on β -myrcene, each has precedent in inducible systems for hydrocarbon degradation in bacteria described previously. An aldehyde dehydrogenase of theoretical molecular mass 54.3 kDa, similar to that observed in Figure 99, gel B, was one of the proteins encoded in a putative operon for β -myrcene degradation in *Pseudomonas* sp. M1 [Iurescia et al. 1999]. A 13-fold upregulation of expression of the GroEL chaperone proteins was observed in *Rhodococcus* sp. RHA1 when induced by propane, the degradation of which is also dependent on a multicomponent monooxygenase [Sharp et al. 2007]. A 1.8 fold increase in expression of GroEL in addition to a number of other chaperones, has also been found as part of a response to growth of *Pseudomonas* sp. M1 on β -myrcene as the SCS [Santos and Correia 2009]. Given the established pathways for the degradation of geraniol by, for example, *Pseudomonas*, through the formation and subsequent degradation of a geranyl-CoA thioester [Förster-Fromme et al. 2006], the involvement of an acyl-CoA dehydrogenase as suggested by MS analysis of induced proteins, would also not be unexpected; indeed an acyl-CoA dehydrogenase with

specificity for citronellyl-CoA was recently described [Förster-Fromme et al. 2008]. The unambiguous identification of the enzymes responsible for degradation of β -myrcene in MLT1 awaits the cloning of the relevant genes and characterisation of their expressed products. Further sub-cellular work is described in the following chapter of work, which aims to uncover mechanistic details for this novel biotransformation identified here.

Enzymes involved in the metabolism of β -myrcene by bacteria may in the future be usefully applied as biocatalysts in the production of natural-equivalent flavour and fragrance compounds. Control experiments for the biotransformation described in this chapter have demonstrated that geraniol is a biogenic product of β -myrcene incubation with *R. erythropolis* MLT1 rather than an artefact of effects due to reaction medium, inactive biological material or pH. The one-pot biotransformation of β -myrcene to geraniol might present therefore a potentially attractive industrial biocatalytic route towards a fragrant monoterpene, from an inexpensive and naturally abundant hydrocarbon starting material.

7. Chapter 7: Sub-cellular studies of the myrcene degrading strain *Rhodococcus erythropolis* MLT1

7.1. Introduction

Work from the previous chapter of this thesis described how the biotransformation of myrcene to geraniol by *Rhodococcus erythropolis* MLT1 was found to be inducible when the organism was grown on myrcene as the sole carbon source. Comparative SDS-PAGE analysis of soluble and insoluble extracts from cells grown on myrcene, glucose and succinate as SCS revealed induction of: a 60 kDa chaperonin GroEL, a putative acyl-CoA dehydrogenase, and an aldehyde dehydrogenase in extracts from those cells viable for this biotransformation. A precedent for each of these proteins has been described in the characterisation of gene clusters responsible for the degradation of hydrocarbon substrates including myrcene. Genes have been identified in *Pseudomonas* strain M1 which confer an ability to grow on myrcene as SCS. Four open reading frames were assigned to encode genes involved in the conversion of myrcene to myrcen-8-ol, which included aldehyde and alcohol dehydrogenase enzymes.

The involvement of an acyl-CoA dehydrogenase in the catabolism of the acyclic monoterpene alcohols citronellol and geraniol has been studied in other *Pseudomonas*

strains [Forster-Fromme et al. 2006, Forster-Fromme and Jendrossek 2006, Diaz-Perez et al. 2004] (fig. 103). The proposal of an acyclic terpene utilisation (ATU) pathway preceded characterisation of a subgroup of acyl-CoA dehydrogenases with specificity for terpenoid structures [Forster-Fromme et al. 2008].

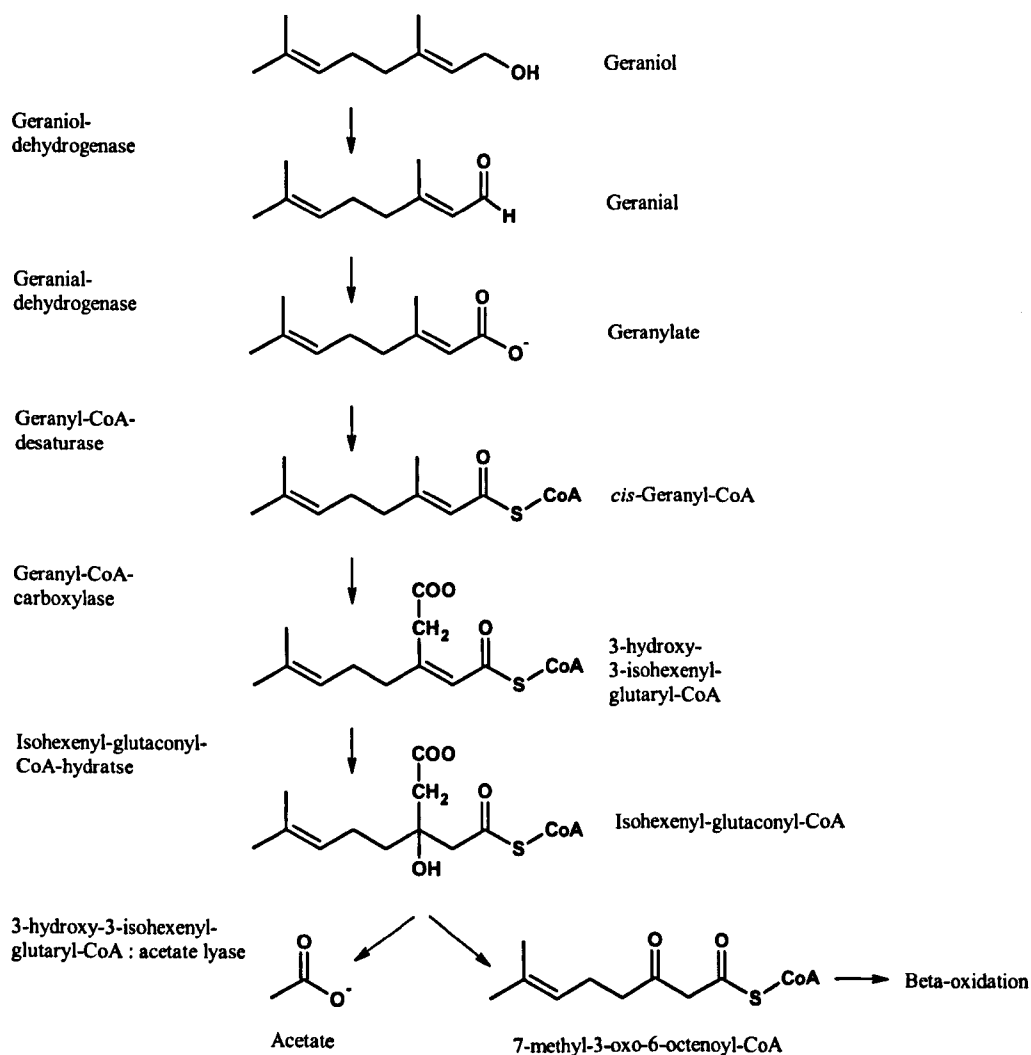


Figure 103: The acyclic terpene utilisation (ATU) pathway showing the degradation of geraniol in *Pseudomonas citronellolis* [Hoschle and Jendrossek 2005, Forster-Fromme and Jendrossek 2006].

The degradation of *N*-nitrosodimethylamine (NDMA) has been demonstrated in *Rhodococcus* sp. RHA1, with activity towards this compound found to be inducible by approximately 500-fold when the organism was grown on propane [Sharp et al. 2007]. Amongst a number of genes which were up-regulated in this response, a 13-fold increase in expression of a 60 kDa chaperonin GroEL protein was determined *via* quantitative RT-PCR analysis. This protein in addition to the alkene monooxygenase activity responsible for NDMA degradation, were found encoded as part of a 13-gene operon. Other multicomponent monooxygenase enzymes have been highlighted as part of gene clusters involved in the metabolism of alkenes. Utilisation of the volatile alkene isoprene (2-methyl-1,3-butadiene) as a SCS for growth in *Rhodococcus* strain AD45 was facilitated by an initial monooxygenase step, leading to the formation of an epoxide prior to glutathione conjugation and further metabolism (fig. 104) [Van Hylckama Vlieg et al. 2000].

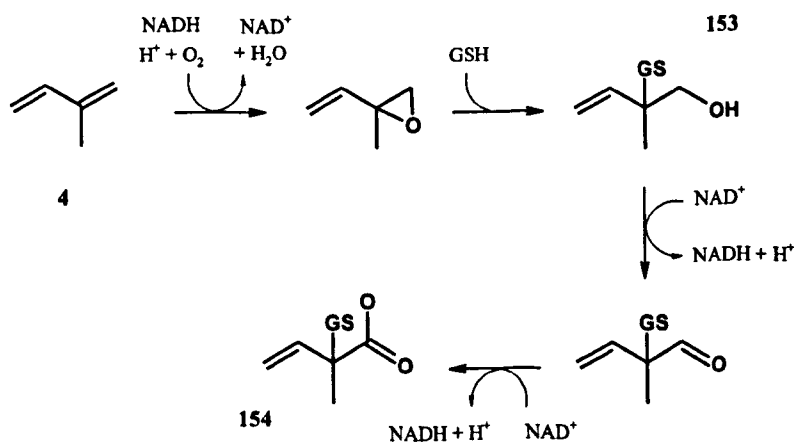


Figure 104: An initial monooxygenase catalysed step in the pathway of isoprene degradation in *Rhodococcus* strain AD45 from Van Hylckama Vlieg et al. 2000.

An enzyme capable of incorporating oxygen functionality into alkene substrates could not be identified in chapter 6 to help explain the potential mechanism by which *R. erythropolis* is able to convert myrcene to geraniol. Attempts will be made in this chapter of work to clone the myrcene induced genes already identified, and also those genes neighbouring the 60 kDa GroEL, and aldehyde- and acyl-CoA dehydrogenases as part of a potential myrcene degradation cluster. The expressed products of these genes may yield the enzyme(s) responsible for the conversion of myrcene to geraniol to complement those already identified with a proposed role in the further metabolism of geraniol by this strain of *Rhodococcus*.

7.2. Experimental

7.2.1. Fermentation of *R. erythropolis* MLT1

10 x 50 mL shake-flask pre-cultures of M9 medium with either glucose 1.0 g/L or β -myrcene (vapour phase) as sole carbon sources were inoculated with *R. erythropolis* MLT1 from agar plates and incubated at 30°C for 24 h to provide a 10% (v/v) inoculum for fermentation. A fermentation vessel containing 5 L of M9 minimal medium was sealed and autoclaved for 2 h at 120°C (FeSO₄·7H₂O 2.5 g/L was filtered in afterwards). Carbon sources to be supplied to the fermentation media were either syringe filtered into the vessel (glucose 0.5 or 1 g/L), or the vapour bubbled in through the air supply (β -myrcene). The fermentation medium was stirred at a temperature of 30°C, and samples extracted over a time-course for measurements of growth (A_{600}) until stationary phase. The cells were harvested using a Beckman Avanti centrifuge – JLA 8.1000 rotor (6,000 x g, 40 min, 4°C). Resting whole cell assays with myrcene as the substrate were carried out as described in chapter 6.

7.2.2. Purification of a 15 kDa myrcene induced protein

7.2.2.1. Preparation of soluble protein

Rhodococcus erythropolis MLT1 cultures (prepared as described in chapter 6) were grown in 50 mL volumes of M9 minimal medium with β -myrcene as the SCS in the vapour phase. A combined culture volume of 1.5 L was harvested once the cells had reached stationary phase of growth using a Sorvall RC5B – GS3 rotor (6,000 x g, 45 min, 4°C) and the cell pellet re-suspended in one-tenth growth volume of 50 mM potassium phosphate buffer pH 7.0. The cells were lysed by three passages through a continuous flow French press at 270 MPa. The cell debris was removed by centrifugation using a Sorvall RC5B – SS34 rotor (34,500 x g, 20 min, 4°C) before retaining the soluble cell extract which was filtered using a 0.45 μ m filter (Millipore – PES membrane).

7.2.2.2. Anion exchange chromatography (1st step)

An anion exchange FFQ column (volume 50 mL) was pre-equilibrated with 50 mM potassium phosphate buffer (pH 7.0), and the column loaded with the filtered cell extract. The protein of interest was found to pass through this column between a 40-90 mL elution of 50 mM phosphate buffer. An increasing step-wise gradient of NaCl

concentration from 0-1.5 M was applied for elution of bound proteins. Fractions found to contain the 15 kDa protein, were pooled and concentrated using a centricon 3k molecular-weight cut-off filter (centrifuged at 4,500 x g, 1 h, 4°C) prior to a second step of purification.

7.2.2.3. Gel filtration chromatography (2nd step)

A Superdex S75 10/30 gel filtration column (volume 24 mL) was equilibrated and run with 50 mM potassium phosphate buffer (pH 7.0), collecting 0.4 mL fractions. The 15 kDa protein was found to elute from the column between 11.5-13 mL. The progress of protein purification was monitored by SDS-PAGE, and concentration of proteins determined using the method of Bradford [Bradford 1976].

7.2.3. Assaying sub-cellular fractions for activity towards myrcene and linalool

Incubations of the crude cell extract (1 mg/mL) and the purified 15 kDa protein (0.09 mg/mL) with myrcene and linalool as the substrates (1 µL/mL) were carried out at 30°C in sealed glass vials; with samples extracted over a 17 h period using a 1:1 mixture of petroleum ether and ethyl acetate for GC analysis (as before).

7.2.4. PCR for genes encoding myrcene induced proteins

A standard PCR mixture contained 0.4 μM of forward and reverse primers (ordered from MWG), 0.2 mM dNTPs, 1 μL KOD hot start DNA polymerase (1 unit/ μL), 1 mM MgSO_4 , 5 μL 10x buffer, 50 ng template DNA, 5% v/v DMSO, and water to 50 μL . Thermocycling conditions were as follows: initial denature 4 min at 94°C, followed by 35 cycles of: denature 1 min at 94°C, annealing 1 min at 48°C, and extension 1.5 min at 72°C, with a final extension step 3 min at 72°C. For optimisation in individual reactions changes were made to the concentration of MgSO_4 (0.5-2.5 mM), DMSO (0-10% v/v), and annealing temperature (45-70°C). For the use in touchdown PCR programs a decreasing annealing temperature (-1°C per cycle) was used.

Primers for 60 kDa chaperonin GroEL:

GroEL for1: 5'-TGGGGCGCSCCSACATCACS-3'
GroEL for2: 5'-ATCATCGCGTTCGAC-3'
GroEL rev1: 5'-CACASAGSAGGATGTASGCGTA -3'
GroEL rev2: 5'-CTTGAGCTCACGAG-3'

Primers for unknown 15 kDa protein:

15 kDa for1: 5'-GCSGACGCSGCSGAG-3'
15 kDa for2: 5'-GACTACMAGGTSGTSACSGGC-3'
15 kDa rev1: 5'-CTCSGCSGCGTCSGC-3'
15 kDa rev2: 5'-GCCGGTGACGACCTKGTAGTC-3'

(where K = G or T; S = G or C; W = A or T; H = A or T or C)

7.3. Results and discussion

7.3.1. Investigation into fermentation as a method of generating increased biomass for sub-cellular studies

To enable activity assays with sub-cellular fractions and purification of myrcene induced proteins, a method of generating significant *R. erythropolis* biomass was required. Cells from shake-flask cultures supplemented with succinate and glucose were shown in the previous chapter to be inactive towards the biotransformation of myrcene to geraniol. Attempts to induce the activity in cultures which were initially grown on M9 media enriched with succinate and glucose also failed to generate cells which are viable for this biotransformation.

An initial fermentation of *R. erythropolis* with glucose supplied as the SCS provided a control for which comparisons with myrcene addition as the growth substrate could be made. After a 10% v/v inoculation of the 5 L fermentation, an initial lag phase of ~3 h preceded a 20 h log phase of growth with a maximum optical density (A_{600}) of 1.25 reached when using glucose (1 g/L) as SCS (fig. 105A). As observed in *R. erythropolis* cultures grown in shake-flasks, the cells harvested from this particular fermentation were found to be inactive towards the biotransformation of myrcene to geraniol in resting cell assays. Another fermentation run aimed to induce cells that had initially utilised glucose as the carbon source for growth (fig. 105B). Myrcene

was supplied into the fermentation medium containing 0.5 g/L glucose however after reaching an optical density of 1.55 and thus yielding a good quantity of biomass, the same observations of inactive cells were found as for the shake-flask grown cultures in the previous chapter.

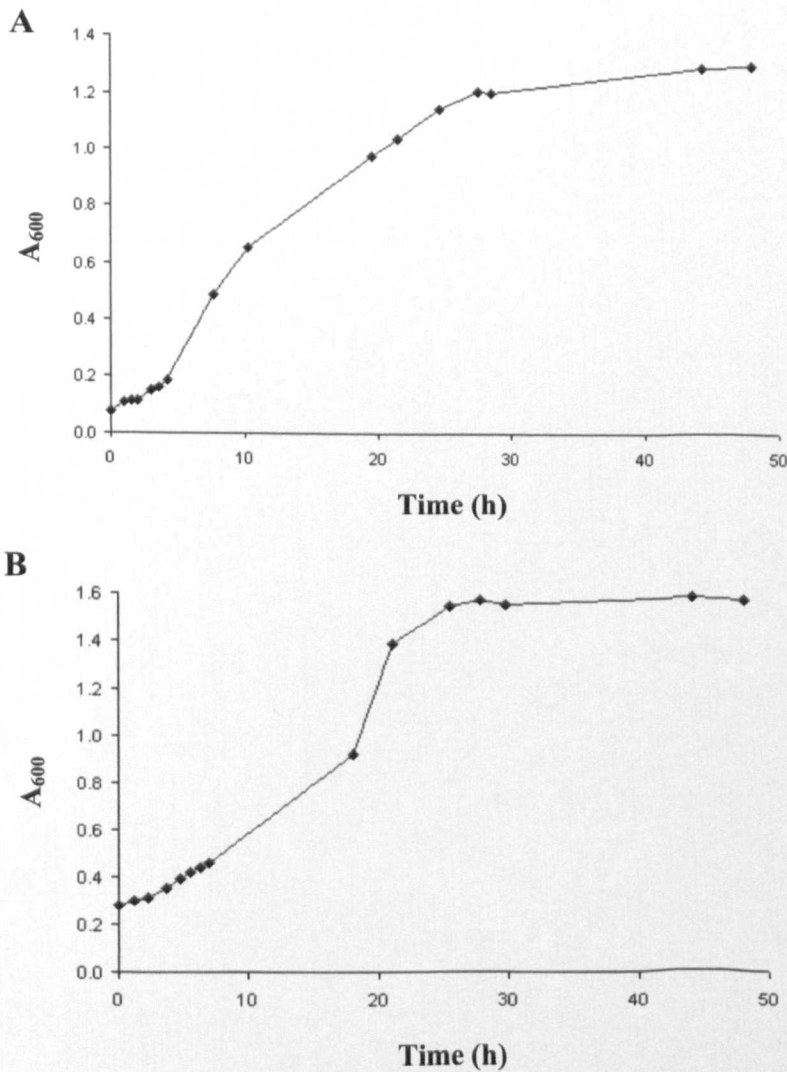


Figure 105: Growth curves plotting absorbance recorded at 600 nm (A_{600}) against time for the fermentation of *R. erythropolis* MLT1 in M9 minimal media with (A): glucose (1 g/L) as the SCS. (B): glucose (0.5 g/L) supplemented with myrcene.

R. erythropolis cells grown on myrcene as SCS have proved active for the biotransformation of myrcene to geraniol when grown in 50 mL cultures (in 250 mL flasks), however an inability to generate active cells upon scale-up to 400 mL incubations in 2 L flasks (with myrcene also in the vapour phase) was thought to be a result of a reduced vapour concentration of the growth substrate. Investigations into the fermentation of this organism with myrcene as the sole carbon source were made, as a potential 100-fold scale-up in growth volume would be desirable for both prospective biotransformation yields whilst also facilitating further sub-cellular studies.

Activity for the biotransformation to geraniol was verified for the *R. erythropolis* pre-culture prior to use as an inoculum in a 5 L fermentation in M9 with myrcene as SCS in the vapour phase. After a prolonged lag-phase of ~10 h a short exponential phase of growth was observed with an increase in optical density from 0.1 to 0.3 (A_{600}) over a 2.5 h period (fig. 106A). It was noted however from GC analysis of extracts from the growth medium, that as a result of supplying the myrcene vapour direct to the culture medium (from $t = 0$) it had accumulated to concentrations that appear to limit growth. An oily film of the growth substrate had accumulated in the fermentation vessel with approximate concentrations of myrcene measured up to 200 μM .

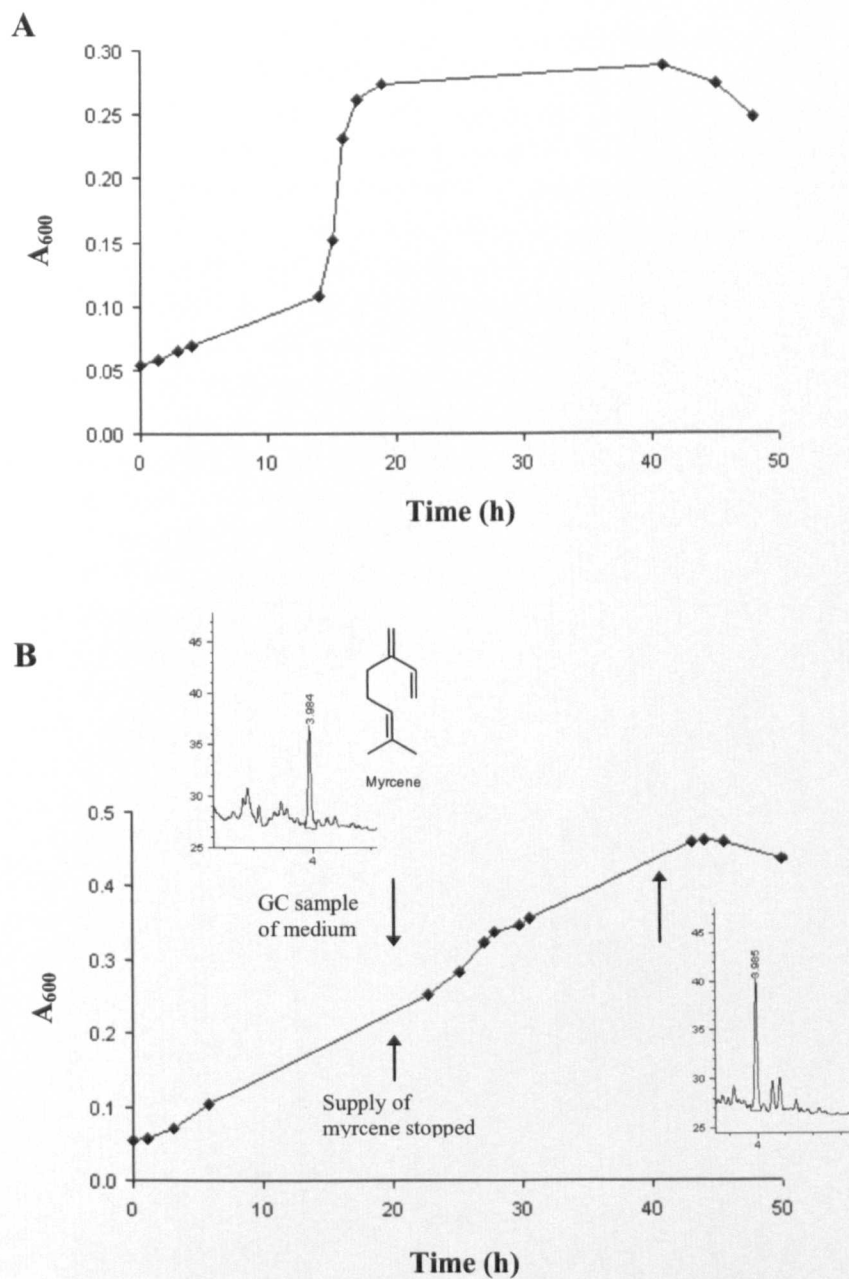


Figure 106: Growth curves plotting absorbance recorded at 600 nm (A_{600}) against time for the fermentation of *R. erythropolis* MLT1 in M9 minimal media with (A): myrcene supplied as the SCS continuously from the start until the end of fermentation. (B): the supply of myrcene stopped after 20 h growth.

For comparison a second fermentation was setup with myrcene as SCS, however the supply of this hydrocarbon to the medium was stopped after a 20 h period when the culture had reached an apparent mid-point in the exponential phase of growth at an OD of 0.2 (fig. 106B). Further growth of *R. erythropolis* was observed to an optical density of 0.45 over an additional 25 h period. The concentration of myrcene in the growth medium measured by GC during this period was $\sim 35 \mu\text{M}$ (fig. 106B). In an attempt to further enhance the levels of growth, myrcene supply was stopped at the start of log-phase (after 4.5 h) in a separate fermentation experiment. The levels of growth in this instance were found not to exceed an OD 0.32, with only trace amounts of myrcene detected through GC analysis (results not shown).

During fermentations with myrcene as the SCS, geraniol could not be detected in the extracts from the growth medium. Despite inoculating the fermentations with cells active for the biotransformation of myrcene to geraniol (figure 107B showing production of $41 \mu\text{M}$ geraniol during a 1 h period), cultures harvested at the end of these fermentations proved inactive during resting cell assays (fig. 107A).

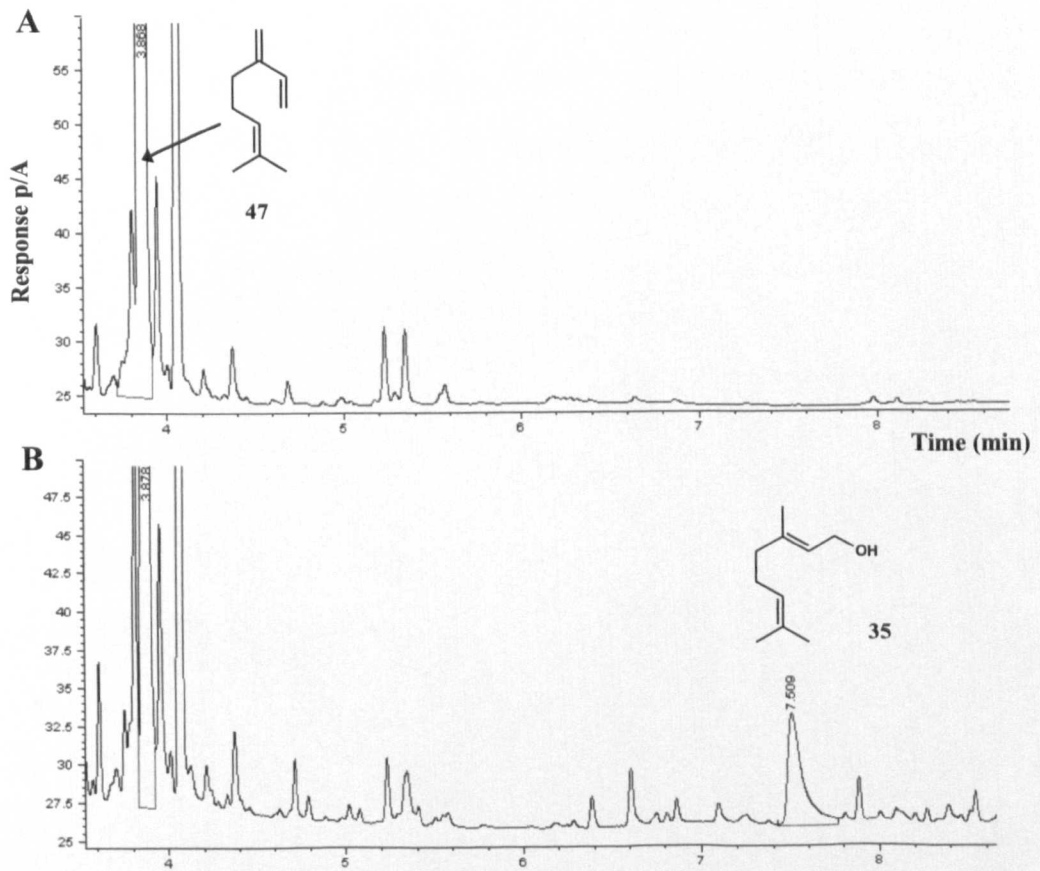


Figure 107: Resting cell assay with myrcene using cells harvested from a 5 L fermentation with myrcene as the SCS (A), and cells from a active shake flask culture used in the initial inoculation of the fermentation medium (B). Samples extracted at $t = 1$ h.

7.3.2. Purification of a 15 kDa myrcene induced protein

Previous investigations into proteins that are induced upon growth of *R. erythropolis* on myrcene as the SCS revealed four which were clearly expressed at greater levels when compared to extracts from glucose grown cells (chapter 6). Identification of three of these proteins was possible *via* sequencing of fragments from tryptic digests, and alignment with homologous proteins in the databases. A 60 kDa chaperonin GroEL, a putative acyl-CoA dehydrogenase, and an aldehyde dehydrogenase were identified through these methods, however an identity to a strongly myrcene induced band at ~15 kDa (fig. 108) could not be assigned.

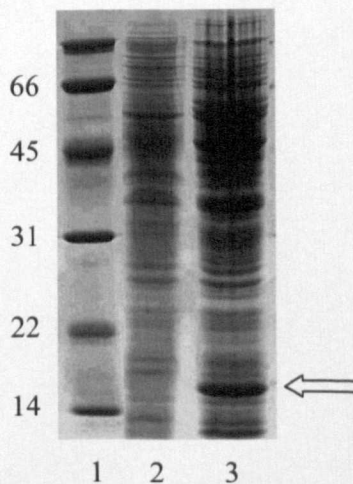


Figure 108: SDS-PAGE analysis from chapter 6. Soluble extracts of *R. erythropolis* MLT1 grown on glucose (*lane 2*), and myrcene (*lane 3*) as SCS. BioRad low molecular mass markers with molecular mass shown in kDa (*lane 1*). Highlighted is the ~15 kDa myrcene induced protein band that could not be identified by initial peptide sequencing.

The following experiments aimed to purify this protein to homogeneity in order to facilitate identification using mass spectrometry. Despite generating increased amounts of biomass, fermentation methods of growth failed to yield cells that are active for the biotransformation of myrcene to geraniol; and comparative analysis of the cell extracts from glucose and myrcene fermentations did not show the apparent induction of proteins that was previously observed in 50 mL shake-flask cultures (results not shown). Growth in 50 mL shake-flask cultures (30x) with myrcene supplied as the SCS in the vapour phase was utilised to provide the biomass for this purification. Anion exchange chromatography was used as the first step of purification. The induced ~15 kDa protein did not bind to a 50 mL FFQ column and eluted in the flow-through fractions (fig. 109A and fig. 109C *lane 3*). The majority of proteins in the cell extract became bound to this column with varying affinity, and could be eluted through an increasing step-wise concentration of NaCl. Fractions from the flow-through containing the induced protein were pooled and concentrated prior to a second purification step of gel filtration chromatography. A peak corresponding to the purified protein was obtained at an elution volume of 12.5 mL from a Superdex S75 10/30 column (fig. 109B and fig. 109C *lane 4*). A comparison of the retention time on this column with those for a standard calibration suggest a monomeric protein composition (fig. 110). The myoglobin standard of MW 17,600 Da is known to elute at a retention time of 23.7 min at a flow rate of 0.5 mL/min (fig. 110). For comparison, this unknown ~15,000 Da protein elutes at 25 min under these conditions.

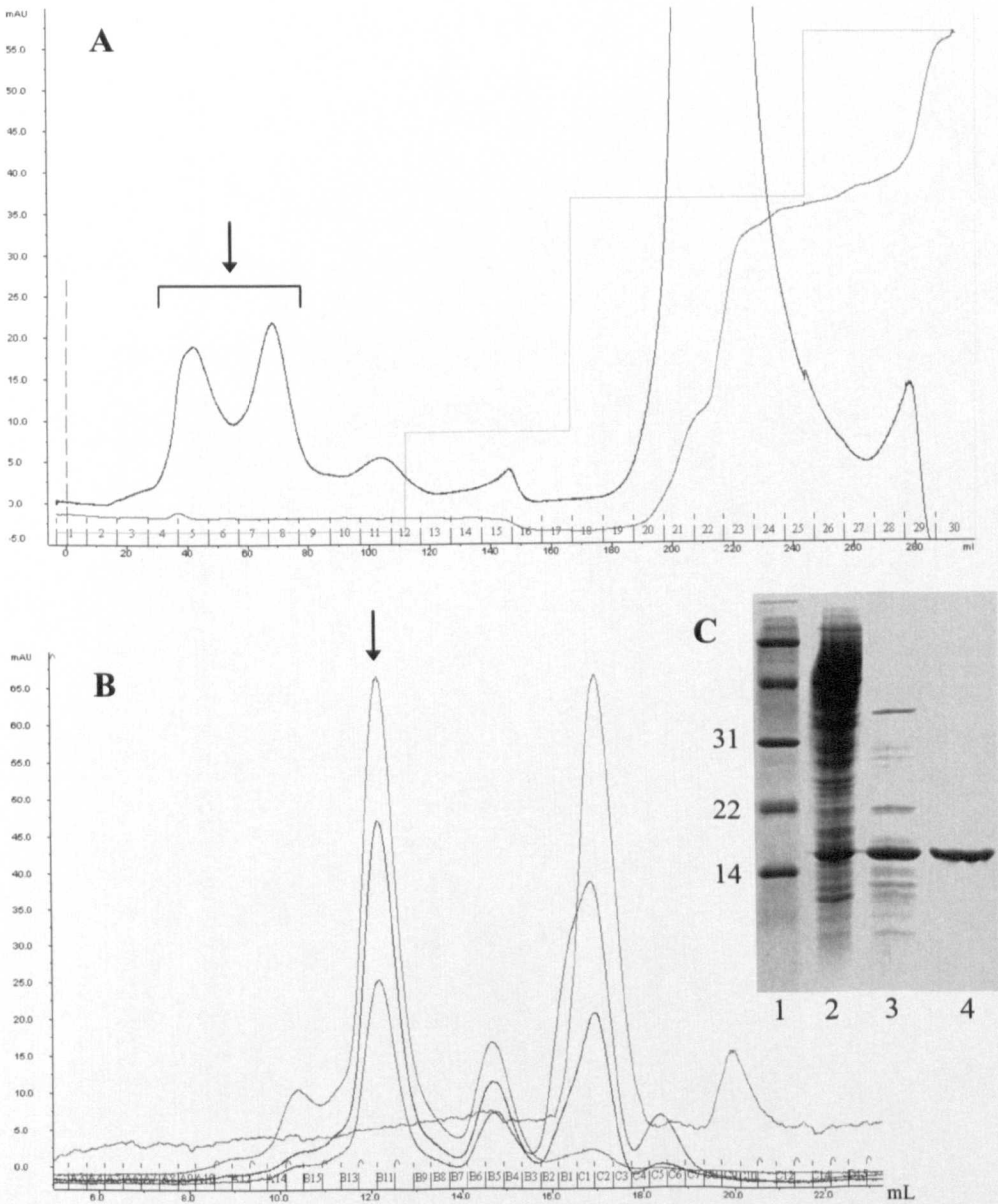


Figure 109: Purification of the unknown ~15 kDa myrcene induced protein from *R. erythropolis* cell extracts. **(A):** First step of purification – anion exchange chromatography. **(B):** Second step of purification – gel filtration chromatography. **(C):** SDS-PAGE analysis. *Lane 1;* BioRad molecular weight marker (kDa). *Lane 2;* Soluble cell extract from myrcene induced cells. *Lane 3;* Highlighted fractions from anion exchange. *Lane 4;* Highlighted fraction from GF.

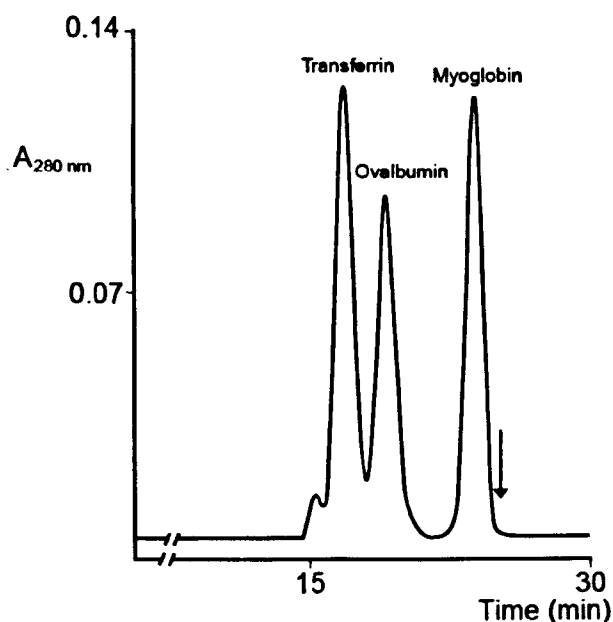


Figure 110: Calibration of the Superdex gel filtration column (S75 10/30) used in the second step of purification (taken from the manufacturer's column specification file). The standard proteins with their retention time on this column are: Transferrin MW 81,000 (16.8 min); Ovalbumin MW 43,000 (19.2 min); Myoglobin MW 17,600 (23.7 min). The unknown protein at a MW ~15,000 elutes with a retention time of 25 min under these conditions (at a relative position indicated by the arrow above).

The absorption spectrum for this purified protein did not show any additional peaks which would suggest a specific functional role for this protein other than the characteristic absorbance at 200 nm due to peptide bonds, and at 280 nm for aromatic amino acids. Sub-cellular fractions were assayed for activity towards myrcene, though neither the soluble cell extract nor the purified ~15 kDa protein fraction showed activity when compared to the whole resting cell conversion to geraniol.

7.3.3. Attempted identification of a 15 kDa myrcene induced protein

Mass spectrometry analysis of the purified protein revealed a parent peak at 14,787 Da (fig. 111). Smaller fragments of 2389 and 1979 Da were sequenced corresponding to the following peptides, to which forward and reverse PCR primers were designed in an attempt to amplify and sequence the majority of the gene encoding this protein.

Peptide fragments from MS (PCR primers designed towards underlined sequence):

- (1) FGFFADAAELDEMAADTFR
- (2) EDYKVVTGALDLKPDLTLLMR

It is anticipated that a 14,787 Da peptide would correspond to a gene sequence of ~410bp. A range of PCR conditions were screened in an attempt to obtain a product resulting from binding of these primers to the target gene. With the addition of 5% DMSO and an annealing temperature of 50°C, a ~300bp PCR product was yielded which could potentially encode 75% of this gene (fig. 112). Sequencing of the PCR product however revealed this to be a result of non-specific binding rather than annealing using the designed primers.

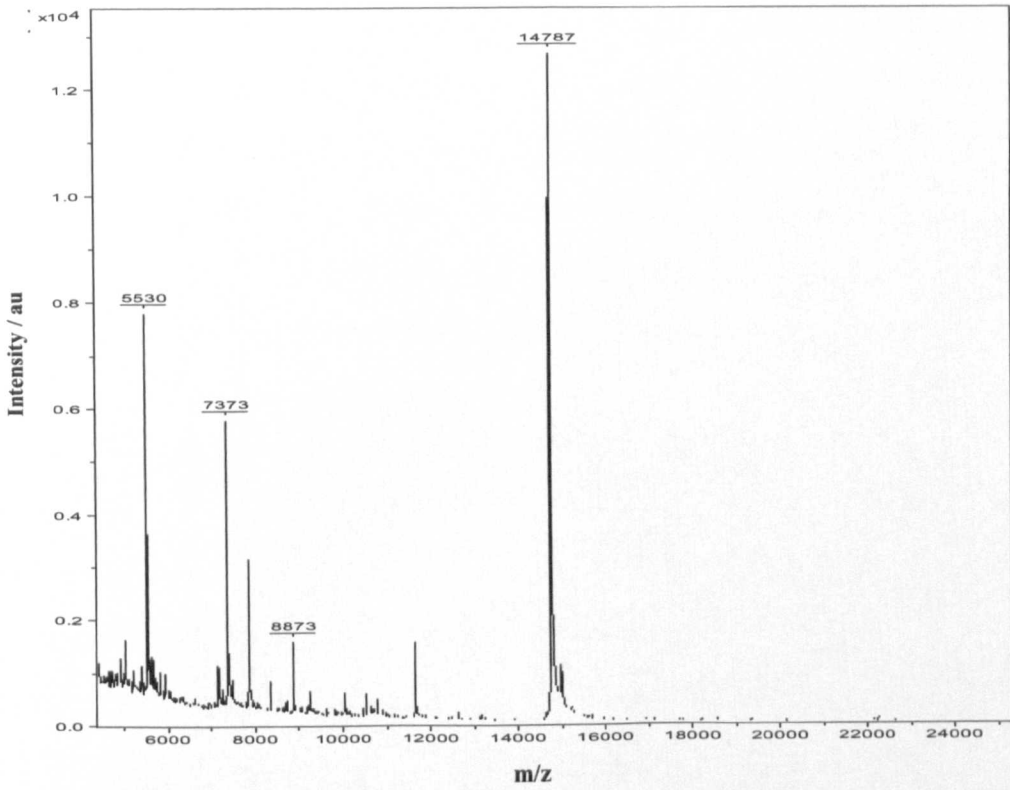


Figure 111: Mass spectrometry (MS) analysis for the purified ~15 kDa myrcene induced protein.

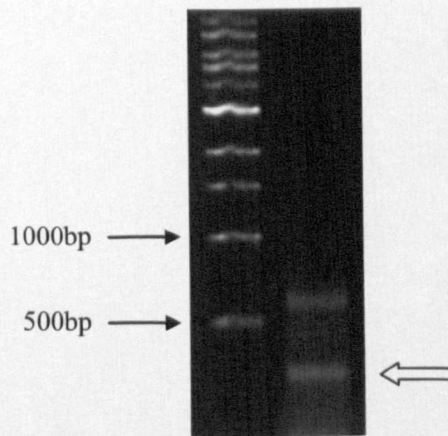


Figure 112: Agarose gel for PCR using primers designed towards the ~15 kDa myrcene induced protein based upon the sequence information from MS.

7.3.4. Attempts towards cloning of a myrcene degradation gene cluster

In order to establish a potential enzymatic mechanism, the cloning of a gene cluster responsible for the biotransformation of myrcene to geraniol in *R. erythropolis* is targeted in this section of work. PCR primers were designed towards the 60 kDa chaperonin GroEL (fig. 113) and acyl-CoA dehydrogenase (fig. 114) genes previously identified by peptide sequencing of tryptic digest fragments. Amplification from the known sequence fragments was attempted in both forward and reverse directions; however no specific PCR products of the expected size could be obtained for either the GroEL or aldehyde dehydrogenase genes. It was anticipated that if these two genes are encoded within the same operon up-regulated in the myrcene degrading strain *R. erythropolis* MLT1, it may be possible to amplify a stretch of DNA sequence incorporating any genes that may be found neighbouring / in-between the two already proposed. Using combinations of the various GroEL and aldehyde dehydrogenase primers available, a range of PCR conditions were tested, but as before only resulted in non-specific amplification of DNA. Increasing the stringency of conditions in both cases did not led to any improvement in these PCR experiments.

Chapter 7: Sub-cellular studies of the myrcene degrading strain *Rhodococcus erythropolis* MLT1

gi|111019139 Mass: 56617 Score: 216 Queries matched: 6
 60 kDa chaperonin GroEL [*Rhodococcus* sp. RHA1]

Check to include this hit in error tolerant search or archive report

Query	Observed	Mr(expt)	Mr(calc)	ppm	Miss	Score	Expect	Rank	Peptide
<input checked="" type="checkbox"/> 1	1063.5184	1062.5111	1062.5345	-22.04	0	45	0.29	1	K.IIAFDEEAR.R
<input checked="" type="checkbox"/> 4	1529.7894	1528.7821	1528.7886	-4.21	0	37	1.4	1	K.WGAPTIINDGVSIAK.E
<input checked="" type="checkbox"/> 7	1777.9586	1776.9513	1776.9509	0.24	0	50	0.058	1	R.QEAVLEDAYILLVSSK.I
<input checked="" type="checkbox"/> 8	2075.0693	2074.0620	2074.0543	3.74	0	28	9.2	1	K.TDDVAGDGTITATVLAQALVR.E
<input checked="" type="checkbox"/> 9	2203.1619	2202.1546	2202.1492	2.46	1	35	1.7	1	K.KTDDVAGDGTITATVLAQALVR.E
<input checked="" type="checkbox"/> 11	2552.2637	2551.2564	2551.2476	3.47	0	21	31	2	K.EGVITVEESNTFGLQLELTEGMR.F

1	MAK	<u>IIAFDEE</u>	ARRGLERGLN	ALADAVKVTL	GPKGRNVVLE	KK	<u>WGAPITIN</u>
51	<u>DGVSIAK</u>	EIE	LEDPYEKIGA	ELVKEVAK	<u>KT</u>	<u>DDVAGDGTIT</u>	<u>ATVLAQALVR</u>
101	EGLRNVAAGA	NPLGLKRGIE	KAVEAVTVRL	LETAKEIDTK	EQIAATAGIS		
151	AGDPSIGELI	AEAMDKVG	<u>KE</u>	<u>GVITVEESNT</u>	<u>FGLQLELTEG</u>	<u>MR</u>	FDKGYISA
201	YFATDPER	<u>QE</u>	<u>AVLEDAYILL</u>	<u>VSSK</u>	ISTVKD	LLPLLEKVIQ	SGKPLVIAE
251	DVEGEALSTL	VVNKIRGTFK	SVAVKAPGFG	DRRKAQLADI	AILTGGEVIS		
301	EEVGLSLETA	GLELLGQARK	VVITKDETTI	VEGAGDPEAI	AGRVAQIRAE		
351	IENSDDSYDR	EKLQERLAKL	AGGVAVIKAG	AATEVELKER	KHRIEDAVRN		
401	AKAAVEEGIV	AGGGVALLQS	APALDDLKLE	GDEATGANIV	RVALEAPLKQ		
451	IAFNAGLEPG	VVAEKVRNLP	AGHGLNASTN	EYGDLEAGI	NDPVKVRTSA		
501	LQNAASIAAL	FLTTEAVVAD	KPEKAGAPVG	DPTGGMGGM	D		

Figure 113: Fragments from peptide MS highlighted in red used in the identification of a myrcene induced protein as a 60 kDa chaperonin GroEL (*Rhodococcus* sp. RHA1). PCR primers were designed towards the underlined regions of this gene for which the sequence is shown.

```

Q0S2R1_RHOSR      MINLELPKCLKASAN-----QAHQVAAEIFRP--ISRKYDLAEHAYPKEL 43
Q0RIZ9_FRAAA      MASDRPPTTLAPDAVGEVPRQTQNRMTHDVWLPDETVALRAQARAADVCKRL 50
* . . *..* ..*          :::: ::: *          * . * *.*

Q0S2R1_RHOSR      DTMAAMVEGLNDSGKGAAGAALGRGDEPKVIGNVNGNMSSLSLMNVIETCW 93
Q0RIZ9_FRAAA      APHAREIQREESADSPWAAFRGLAEEGLFAVPPFGDDFG--RGLAYPML 98
. * :   ::*... . ** : *   ::. *::: . : .

Q0S2R1_RHOSR      GDVGLTLAIPYQG-----LGNSAIAAVATDEQLERF 124
Q0RIZ9_FRAAA      GTCTVTTEEIAYHSSSMAGVYDGCILVPQTLTFASPALRARLVPPELVE-- 146
*   :* *..*..          :...*: * . * :.*

Q0S2R1_RHOSR      GKVWASMAITEPGFGSDSAAVTTTAVLD--GDEYVLNGEKIFVTAGERST 172
Q0RIZ9_FRAAA      GRTAFSFATTEPETSSDLTAARMQTVADRTADGFVNGRKRWITNSVVAG 196
*:. *:* *** .** :*. : * * . * :*:**.* :* . :

Q0S2R1_RHOSR      HIVWATVDKTKGRAAIKSFVVPRDAPGLSVARLEHKLGIKASDTAVLLL 222
Q0RIZ9_FRAAA      WVSVLVRAGRS---RATMLLDLSSPGVVRVGPDLKMGHRGQLTADIVF 243
: * . . . . . . ::* .:***: * . : *:* ... ** :::

Q0S2R1_RHOSR      QDCRIPKDNLLGTPEVNVKGFAGVMQTFDNTRPIVAGMAVGLGRAALEE 272
Q0RIZ9_FRAAA      TDVHVPADNVLGPPDG---GLGVALSALVRGRIGIGAAGVGVAQAALDL 289
* ::* **:*:*.*:   *.. .:..: . *   .. **:*:***:

Q0S2R1_RHOSR      LRSILSDAGVEISYDTPAYNQHAAAAEFLQLEADWEAAYLLALRATWMAD 322
Q0RIZ9_FRAAA      AVHRLRTR---HVFGAPLQALQHWQFQMAQRATEIECARSLYQKAAILLD 336
*           :::* :   : * : * : * * * :* : *

Q0S2R1_RHOSR      -NKKPNSLEASMSKAKAGRTGTAISLKAVELAGTLGYS-----ERPLL 364
Q0RIZ9_FRAAA      RGDRAEPEAAMAKAYGTRLANDVVREAIQIHGAVGFARRVAESGESVRL 386
... . **:*:* * . . . :*::: *::*: * *

Q0S2R1_RHOSR      EKWARDKILDIFEGTQQIQQLIVARRLLGKSSAELK 401
Q0RIZ9_FRAAA      EEMYRDAKILEIFEGANELQQWIARQLIGRDVTG-- 421
*: **:*:*:*:*:::* *:*:*:*:. :

```

Figure 114: Sequence alignment of the putative acyl-CoA dehydrogenase from *Frankia alni* showing the greatest similarity to the myrcene induced protein of 47 kDa (chapter 6), with a homologous acyl-CoA dehydrogenase from *Rhodococcus* sp. RHA1. The region shown in red corresponds to the fragment (ILEIFEGANELQQWIAR) used in the initial identification of the protein (chapter 6). The above alignment was used in the design of PCR primers towards sequence highlighted in blue.

7.4. Conclusions

Scaling-up the growth of *R. erythropolis* cultures active for the biotransformation of myrcene to geraniol could prove desirable for a potential industrial process. However the inability to achieve a product yield greater than 2% in resting cell assays (chapter 6) highlighted the problems of converting this interesting biotransformation to a fragrant monoterpene alcohol, towards a commercially viable scale. It was found in this chapter of work that growth of this organism in fermentation volumes of 5 L could not lead to reproduction of the resting cell biotransformation observed when using cells harvested from 50 mL shake-flask cultures with myrcene as SCS in the vapour phase. Despite supplying the volatile hydrocarbon as the SCS, the inductive effects of growth on myrcene could not be replicated on this larger scale. It was found that an accumulation of myrcene in the fermentation medium limited the growth of *R. erythropolis*. Optimum growth on myrcene as the SCS in the 5 L fermentation was achieved when supply of the hydrocarbon was stopped at the apparent mid-point in the exponential phase of growth, resulting in a final optical density (A_{600}) of 0.45. A measured concentration of $\sim 35 \mu\text{M}$ myrcene was found to subsequently remain constant in the vessel until the cells were harvested. Stringent control of the exact myrcene concentration to the fermentation vessel could not be achieved, and it was not clear to what extent myrcene depletion could be attributed to cell growth. Despite growth of *R. erythropolis* on myrcene as the SCS in these fermentations, the harvested cells were not viable for the biotransformation of myrcene to geraniol. As

with the observations made in the previous chapter, initial growth on glucose followed by a supply of myrcene to the culture did not result in an induction of activity either. A more appropriate method of achieving a scalable process would be to identify the genes responsible for the biocatalytic activity, for cloning and over-expression of the proteins in *E. coli*.

Work for this chapter targeted the identification of potentially up-regulated genes involved in biotransformation of myrcene to geraniol. The previous chapter described a possible role for three myrcene induced proteins in the further metabolism of geraniol however one strongly induced protein band from SDS-PAGE analysis at ~15 kDa could not be identified. Purification of this unknown protein / subunit to homogeneity was achieved here. Elution during gel filtration chromatography suggests that this protein is in a monomeric state. It is not clear as to what a potential function for such a small protein may be, which appears strongly inducible from analysis of *R. erythropolis* cell extracts grown on myrcene as the SCS. Expression of this protein appears absent in those cells which were grown on alternate carbon sources (chapter 6). Further attempts to uncover the identity of this purified protein through mass spectrometry and peptide sequencing revealed two short peptide sequences; however a search for homologous regions in other proteins from the databases did not provide any clear matches. From the sequence information that was available, PCR experiments targeted the amplification of DNA encoded between these regions; however binding of primers to these sequences could not be achieved.

More reliable sequence information was yielded from previous studies into the myrcene induced GroEL and acyl-CoA dehydrogenase proteins. Based upon the *Rhodococcus* sp. RHA1 sequence for these genes a number of PCR primers were designed to amplify regions within these genes and also DNA that may be encoded between them as part of a proposed myrcene degradation operon.

Clusters of genes that are up-regulated in response to growth of organisms on hydrocarbons related to, and including myrcene have been illustrated in the introduction to this chapter. It was anticipated that this simple PCR approach described would provide further sequence information for neighbouring genes; and may highlight the roles of other types of enzyme in the biotransformation of myrcene to geraniol in this organism. Sequencing of the *R. erythropolis* genome would also prove very useful in helping to identify the genes that are involved in this process. A lack of success in these experiments suggest that an alternative route through creation of gene libraries and screening for the fragments identified so far, should perhaps be considered for uncovering a gene cluster involved in myrcene biotransformation.

8. Chapter 8: Conclusions and future work

An increase in demand for a wide diversity of natural products has created a wealth of opportunity in the discovery and development of biocatalytic processes for the generation of fine chemicals. Changes in legislation have driven increased study towards the use of biocatalysis which can satisfy production of these compounds *via* a 'natural' route. Of particular emphasis for study in this thesis are the monoterpene alcohols which find many applications within the flavour and fragrance industries. The overall aim of this investigation was to uncover and develop novel biocatalytic routes towards these monoterpene alcohols. Where specific enantioselectivity was required in the product, this was also targeted, particularly with regard to the differing organoleptic properties of *R*- and *S*- linalool, a monoterpene alcohol of significant interest for this project. A scheme showing a summary of biocatalytic routes taken towards the monoterpene alcohols in this thesis is shown in figure 115 on the following page.

Figure 115 (following page): Summary of the biocatalytic routes observed during this project. **(A)**: Acid catalysed conversion of geraniol and nerol to α -terpineol and linalool in the growth medium of *A. niger*. **(B)**: Biotransformation of geraniol to citral by *A. niger* in resting cell assays. **(C)**: Enantioselective hydrolysis of linalyl acetate by *R. ruber* DSM 43338, with sub-cellular fractions of complementary selectivity. **(D)**: A recombinant GGG(A)X motif esterase (N3) from *N. farcinica* catalyses the highly enantioselective hydrolysis of menthyl acetate, in addition to the hydrolysis of citronellyl- and lavandulyl- acetates. **(E)**: The purified N3 esterase did not hydrolyse the tertiary linalyl- or α -terpinyl- acetates. **(F)**: *Rhodococcus erythropolis* MLT1 isolated by selective enrichment from hop plants catalyses the biotransformation of β -myrcene to geraniol.

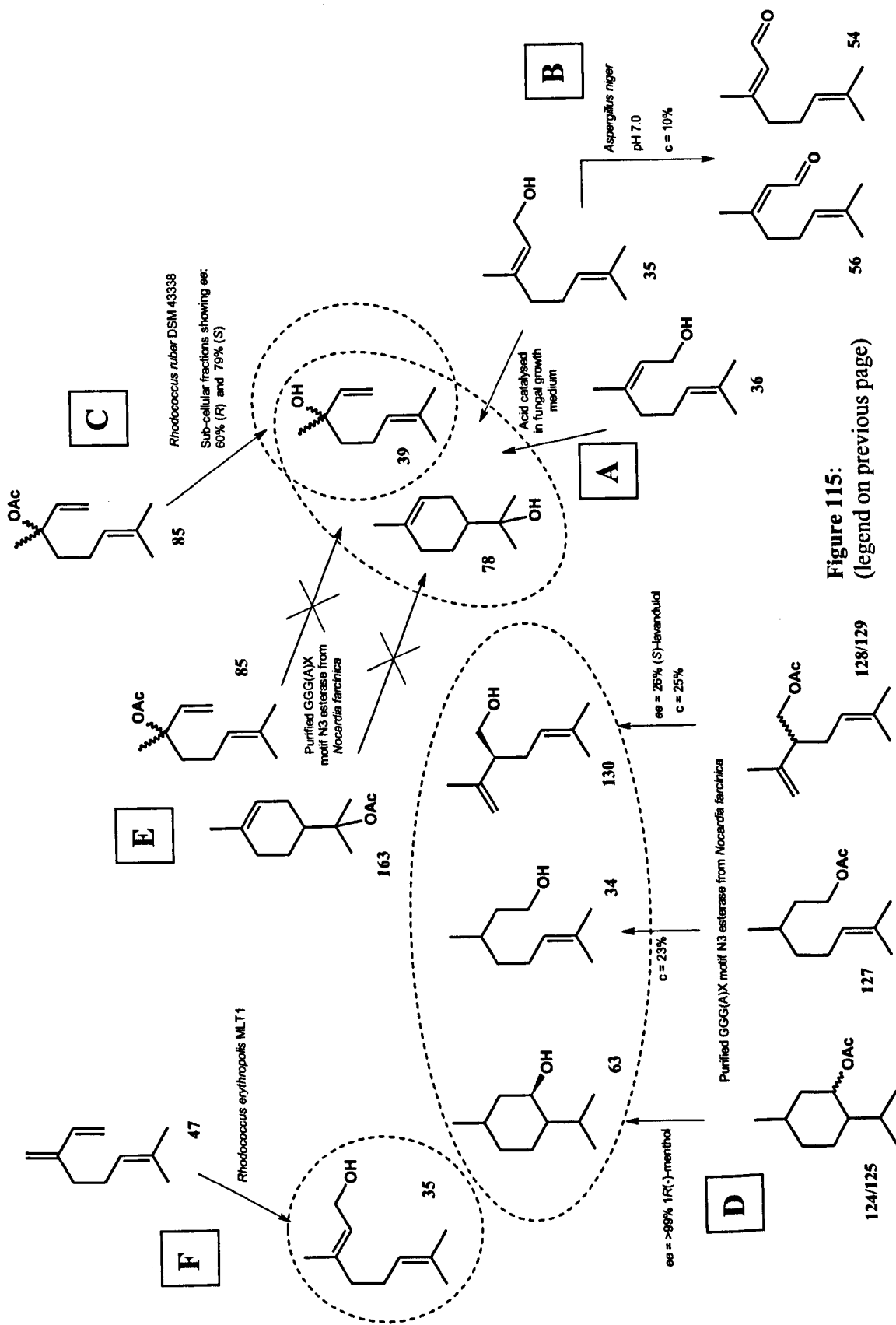


Figure 115:
(legend on previous page)

The work in chapter 3 described an investigation into the suitability of fungal biocatalysts for generation of the tertiary monoterpene alcohol linalool. Linalool and α -terpineol were produced in growing cell assays using *Aspergillus niger*, however an investigation into the effects of the growth medium on this production, found that it occurred as a result of the acidic pH rather than a biogenic process (fig. 115A). Linalool has been found among a number of products including α -terpineol, from biotransformations of geraniol and nerol by sporulated surface cultures of *Aspergillus niger* and *Penicillium rugulosom* [Demyttenaere et al. 2000]. Acid-catalysed rearrangements of geraniol and nerol into linalool, nerol, and α -terpineol are known to exist (chapter 3 – fig. 42) however the effects of low pH are not extensively referred to in previously described fungal biotransformations which lead to linalool formation [Farooq et al. 2004, Bock et al. 1988, Busmann et al. 1994]. It was noted during the screening of fungal strains with the three monoterpene substrates geraniol, nerol, and myrcene, that oxidation of geraniol to citral (geraniol / neral mixture) could be achieved in pH 7 resting cell assays with *A. niger* (fig. 115B). Citral finds application in the fragrance industry as a main component of citrus aroma however attempts to optimise the production of this compound in biotransformations either through the use of acetone as a co-substrate or changes in pH failed to increase the conversion beyond 10%.

An alternative route towards linalool production was considered in chapter 4. Esterases from *Rhodococcus ruber* DSM 43338 have previously shown activity for

the enantioselective hydrolysis of linalyl acetate [Osprian et al. 1996, Pogorevc et al. 2000]. Attempts in literature to purify these esterases resulted in the isolation of fractions showing complementary enantioselectivity towards the hydrolysis of this substrate, and prompted investigation during chapter 4 towards isolation of these enzymes to homogeneity. Screening this species and a further 24 *Rhodococcus* strains uncovered four (*R. aetherivorans* AM1, *R. ruber* DSM 43338, *R. sp.* HS2, *R. rhodochrous* sp. 11Y) which showed whole cell activity towards the hydrolysis of linalyl acetate. These strains demonstrated significant hydrolytic activity towards this sterically demanding ester with levels of conversion ranging from 15-50% in whole cell assays displaying a predominant *S*- enantioselectivity (*ee* 15-20%). Partial purification of extracts from strains AM1, HS2, and 11Y led to an enhancement of selectivity towards (*S*)-linalyl acetate (*ee* 33-50%) when compared to the crude cell extract from which the fractions were derived. However the most interesting results were achieved with sub-cellular extracts from *R. ruber* DSM 43338 whereby two distinct sets of fractions of opposing enantioselectivity were separated during a single step of anion exchange chromatography, with enantiomeric excess values ranging from 60% (*R*) to 76% (*S*) (chapter 4 – fig. 55 and 56). A two step purification strategy was developed yielding a fraction which upon assaying for linalyl acetate hydrolysis showed an *ee* of 79% (*S*)-linalool (fig. 115C). Although carrying out two successive chromatographic steps, purification to homogeneity of an enantioselective esterase could not be achieved from cell extracts of *R. ruber*. Active fractions at this stage of purification were noted to still contain a number of proteins, and following attempts

to yield further protein purification resulted in a subsequent loss of esterase activity. Despite induction of tertiary alcohol esterase activity by 6-fold with the application of *tert*-butyl acetate, it was not possible to isolate a single protein band from SDS gel electrophoresis which could represent the enantioselective activity observed in the partially purified protein fractions. Attempts to highlight esterase bands on a protein gel by soaking in a stain containing α -naphthyl acetate and fast blue dye did not reveal which bands were accounting for the observed esterase activity. Improved methods of staining and investigation of different methods for screening esterase activity in protein containing fractions are planned for future progress with this work. An alternative high-throughput assay for screening of esterase activity and enantioselectivity has been described in the literature [Bottcher and Bornscheuer 2006]. In this instance the hydrolysis of secondary alcohol acetates was studied. The release of acetic acid in this reaction leads to the stoichiometric formation of NADH which was quantified spectrophotometrically at 340 nm. The use of optically pure acetates also enables the calculation of enantioselectivity. A similar assay based upon the hydrolysis of linalyl acetate could be utilised for the purposes of this investigation.

Based upon sequence information known for tertiary alcohol esterases from other organisms, an alternative approach was devised in chapter 5 for the isolation of such enzymes from the 43338 strain, for which enantioselective activity towards *R*- and *S*-linalyl acetate had previously been demonstrated. Hydrolases containing a highly conserved GGG(A)X motif in the active site are able to accept TAEs as substrates by

stabilising the tetrahedral intermediate formed during ester hydrolysis within an oxyanion hole. Relatively few GGG(A)X esterases are known to exist when compared to GX type enzymes in which the binding pocket is 1.5-2Å narrower; and thus activity towards sterically challenging TAEs substrates is not so widely described. In those cases where activity towards linalyl acetate is demonstrated, the enantioselectivity of this hydrolysis tends to remain relatively low due to the steric similarity of the methyl and ethenyl groups impeding the chiral recognition process. Searching the genome of the sequenced *Rhodococcus* sp. RHA1 strain revealed five esterases containing the GGG(A)X motif. Design of PCR primers based upon RHA1 codon usage against conserved regions encoding the catalytic serine and oxyanion hole residues, preceded the cloning of a 288bp fragment (~20%) of a potential tertiary alcohol esterase from the un-sequenced 43338 strain. Sequencing and alignment of this cloned fragment against all bacterial genomes highlighted the closest homologues, from which it was possible to clone and sequence an extended stretch of DNA corresponding to approximately 75% of a tertiary alcohol esterase from *R. ruber*. Attempts to amplify a full-length gene *via* design of N- and C- terminal primers, and various PCR approaches, were not successful. For progression of this work, it would be interesting to examine the whole cell activity of the *Rhodococcus* strain RHA1 for which the genome sequence is known, towards the hydrolysis of linalyl acetate. If active it would be relatively straightforward to clone the five genes containing a GGG(A)X motif, for overexpression and purification of a potentially active tertiary alcohol esterase. Studies of the RHA1 strain and the use of its genomic DNA could

unfortunately not be utilised within this project due to an industrial conflict. Sequencing of the 43338 strain which is known to contain esterases of complementary enantioselectivity could precede such an approach; and it may be possible to generate highly selective biocatalytic routes towards *R*- and *S*- linalool through this method. Working with a recombinant esterase would facilitate a scaled-up process towards this commercially desirable monoterpene alcohol, whilst also enabling a more detailed characterisation of enzyme activity and specificity.

Although a tertiary alcohol esterase could not be purified or cloned from those *Rhodococcus* strains showing desirable enantioselectivity towards linalyl acetate hydrolysis in whole cell assays and sub-cellular fractions; a GGG(A)X motif esterase from the related actinomycete *Nocardia farcinica* was cloned, over-expressed and purified. This esterase which shared high sequence homology to those enzymes from RHA1 and the model BS2 esterase displayed promising characteristics for the biocatalytic preparation of the commercially significant enantiomer of the monoterpene alcohol menthol. The purified esterase was found to be highly enantioselective towards the hydrolysis of racemic menthyl acetate ($ee_p = >99\%$ 1*R*(-)-menthol), with substrate specificity extending to the other monoterpene esters citronellyl acetate, and lavandulyl acetate (fig. 115D). Whilst activity of the purified esterase was described towards these primary and secondary monoterpene alcohol esters it has yet to show substrate specificity extending towards the TAEs (fig. 115E)

which may lead to a biocatalytic route towards linalool, one of the principal targets of this investigation.

The importance of linalool within the flavour and fragrance industries has previously been described in the introduction to this thesis, yet whilst common synthetic routes towards this compound from α -pinene and 2-methyl-hepten-6-one do not lead to a 'natural' product classification; isolated enzymatic routes towards 'natural' linalool that show high enantioselectivities are not widely described. Previous studies of *Rhodococcus ruber* DSM 43338 have been used to obtain a conversion of 25% from hydrolysis of linalyl acetate, with (*S*)-linalool produced at an enantiomeric excess (*ee*) 56%, and selectivity (*E*) of 4.2 [Osprian et al. 1996]. Later work studying purification from cell extracts from this strain led to the isolation of two active fractions with opposite enantiopreference for the acetate, showing that the low selectivities generally observed in whole cell assays is due to the presence of competing carboxyl esterases [Pogorevc et al. 2000]. Selectivities up to $E = 100$ were obtained for the individual fractions. However as with the observations made in chapter 4 of this investigation, instability of the semi-purified enzyme preparations and low yield prevented purification to homogeneity of a linalyl acetate esterase.

Although few hydrolases accept TAEs as substrates, when compared to enzymes accepting esters of primary and secondary alcohols [Henke et al. 2002, Pogorevc et al. 2000], the identification and expression of an enantioselective linalyl acetate esterase

in a recombinant system would prove highly desirable. Such esterases have been found to catalyse the hydrolysis of racemic linalyl acetate with only moderate enantioselectivity (enantiomeric excesses of up to 54% for the product (*S*)-linalool and a selectivity $E = 5$ have been yielded) [Kourist et al. 2007]. Whilst negligible activity was observed towards linalyl- and terpinyl acetates using this purified GGG(A)X motif esterase from *N. farcinica* (fig. 115E), future work will target the hydrolysis of more diverse TAEs for generation of other important tertiary alcohols, some of which find importance as pharmacological precursors [Kourist et al. 2007]. The presence of a GGG(A)X motif in the peptide sequence of esterases whilst conferring activity towards TAEs, does not guarantee activity towards all substrates of this class [Henke et al. 2002]. Many enzymes show inactivity towards linalyl- and terpinyl acetate, yet still show high levels of conversion and enantioselectivity for the hydrolysis of other TAEs. Further work with this purified esterase will aim to uncover function for hydrolysis of a tertiary alcohol ester by screening a wide range of compounds from this class. The high levels of expression for this recombinant enzyme and the ability to purify to homogeneity also offer the potential for future structural studies. It would also be of interest to increase the knowledge of substrate specificity and selectivity for hydrolysis of other menthyl esters, and investigate the potential use of this enzyme in enantioselective esterifications as an alternative route for generation of optically pure monoterpene alcohols.

In addition to linalool and menthol, another monoterpene alcohol geraniol is also to be found widely used in both the flavour and fragrance industries. Chapter 6 described a novel biotransformation from β -myrcene to geraniol utilising a strain of *R. erythropolis* isolated by selective enrichment from hop plant material (fig. 115F) [Thompson et al. 2010]. Control experiments demonstrated that the product was biogenic and that an aerobic environment was required. This biotransformation was found to be inducible when the organism was grown on β -myrcene as the SCS. Pre-incubation of cells with the cytochrome P450 inhibitors metyrapone or 1-aminobenzotriazole reduced geraniol production by 23% and 73% respectively but reduction in activity was found not to correlate with inhibitor concentration, and thus it could not be ascertained whether or not this reaction is catalysed by a cytochrome P450 monooxygenase. In an attempt to uncover the mechanism involved in the biotransformation of myrcene to geraniol, a comparative analysis of insoluble and soluble cell extracts from cells of *R. erythropolis* MLT1 grown on either β -myrcene or glucose was made. Mass spectrometric analysis of tryptic digests revealed a 60 kDa chaperonin GroEL, an acyl-CoA dehydrogenase, and an aldehyde dehydrogenase which were overproduced in response to growth on β -myrcene. Each of these proteins finds precedent in gene clusters for the degradation of terpenes and related hydrocarbons, however would not seem to fit into a mechanism for the β -myrcene to geraniol conversion, but rather act in a pathway for the further metabolism of geraniol by this organism. The biotransformation of β -myrcene to myrcen-8-ol by a strain of *Pseudomonas* [Iurescia et al. 1999] led to the identification of four open reading

frames which were up-regulated in response to growth on myrcene encoding for; an aldehyde dehydrogenase, an alcohol dehydrogenase, an acyl-CoA synthetase, and an enoyl-CoA hydratase. The involvement of these induced genes in a proposed β -myrcene catabolism pathway is shown in figure 116.

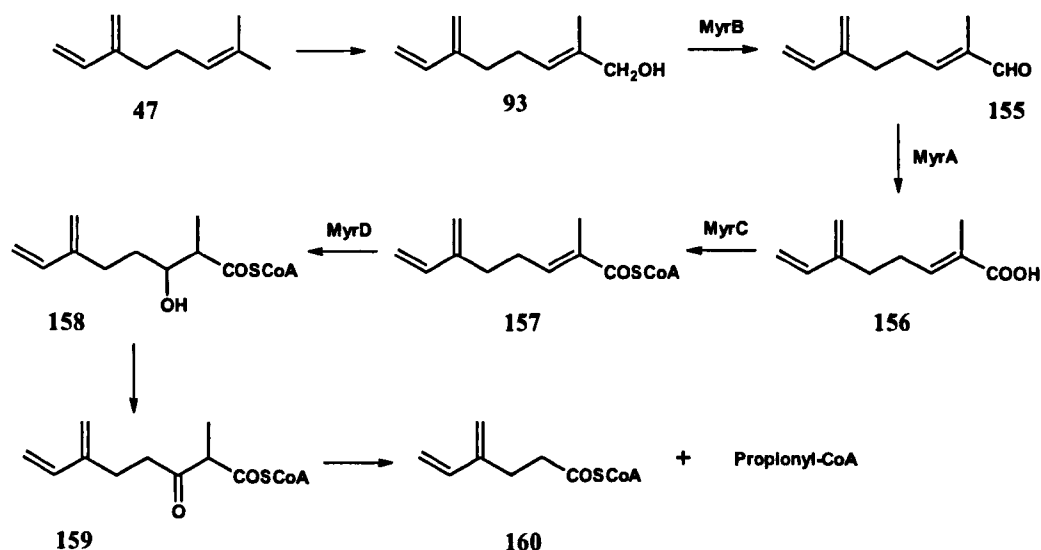


Figure 116: A proposed catabolic pathway of β -myrcene in the *Pseudomonas* strain M1 from Iurescia et al. 1999, showing the involvement of up-regulated genes: MyrB, alcohol dehydrogenase; MyrA, aldehyde dehydrogenase; MyrC, CoA ligase; MyrD, enoyl-CoA hydratase.

A similar mechanism as to that for myrcen-8-ol degradation shown in figure 116 may exist for the further metabolism of geraniol in *R. erythropolis* MLT1, which also shows induction of alcohol dehydrogenase and aldehyde dehydrogenase genes in response growth on β -myrcene as SCS. The metabolism of geraniol and citronellol has been characterised in detail in *Pseudomonas* strains [Hoschle and Jendrossek

2005, Forster-Fromme and Jendrossek 2006] and is described in the introduction to chapter 7, however a definitive mechanism for the transformation of β -myrcene to geraniol has yet to be shown. Related biotransformations of myrcene to other monoterpene alcohols have been discussed previously and may give an indication of the type of enzymes that can expect to be found in such a mechanism from β -myrcene to geraniol [Busmann and Berger 1994]. Recently a linalool dehydratase enzyme has been characterised from the denitrifying Proteobacteria *Castellaniella defragrans* (formally *Alcaligenes defragrans*) (fig. 117) [Brodkorb and Harder 2009].

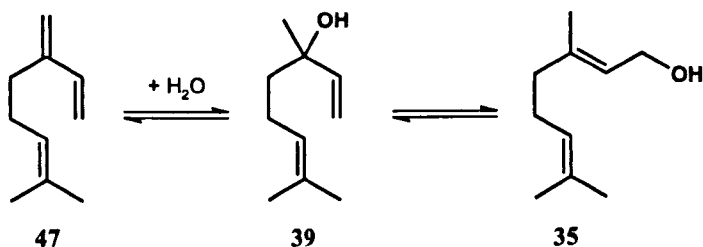


Figure 117: The dehydration of linalool 39 to β -myrcene 47, and isomerisation of geraniol 35 to linalool catalysed by a *linalool dehydratase* in *Castellaniella defragrans* [Brodkorb and Harder 2009 – conference abstract].

Under anaerobic conditions and in the presence of reducing agents the enzyme was able to catalyse the dehydration of linalool to β -myrcene, whilst also able to isomerise geraniol to linalool. The microbial transformation of linalool to geraniol has also been illustrated through activity of a putative 3,1-hydroxyl- Δ^1 - Δ^2 -mutase [Harder and Probian 1995, Fo β and Harder 1997]. In the biotransformation catalysed by *R. erythropolis* MLT1 in this investigation, a reaction proceeding *via* hydration of β -myrcene to linalool followed subsequently by isomerisation to geraniol may provide

a possible explanation as to the mechanism involved. A hydration mechanism has also been discussed for the fungal catalysed biotransformation of α -myrcene to nerol (fig. 118). A variety of oxygenated acyclic and monocyclic metabolites were observed in extracts from the medium, amongst which nerol but not geraniol was formed. An oxygenase-type enzyme system was proposed by the authors that 'double bonds were stereoselectively hydroxylated and that isolated double bonds could be hydrated while maintaining a conjugated unsaturated system'. It is also suggested that many acyclic metabolites could have originated from incorporation of oxygen functionality to intermediary acyclic cations, and which may account for nerol formation (fig. 118).

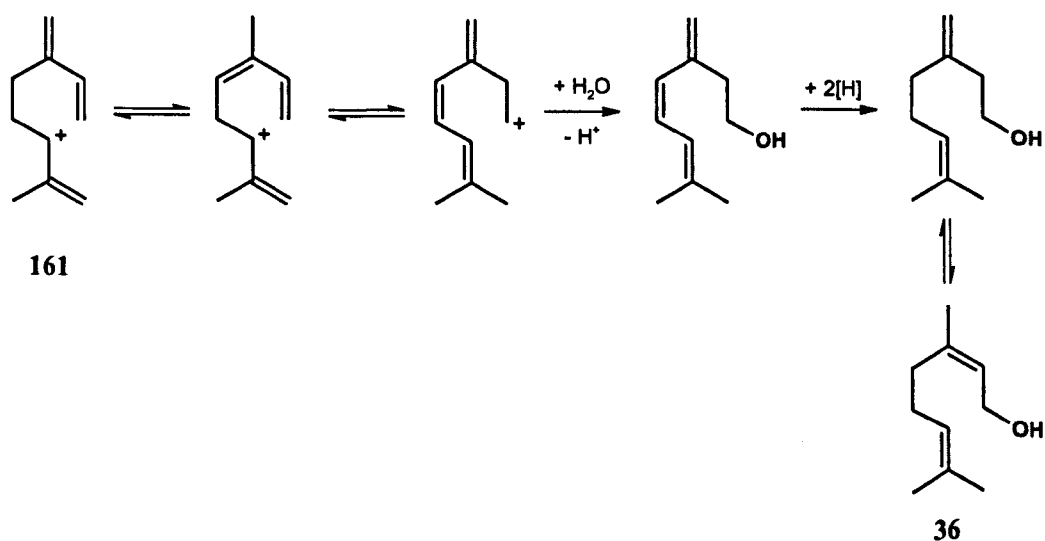


Figure 118: A proposed mechanism for the conversion of α -myrcene **161** to nerol **36** by different strains of basidiomycetes, from Busmann and Berger 1994.

A study of the metabolism of unsaturated monoterpenes including α -pinene, limonene, and β -myrcene by *Alcaligenes defragrans*, revealed the production of geranic acid in cell-suspensions and sub-cellular cytosolic fractions (fig. 119) [Heyen and Harder 2000]. An un-characterised pathway for β -myrcene oxidation is suggested with the potential intermediates geraniol and linalool, though neither of these monoterpene alcohols was detected in these assays described.

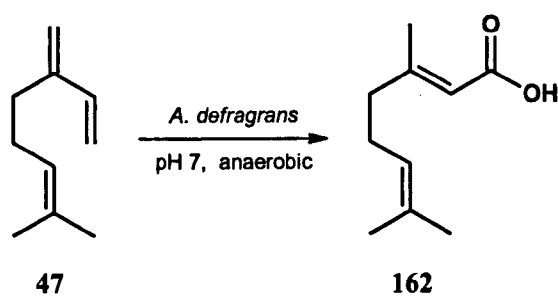


Figure 119: The anaerobic biotransformation of β -myrcene 47 to geranic acid 162 by *Alcaligenes defragrans* [Heyen and Harder 2000].

Attempts to clone the myrcene induced genes identified in *R. erythropolis* MLT1, and also those genes neighbouring the 60 kDa GroEL, and aldehyde- and acyl-CoA dehydrogenases as part of a potential β -myrcene degradation cluster were made in chapter 7. It was anticipated that by gaining sequence information for these genes, that enzyme(s) involved in the biotransformation of β -myrcene to geraniol could be identified as part of a gene cluster involved in β -myrcene degradation. Operons describing up-regulated genes involved in the metabolism of terpenes have previously been illustrated. Future work aims to uncover the enzymatic mechanism by first identifying those genes responsible for this inducible biotransformation. Sequencing

of the genome of the *R. erythropolis* strain would prove useful in this regard. An alternative route through creation of gene libraries and screening for the fragments already identified by mass spectrometric analysis of tryptic digests could also be applied towards identification of a gene cluster. The chemical mechanism by which β -myrcene is converted to geraniol in this aerobic biotransformation remains unclear; however the use of labelled oxygen (^{18}O) in experiments could be used to ascertain whether the oxygen atom originates from molecular oxygen (and thus oxygenase catalysed), or from water (and thus catalysed by a lyase-type mechanism).

The work for this thesis has strived to uncover novel and interesting biocatalytic routes towards the monoterpene alcohols, and thus offer approaches to 'natural' products that are desired for application within the flavour and fragrance industries. A number of the routes that have been identified in the chapters presented here, offer potential in future selective biotransformations and could eventually lead to scalable reactions. The presence of tertiary alcohol esterases in *R. ruber* DSM 43338 offer an enantioselective route towards (*R*)- and (*S*)- linalool from the hydrolysis of linalyl acetate. The identification of sub-cellular fractions of complementary activity preceded a gene-based approach towards these esterases that whilst not resulting in the cloning of a full length gene, enabled cloning and sequencing of a fragment containing the conserved motifs that confer esterase activity towards the sterically demanding tertiary alcohol esters. The results of experiments from chapters 4 and 5 reveal it should be possible to clone and over-express an enantioselective linalyl

acetate esterase from *R. ruber* DSM 43338, and thus such a recombinant system would offer potential for commercial production of 'natural' optically pure linalool. Biocatalytic routes towards a further two monoterpene alcohols of industrial interest have also been described. A highly enantioselective hydrolysis of menthyl acetate to the preferred 1(*R*)- enantiomer of menthol that yields its characteristic mint aroma was described in chapter 5, *via* the activity of a recombinant GGG(A)X motif esterase from *N. farcinica*. Further work is required to fully characterise the substrate specificity and enantioselectivity of this enzyme, and to determine hydrolytic activity towards some TAEs from which sequence analysis seems confer upon it. Another fragrant monoterpene alcohol, geraniol, was generated in a novel biotransformation from β -myrcene, using a strain of *R. erythropolis* isolated by selective enrichment from a hop plant. This biocatalytic route would also require further study to fully characterise and understand the mechanism involved. The work for this thesis has set out to create the foundation for biotransformations leading to some of the more desirable monoterpene alcohols. Based upon the results presented in this work, each biocatalytic route offers great potential for further detailed study that would present both increased understanding and optimisation of the pathways involved.

References

- Adams, R. P. *Identification of essential oil components by gas chromatography – mass spectrometry*. 1995, Allured, IL.
- Akutagawa, S. *Topics in Catalysis* 1997, 4, 271-274.
- Aleu, J.; Collado, I. G. *Journal of Molecular Catalysis B-Enzymatic* 2001, 13, 77-93.
- Aslanidis, C.; Dejong, P. J. *Nucleic Acids Research* 1990, 18, 6069-6074.
- Bartsch, S.; Kourist, R.; Bornscheuer, U. T. *Angewandte Chemie-International Edition* 2008, 47, 1508-1511.
- Bell, K. S.; Kuyukina, M. S.; Heidbrink, S.; Philp, J. C.; Aw, D. W. J.; Ivshina, I. B.; Christofi, N. *Journal of Applied Microbiology* 1999, 87, 472-480.
- Bernotiene, G.; Nivinskiene, O.; Butkiene, R.; Mockute, D. *Chemija* 2004, 15, 31-36.
- Bock, G.; Benda, I.; Schreier, P. *Applied Microbiology and Biotechnology* 1988, 27, 351-357.
- Bonsor, D.; Butz, S. F.; Solomons, J.; Grant, S.; Fairlamb, I. J. S.; Fogg, M. J.; Grogan, G. *Organic & Biomolecular Chemistry* 2006, 4, 1252-1260.
- Bornscheuer, U. T. *FEMS Microbiol Reviews* 2002, 26, 73-81.
- Bornscheuer, U. T. *Current Opinion in Biotechnology* 2002, 13, 543-547.
- Bottcher, D.; Bornscheuer, U. T. *Nature Protocols* 2006, 1, 2340-2343.
- Bradford, M. M. *Analytical Biochemistry* 1976, 72, 248-254.
- Brenna, E.; Fuganti, C.; Serra, S. *Tetrahedron-Asymmetry* 2003, 14, 1-42.
- Brodkorb, D.; Harder, J. *Conference abstract - Biotrans2009* 2009.
- Busmann, D.; Berger, R. G. *Journal of Biotechnology* 1994, 37, 39-43.
- Casabianca, H.; Graff, J. B.; Faugier, V.; Fleig, F. *Journal of High Resolution Chromatography* 1998, 21, 107-112.
- Cheetham, P. S. J. *Trends in Biotechnology* 1993, 11, 478-488.

- Chen, C. S.; Fujimoto, Y.; Girdaukas, G.; Sih, C. J. *Journal of the American Chemical Society* **1982**, *104*, 7294-7299.
- Chen, C. S.; Wu, S. H.; Girdaukas, G.; Sih, C. J. *Journal of the American Chemical Society* **1987**, *109*, 2812-2817.
- Cheng, A. X.; Lou, Y. G.; Mao, Y. B.; Lu, S.; Wang, L. J.; Chen, X. Y. *Journal of Integrative Plant Biology* **2007**, *49*, 179-186.
- Cori, O.; Chayet, L.; Perez, L. M.; Bunton, C. A.; Hachey, D. *Journal of Organic Chemistry* **1986**, *51*, 1310-1316.
- Croteau, R. B.; Davis, E. M.; Ringer, K. L.; Wildung, M. R. *Naturwissenschaften* **2005**, *92*, 562-577.
- de Carvalho, C.; da Fonseca, M. M. R. *Tetrahedron-Asymmetry* **2003**, *14*, 3925-3931.
- de Carvalho, C.; da Fonseca, M. M. R. *Applied Microbiology and Biotechnology* **2005**, *67*, 715-726.
- de Carvalho, C.; da Fonseca, M. M. R. *FEMS Microbiology Ecology* **2005**, *51*, 389-399.
- de Carvalho, C.; Parreno-Marchante, B.; Neumann, G.; da Fonseca, M. M. R.; Heipieper, H. J. *Applied Microbiology and Biotechnology* **2005**, *67*, 383-388.
- de Carvalho, C.; da Fonseca, M. M. R. *Biotechnology Advances* **2006**, *24*, 134-142.
- de Carvalho, C.; da Fonseca, M. M. R. *Food Chemistry* **2006**, *95*, 413-422.
- de Oliveira, A.; Ribiero-Pinto, L.; Otto, S. *Toxicology* **1997**, *124*, 135-140.
- de Oliveira, B. H.; dos Santos, M. C.; Leal, P. C. *Phytochemistry* **1999**, *51*, 737-741.
- Demyttenaere, J. C. R.; Herrera, M. D.; De Kimpe, N. *Phytochemistry* **2000**, *55*, 363-373.
- Demyttenaere, J.; De Kimpe, N. *Journal of Molecular Catalysis B-Enzymatic* **2001**, *11*, 265-270.
- Diaz-Perez, A. L.; Zavala-Hernandez, A. N.; Cervantes, C.; Campos-Garcia, J. *Applied and Environmental Microbiology* **2004**, *70*, 5102-5110.

- Drawert, F.; Barton, H. *Journal of Agricultural and Food Chemistry* **1978**, *26*, 765-766.
- Edegger, K.; Mang, H.; Faber, K.; Gross, J.; Kroutil, W. *Journal of Molecular Catalysis A-Chemical* **2006**, *251*, 66-70.
- Ensign, S. A. *Biochemistry* **2001**, *40*, 5845-5853.
- European Economic Community Directive 88/388/EEC **1988**
- Faber, K. *Biotransformations in Organic Chemistry 5th Ed.* **2004**. Springer.
- Fagan, G. L.; Kepner, R. E.; Webb, A. D. *Vitis* **1981**, *20*, 36-42.
- Farooq, A.; Rahman, A.; Choudhary, M. I. *Current Organic Chemistry* **2004**, *8*, 353-367.
- Feron, G.; Bonnarme, P.; Durand, A. *Trends in Food Science & Technology* **1996**, *7*, 285-293.
- Fogg, M. J.; Wilkinson, A. J. *Biochemical Society Transactions* **2008**, *36*, 771-775.
- Forster-Fromme, K.; Jendrossek, D. *FEMS Microbiology Letters* **2005**, *246*, 25-31.
- Forster-Fromme, K.; Jendrossek, D. *FEMS Microbiology Letters* **2006**, *264*, 220-225.
- Forster-Fromme, K.; Hoschle, B.; Mack, C.; Bott, M.; Armbruster, W.; Jendrossek, D. *Applied and Environmental Microbiology* **2006**, *72*, 4819-4828.
- Forster-Fromme, K.; Chattopadhyay, A.; Jendrossek, D. *Microbiology-SGM* **2008**, *154*, 789-796.
- Foß, S.; Harder, J. *FEMS Microbiology Letters* **1997**, *149*, 71-75.
- Fukuda, H.; Kondo, A.; Tamalampudi, S. *Biochemical Engineering Journal* **2009**, *44*, 2-12.
- Gershenson, J.; Dudareva, N. *Nature Chemical Biology* **2007**, *3*, 408-414.
- Gudelj, M.; Valinger, G.; Faber, K.; Schwab, H. *Journal of Molecular Catalysis B-Enzymatic* **1998**, *5*, 261-266.
- Harder, J.; Probian, C. *Applied and Environmental Microbiology* **1995**, *61*, 3804-3808.

- Heinze, B.; Kourist, R.; Fransson, L.; Hult, K.; Bornscheuer, U. T. *Protein Engineering Design & Selection* **2007**, *20*, 125-131.
- Heipieper, H. J.; Diefenbach, R.; Keweloh, H. *Applied and Environmental Microbiology* **1992**, *58*, 1847-1852.
- Hellstrom, H.; Steinreiber, A.; Mayer, S. F.; Faber, K. *Biotechnology Letters* **2001**, *23*, 169-173.
- Henke, E.; Bornscheuer, U. T. *Applied Microbiology and Biotechnology* **2002**, *60*, 320-326.
- Henke, E.; Pleiss, E.; Bornscheuer, U. T. *Angewandte Chemie-International Edition* **2002**, *41*, 3211-3213.
- Henke, E.; Bornscheuer, U. T.; Schmid, R. D.; Pleiss, J. *ChemBioChem* **2003**, *4*, 485-493.
- Heyen, U.; Harder, J. *Applied and Environmental Microbiology* **2000**, *66*, 3004-3009.
- Hibbert, H.; Cannon, L. T. *Journal of the American Chemical Society* **1924**, *45*, 119-130.
- Holland, H. L.; Gu, J. X. *Biotechnology Letters* **1998**, *20*, 1125-1126.
- Hook, I.; Lecky, R.; McKenna, B.; Sheridan, H. *Phytochemistry* **1990**, *29*, 2143-2144.
- Hop Union Directory of Hop Data, available at <http://www.hopunion.com/education.shtml>
- Hoschle, B.; Gnau, V.; Jendrossek, D. *Microbiology-SGM* **2005**, *151*, 3649-3656.
- Hoschle, B.; Jendrossek, D. *Microbiology-SGM* **2005**, *151*, 2277-2283.
- Howell, A. R.; Pattenden, G. *Journal of the Chemical Society-Perkin Transactions 1* **1990**, 2715-2719.
- Howell, A. R.; Pattenden, G. *Journal of the Chemical Society-Chemical Communications* **1990**, 103-104.
- Ishida, T. *Chemistry & Biodiversity* **2005**, *2*, 569-590.
- Ishikawa, J.; Yamashita, A.; Mikami, Y.; Hoshino, Y.; Kurita, H.; Hotta, K.; Shiba, T.; Hattori, M. *Proceedings of the National Academy of Sciences of the United States of America* **2004**, *101*, 14925-14930.

- Iurescia, S.; Marconi, A. M.; Tofani, D.; Gambacorta, A.; Paterno, A.; Devirgiliis, C.; van der Werf, M. J.; Zennaro, E. *Applied and Environmental Microbiology* **1999**, *65*, 2871-2876.
- Jablonski, E. L.; Vilella, I. M. J.; Maina, S. C.; de Miguel, S. R.; Scelza, O. A. *Catalysis Communications* **2006**, *7*, 18-23.
- Jenkins, G. N.; Ribbons, D. W.; Widdowson, D. A.; Slawin, A. M. Z.; Williams, D. J. *Journal of the Chemical Society-Perkin Transactions 1* **1995**, 2647-2655.
- Jennings, W.; Shibamoto, T. *Qualitative analysis of flavour and fragrance volatiles by glass capillary gas chromatography* **1980**, Academic, New York.
- Kang, H. K.; Lee, S. S. *Archives of Pharmaceutical Research* **1997**, *20*, 519-524.
- Kazlauskas, R. J.; Weber, H. K. *Current Opinion in Chemical Biology* **1998**, *2*, 121-126.
- King, A.; Dickinson, J. R. *Yeast* **2000**, *16*, 499-506.
- King, A. J.; Dickinson, J. R. *FEMS Yeast Research* **2003**, *3*, 53-62.
- Kirimura, K.; Furuya, T.; Sato, R.; Ishii, Y.; Kino, K.; Usami, S. *Applied and Environmental Microbiology* **2002**, *68*, 3867-3872.
- Kishimoto, T.; Wanikawa, A.; Kagami, N.; Kawatsura, K. *Journal of Agricultural and Food Chemistry* **2005**, *53*, 4701-4707.
- Kishimoto, T.; Wanikawa, A.; Kono, K.; Shibata, K. *Journal of Agricultural and Food Chemistry* **2006**, *54*, 8855-8861.
- Klingenberg, A.; Sprecher, E. *Planta Medica* **1985**, *3*, 264-265.
- Kosjek, B.; Stampfer, W.; Glueck, S. M.; Pogorevc, M.; Ellmer, U.; Wallner, S. R.; Koegl, M. F.; Poessl, T. M.; Mayer, S. F.; Ueberbacher, B.; Faber, K.; Kroutil, W. *Journal of Molecular Catalysis B-Enzymatic* **2003**, *22*, 1-6.
- Kourist, R.; Bartsch, S.; Bornscheuer, U. T. *Advanced Synthesis & Catalysis* **2007**, *349*, 1393-1398.
- Kourist, R.; Krishna, S. H.; Patel, J. S.; Bartnek, F.; Hitchman, T. S.; Weiner, D. P.; Bornscheuer, U. T. *Organic & Biomolecular Chemistry* **2007**, *5*, 3310-3313.
- Kourist, R.; Nguyen, G. S.; Strubing, D.; Bottcher, D.; Liebeton, K.; Naumer, C.; Eck, J.; Bornscheuer, U. T. *Tetrahedron-Asymmetry* **2008**, *19*, 1839-1843.

- Kourist, R., Dominguez de Maria, P., Bornscheuer, U.T. *ChemBioChem* **2008**, *9*, 491-498.
- Krings, U.; Berger, R. G. *Applied Microbiology and Biotechnology* **1998**, *49*, 1-8.
- Krings, U.; Hapetta, D.; Berger, R. G. *Applied Microbiology and Biotechnology* **2008**, *78*, 533-541.
- Kroutil, W.; Mang, H.; Edegger, K.; Faber, K. *Current Opinion in Chemical Biology* **2004**, *8*, 120-126.
- Krugener, S.; Schaper, C.; Krings, U.; Berger, R. G. *Bioresource Technology* **2009**, *100*, 2855-60.
- Kulikova, A. K.; Bezborodov, A. M. *Applied Biochemistry and Microbiology* **2000**, *36*, 227-230.
- Kulikova, A. K.; Bezborodov, A. M. *Applied Biochemistry and Microbiology* **2001**, *37*, 164-167.
- Larkin, M. J.; Kulakov, L. A.; Allen, C. C. R. *Current Opinion in Biotechnology* **2005**, *16*, 282-290.
- Lichtenthaler, H. K. *Annual Review of Plant Physiology and Plant Molecular Biology* **1999**, *50*, 47-65.
- Lindwall, G.; Chau, M. F.; Gardner, S. R.; Kohlstaedt, L. A. *Protein Engineering* **2000**, *13*, 67-71.
- Madyastha, K. M. *Xenobiotica* **1987**, *17*, 539-549.
- Maia, O.; Perecin, M.O.M. Marques, N.P. Granja, A.L. *Conference abstract* **2004**.
- McGarvey, D. J.; Croteau, R. *Plant Cell* **1995**, *7*, 1015-1026.
- McKemy, D. D.; Neuhausser, W. M.; Julius, D. *Nature* **2002**, *416*, 52-58.
- McLeod, M. P.; Warren, R. L.; Hsiao, W. W. L.; Araki, N.; Myhre, M.; Fernandes, C.; Miyazawa, D.; Wong, W.; Lillquist, A. L.; Wang, D.; Dosanjh, M.; Hara, H.; Petrescu, A.; Morin, R. D.; Yang, G.; Stott, J. M.; Schein, J. E.; Shin, H.; Smailus, D.; Siddiqui, A. S.; Marra, M. A.; Jones, S. J. M.; Holt, R.; Brinkman, F. S. L.; Miyauchi, K.; Fukuda, M.; Davies, J. E.; Mohn, W. W.; Eltis, L. D. *Proceedings of the National Academy of Sciences of the United States of America* **2006**, *103*, 15582-15587.

- Miyazawa, M.; Murata, T. *Journal of Agricultural and Food Chemistry* **2000**, *48*, 123-125.
- Mockute, D.; Bernotiene, G.; Nivinskiene, O.; Butkiene, R. *Journal of Essential Oil Research* **2008**, *20*, 96-101.
- Murakami, A.; Darby, P.; Javornik, B.; Pais, M.; Seigner, E.; Lutz, A.; Svoboda, P. *Heredity* **2006**, *97*, 66-74.
- Noyori, R. *Advanced Synthesis & Catalysis* **2003**, *345*, 15-32.
- Ojala, M.; Ketola, R. A.; Mansikka, T.; Kotiaho, T.; Kostianen, R. *Talanta* **1999**, *49*, 179-188.
- Ollis, D. L.; Cheah, E.; Cygler, M.; Dijkstra, B.; Frolow, F.; Franken, S. M.; Harel, M.; Remington, S. J.; Silman, I.; Schrag, J.; Sussman, J. L.; Verschueren, K. H. G.; Goldman, A. *Protein Engineering* **1992**, *5*, 197-211.
- Osprian, I.; Steinreiber, A.; Mischitz, M.; Faber, K. *Biotechnology Letters* **1996**, *18*, 1331-1334.
- Panke, S.; Witholt, B.; Schmid, A.; Wubbolts, M. G. *Applied and Environmental Microbiology* **1998**, *64*, 2032-2043.
- Patel, T.; Ishiiji, Y.; Yosipovitch, G. *Journal of the American Academy of Dermatology* **2007**, *57*, 873-878.
- Peier, A. M.; Moqrigh, A.; Hergarden, A. C.; Reeve, A. J.; Andersson, D. A.; Story, G. M.; Earley, T. J.; Dragoni, I.; McIntyre, P.; Bevan, S.; Patapoutian, A. *Cell* **2002**, *108*, 705-715.
- Pichersky, E.; Lewinsohn, E.; Croteau, R. *Archives of Biochemistry and Biophysics* **1995**, *316*, 803-807.
- Pleiss, J.; Fischer, M.; Peiker, M.; Thiele, C.; Schmid, R. D. *Journal of Molecular Catalysis B-Enzymatic* **2000**, *10*, 491-508.
- Pogorevc, M.; Faber, K. *Journal of Molecular Catalysis B-Enzymatic* **2000**, *10*, 357-376.
- Pogorevc, M.; Strauss, U. T.; Hayn, M.; Faber, K. *Monatshefte Fur Chemie* **2000**, *131*, 639-644.
- Raguso, R. A.; Pichersky, E. *Plant Species Biology* **1999**, *14*, 95-120.

Rocha, S. M.; Coelho, E.; Zrostlikova, J.; Delgadillo, I.; Coimbra, M. A. *Journal of Chromatography A* **2007**, *1161*, 292-299.

Rohmer, M. *Natural Product Reports* **1999**, *16*, 565-574.

Rondon, M. R.; August, P. R.; Bettermann, A. D.; Brady, S. F.; Grossman, T. H.; Liles, M. R.; Loiacono, K. A.; Lynch, B. A.; MacNeil, I. A.; Minor, C.; Tiong, C. L.; Gilman, M.; Osburne, M. S.; Clardy, J.; Handelsman, J.; Goodman, R. M. *Applied and Environmental Microbiology* **2000**, *66*, 2541-2547.

Sandstrom, P.; Welch, W. H.; Blomquist, G. J.; Tittiger, C. *Insect Biochemistry and Molecular Biology* **2006**, *36*, 835-845.

Santos, P. M.; Correia, I. S. *Proteomics* **2009**, *22*, 5101-5111.

Savithiry, N.; Cheong, T. K.; Oriel, P. In *18th Symposium on Biotechnology for Fuels and Chemicals 1996*, 213-220, Humana Press Inc, Gatlinburg.

Schwab, W.; Davidovich-Rikanati, R.; Lewinsohn, E. *Plant Journal* **2008**, *54*, 712-732.

Sell, C. S. *Fragrant introduction to terpenoid chemistry 2003*, Royal Society of Chemistry.

Semikolenov, V. A.; Ilyna, II; Simakova, I. L. *Applied Catalysis A-General* **2001**, *211*, 91-107.

Serra, S.; Fuganti, C.; Brenna, E. *Trends in Biotechnology* **2005**, *23*, 193-198.

Sharp, J. O.; Sales, C. M.; LeBlanc, J. C.; Liu, J.; Wood, T. K.; Eltis, L. D.; Mohn, W. W.; Alvarez-Cohen, L. *Applied and Environmental Microbiology* **2007**, *73*, 6930-6938.

Shevchenko, A.; Sunyaev, S.; Loboda, A.; Shevehenko, A.; Bork, P.; Ens, W.; Standing, K. G. *Analytical Chemistry* **2001**, *73*, 1917-1926.

Small, F. J.; Ensign, S. A. *Journal of Biological Chemistry* **1997**, *272*, 24913-24920.

Stampfer, W.; Kosjek, B.; Kroutil, W.; Faber, K. *Biotechnology and Bioengineering* **2003**, *81*, 865-869.

Takahashi, M.; Suzuki, H.; Morooka, Y.; Ikawa, T. *Chemistry Letters* **1979**, 53-56.

Thompson, M. L.; Marriott, R.; Dowle, A.; Grogan, G. *Applied Microbiology and Biotechnology* **2010**, *85*, 721-730.

Van der Geize, R.; Dijkhuizen, L. *Current Opinion in Microbiology* **2004**, *7*, 255-261.

Vlieg, J.; Leemhuis, H.; Spelberg, J. H. L.; Janssen, D. B. *Journal of Bacteriology* **2000**, *182*, 1956-1963.

Wackett, L. P.; Hershberger, C. D. *Biocatalysis and Biodegradation. Microbial Transformation of Organic Compounds*. **2001**, ASM press, Washington D.C.

Wu, W. H.; Akoh, C. C.; Phillips, R. S. *Enzyme and Microbial Technology* **1996**, *18*, 536-539.

Yamazaki, Y.; Hayashi, Y.; Hori, N.; Mikami, Y. *Agricultural and Biological Chemistry* **1988**, *52*, 2921-2922.

Yao, G.; Haque, S.; Sha, L.; Kumaravel, G.; Wang, J.; Engber, T. M.; Whalley, E. T.; Conlon, P. R.; Chang, H. X.; Kiesman, W. F.; Petter, R. C. *Bioorganic & Medicinal Chemistry Letters* **2005**, *15*, 511-515.

Yu, L. J.; Xu, Y.; Wang, X. Q.; Yu, X. W. *Journal of Molecular Catalysis B-Enzymatic* **2007**, *47*, 149-154.

Yu, L. J.; Xu, Y.; Yu, X. W. *Journal of Molecular Catalysis B-Enzymatic* **2009**, *57*, 27-33.

List of structures

<u>Structure</u>	<u>Page</u>
1. Quinine	2
2. Caffeine	2
3. Erythromycin	2
4. Isoprene	3
5. Limonene	3
6. Menthol	3
7. Camphor	3
8. Caryophyllene	4
9. Retinol	4
10. α -pinene	5
11. 3-carene	5
12. Abietic acid	5
13. Acetyl-CoA	6
14. HMG-CoA	6
15. Mevalonic acid	6
16. Isopentenyl diphosphate (IPP)	6
17. Dimethylallyl diphosphate (DMAPP)	6
18. Geranyl diphosphate (GPP)	6
19. Farnesyl diphosphate (FPP)	6
20. Geranyl geranyl diphosphate (GGPP)	6

<u>Structure</u>	<u>Page</u>
21. Pyruvate	7
22. Glyceraldehyde-3-phosphate	7
23. 1-deoxy-D-xylulose 5-phosphate (DOXP)	7
24. Methylerythritol phosphate (MEP)	7
25. 4-diphosphocytidyl-2-methylerythritol (CDP-ME)	7
26. 4-diphosphocytidyl-2-methyl-erythritol-2-phosphate (CDP-MEP)	7
27. 2-methyl-erythritol-2,4-cyclopyrophosphate (MEcPP)	7
28. 4-hydroxy-3-methyl-but-2-enyl pyrophosphate (HMB-PP)	7
29. Ambrein	9
30. Patchouli alcohol	9
31. Azulene	9
32. Vanillin	9
33. Eugenol	9
34. Citronellol	9
35. Geraniol	9
36. Nerol	9
37. (<i>R</i>)-Linalool	9
38. (<i>S</i>)-Linalool	9
39. (<i>R,S</i>)-Linalool	10
40. Pinane	12
41. Pinane-hydroperoxide	12
42. Pinanol	12
	223

<u>Structure</u>	<u>Page</u>
43. 2-methyl-2-hepten-6-one	12
44. Dihydro-linalool	12
45. Intermediate linalyl cation	13
46. Linalyl diphosphate	13
47. β -myrcene	14
48. Neryl chloride	14
49. Linalyl chloride	14
50. Geranyl cobaloxime	15
51. Tertiary radical intermediate	15
52. Primary radical intermediate	15
53. Hydroxylamine intermediate	15
54. Geranial	16
55. Enol-intermediate	16
56. Neral	16
57. 4S(+)-limonene	18
58. (+)-isopiperitenol	18
59. (+)-isopiperitenone	18
60. (+)-isopulegone	18
61. (+)-pulegone	18
62. (-)-menthone	18
63. 1R(-)-menthol	18
64. β -pinene	14

<u>Structure</u>	<u>Page</u>
65. Allylic amine intermediate	19
66. Isomerised allylic amine intermediate	19
67. <i>S</i> -citronellal	19
68. 1 <i>R</i> -(-)-isopulegol	19
69. DL-(±)-menthyl acetate	20
70. D-1 <i>S</i> (+)-menthyl acetate	20
71. 17 α -hydroxyprogesterone	21
72. 6 β -17 α -hydroxyprogesterone	21
73. 3-(<i>p</i> -tolyl)-butenol	22
74. (<i>S</i>)-(+)- 3-(<i>p</i> -tolyl)-butanol	22
75. (±)-2-phenylbut-3-yn-2-ol	22
76. (+)-2-phenylbut-3-yn-2-ol	22
77. (-)-2-phenylbut-3-yn-2-acetate	22
78. α -terpineol	23
79. Terpin hydrate	23
80. naphtho[2-1- <i>b</i>]thiophene	24
81. naphtho[2-1- <i>b</i>]furan	24
82. 2-hydroxynaphthylethene	24
83. Carveol	25
84. Carvone	25
85. (±)-linalyl acetate	27
86. Racemic menthyl esters	27
	225

<u>Structure</u>	<u>Page</u>
87. <i>ent</i> -16-ketobeyeran-19-oic acid (isosteriol)	42
88. <i>ent</i> -7 α -hydroxy-16-ketobeyeran-19-oic acid	42
89. <i>ent</i> -17 α -hydroxy-16-ketobeyeran-19-oic acid	42
90. Myrcene-6,7-glycol	42
91. Myrcene-1,2-glycol	42
92. Myrcene-3(10)-glycol	42
93. Myrcenol (2-methyl-6-methylen-2,7-octadien-1-ol)	43
94. <i>p</i> -mentha-1,5-diene-8-ol	43
95. (<i>Z</i>)-2-methyl-2-hepten-6-one-1-ol	44
96. 2,6-dimethyl-2,7-octadien-1,6-diol	44
97. 2,6-dimethyl-octan-diol	44
98. (<i>Z</i>)-3,7-dimethyl-2-octen-1,8-diol	44
99. <i>p</i> -menth-1-ene-9-ol	44
100. (<i>Z</i>)-2-methyl-2-heptan-1-ol	44
101. 3,7-dimethyl-1,8-octandiol	44
102. (2 <i>Z</i> ,6 <i>E</i>)-3,7-dimethyl-2,6-octadien-1,8-diol	44
103. 7-hydroxy-6-methyl-2-heptanone	44
104. (<i>Z</i>)-3,7-dimethyl-2,6-octadiene-1,8-diol	44
105. (<i>E</i>)-3,7-dimethyl-2-octen-1,8-diol	44
106. Unknown epoxide product	50
107. Unknown cyclic product	50
108. Acetone	61

<u>Structure</u>	<u>Page</u>
109. ψ -ionone	61
110. α -ionone	61
111. Benzoic acid	68
112. (1 <i>S</i> , 2 <i>R</i>)-dihydroxy-benzoic acid	68
113. <i>Tert</i> -butyl octanoate	68
114. <i>Tert</i> -butyl alcohol	68
115. <i>Tert</i> -butyl octanoic acid	68
116. (<i>R,S</i>)-2-methylglycidyl benzyl ether	68
117. (<i>R</i>)-2-methylglycidyl benzyl ether	68
118. (<i>S</i>)-2-methyl-propan-2,3-diol benzyl ether	68
119. Tributyrin	84
120. α -naphthyl acetate	84
121. <i>tert</i> -butyl acetate	84
122. <i>p</i> -nitrophenyl acetate	131
123. <i>p</i> -nitrophenol	131
124. 1 <i>R</i> (-)-menthyl acetate	134
125. 1 <i>S</i> (+)-menthyl acetate	134
126. 1 <i>S</i> (+)-menthol	134
127. Citronellyl acetate	135
128. (<i>R</i>)-lavandulyl acetate	136
129. (<i>S</i>)-lavandulyl acetate	136
130. (<i>S</i>)-lavandulol	136

<u>Structure</u>	<u>Page</u>
131. (<i>R</i>)-lavandulol	136
132. Humulone	141
133. Lupulone	141
134. Xanthohumol	141
135. Myrcene-3,10-diol	142
136. A myrcene hydroxy acid	142
137. Myrcene-1,2-diol	142
138. A myrcene hydroxy acid	142
139. (4 <i>R</i>)-(-)-ips-dienol	144
140. 2-methyl-6-methylene-7-octene-2,3-diol	144
141. 6-methyl-2-ethenyl-5-heptene-1,2-diol	144
142. 7-methyl-3-methylene-6-octene-1,2-diol	144
143. α -(<i>Z</i>)-acaridiol	144
144. Myrcene 1,2-endoperoxide	144
145. Myrcene 1,4-endoperoxide	144
146. Styrene	167
147. Styrene oxide	167
148. Phenylacetaldehyde	167
149. Phenylacetic acid	167
150. 3-methyl and 3-ethylbutanolide	168
151. (<i>R</i>)-3-hydroxy-3-alkylbutanolides	168
152. Perillyl alcohol	168
	228

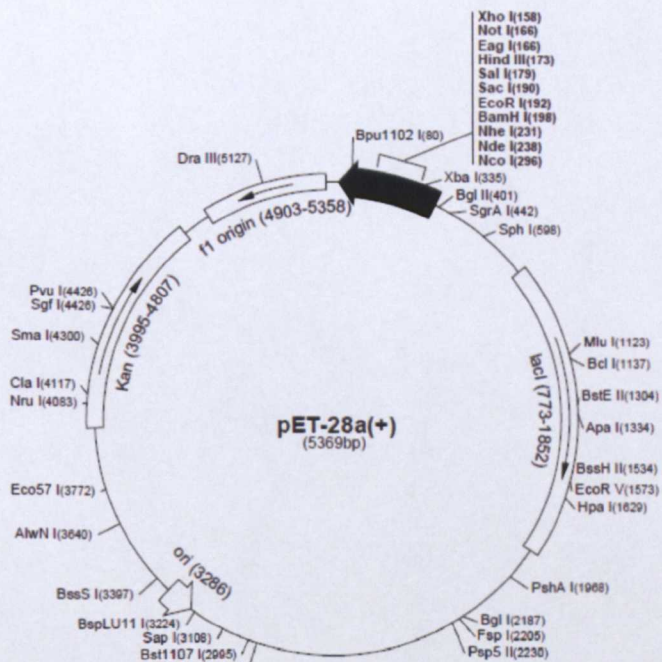
<u>Structure</u>	<u>Page</u>
153. 1-hydroxy-2-glutathionyl-2-methyl-3-butene	173
154. 1-hydroxy-2-glutathionyl-2-methyl-3-butenic acid	173
155. 2-methyl-6-methylen-2,7-octadienal	207
156. 2-methyl-6-methylen-2,7-octadienoic acid	207
157. 2-methyl-6-methylen-2,7-octadienoyl-CoA	207
158. 2-methyl-3-hydroxy-6-methylen-7-octenoyl-CoA	207
159. 2-methyl-3-keto-6-methylen-7-octenoyl-CoA	207
160. 4-methylen-5-hexenoyl-CoA	207
161. α -myrcene	209
162. Geranic acid	210
163. α -terpinyl acetate	198

Appendix

A plasmid map of the pET-YSBL3C vector used in ligation independent cloning is shown below [Fogg and Wilkinson 2008]. A pET-28a vector had been modified between the *NcoI* and *NdeI* restriction enzyme sites to incorporate a 3C protease cleavage site and a His-tag in place of the thrombin cleavage site, yielding the pET-YSBL3C construct. Selection is achieved *via* kanamycin resistance.

pET-28a(+) sequence landmarks

T7 promoter	370-386
T7 transcription start	369
His•Tag coding sequence	270-287
T7•Tag coding sequence	207-239
Multiple cloning sites (<i>Bam</i> HI - <i>Xho</i> I)	158-203
His•Tag coding sequence	140-157
T7 terminator	26-72
<i>lacI</i> coding sequence	773-1852
pBR322 origin	3286
Kan coding sequence	3995-4807
f1 origin	4903-5358



CCATGG *NcoI* restriction site

GAGGAG *BseRI* restriction site

CATATG *NdeI* restriction site

CTGGAA GTTCTGTTCCAGGGACCA (3C) Protease cleavage site

5'-ATAC**CCATGG**GCAGCAGCCATCATCATCATCACAGCAGCGGC**CTGGAA GTTCTGTTCCAGGGACCA**GCAAGGCCGCCTT**CTCTCACATATG**-3'
 3'-TAT**GGTACC**CGTCGTCGGTAGTAGTAGTAGTGTCTGTCGCCG**GACCTTCAA GACAAAGTCCCTGGT**CGTCCGCGCGGAA**GAGGAGTG**TATAC-5'

MetGlySerSerHisHisHisHisHisHisHisSerSerGly**LeuGluValLeuPheClnGlyProAla**

21/22 additional N-terminal amino acids
 encoding a cleavable His-tag

3C Cleavage site

Biotransformation of β -myrcene to geraniol by a strain of *Rhodococcus erythropolis* isolated by selective enrichment from hop plants

Mark L. Thompson · Ray Marriott · Adam Dowle · Gideon Grogan

Received: 2 July 2009 / Revised: 4 August 2009 / Accepted: 4 August 2009 / Published online: 26 August 2009
© Springer-Verlag 2009

Abstract The biocatalytic generation of high-value chemicals from abundant, cheap and renewable feedstocks is an area of great contemporary interest. A strain of *Rhodococcus erythropolis* designated MLT1 was isolated by selective enrichment from the soil surrounding hop plants, using the abundant triene β -myrcene from hops as a sole carbon source for growth. Resting cells of the organism were challenged with β -myrcene, and the major product of biotransformation was determined by mass spectrometric analysis to be the monoterpene alcohol geraniol. Controls demonstrated that the product was biogenic and that an aerobic environment was required. The ability to transform β -myrcene was shown to be restricted to cells that had been grown on this substrate as sole carbon source. Pre-incubation of cells with the cytochrome P450 inhibitors metyrapone or 1-aminobenzotriazole reduced geraniol production by 23% and 73% respectively, but reduction in activity was found not to correlate with the inhibitor concentration. A comparative analysis of insoluble and soluble cell extracts derived from cells of MLT1 grown on either β -myrcene or glucose revealed at least four proteins that were clearly overproduced in response to growth on β -myrcene. Mass

spectrometric analysis of tryptic digests of three of these protein bands suggested their identities as an aldehyde dehydrogenase, an acyl-CoA dehydrogenase and a chaperone-like protein, each of which has a precedented role in hydrocarbon metabolism clusters in *Rhodococcus* sp. and which may therefore participate in a β -myrcene degradation pathway in this organism.

Keywords Hops · Enrichment · *Rhodococcus* · Biotransformation · Myrcene · Geraniol

Introduction

The biotransformation of abundant, low-value renewable organic materials from plants to higher value compounds is an area of great contemporary interest, as the use of microbial or enzymatic catalysis can offer a route to natural-equivalent products which resonate with green technologies in industry (Chen et al. 2007; Woodley 2008). The C-10 monoterpenes represent one such source of potential renewable chemicals of value to the flavour and fragrance industry (Klings and Berger 1998; Vandamme and Soetaert 2002; Rozenbaum et al. 2006), with compounds such as limonene (de Carvalho and da Fonseca 2003; Duetz et al. 2003) carvone (de Carvalho and da Fonseca 2006) and menthol (Serra et al. 2005) having been studied extensively.

Hops, from the genus *Humulus*, are an abundant crop largely grown in central temperate regions and are widely cultivated for beer production. The lupulin glands from the flowers (cones) of the female *Humulus lupulus* plant are known to contain a complex mixture of C-10 terpenes as part of their natural essential oils, including the fragrant monoterpene alcohols linalool and geraniol (Kishimoto et

M. L. Thompson · G. Grogan (✉)
York Structural Biology Laboratory, Department of Chemistry,
University of York,
YO10 5YW York, UK
e-mail: grogan@ysbl.york.ac.uk

R. Marriott
Department of Chemistry, University of York,
YO10 5DD York, UK

A. Dowle
Technology Facility, Department of Biology, University of York,
YO10 5YW York, UK

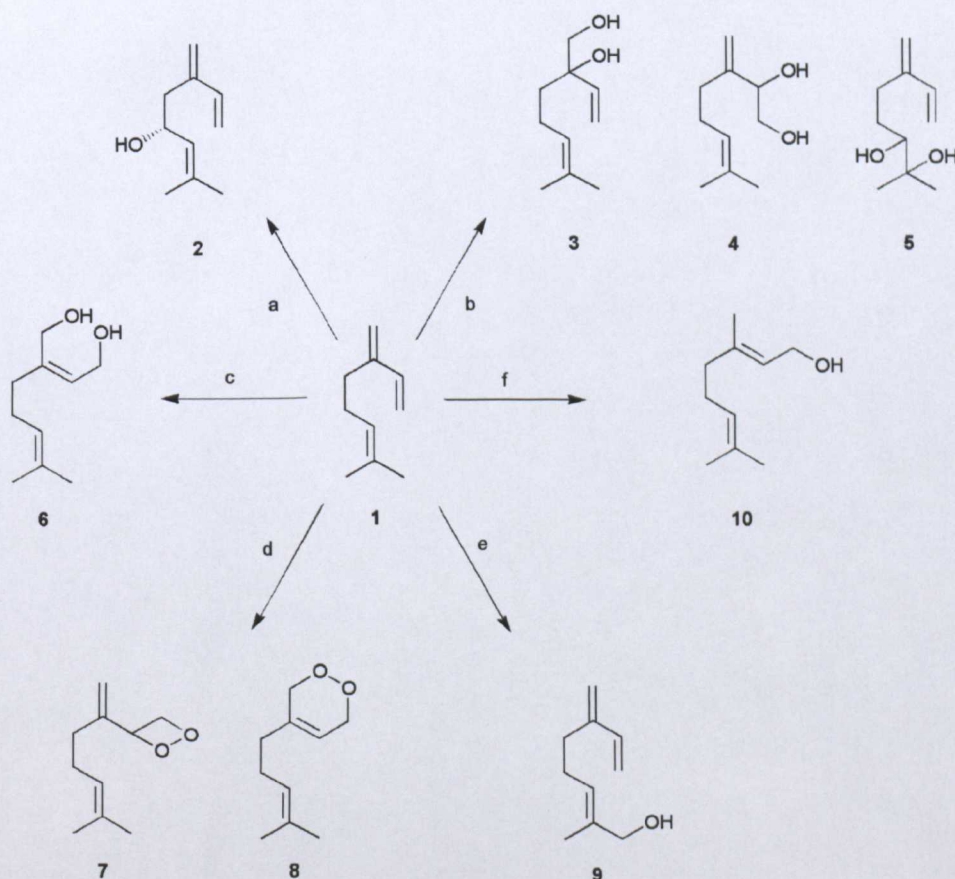
al. 2005; Cheng et al. 2007). The acyclic monoterpene β -myrcene (7-methyl-3-methylene-1,6-octadiene; **1**, Fig. 1) accounts for a relatively large fraction (up to 70%) of monoterpenes extracted from the essential oils of *H. lupulus* (from the Hop Union Directory of Hop Data, available at <http://www.hopunion.com/education.shtml>). β -Myrcene may therefore be considered as a relatively inexpensive starting material for biotransformations that target more commercially attractive derivatives.

β -Myrcene has been the subject of a number of biotransformation studies in the past (Ishida 2005), including descriptions of its metabolism in mammalian (de Oliveira et al. 1997; Madyastha 1987) and insect cells (Miyazawa and Murata 2000). One example of a natural biotransformation involving myrcene is found in the biosynthetic pathway of aggregation pheromones in the pine engraver beetle *Ips pini*, in which β -myrcene was demonstrated to be hydroxylated stereoselectively to (4*R*)-(–)-ipsdienol (**2**, Fig. 1; Sandstrom et al. 2006). β -Myrcene has also been used as a substrate in microbial reactions. Biotransformation of **1** by *Aspergillus niger* yielded different 1, 2-diol compounds **3**, **4** and **5** (Fig. 1) via the apparent epoxidation, followed by hydrolysis, of β -myrcene at each of the three double bonds (Farooq et al.

2004; Yamazaki et al. 1988). A wide range of fragrant monoterpene alcohols was also produced by incubation of **1** with submerged cultures of *Ganoderma applanatum*, *Pleurotus flabellatus* and *Pleurotus sajor-caju* (Busmann and Berger 1994). Further strains of *Pleurotus* have been shown to metabolise **1** to, in one instance, α -acaridiol **6** (Klings et al. 2008) and in another, two endoperoxide derivatives **7** and **8** (Krugener et al. 2009).

Reports of the biotransformation of β -myrcene by bacterial species are rare, but in one study, it was used as the sole source of carbon for growth by *Pseudomonas* sp. M1 (Iurescia et al. 1999). Resting cells of a β -myrcene negative mutant of M1, created using transposon mutagenesis and designated N22, accumulated 2-methyl-6-methylen-2,7-octadien-1-ol **9** (myrcen-8-ol) as the major metabolite of biotransformation of **1** (Fig. 1). The ability to grow on **1** was conferred on N22 through the transfer of a cosmid which contained four open-reading frames *myrA*, *myrB*, *myrC* and *myrD*, potentially encoding an aldehyde dehydrogenase, an alcohol dehydrogenase, an acyl-coenzyme A synthetase and an enoyl-CoA hydratase respectively. The identification of these genes enabled the authors to propose a pathway for degradation of **1** by *Pseudomonas* sp. M1.

Fig. 1 Some biotransformations of β -myrcene in the literature. Pathway (a): to ipsdienol **2** in the bark beetle *Ips pini* (Sandstrom et al. 2006); (b): to three diol **3**, **4** and **5** compounds by *A. niger* (Farooq et al. 2004; Yamazaki et al. 1988); (c): to α -(*Z*)-acaridiol **6** by *Pleurotus ostreatus* (Klings et al. 2008); (d): to myrcene 1, 2-endoperoxide **7** and myrcene 1,4-endoperoxide **8** by *Pleurotus* spp. (Krugener et al. 2009); (e): to 2-methyl-6-methylen-2,7-octadien-1-ol **9** (myrcen-8-ol) by *Pseudomonas* sp. strain M1 (Iurescia et al. 1999); (f): to geraniol **10** in this study



Geraniol (**10**, Fig. 1) is a monoterpene alcohol with a wide range of uses in perfumery, food and also as an insect repellent. The global production of geraniol together with its derived esters was estimated recently to be 12,000 tonnes per year (Schwab et al. 2008). Whilst some of this material is extracted directly from natural products, the majority is based on an industrial chemical synthesis from naturally derived β -pinene. Selective abiotic routes from β -myrcene towards geraniol have also been described, through regio-selective hydroxylation of Pd(II) (Takahashi et al. 1979) and cobalt (Howell and Pattenden 1990a, 1990b) complexes. Production of geraniol in any of these respects would preclude the potential use of the natural-equivalent label and so a direct biocatalytic route from β -myrcene to geraniol would be highly desirable. In this report, we describe the enrichment selection of a *Rhodococcus* strain designated MLT1 using β -myrcene as sole carbon source. Growth of the organism on β -myrcene induces the activity for biotransformation of the substrate to geraniol.

Materials and methods

Chemicals

Myrcene of 90% purity was purchased from Fluka. For use in enrichment and biotransformation experiments, the commercial compound was distilled by heating at 120°C under a reduced pressure of 15 mbar. Authentic geraniol (purity $\geq 96\%$) and nerol ($\geq 90\%$) standards were purchased from Fluka. A *H. lupulus* plant (Goldings variety) and soil surrounding the roots were obtained from Botanix Ltd.

Enrichment cultures and isolation of *Rhodococcus erythropolis* MLT1

Soil, root, leaf and flower samples from *H. lupulus* were homogenised individually in 20 mL of sterile water, 5 mL of which was used to inoculate 250-mL Erlenmeyer flasks containing 50 mL of M9 minimal medium (KH₂PO₄ 3.1 g/L, K₂HPO₄ 8.2 g/L, (NH₄)₂SO₄ 2.4 g/L, yeast extract 0.1 g/L, tryptone 0.1 g/L, MgSO₄·7H₂O 0.5 g/L, MnSO₄·H₂O 0.05 g/L, CaCl₂·2H₂O 0.01 g/L, molybdic acid 0.01 g/L, FeSO₄·7H₂O 2.5 g/L). The cultures were incubated aerobically at 25°C for 7 days with shaking at 150 rpm, before the addition of myrcene (1 g/L). After a further 12 days incubation, samples showing growth from the soil incubations were transferred (2% inoculum) to fresh M9 media (50 mL) with concentrations of myrcene at 1 and 5 g/L. At these concentrations, the myrcene was not completely soluble and tended to form emulsions. However, this did not seem to limit growth or result in uneven patterns of growth on the plates. After 6 days of growth,

M9 agar plates containing myrcene (5 g/L) were inoculated with 100 μ L dilutions (10^{-2} – 10^{-4}) of this culture, and incubated at 30°C for 7 days. Plates were sub-cultured onto the same medium and incubated for a further 7 days, before picking individual colonies and plating again. Further incubation led to the appearance of a single strain. 16S rRNA sequence analysis of this strain was carried out by the National Collection of Industrial and Marine Bacteria (NCIMB, Aberdeen, Scotland). The strain has been deposited with NCIMB with the accession number NCIMB 14574.

Growth of *R. erythropolis* MLT1

To enable growth on β -myrcene in the vapour phase, adaptations of 250-mL Erlenmeyer flasks were made using glassblowing facilities. Glass tubing (50 mm in length, and 6 mm diameter) was attached to the internal base of the flask, the top of which protrudes 25 mm above the level of a 50 mL culture shaken at 150 rpm. Myrcene (0.5 mL) was added into this hollow central well allowing the vapour to fill into the headspace above the culture medium. For the monitoring of growth, 50-mL cultures of M9 media with either glucose 1.0 g/L, succinate 1.0 g/L, or myrcene (vapour phase) as sole carbon sources were inoculated from agar plates as described previously and incubated at 30°C for 24 h. The optical density (OD, measured at a wavelength of 600 nm) of these pre-cultures was measured prior to inoculation (10%) of three separate 50 mL cultures for each of glucose, succinate and myrcene. OD measurements were taken from each flask over a period of time, until stationary phase of the growth curve was reached.

Preparation of cell extracts

Cells were harvested using a Sorvall RC5B centrifuge equipped with an SS34 rotor (4°C, 20 min, 27,000 \times g) then resuspended in one-tenth growth volume of 50 mM potassium phosphate (KH₂PO₄ 6.8 g/L, K₂HPO₄ 8.7 g/L) buffer (pH 7.0). Cells were lysed by three passages through a continuous flow French press at 270 MPa. The cell debris was removed by centrifugation (4°C, 40 min, 34,500 \times g) before retaining the soluble cell extract, which was concentrated by ultracentrifugation using a Centricon with a 3,000-molecular-weight cut-off filter (Millipore, Amicon Ultra-15). The total concentration of protein was estimated after lysis using the method of Bradford (Bradford 1976).

Biotransformation of myrcene by *R. erythropolis* MLT1

R. erythropolis MLT1 was incubated in M9 media as described above, with myrcene as the sole carbon source administered in the vapour phase for 3 days. Harvested

cells were washed twice with phosphate buffer, before resuspension (50 g/L) in 5 mL of buffer and the addition of myrcene (1 $\mu\text{L}/\text{mL}$, 7.4 mM). Controls with dead (autoclaved) cells, and myrcene (1 $\mu\text{L}/\text{mL}$) in buffer (no cells) were prepared under the same conditions. The samples were incubated for 1 h with shaking at 30°C. Cells were separated by centrifugation as before, and the solution saturated with NaCl before extracting three times with 5 mL of a 1:1 (petroleum ether:ethyl acetate) mixture. The organic layers were recombined, and dry MgSO_4 added to remove excess water. The MgSO_4 was filtered off, and the solution concentrated by leaving to evaporate overnight, before re-dissolving the resultant oil with 300 μL of a 1:1 petroleum ether:ethyl acetate mixture. For cytochrome P450 inhibition studies, cells were prepared using the methods previously mentioned, then pre-incubated with 1 and 5 mM concentrations of the inhibitors metyrapone and 1-aminobenzotriazole (ABT), shaking at 30°C for 0.5, 1 and 2 h before repeating the resting cell assay with myrcene.

Anaerobic resting cell assay

Resuspended cells were split into two aliquots. The standard resting cell assay with myrcene was repeated with one aliquot by incubating for 1 h at 25°C, whilst the other aliquot was stirred for 15 min in an anaerobic chamber to remove any dissolved oxygen from the solution prior to the addition of pre-equilibrated myrcene (1 $\mu\text{L}/\text{mL}$). The stirred solution was incubated for 1 h at 25°C under anaerobic conditions, and extracted with a pre-equilibrated 1:1 (petroleum ether:ethyl acetate) mixture. Samples were kept sealed airtight prior to GC analysis.

Metabolite identification

Gas chromatographic analysis of samples was performed routinely using an Agilent 6890 N gas chromatograph equipped with a J&W HP5 column (length 30 m, internal diameter 0.32 mm, film 0.25 μm). Two-microlitre samples were injected at 250°C in the split mode. For analysis of myrcene–geraniol biotransformations, an initial oven temperature of 60°C was increased through a 10°C/min gradient to 200°C, with a flow rate of the carrier gas helium at 10 mL/min. GC-MS analysis was performed with a Clarus 500 gas chromatograph (Perkin-Elmer) equipped with a J&W DB-1 column (30 m \times 0.32 mm \times 1 μm), coupled with a Clarus 500 mass spectrometer. One-microlitre samples were injected at 250°C in the split mode. An initial oven temperature of 60°C was held for 1.5 min before increasing at 4°C/min to 280°C with a further hold at this temperature for 15 min. The carrier gas helium was provided at a flow rate of 1.5 mL/min. The instrument was run

in EI mode at an energy of 70 eV. Mass spectra were scanned in the range of 25 to 250 m/z .

Gel analysis of cell extracts and peptide MS analysis

Cell extract samples were diluted 1:1 in a loading buffer 50 mM Tris/HCl (pH 6.8), containing: glycerol 10%, SDS 2%, bromophenol blue 0.005% and β -mercaptoethanol 5%. Resolving gels (12% acrylamide) were set by adding tetramethylethylenediamine (TEMED) to a resolving gel buffer (1.5 M Tris, 0.4% SDS, pH 8.8) containing acrylamide and ammonium persulphate (APS). Stacking gels were poured from a 0.5 M Tris buffer (0.4% SDS, pH 6.8) containing acrylamide, APS and TEMED. A BioRad low molecular mass marker mixture from 14.4–97.4 kDa was used. Gels were stained with Coomassie Blue and destained using a 6:3:1 mixture of water: propan-2-ol: glacial acetic acid.

In-gel tryptic digestion was performed after reduction with dithioerythritol (DTE) and *S*-carbamidomethylation with iodoacetamide. Gel pieces were washed twice with 50% (v:v) aqueous acetonitrile containing 25 mM ammonium bicarbonate, and then once with acetonitrile before drying in a vacuum concentrator for 20 min. Sequencing-grade, modified porcine trypsin (Promega) was dissolved in 50 mM acetic acid, then diluted fivefold by adding 25 mM ammonium bicarbonate to give a final trypsin concentration of 0.01 $\mu\text{g}/\mu\text{L}$. Gel pieces were rehydrated by adding 10 μL of trypsin solution, and after 30 min, the gel pieces were submerged in a 25-mM ammonium bicarbonate solution. Digests were incubated overnight at 37°C. A 0.5- μL aliquot of each peptide mixture was applied directly to the ground steel MALDI target plate, followed immediately by an equal volume of a freshly prepared 5 g/L solution of 4-hydroxy- α -cyano-cinnamic acid (Sigma) in 50% aqueous (v:v) acetonitrile containing 0.1% , trifluoroacetic acid (v:v).

Positive-ion MALDI mass spectra were obtained using an Applied Biosystems 4700 Proteomics Analyzer (Applied Biosystems, Foster City, CA, USA) in reflectron mode, equipped with a Nd:YAG laser. MS spectra were acquired over a mass range of m/z 800–4,000. Final mass spectra were internally calibrated using the tryptic autoproteolysis products at m/z 842.509 and 2,211.104. Monoisotopic masses were obtained from centroids of raw, unsmoothed data. The 20 strongest peaks with a signal to noise greater than 40 were selected for CID-MS/MS analysis.

For CID-MS/MS, a Source 1 collision energy of 1 kV was used, with air as the collision gas. The precursor mass window was set to a relative resolution of 50, and the metastable suppressor was enabled. The default calibration was used for MS/MS spectra, which were baseline-

subtracted (peak width 50) and smoothed (Savitsky–Golay with three points across a peak and polynomial order 4); peak detection used a minimum S/N of 5, local noise window of $50m/z$, and minimum peak width of 2.9 bins. Filters of S/N 20 and 30 were used for generating peak lists from MS and MS/MS spectra, respectively.

Tandem mass spectral data were submitted to database searching against the NCBI non-redundant database (20070926 version, 5519594 sequences, 1911975371 residues) and the *Rhodococcus jostii* RHA1 genome (<http://www.rhodococcus.ca>; 9161 sequences, 2893055 residues) using a locally running copy of the Mascot programme (Matrix Science Ltd., version 2.1), through the Applied Biosystems GPS Explorer software interface (version 3.6).

Where required MS/MS spectral data were also submitted to de novo sequencing using GPS Explorer TM software—DeNovo Explorer Version 3.6. The following parameters were used: Enzyme: trypsin, mass tolerance; 0.2 Da, fixed modifications; carbamidomethyl (C), variable modification; oxidation (M). The top ten sequence matches were submitted to an MSBlast search against the nrdb95 database using the facility provided by the European Molecular Biology Laboratory (Shevchenko et al. 2001).

Results

Enrichment selection and characterisation of *R. erythropolis* MLT1

R. erythropolis MLT1 was isolated from an enrichment culture using β -myrcene as a sole carbon source (SCS) inoculated initially with soil surrounding the roots of a hop plant, as described in the “Materials and methods” section, and identified through 16S rRNA sequence analysis (NCIMB). Growth of this strain in liquid media with myrcene (0.1–0.5 g/L) was very limited, and was likely to be a result of the poor solubility and toxicity observed at higher concentrations of myrcene. Improved growth was observed when the myrcene was supplied in the vapour phase in Erlenmeyer flasks that had been fitted with a central glass well, into which the β -myrcene was deposited. GC analysis of organic extracts of the growth medium at intervals showed an absence of β -myrcene, and it appears therefore that the substrate in the vapour phase is taken up from the flask headspace by the cells. In cultures using β -myrcene in the vapour phase as SCS a prolonged exponential phase of 15 h preceded a maximum OD (recorded at 600 nm) of 0.45 (Fig. 2). Growth rates were increased using glucose or succinate as SCS with exponential phases lasting 7 and

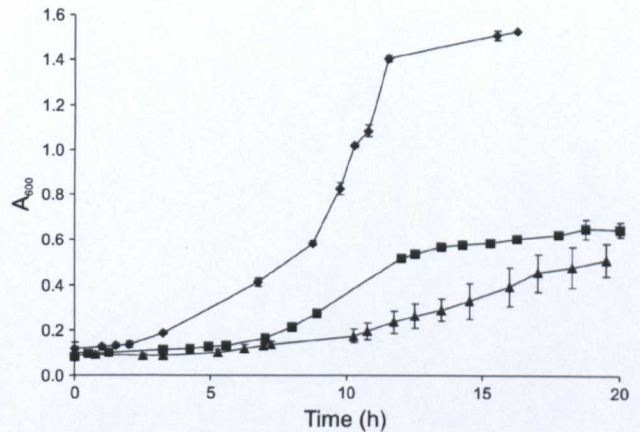


Fig. 2 Growth curves plotting absorbance recorded at 600 nm (A_{600}) against time for *R. erythropolis* MLT1 utilising: succinate (filled diamond), glucose (filled square) and myrcene (filled upright triangle) as the sole sources of carbon for growth. Each point corresponds to the average value calculated on the basis of results recorded for three cultures grown in parallel

9 h, respectively, before reaching optical densities as measured by absorbance at 600 nm of 0.6 and 1.5, respectively (Fig. 2).

Biotransformation of β -myrcene

Resting cells of *R. erythropolis* MLT1 harvested from the late exponential phase of growth were resuspended (50 g/L) in a pH 7.0 phosphate buffer and incubated with myrcene (7.4 mM) for 1 h at 30°C (Fig. 3a). A

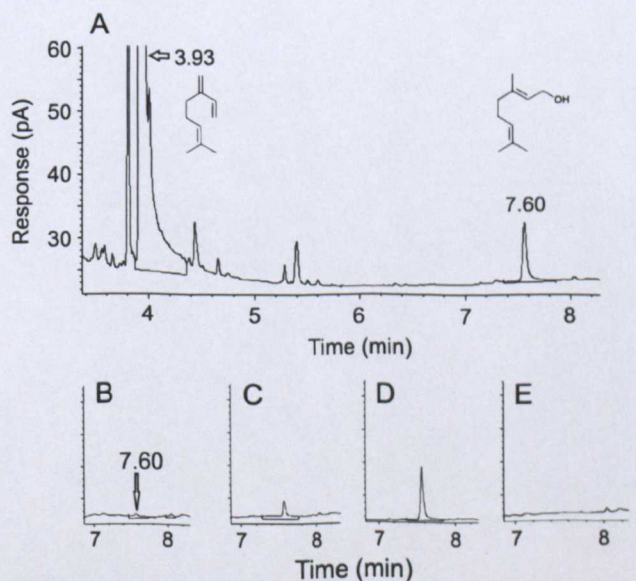


Fig. 3 Chromatograms of injections of the myrcene biotransformation extracts after: a $t=1$ h; b $t=0.1$ min; c $t=0.5$ min; d $t=5$ min; e dead cell control at $t=1$ h. β -myrcene eluted at 3.93 min and geraniol at 7.60 min

variety of control experiments was performed that included incubating cells without myrcene, and incubating phosphate buffer and cells inactivated through autoclaving, with the substrate (Fig. 3e). No biotransformation products were observed in any of the controls; however, a single GC peak with retention time 7.60 min not present in the background was found to be produced only on incubation of β -myrcene-grown cells with β -myrcene. A time-course for this assay showed an increasing concentration of this product over an initial 5-min period (Fig. 3b–d), after which the concentration remained constant for approximately 2 h.

The dependence of this biotransformation on the presence of molecular oxygen was studied in a control experiment carried out under anaerobic conditions. A single batch of cells was prepared as before with myrcene as the SCS in the vapour phase. Division of the cell resuspension into two aliquots enabled reproduction of the standard biotransformation, again showing the formation of the peak at 7.60 min from 1 h incubation at a temperature of 25°C, replicating the ambient temperature measured in the anaerobic hood for the control assay. The second aliquot of active cells was pre-equilibrated in the anaerobic environment, and then challenged with the substrate. GC analysis of the anaerobic biotransformation mixture

revealed no production of the peak at 7.60 min under anaerobic conditions.

Metabolite identification

The MS spectrum of the biotransformation product (Fig. 4) revealed good correlation to existing published data (Adams 1995; Jennings and Shibamoto 1980; Ojala et al. 1999) for the GC-MS analysis of geraniol (3,7-dimethylocta 2,6-dien-1-ol) **10** (Fig. 1). Evidence was also obtained to demonstrate that isomers of geraniol are not responsible for the major product peak. An authentic standard of the stereoisomer nerol ((2Z)-3,7-dimethylocta-2,6-dien-1-ol) run under the same GC conditions was found to have a HP5 retention time of 7.25–7.30 min compared to that for geraniol of 7.60 min. The structural isomer, isogeraniol ((3Z)-3,7-dimethylocta-3,6-dien-1-ol) has published retention indexes lower than those for nerol (Rocha et al. 2007). A calibration line generated from a geraniol standard shows an approximate 50 μ M product concentration from the biotransformation in a 1-h assay representing a conversion from β -myrcene of ~2%. Further samples were prepared from three separate cultures for the biotransformation of myrcene each showing the product with a retention time of 7.60 min. In addition to these

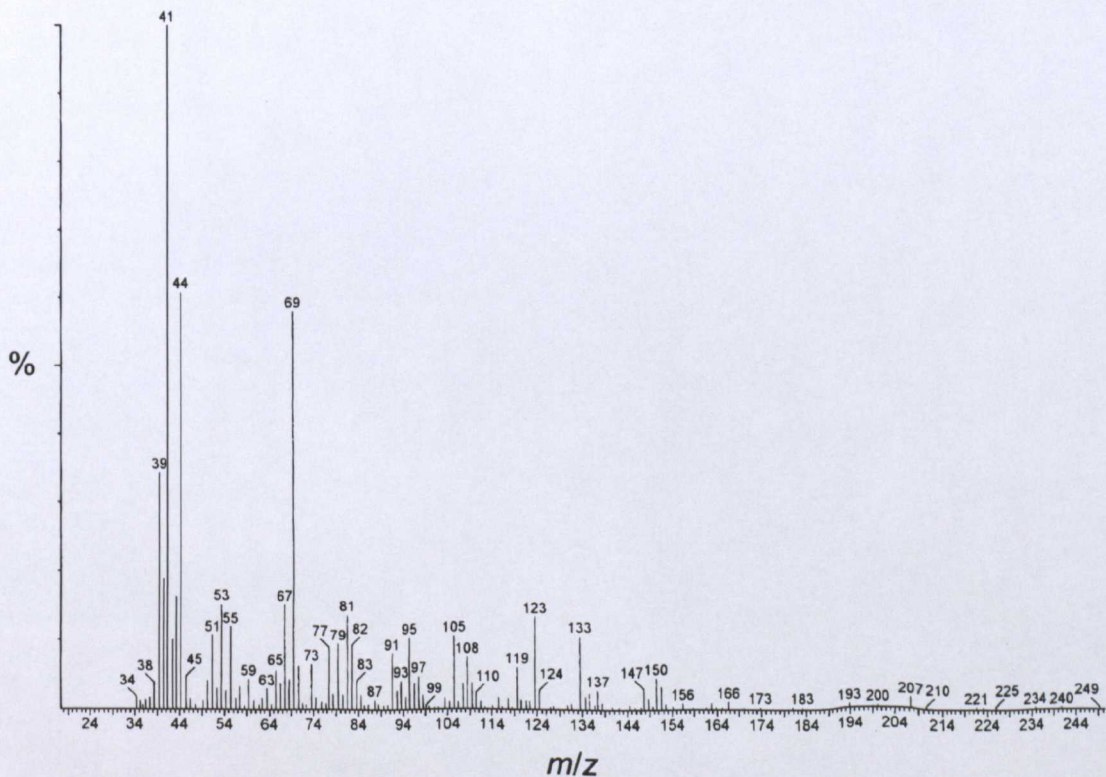


Fig. 4 Mass spectrum for the major metabolite of biotransformation of β -myrcene by *R. erythropolis* MLT1, eluting at a retention time of 7.60 min in Fig. 3 and identified as geraniol

samples, three standards of geraniol at: 0.03, 0.05 and 0.5 mM were also prepared for further analytical work to confirm the product identity. A standard linear *n*-alkane series (C10–C18) was run on both DB5 (non-polar) and DB17 (polar) GC columns giving incremental retention times with increasing chain length. All samples and standards were then run on the DB17 column where a shift (increase) in retention time was observed for geraniol due to interactions of the hydroxyl group with the polar column, when compared to the standard alkane series (giving a retention time similar to the C14 alkane on the same column). The retention times of the three samples run on DB17 column (11.16–11.21 min) overlapped with those for the geraniol standards (11.13–11.20 min). Peak areas were proportional in samples and standards run on both HP5 and DB17 columns, again confirming the identity of the product peak as geraniol.

Cytochrome P450 inhibition studies

Cells were harvested from cultures grown in parallel and combined before splitting into separate aliquots to study the effects of cytochrome P450 inhibition on the biotransformation. GC analysis of the reactions catalysed by cells in the absence of inhibitors revealed concentrations of geraniol that were consistent with previous observations. Pre-incubation of cells at 30°C for 1 h with metyrapone led to a 23% reduction in the concentration of geraniol produced. The effect of incubation with 5 mM 1-aminobenzotriazole for the same period was a 73% decrease in the yield of geraniol. A range of concentrations from 0–5 mM was investigated for both inhibitors however there was no correlation observed between concentration of inhibitor and the negative effect on myrcene biotransformation. Extended pre-incubation times of up to 2 h with the inhibitors also did not result in greater levels of inhibition. Complete inhibition of the biotransformation of β -myrcene to geraniol was not observed for any of the assays conducted using cytochrome-P450 inhibitors.

Inducibility of β -myrcene biotransformation

The resting cell assay was repeated using cells grown on glucose or succinate as SCS. GC analysis of the extracts from these assays showed no geraniol product peak as previously described for those cells grown on β -myrcene as SCS. Insoluble and soluble extracts from cells grown on either glucose or β -myrcene were obtained and analysed by SDS-PAGE (Fig. 5a). Gel a clearly shows induced expression of a band of protein at a MW of approximately 16 kDa-labelled I. Analysis of tryptic digests of this band by mass spectrometry with subsequent comparison of

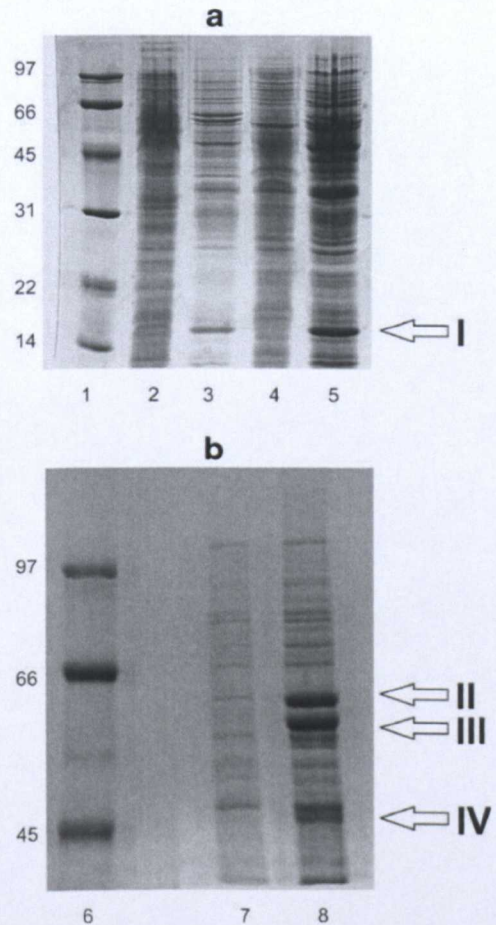


Fig. 5 SDS-PAGE analysis of the crude soluble cell extracts of *R. erythropolis* MLT1 grown on either glucose or β -myrcene as SCS. Gel **a** shows denatured proteins in the molecular mass range 14–97 kDa analysed on a 12% acrylamide gel: *lane 1* BioRad low molecular mass markers with molecular mass shown in kDa; *lane 2* Soluble extract from cells grown on glucose; *lane 3*, soluble extract from cells grown on β -myrcene; *lane 4* Insoluble extract from cells grown on glucose; *lane 5* Insoluble extract from cells grown on β -myrcene. Protein band labelled *I* could not be identified using mass spectrometric analysis of tryptic fragments. Gel **b** shows denatured proteins in the molecular mass range 45–97 kDa analysed on an 8% acrylamide gel: *lane 6* BioRad low molecular mass markers with molecular mass shown in kDa; *lane 7* soluble extract from cells grown on glucose; *lane 8*, soluble extract from cells grown on β -myrcene. MS analysis of tryptic fragments suggested that proteins *II*, *III* and *IV* may be homologues of a GroEL-like chaperone, an aldehyde dehydrogenase and an acyl-CoA dehydrogenase, respectively

peptide mass fragments against database searches using Mascot failed to identify any clear hits. Gel **a** also shows additional bands induced in the molecular mass region corresponding to between 43 and 66 kDa. Increased resolution of proteins in this region was achieved between these molecular masses (Fig. 5b) by decreasing the percentage acrylamide in the gel, and running for a longer period of time. At least three further bands, *II*, *III* and *IV* on the gel were enhanced in samples having been obtained

from cells grown on β -myrcene. MS analysis of tryptic fragments obtained from bands II and IV followed by a BLAST search and comparison with entries in the Mascot database suggested II was homologous to the 60-kDa chaperonin GroEL from *R. jostii* RHA1 (Table 1). IV was assigned as a putative acyl-CoA dehydrogenase based on the similarity to a peptide fragment from *Frankia alni* (Table 1). Equivalent analysis of band III did not yield any clear hits within the Mascot database, however, de novo sequencing followed by searching against the BLAST database suggested that the protein was homologous to 2-hydroxybutyrate semialdehyde dehydrogenase from *Pseudomonas*, based on the identification of peptide fragments LSYVEEAVSEGATLVGG and DEFVAR.

Discussion

Little is known about the enzymatic systems that exist for the metabolism of β -myrcene in bacteria. In this report, a strain of *R. erythropolis* was isolated that is observed in resting cell biotransformations to convert β -myrcene to the important flavour compound geraniol. The chemical-enzymatic mechanism of this transformation is at this stage unclear, and an explanation must await labelling experiments to reveal if the oxygen atom introduced originates from molecular oxygen, and is thus catalysed by an oxygenase; or water, and thus catalysed by a lyase, each discussed below.

Much is known about the mechanisms by which some bacteria oxygenate alkene substrates (Ensign 2001), but these mechanisms routinely involve epoxidation by a multicomponent monooxygenase enzyme, of which different types have been observed in, for example *Xanthobacter* strain Py2 (Small and Ensign 1997) and *Rhodococcus* strain AD45 (Van Hylckama Vlieg et al. 2000). No component of such a monooxygenase was yet identified in 1-D gels of extracts

resulting from cells induced with β -myrcene from mass spectrometric analysis of tryptic fragments, although the biotransformation of β -myrcene by *Rhodococcus* MLT1 clearly required an aerobic environment. Another possible route for the incorporation of a single atom of molecular oxygen into an alkene substrate was described in styrene-oxidising bacteria, in which the successive action of styrene monooxygenase, followed by an isomerase enzyme, results in the terminally monooxygenated compound phenylacetaldehyde from styrene oxide (Panke et al. 1998), but as yet, no such system has been described in the metabolism of aliphatic alkenes. Of other enzymes that catalyse the incorporation of a single atom of oxygen into an alkene substrate, the contribution of cytochrome-P450 in the oxygenation of β -myrcene by MLT1 has not been absolutely ruled out by the relevant inhibition studies. Such alkenes are certainly substrates for cyt-P450 (Sandstrom et al. 2006), although in previous studies, such as those on the cytochrome-P450 steroid 9- α hydroxylase from *Mycobacterium fortuitum* (Kang and Lee 1997), the level of inhibition by metyrapone increased with increasing inhibitor concentration. This was not the case for the transformation by MLT1 presented herein.

The chemical transformation of β -myrcene to geraniol is formally a hydration reaction. The hydration of myrcene could also lead to linalool, and, whilst there is a precedent for the microbial transformation of linalool to geraniol through a putative 3,1-hydroxyl- Δ^1 - Δ^2 -mutase (Foß and Harder 1997), few appropriate lyase enzymes have been described, to our knowledge, that might hydrate the double bond of an alkene that was not conjugated, as part of an α , β -unsaturated system conjugated to a ketone or (thio)ester. One example was the limonene hydratase described by Oriel and co-workers, which was used to convert limonene to α -terpineol and carvone (Savithiry et al. 1997). The other chemical methods of conversion described in the "Introduction" section are dependent on,

Table 1 Identification of protein bands II and IV (Fig. 5) using MS analysis of peptide fragments followed by matching against the Mascot database

Band	Protein	Database	Peptide Sequences matched	Mowse score	Mowse score identity threshold	Expect score
II	60 kDa chaperonin GroEL	<i>Rhodococcus jostii</i> RHA1	IIFAFDEEAR	45	22	0.00032
			WGAPTIINDGVSIK	37	22	0.0018
			QEAVLEDAYILLVSSK	50	21	7.50E-05
			TDDVAGDGTATVLAQALVR	28	21	0.012
			KTDDVAGDGTATVLAQALVR	35	21	0.0023
			EGVITVEESNTFGLQLELLEGMR	20	20	0.053
IV	Putative Acyl-CoA dehydrogenase [<i>Frankia alni</i> ACN 14a]	NCBIInr	ILEIFEGANELQQWIAR	117	49	8.60E-09

for example, hydrocobaltation of the terminal alkene, followed by radical trapping with TEMPO and subsequent reduction with zinc (Howell and Pattenden 1990a). Whilst these mechanisms of hydroxylation have no formal equivalent in biochemistry, the use of metal-assisted catalysis for the transformation of β -myrcene by MLT1 cannot at this stage be ruled out.

Of the enzymes that are apparently induced in MLT1 by growth on β -myrcene, each has precedent in inducible systems for hydrocarbon degradation in bacteria described previously. An aldehyde dehydrogenase of theoretical molecular mass 54.3 kDa, similar to that observed in Fig. 5, gel b, was one of the proteins encoded in a putative operon for β -myrcene degradation in *Pseudomonas* sp. M1 (Iurescia et al. 1999). A 13-fold upregulation of expression of the GroEL chaperone proteins was observed in *Rhodococcus* sp. RHA1 when induced by propane, the degradation of which is also dependent on a multicomponent monooxygenase (Sharp et al. 2007). Given the established pathways for the degradation of geraniol by, for example, *Pseudomonas*, through the formation and subsequent degradation of a geranyl-CoA thioester (Förster-Fromme et al. 2006), the involvement of an acyl-CoA dehydrogenase as suggested by MS analysis of induced proteins, would also not be unexpected; indeed an acyl-CoA dehydrogenase with specificity for citronellyl-CoA was recently described (Förster-Fromme et al. 2008). The unambiguous identification of the enzymes responsible for degradation of β -myrcene in MLT1 awaits the cloning of the relevant genes and characterisation of their expressed products.

Enzymes involved in the metabolism of β -myrcene by bacteria may, in the future, be usefully applied as biocatalysts in the production of natural-equivalent flavour and fragrance compounds. Control experiments for the biotransformation described in this report have demonstrated that geraniol is a biogenic product of β -myrcene incubation with *R. erythropolis* MLT1 rather than an artefact of effects due to reaction medium, inactive biological material or pH. The one-pot biotransformation of β -myrcene to geraniol might present therefore a potentially attractive industrial biocatalytic route towards a fragrant monoterpene, from an inexpensive and naturally abundant hydrocarbon starting material. We are currently exploring the nature of the key enzymes involved in β -myrcene metabolism by *R. erythropolis* MLT1, with a view both to proposing a mechanism for the biotransformation, and to developing a scaleable process for geraniol production.

also grateful to Botanix for providing plant material, chemicals and GC-MS services.

References

- Adams RP (1995) Identification of essential oil components by gas chromatography – mass spectrometry. Allured, IL
- Bradford MM (1976) A rapid and sensitive method for the quantitation of microgram quantities of protein utilizing the principle of protein-dye binding. *Anal Biochem* 72:248–254
- Busmann D, Berger RG (1994) Conversion of myrcene by submerged cultured basidiomycetes. *J Biotechnol* 37:39–43
- Chen ZM, Liu JH, Tao JH (2007) Biocatalysis for green chemistry and drug development. *Prog Chem* 19:1919–1927
- Cheng AX, Lou YG, Mao YB, Lu S, Wang LJ, Chen XY (2007) Plant terpenoids: biosynthesis and ecological functions. *J Integr Plant Biol* 49:179–186
- de Carvalho C, da Fonseca MMR (2003) Towards the bio-production of trans-carveol and carvone from limonene: induction after cell growth on limonene and toluene. *Tetrahedron Asymmetry* 14:3925–3931
- de Carvalho C, da Fonseca MMR (2006) Carvone: why and how should one bother to produce this terpene. *Food Chem* 95:413–422
- de Oliveira A, Ribiero-Pinto L, Otto S (1997) Induction of liver monooxygenases by beta-myrcene. *Toxicology* 124:135–140
- Duetz WA, Bouwmeester H, van Beilen JB, Witholt B (2003) Biotransformation of limonene by bacteria, fungi, yeasts, and plants. *Appl Microbiol Biotechnol* 61:269–277
- Ensign SA (2001) Microbial metabolism of aliphatic alkenes. *Biochemistry* 40:5845–5853
- Farooq AR, Rahman A, Choudhary AI (2004) Fungal transformation of monoterpenes. *Curr Org Chem* 8:353–367
- Förster-Fromme K, Chattopadhyay A, Jendrossek D (2008) Biochemical characterization of AtuD from *Pseudomonas aeruginosa*, the first member of a new subgroup of acyl-CoA dehydrogenases for citronellyl-CoA. *Microbiology* 154:789–796
- Förster-Fromme K, Höschle B, Mack C, Bott M, Armbruster W, Jendrossek D (2006) Identification of genes and proteins necessary for catabolism of acyclic terpenes and leucine/isovalerate in *Pseudomonas aeruginosa*. *Appl Environ Microbiol* 72:4819–4828
- Foß S, Harder J (1997) Microbial transformation of a tertiary allyl alcohol: regioselective isomerisation of linalool to geraniol without nerol formation. *FEMS Microbiol Lett* 149:71–75
- Howell AR, Pattenden G (1990a) Hydrocobaltation reactions of 1, 3-dienes - regioselective hydroxylation of myrcene to geraniol and to (+/-)-linalool via allylcobaloxime intermediates. *J Chem Soc, Perkin Trans 1*:2715–2719
- Howell AR, Pattenden G (1990b) Regioselective hydroxylations of 1, 3-dienes via hydrocobaltation reactions—facile conversion of myrcene to geraniol and to (+/-)-linalool. *J Chem Soc Chem Commun* 2:103–104
- Ishida T (2005) Biotransformation of terpenoids by mammals, microorganisms, and plant-cultured cells. *Chem Biodivers* 2:569–590
- Iurescia S, Marconi AM, Tofani D, Gambacorta A, Paterno A, Devirgiliis C, van der Werf MJ, Zennaro E (1999) Identification and sequencing of beta-myrcene catabolism genes from *Pseudomonas* sp strain M1. *Appl Environ Microbiol* 65:2871–2876
- Jennings W, Shibamoto T (1980) Qualitative analysis of flavour and fragrance volatiles by glass capillary gas chromatography. Academic, New York

Acknowledgments We are grateful to Botanix Ltd, Paddock Wood, Kent, U.K. and to the Biotechnology and Biological Sciences Research Council for funding a CASE studentship to M.L.T. We are

- Kang HK, Lee SS (1997) Heterogeneous natures of the microbial steroid 9 α -hydroxylase in nocardioforms. *Arch Pharm Res* 20:519–524
- Kishimoto T, Wanikawa A, Kagami N, Kawatsura K (2005) Analysis of hop-derived terpenoids in beer and evaluation of their behavior using the stir bar-sorptive extraction method with GC-MS. *J Agric Food Chem* 53:4701–4707
- Krings U, Berger RG (1998) Biotechnological production of flavours and fragrances. *Appl Microbiol Biotechnol* 49:1–8
- Krings U, Hapetta D, Berger RG (2008) A labeling study on the formation of perillene by submerged cultured oyster mushroom, *Pleurotus ostreatus*. *Appl Microbiol Biotechnol* 78:533–541
- Krugener S, Schaper C, Krings U, Berger RG (2009) *Pleurotus* species convert monoterpenes to furanoterpenoids through 1, 4-endoperoxides. *Biores Technol* 100:2855–2860
- Madyastha KM (1987) Metabolism of beta-myrcene in-vivo and in-vitro - its effects on rat-liver microsomal-enzymes. *Xenobiotica* 17:539–549
- Miyazawa M, Murata T (2000) Biotransformation of beta-myrcene by the larvae of common cutworm (*Spodoptera litura*). *J Agric Food Chem* 48:123–125
- Ojala M, Ketola RA, Mansikka T, Kotiaho T, Kostianen R (1999) Determination of mono- and sesquiterpenes in water samples by membrane inlet mass spectrometry and static headspace gas chromatography. *Talanta* 49:179–188
- Panke S, Witholt B, Schmid A, Wubbolts MG (1998) Towards a biocatalyst for (*S*)-styrene oxide production: characterization of the styrene degradation pathway of *Pseudomonas* sp. strain VLB120. *Appl Environ Microbiol* 64:2032–2043
- Rocha SM, Coelho E, Zrostlikova J, Delgadillo I, Coimbra MA (2007) Comprehensive two-dimensional gas chromatography with time-of-flight mass spectrometry of monoterpenoids as a powerful tool for grape origin traceability. *J Chromatogr A* 1161:292–299
- Rozenbaum HF, Patitucci ML, Antunes OAC, Pereira N (2006) Production of aromas and fragrances through microbial oxidation of monoterpenes. *Br J Chem Eng* 23:273–279
- Sandstrom P, Welch WH, Blomquist GJ, Fittiger C (2006) Functional expression of a bark beetle cytochrome P450 that hydroxylates myrcene to ipsdienol. *Insect Biochem Mol Biol* 36:835–845
- Savithiry N, Cheong TK, Oriel P (1997) Production of alpha-terpineol from *Escherichia coli* cells expressing thermostable limonene hydratase. *Appl Biochem Biotechnol* 63–65:213–220
- Schwab W, Davidovich-Rikanati R, Lewinsohn E (2008) Biosynthesis of plant-derived flavor compounds. *Plant J* 54:712–732
- Serra S, Fuganti C, Brenna E (2005) Biocatalytic preparation of natural flavours and fragrances. *Trends Biotechnol* 23:193–198
- Sharp JO, Sales CM, LeBlanc JC, Liu J, Wood TK, Eltis LD, Mohn WW, Alvarez-Cohen L (2007) An inducible propane monooxygenase is responsible for *N*-nitrosodimethylamine degradation by *Rhodococcus* sp strain RHA1. *Appl Environ Microbiol* 73:6930–6938
- Shevchenko A, Sunyaev S, Loboda A, Shevchenko A, Bork P, Enz W, Standing KG (2001) Charting the proteomes of organisms with unsequenced genomes by MALDI quadrupole time-of-flight mass spectrometry and BLAST homology searching. *Anal Chem* 73:1917–1926
- Small FJ, Ensign SA (1997) Alkene monooxygenase from *Xanthobacter* strain Py2. *J Biol Chem* 272:24913–24920
- Takahashi M, Suzuki H, Morooka Y, Ikawa T (1979) Regioselective hydroxylation of beta-myrcene using Pd(II) complexes. *Chem Lett* 8:53–56
- Van Hylckama Vlieg JET, Leemhuis H, Lutje Spelberg JH, Janssen DB (2000) Characterisation of the gene cluster involved in isoprene metabolism in *Rhodococcus* sp. strain AD45. *J Bacteriol* 182:1956–1963
- Vandamme EJ, Soetaert W (2002) Bioflavours and fragrances via fermentation and biocatalysis. *J Chem Technol Biotechnol* 77:1323–1332
- Woodley JM (2008) New opportunities for biocatalysis: making pharmaceutical processes greener. *Trends Biotechnol* 26:321–327
- Yamazaki Y, Hayashi Y, Hori N, Mikami Y (1988) Microbial conversion of β -myrcene by *Aspergillus niger*. *Agric Biol Chem* 52:2921–2922